FACULDADE DE ENGENHARIA DA UNIVERSIDADE DO PORTO

Advanced functionalities for the future smart secondary substation

Konstantinos Kotsalos

Doctoral Program of Electrical and Computer Engineering

Supervisor: Prof. Dr. Helder Filipe Duarte Leite

Co-supervisor: Dr. Ismael Tiago Sá Miranda

Co-supervisor: Dr. Nuno Filipe Gonçalves da Silva

July 2020

Advanced functionalities for the future smart secondary substation

Konstantinos Kotsalos

Doctoral Program of Electrical and Computer Engineering

July 2020

This project has received funding from the European Union's Horizon 2020 research and innovation programme under the Marie Skłodowska-Curie grant agreement No 675318 (INCITE).

Abstract

The emphasis on climate change policy across EU has been to decrease greenhouse gas emissions through reductions and efficiency savings in the power sector. There is clear focus on promoting low carbon and renewable energy technologies for generation with the new and binding objectives of 50% by 2030. The ever-increasing integration of Renewable Energy Resources (RES) or more widely Distributed Energy Resources (DER) such as Electric Vehicles (EVs), rooftop photovoltaic installations, Battery Energy Storage Systems (BESS) and Controllable Loads (CLs), pose several challenges on the planning and operation of distribution networks. Yet, such installations may bring novel and diverse opportunities providing ancillary services to the power system operation through their operational flexibility. This flexibility is generally performed with temporal shifting of energy to be consumed or injected.

The main scope of this thesis is to develop control and management schemes, exploiting operational DER flexibility in Low Voltage (LV) distribution networks in a cost-efficient manner ensuring safe operation. A flexible Distribution Management System (DMS) application is implemented based on a substation centered technical approach, capable to coordinate several active measures such as BESS, microgeneration, EVs, CLs and On-Load Tap Changer (OLTC). The proposed Distribution System Operator (DSO) decision making tool is framed with a three-phase unbalanced multi-period AC Optimal Power Flow (MACOPF) solved as a multi-objective nonlinear optimization problem. More specifically, the dissertation proposes computational techniques to provide a tractable version of the non-linear large-scale optimization problem.

The DMS application is extended to orchestrate the operation of LV networks through a three-stage temporal scheme. Initially, the operational planning is obtained by performing MACOPF to derive schedules for multiple DER. Following an event-triggered MACOPF takes place to mitigate forecast errors or unpredicted behaviors by end-users that provoke operational constraints. Thirdly, typical droop-based controls at the smart-inverters are suggested for close to real-time operation. By using yearly synthetic profiles MACOPF formulation is, also, used to derive efficient planning of the network particularly for the sizing and placement of BESS owned by the DSO.

The thesis provides several study cases showing that active participation of DER in the operation of grid may address technical challenges provoked by their extensive integration. The efficient management of DER flexibility may, additionally, act as an investment deferral (for wire and non-wire alternatives) measure. An analytical techno-economical assessment compares the coordinated operation of a BESS (i.e. owned and operated by the DSO) investment against the option of retrofitting a typical transformer with OLTC hardware, both in active distribution networks. The OLTC appears to be the most efficient option to mitigate overvoltages when high PV integration is encountered, along with the accomplishment of loss minimization. Nonetheless, any phase unbalances could be treated by coordinating OLTC with other DER, or the installation of BESS.

Resumo

O ênfase na política relativa às alterações climáticas da UE tem sido focada na redução das emissões de gases com efeito de estufa e na eficiência no sector da energia. Há assim, um claro ênfase na promoção de tecnologias com baixas emissões de carbono e de energias renováveis para a produção, com os novos objetivos vinculativos de 50% até 2030. A integração dos Recursos Energéticos Renováveis (RER) ou dos Recursos Energéticos Distribuídos (DER), como os Veículos Eléctricos (VE), as instalações fotovoltaicas, os Sistemas de Armazenamento de Energia em Baterias (SAEBs) e as Cargas Controláveis (CC), colocam vários desafios ao planeamento e funcionamento das redes de distribuição. No entanto, tais instalações através da sua flexibilidade operacional, podem criar oportunidades para a prestação de serviços ao sistema elétrico de energia. Esta flexibilidade operacional é geralmente realizada com o deslocamento temporal da produção ou consumo de energia.

O principal objetivo deste trabalho foi desenvolver sistemas de controlo e gestão, explorando a flexibilidade operacional dos DER nas redes de distribuição de baixa tensão (BT) de uma forma eficiente em termos de custos, garantindo o funcionamento seguro da rede. Um Sistema de Gestão da Distribuição (SGD) que permite a flexibilidade da produção foi implementado com base numa abordagem técnica centrada numa subestação, capaz de coordenar várias medidas ativas, tais como SAEB, microgeração, VEs, CCs e On-Load Tap Changer (OLTC). A ferramenta proposta para uma tomada de decisão do Operador da Rede de Distribuição (ORD) é enquadrada com um trânsito de potência trifásico ótimo multitemporal (MACOPF), resolvido a partir de uma otimização multiobjectivo não-linear. Especificamente, o trabalho desenvolvido nesta tese propõe técnicas computacionais para fornecer uma versão computacionalmente possível do problema de otimização não-linear em grande escala.

A aplicação SGD é estendida ao funcionamento de redes de BT através de um esquema temporal em três fases. Inicialmente, o planeamento operacional é obtido através da execução de MACOPF para a obtenção de planeamento multitemporal dos diferentes DER. Em seguida, será chamado MACOPF para mitigar erros de previsão ou comportamentos imprevistos por parte dos utilizadores finais que têm restrições operacionais. Em terceiro lugar, são sugeridos controlos típicos baseados no controlo do estatismo dos "smart-inverters" para um funcionamento próximo do tempo real. Ao utilizar perfis sintéticos anuais, a formulação MACOPF é também utilizada para obter um planeamento eficiente da rede, especialmente para o dimensionamento e instalação de SAEB como um ativo da ORD.

Este trabalho apresenta vários casos de estudo que demonstram que a participação ativa da DER no funcionamento da rede pode enfrentar os desafios técnicos provocados pela sua extensa integração. A gestão eficiente da flexibilidade da DER pode, adicionalmente, funcionar como uma medida de deferimento do investimento. Uma avaliação técnico-económica compara o funcionamento coordenado de um investimento SAEB (ativo da ORD) com a opção de reequipar um transformador típico sem tomadas em carga com equipamento de tomada em carga (OLTC). O OLTC parece ser a opção mais eficiente para mitigar sobretensões quando se verifica uma injeção

de potência fotovoltaica elevada, juntamente com a realização da minimização das perdas na rede. No entanto, os desequilíbrios de tensão por fases poderiam ser tratados através da coordenação do OLTC com os diferentes DER, ou SAEB da rede de distribuição de energia.

Acknowledgments

Thinking of the amount of people I would like to thank along these last four years of my PhD adventure, this page would most likely not be enough to include them all.

Firstly and most importantly I would like to express my deepest gratitude to my supervisory team Prof. Helder Leite and Dr Nuno Silva for trusting and providing me the chance to join INCITE project, as well as for their valuable advice and support these years. I would also like to thank Prof. Leite for resolving any type of bureaucratic problem and for helping me to settle in Porto! A valuable partner of my supervisory team, but most importantly a great friend that guided me in many different ways is Dr Ismael Miranda, who I would heartfeltly like to thank hereby.

Dr Jose Luis Domingues who hosted me and supervised my activities during my first secondment at Research Energy of Catalonia. Marta Fonrodona, the project manager of INCITE that ended up of being a very good friend!

Prof. Hatziargyriou who supported my idea of conducting this PhD. Without him I wouldn't have made the application for the Marie-Curie fellowship. Additionally, I would like to thank him, as well as the SmartRue Lab members, for hosting and supervising me during my stay at National Technical University of Athens.

Additionally, all my colleagues from Efacec, particularly those from the Smart Grids division, who were a great company in the everyday life. I would like to give special thanks to Luis Acacio Marques for the great technical discussions all along these years in Efacec as well as for the excellent collaboration we had, in the projects we were both involved.

These years in Porto wouldn't be as nice without the following very beautiful people Alexandros, Christie, Kavouras, Tiago, Sonia and Helder (esquadrão Grego) as well as Nina, Lotfi and Motaz! Also, these two amazing guys Bruno Taveira and Francisco Gonçalves for their priceless friendship.

Moreover, I would like to thank my friends and colleagues Nikolas Sapountzoglou and Shantanu Chakraborty, both co-fellows of the INCITE-ITN. Both of them provided constant support and motivation throughout these years.

To all my friends from Greece, I would like to express my gratitude for their remote but vital support!

To Vasia, for her important support and love these last six-months! Thank you for your patience, for lending me your strength when I most need it.

Last and most importantly, I would like to thank my family Efthymios and Maria, Christos, Alexandros and Paty for their limitless love throughout my entire life. All of them have been always teaching me the true virtues of becoming a fighter, to work along personal development and advance in life towards eudaimonia!

Konstantinos Kotsalos
Κωνσταντῖνος Κὸτσαλος

"You cannot hope to build a better world without improving the individuals. To that end, each of us must work for his own improvement and, at the same time, share a general responsibility for all humanity, our particular duty being to aid those to whom we think we can be most useful."

Maria Salomea Skłodowska-Curie (1867-1934)

Contents

List of Figures

List of Tables

Abbreviations

ADMS	Advanced Distribution Management System
ANM	Active Network Management
APC	Active Power Curtailment
API	Application Programming Interface
BESS	Battery Energy Storage System
BFS	Backward-Forward Sweep
CCV	Cost Constrained Variable
CL	Controllable Load
DR	Demand Response
EV	Electric Vehicle
DER	Distributed Energy Resources
DMS	Distribution Management System
DN	Distribution Network
DSO	Distribution System Operator
EV	Electric Vehicle
HEMS	Home Energy Management System
IP	Interior-Point
KKT	Karush-Kuhn-Tucker
LCOE	Levelized Cost of Energy
LICQ	Linear Constraint Qualification
LV	Low Voltage
MACOPF	Multiperiod Alternate Current Optimal Power Flow
OLTC	On-Load Tap Changer
OPF	Optimal Power Flow
PCC	Point of Common Coupling
QR	Reactive Power Control
SST	Solid-State Transformer
ST	Smart Transformer
SoC	State-of-Charge
V2G	Vehicle-to-Grid
μG	micro Generation

Chapter 1

Introduction

1.1 Challenges in the Electrical Power System

Electricity plays a significant role in the evolution of modern societies, improving health, safety and the general field of economic growth. Nowadays, fossil fuels remain the primary resource for the generation of electricity in most countries around the world. Yet, this practice of burning fossil fuels to convert them into electricity has been questioned for its sustainability (i.e. efficiency of conversion, environmental footprint). Therefore, over the past two decades there has been an ongoing energy transition towards green technologies and the so-called decarbonization of the energy sector. This transition in the energy mix is presented in the Figures 1.1a–1.1b. The commencement of energy transition occurred with the energy crisis in the decade of 70s, where the nuclear energy was introduced.

The energy transition brings accordingly several trends in the electricity sector. The increasing integration of solar and wind technologies poses a further challenge of maintaining the balance between supply and demand. In the twentieth century the supply was directed to follow the demand. Lately, the supply is becoming more unpredictable and variable due to the dependence on renewables. Additionally, the so-called *electrification of everything* which implies the electrification across transportation, buildings, and even some industrial uses will be a key strategy for achieving deep decarbonization. Concurrently, the majority of electricity infrastructures has been built during 50s to 70s. The significant expected demand growth: in 2030 is forecasted to raise three times the level it was in the beginning of the millennium, leads to the further aggravation of ageing of distribution networks due to their limited capacity limits. This is related to the lifespan distribution lines and cables as well as distribution transformers. Besides, if precautious operation is followed their life time may be significantly extended. The generation of electricity is increasingly taking place in more decentralised manner, due to the installation of photovoltaics in rooftops, small wind turbines, combined heat and power *etc*. Environmental concerns have spurred this remarkable growth of electricity generation from renewable energy sources the last two decades. Additionally, the endeavor of many countries to subsidize new units such as battery storage systems, electric vehicles and fuel cells, propels a further integration of Distributed Energy

Resources (DERs) into the electric grid. These sources are not consistently owned by the System Operator which essentially hardens the task of managing and operating the network.

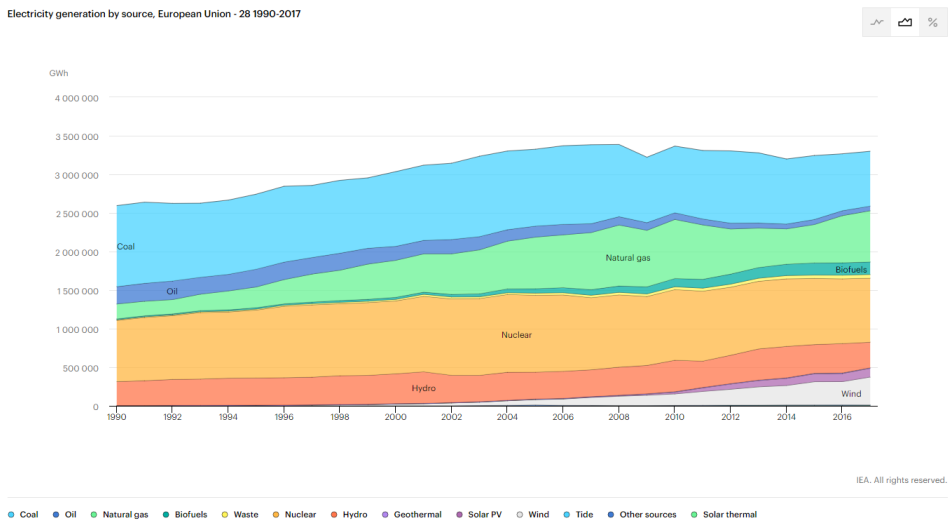

(a)

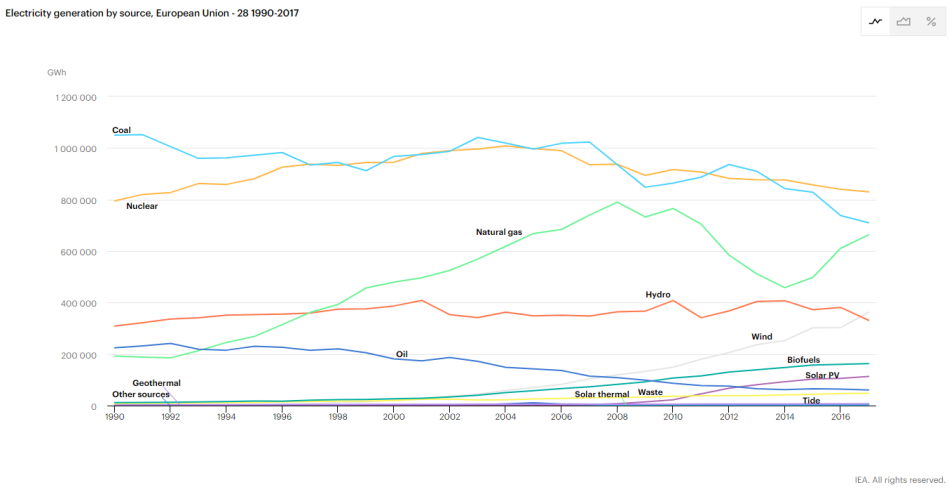

(b)

Figure 1.1: Energy generation by source (IEA, 2020): (a) Cumulative graph.(b) Individual representation for each source.

These evolving changes signify that electricity production is following a more decentralized form, in the sense that a large number of small generation units are connected with the distribution network, delivering their produced energy closer to the location of the consumption. For instance, some of the most commonly connected DERs are microgeneration (typically rooftop PVs), Battery Energy Storage System (BESS), Electric Vehicles (EVs), Controllable Loads (CLs) –such as electric water heat pumps, smart electrical appliances– *etc*. This ongoing shift from centralized to decentralized energy generation requires radical adaptation on the operation and planning stages of the distribution networks.

This leading transition from fossil to renewable generation technologies has, also, direct impacts not only to the conventional power producers, but also, to the typical discrimination of power consumer and power producer. This refers to current consumers with solar panel and/or BESS may contribute on the power production by injecting periodically power into the grid (Figure 1.2). Besides, further implications are made by relevant references on EU wide-level where the challenges towards the phasing-out of fossil fuels are discussed (Erbach, 2016), .

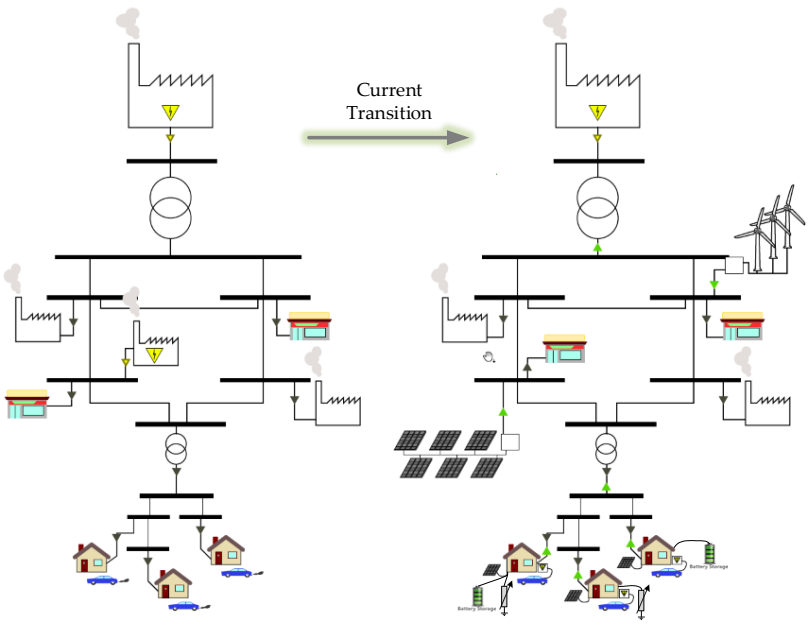

Figure 1.2: Representation of the occurring transition of electrical grids with the extensive integration of DER. The power flow is indicatively shown with the green and black arrows. Edited:(Pedersen).

In the following Section 1.2 a discussion on active network management and future smart secondary substation takes place; Section 1.4 highlights the main contributions of this thesis, Section 1.5 presents its structure, and Section 1.6 enlists the publications published during the doctoral studies.

1.2 Towards active network management

The classical paradigm of electrical power system over the last 60 years has followed a traditional structure, in the sense that it was organized in the layers of generation, transmission, distribution and finally end customers. As per (Kundur et al., 1994), the power system was traditionally "passive", viewed primarily as the delivery of bulk power from the transmission network to consumers at lower voltages.

Focusing particularly on the LV distribution network scale and the integration of mini (mG) and micro (μG), it is more common to consider them in the context of the wider concept of

Distributed Energy Resources (DER). On this document it is rather used the term DER. According to (Evangelopoulos et al., 2016), the meaning of DER embodies the following categories:

- *Distributed Generation (DG)*: which might be further discriminated in Dispatchable DG, referring to all controllable generation such as fueled DGs, Combined Heat and Power (CHG) etc, and the non-dispatchable DG, such as wind turbines and photovoltaics, which are inevitably dependent on the stochastic nature of wind and solar irradiance, respectively.
- *Energy Storage System (ESS)*: the most commonly met on that category is the BESS and EV, while other technologies include mini-pumped hydro storage plant etc.
- *Demand Response (DR) or Demand Side Management (DSM)*, which basically refers to controllable or loads that their operation can be shifted, which might be triggered following a reference signal sent by the DSO or following multiple-pricing signals. There are several other sub-categories of DR.

The presence of DER takes place predominantly in Distribution Networks (DN) in multiple scales, possibly leading to technical and operational challenges. More specifically, there is a wide integration of small-scale embedded generators, typically connected at the LV side. Therefore, the integration of DER is progressively facing limits intrinsic to current power systems. The connection of DERs along the DN results bidirectional power flow, with the possibility of occurring constraints such as branch congestion and voltage unbalances and voltage problems among downstream feeders.

The DER, generally, are enhancing the Distribution System Operator's (DSO's) role providing their flexibility for operational purposes for the distribution network or even for the support of the bulk transmission (usually via the aggregation of their flexibility at the Aggregator level). The incorporation of this DER flexibility for operational purposes is regarded as the active network management.

These evolving changes are already changing radically the end-users' view within the distribution network, provided that they become eventually alternate from consuming to producing energy, acquiring a bilateral interaction with grid and DSO as well. This flexible attribute can be valuable in maintaining the fundamental balance between demand and supply in the overall electric power system. One can notice the potential advantages of smart charging of EVs in the grid among different modes of charging, as explained in Table 1.1. Nevertheless, the exploitation of this operational flexibility necessitates novel active network management functionalities and platforms to be embraced by the DSO. Additionally, grid standards have to be harmonized with these on-going trends and challenges to allow the active operation of DER and consumers.

The utilities are enhancing monitoring functionalities by installing sensory devices to obtain more observable distribution networks and to some extent address these challenges. The advent of smart grids are employed around the concept of deploying smart management systems leveraging communication infrastructures and control functions, usually defined as Advanced Distribution Management Systems (ADMS).

Dumb & inflexible ⟶ *Smart & flexible*

EV Controllability Modes/Strategies	**Conventional**	**Safe**	**Proactive**	**Smart grid Unidirectional**	**Smart grid Bidirectional**
Objective	Maximum comfort max power rate	Charge at maximum power rate exploiting period with better price	min{Charging cost}	min{Charging cost}	min{Charging cost}
Energy flow in EVs	Grid → EV	Grid→ EV	Grid→ EV	Grid→ EV	Grid ↔EV
Remuneration scheme (price)	Fixed	Variable	Variable	Variable	Variable
Type of Charging (Flexibility shape)	On/off	On/off	On/off	Continuous	Continuous

Table 1.1: Towards different EV charging strategies.

These technological changes and challenges, have raised the conceptualization of novel control and management architecture to coordinate the operation of distribution networks, within new market integration models. Concurrently, the proliferation of sensory devices such as smart meters and intelligent electronic devices along with advanced automation, will contribute to this evolution to perform novel control and monitoring schemes, which adopt the active participation of DER. For instance, utilities can adopt innovative power management and voltage control functionalities, in which the distribution resources are substantially involved. Following these notions, the deployment of smart grid concept, has been initiated with the interest of several DSOs to integrate smart metering apparatuses along the LV grid. Smart metering is the key enabler to start facilitating the infrastructure that will allow the commercial and technical management of the electrical power system of the future. While the integration of Advanced Metering Infrastructures (AMI) evokes the necessity to accommodate new mechanisms able to involve user-energy efficiency, new solutions are being implemented up to the LV grid level, by several utilities. Therefore, leveraging metering apparatus together with a set of intelligent automation devices -i.e. Distributed Automation (DA)-, are further propelling contractual operations such as demand response (DR) schemes, leading to a user-centric approach for the operation of the LV grid (Silva, 2010). This can be further enhanced by developing active network technologies that enable a massive deployment and control of industrial and residential generation, possibly through DR programs (Madureira et al., 2009). Along these, the future distribution networks shall require more decentralized management architectures able to incorporate these elements, whilst the operation and planning tools of the network shall consider an active participation of these newly integrated resources, beyond the conventional approaches, through multi-scenario analyses. The alternative “active” future represents the system capacities with distributed generation and demand side fully integrated into system operation under a decentralized operating paradigm that allows in general DER to participate in both energy markets and system management. In Figure 1.3, it is illustrated that the future power systems will pave towards a fully "active" regime, where DER will take lead for the delivery of major system support services, that ultimately will take over the role of central generation. Nonetheless,the "business-as-usual" foresees that an active integration of DG and the demand side into system operation, should follow a decentralized paradigm in both system management and energy markets (Djapic et al., 2007; Shahidehpour and Fotuhi-Friuzabad, 2016).

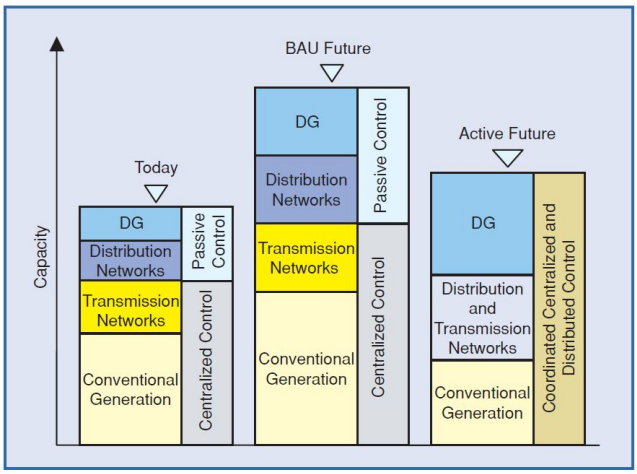

Figure 1.3: Relative levels of system capacity under centralized and distributed control strategies (Djapic et al., 2007).

1.2.1 Portraying the Smart Secondary Substation

The substation composes a primary element of power systems delivering important functions of the utility; therefore, a major breakthrough in substation technology and active management of LV networks is seen as one of the aspects of smart grid revolution. There are several features that need to be facilitated at the secondary substations in order to be retrofitted into intelligent and consistent enough to handle out key tasks (see Figure 1.4).

Towards the "active" way, additional control levels shall be introduced, providing further controllability to the grid. In line with this, the secondary substation equipped with advanced automation devices as well as with proper control management schemes, could serve as an interface between the LV level and the SCADA/DMS (Silva et al.). The secondary substation could be the intermediate pillar to decentralize control and management functionalities down to LV grid.

The main pillars envisaged for the future secondary substation may be outlined as follows :

- *Monitoring*: refers to the aggregation of multiple in-door (i.e. substation's) and network measurements which contributes to the increase of availability and fault localization. Control algorithms can be implemented to track properly any faults and generate alarms of acknowledgement (i.e. task of Advanced Distribution Management System).
- *Telecontrol*: communication interface with switching equipment (e.g. IED), which is a complementary feature that can exploit monitoring information to minimize the down-times.
- *Power Flow Control*: this pillar refers to power management and control functionalities, which will make use of aggregated information to lead to decisions/set-point for distributed resources. These management functionalities target to provide automated control for the LV grid operation.

At the LV level a set of new intelligent devices are being installed, and currently arises the opportunity to enable their capabilities to manage commercial technical functions and advanced services. Furthermore, the need to integrate growing DER facilities emerges, with all related control fea-

tures, and, at the same time, to increase information availability and intelligence (Silva, 2010). Novel control architecture are emerging based on hierarchical or decentralized structure (i.e. different prerequisites for communication infrastructures), which are leveraging the information and advanced automation, to offer control and management functionalities considering an active approach for any distributed resources.

Several works have already focused on retrofitting the secondary substation with advanced automation capabilities which can deliver better controllability of the LV distribution network (Körner et al., 2012). The future of the secondary substation and the MV/LV transformer are foreseen to meet radical hardware changes. For instance, the Smart Transformer (ST) is envisioned as a key element for the controllability of distribution networks in the context of extensive DER integration. The ST is also envisaged to be a solid-state transformer (SST) as a replacement of the conventional power transformer according to (Costa et al., 2017). The presence of ST serving as interface between MV and LV AC grids will, also, enable other key functionalities particularly when BESS capacity is available at ST's DC link, such as frequency and voltage control in the these grids, islanded operation and black-start supported by the ST's electronic power converters (Liserre et al., 2016).

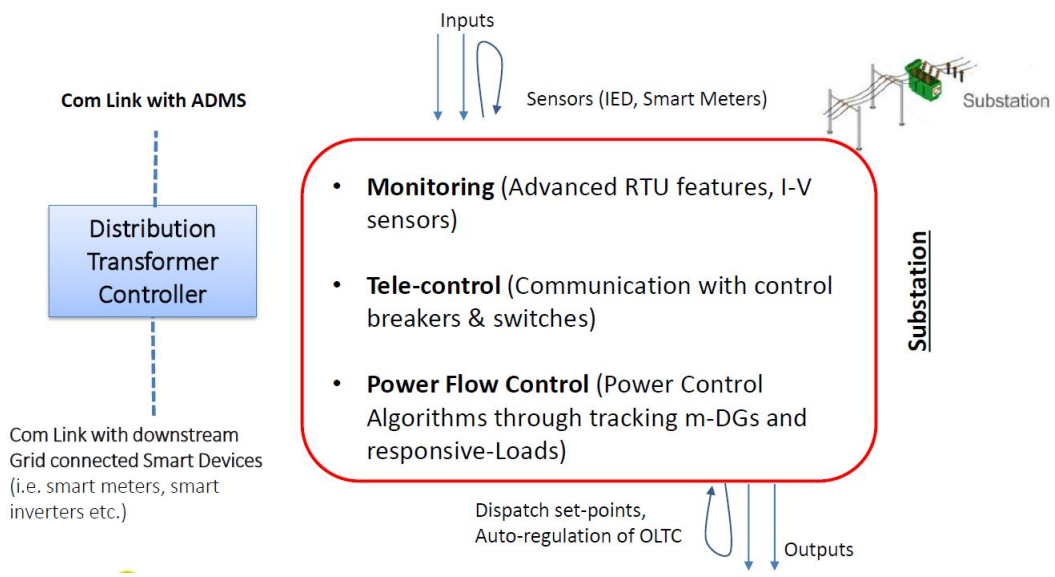

Figure 1.4: Conceptual proposal for the future Smart Secondary Substation, functionalities and technical features.

The secondary substation -as a central entity for the LV grid-, may acquires measurements from sensory devices, IEDs and smart meters through heterogeneous communication, which can feed thereafter control and management strategies. Therefore, the ST, an SST equipped with control and management frameworks as well as communication functionalities, can represent a solution for many of the mentioned problems. These conceptual technical functionalities for the secondary substation provide the capability to facilitate intelligent and autonomous control strategies. This idea leans on dispersing part of the intelligence form the control center to other levels

of the distribution grid e.g. the secondary substation. At the MV/LV substation, close to real-time measurements could be monitored and processed locally, dispatching only requested or statistical information to the control center. Paving towards this line of LV network and secondary substation management, there will be clear benefits for all stakeholders of the network such as the active engagement of the prosumers or consumers on the LV grid operation delivering them compensation fees.

Nowadays, the operation of the LV distribution networks particularly related to voltage regulation and voltage unbalances issues are conventionally handled by the DSO, including manual adjustment of secondary transformer tap position, or manual changes of customers' connection phases respectively. Nevertheless, the manually-controlled techniques are proved to be insufficient, due to the presence of microgeneration together with the variable demand of end-users. Nonetheless, additional voltage compensation devices are proposed to cope with these challenges, such as Automatic Voltage transformer (SVR), active power-line conditioners, Unified Power Flow Controllers (UPFCs). These devices present efficient alternative solutions (Efkarpidis et al., 2016a); although, their application in LV networks is limited due to the investment cost needed for the device itself.

1.3 Thesis scope, objective and research challenges

The purpose of this thesis is to explore scenarios of intensive integration of DER into LV distribution networks, with the subsequent technical challenges (i.e. for the planning and operation stage of LV grids). The integration of DER has clear implications for increased operational flexibility in the frame of active network management. Multiple questions are still unanswered in the planning and operation of LV distribution networks actively utilizing the DER. In order to address several research gaps in this area, some research questions are addressed in this work. Answering these research questions is fundamental to achieve the purpose of this thesis. The addressed research questions are the following:

- Which is the contribution of secondary substation based functionalities to the efficient integration of DER?
- How can DER flexibilities be included in control and management functionalities at the Secondary Substation level?
- Which is the techno-economic impact on the Low Voltage distribution grid operation of a secondary substation centered control approach?

The purpose of this work is to propose control and management functionalities for the operation of LV distribution networks in a context of a substation centered approach. To achieve this, a Distribution Transformer Controller is proposed to be installed at the level of the secondary substation to accommodate the proposed functionalities and control algorithms. Therefore, this thesis aims to at decentralizing the operational and planning stages of the LV distribution network up to the secondary substation level. Analytical control algorithms and solutions are proposed and validated

in scenarios with intensive integration of DER in the LV distribution networks. The benefits of utilizing the substation centered approach is explored comparing different scenarios of coordinated resources, considering also BESS and OLTC as possible investment for the DSO.

1.4 Thesis contributions

The novelties and contribution of this thesis could be summarized as follows:

- The development of an analytical DMS framework for the energy management and scheduling of operation of unbalanced LV distribution networks with increased integration of multiple DER. The tool is capable to derive control actions and schedules for flexible DER and OLTC, subjected to operational constraints such as congestion management, phase balancing, and voltage regulation. The operational framework is formed as multi-objective optimization problem, where the analytical configuration (i.e. objectives, cost setup, control strategy for each DER, operational and technical constraints) can take place through a user interface page. Among the optional objective terms that can be selected are the minimization of operational costs or minimization of flexibility activation costs and minimization of active power losses, as well the minimization of voltage deviations.
- A tractable three-phase multi-period OPF framework based on the exact formulation of the AC power flow equations. The overall problem is formed as a nonlinear optimization problem addressed with the interior-point method. Efficient explicit calculations are suggested for the first-order gradients of constraints and the Hessian of the Lagrangian. Taking advantage of the sparsity of those matrices efficient and storing of variables, a tractable version of the problem with limited memory allocation is obtained.
- Mathematical analysis of inter-temporal constraints (i.e. the limitations of each type of DER) and the counterpart inter-temporal cost dependencies, which cause singularity of the Jacobian matrix of the primal-dual algorithm. In particular, a technique based on slight pivotal adaptations on the Jacobian matrix is proposed to treat those singularities. This methodology presents the advantage that is model-free in the sense that it detects and acts to the binding constraints (i.e. causing the singularity) once needed.
- The operational framework is advanced to bundle multiple operational stage, using the core algorithm for scheduling of operation and intra-day corrective actions, whereas local droop actions are suggested for the near-to-real time operation. In the first two operational stages, active power curtailments and reactive power support are set as the last active measure to be utilized, ensuring maximization of PV generation and anticipate their flexibility in near-to-real time operation through local schemes.
- A technique based on heuristics and continuous variables is proposed to incorporate the OLTC operation avoiding integer decision variables. This practice allows the introduction of OLTC decision variables in the proposed non-linear operational framework.
- An assessment study of the potential impact of managing DER operational flexibilities for the support of the operation of LV. Several scenarios are focusing particularly on increased

integration of EV and PV. The minimum necessary flexibility engagement provided by EVs is identified to respect all grid constraints. The importance of coordinated smart charging is explored and compared with different alternatives either on installing a BESS –owned by the DSO– or by replacing the most congested line.

- The proposed DMS tool is extended for the efficient sizing and placement of BESS solutions (i.e., distributed or centralized). The co-optimization of planning and operation stages is also explored, providing insights for the active participation of DER as investment-deferral practice.
- An analytical techno-economic study is conducted to compare the alternatives among OLTC, BESS, active network management, or their coordinated operation for scenarios with increased DER integration. The comparison, essentially, examines the retrofit of an existing secondary substation with OLTC equipment against the investment on a three-phase BESS –owned by the DSO–.
- A sensitivity analysis for coordinated operation between BESS and EVs exploring variable base pricing for the BESS investment and the variable price of EV flexibility. Following different operational cost for the BESS (i.e. based on its levelized cost of energy) and a range for EV flexibility cost, the tool decides the optimal coordination of those. Several such scenarios are built to explore the participation of each operational measure at each time.

1.5 Thesis organization

The thesis organization, regarding its developed schemes, coordinated units and objectives, is framed in Table 1.2.

Table 1.2: Thesis summary based on optimization method, purpose, objective and the controllable DER considered.

Chapter	**controllable DER & assets considered**	**Objective**	**Purpose**	**Optimization type**
2	PV, EV	min{operating costs}	Comparison : (AC OPF , local droop controls)	3-phase unbalanced AC OPF
3	BESS, PV, EV (v2g)	min{DSO operating costs}	optimal operational planning	3-phase unbalanced MACOPF
4	BESS, PV, EV (v2g)	min{DSO operating costs}	1: optimal scheduling 2: corrective actions 3:close to real-time operation	1: 3-phase unbalanced MACOPF 2: event-triggered MACOPF 3: droop based controls
5	OLTC, BESS, PV, EV (v2g)	min [DSO operating costs, flexibility activation costs, grid losses, fast OLTC changes, tap operation]	operational planning	multi-objective MACOPF

The thesis is organized in five Chapters which can be outlined as follows:

- **Chapter 2** is an introductory chapter on the classical view and operation LV distribution networks and the ongoing challenges. A discussion on the modeling of the LV grids' components and the connected DER. Literature reviews and overview on the conventional unbalanced power flow and optimal power applications is also conducted. Particular emphasis is given on the comparison between a centralized OPF based scheme with local droop scheme for the operation of unbalanced LV networks.
- **Chapter 3** provides the formulation and the methodological steps to obtain a tractable version of the multi-period three-phase AC Optimal Power Flow (MACOPF) addressed as a nonlinear optimization problem. The proposed scheme is validated within an LV distribution network through multiple case scenarios with high microgeneration and electric vehicle integration providing admissible voltage limits and avoiding unnecessary active power curtailments
- **Chapter 4** suggests a taxonomy of research works on the control and management of DER operational flexibility. A conceptual technical architecture is proposed based on an hierarchical substation centered approach. A complete and flexible DMS application is proposed for the efficient planning and optimal DER operational flexibility for unbalanced distribution networks. The core of the proposed leans on the MACOPF formulation. The DSO operational tool is comprised of three stages: the initial for the scheduling of operation, subsequently an event-trigged scheme to provide corrective actions to mitigate uncertainties, and lastly the droop controls based on local measurements.
- **Chapter 5** advances the operational framework into multi-objective programming one. A three-stage scheme is proposed to allow the incorporation of OLTC decision variables into the MACOPF non-linear formulation, avoiding the use of integer variables. A thorough techno-economical analysis in this Chapter provides insights regarding the alternatives among OLTC, BESS, active network management, or their coordinated operation for scenarios with increased DER integration.
- **Chapter 6** summarizes the key findings of the thesis and proposes directions for future work.

1.6 List of publications

The following list of research works were publish during the doctoral course: **Journal papers**

1. **Kotsalos, K.**, Miranda, I., Dominguez-Garcia, J. L., Leite, H., Silva, N., & Hatziargyriou, N. (2020). *Exploiting OLTC and BESS Operation Coordinated with Active Network Management in LV Networks*. Sustainability, 12(8), 3332. [Online]
2. **Kotsalos, K.**, Miranda, I., Silva, N., & Leite, H. (2019). *A horizon optimization control framework for the coordinated operation of multiple distributed energy resources in low voltage distribution networks*. Energies, 12(6), 1182.[Online]

Conference papers

1. **Kotsalos, K.**, Dominguez-Garcia, J. L., Hatziargyriou, N., Miranda, I., Leite, H., & Silva, N. (2019, October). *Coordinated Management of Distributed Energy Resources in Smart Microgrids*. In Proceedings of IECON 2019-45th Annual Conference of the IEEE Industrial Electronics Society (Vol. 1, pp. 4133-4138). Lisbon, Portugal.[Online]
2. **Kotsalos, K.**, Miranda, I., Silva, N., & Leite, H. (2019). *A centralized control for the operation of low voltage distribution networks with multiple distributed energy resources.* In Proceedings of CIRED 2019, Madrid, Spain.[Online]
3. **Kotsalos, K.**, Silva, N., Miranda, I., & Leite, H. (2018). *Scheduling of operation in Low Voltage distribution networks with multiple Distributed Energy Resources*. In Proceedings of CIRED 2018, Ljubljana, Slovenia.[Online]

The following papers have been outcomes of collaborative work along the PhD studies with the R&D of Smart Grid of Efacec, but their content is not discussed in the thesis:

1. **Kotsalos, K.**, Marques, L., Sampaio, G., Pereira, J., Gouveia, C., Teixeira, H., ... & Campos, F. (2019, September). *On the development of a framework for the advanced monitoring of LV grids*. In 2019 International Conference on Smart Energy Systems and Technologies (SEST) (pp. 1-6).[Online]
2. **Kotsalos, K.**, Simões, A., Marques, L., Campos, F., Gouveia, C., Teixeira, H., ... & Pereira, J. (2019). *(ADMS4LV)–Improved observability of LV grids based on advanced analytics*. In Proceeding of CIRED 2019, Madrid, Spain.[Online]
3. Campos, F., Marques, L., & **Kotsalos, K.** (2018, October). *Electric vehicle CPMS and secondary substation management*. In Proceedings of the 8th Solar & 17th Wind Integration Workshop, Stockholm, Sweden (pp. 16-17).[Online]
4. Marques, L., **Kotsalos, K.**& Campos, F. (2018, November). *Distribution Control Units – A Solution to Leverage Distribution Network's Operation Through Distribution Automation*. In Proceedings of CIDEL 2018, Argentina.

Chapter 2

Unbalanced distribution networks and Distributed Energy Resources modeling

Typically, the operation of transmission grids is followed by advanced automation and optimized controls, whereas distribution grids have very limited or absence of control and monitoring functionalities –particularly Low Voltage (LV) grids–. This is due to the fact that LV grids were mainly treated as a passive segment of the overall power system, consuming energy. Nonetheless, the previous two decades several types of Distributed Energy Resources (DER) have being connected such as microgeneration (μG) –e.g. Photovoltaics (PVs) and micro Wind Turbines (WTs)–, Electric Vehicles (EVs) and Controlable Loads (CLs), creating several technical challenges in the operation of LV grids. Concurrently, DER may provide several types of flexibility for the operation of the grids through their active participation. Despite several control approaches are applied in transmission networks which could be adopted in distribution grids, this chapter overviews the crucial differences and explores the conventional operation and monitoring of LV grids. The modelling of distribution network and DER is also described hereby, together with basic functions for unbalanced power flow and optimal power flow. This chapter also contains literature overview on unbalanced power flow and optimal power flows along with a basic centralized control scheme for the operation of unbalanced distribution networks.

2.1 Introduction on Low Voltage distribution networks

The LV distribution networks are the final link for most customers in the electricity supply chain, delivering energy from the secondary substation (Medium Voltage/Low Voltage (MV/LV)) to the service cables. Distribution networks are generally very large networks; in Portugal, the LV network is 140.000 km, the MV lines 74.000 km and the transmission lines 9.000 km (Vieira, 2015). The LV network is either underground or overhead, and in some cases mixed as follows:

- *Underground LV Distribution Network*: typically, it is supplied by a three-phase, ground-mounted, distribution transformer that its rated power is in the range of 300 to 1000kVA, which could supply up to 500 customers.
- *Overhead LV Distribution Network*: it is usually connected to a pole-mounted distribution transformer with rated power between 50 and 100kVA, capable to feed about 30 customers. Distribution networks might be also a combination of overhead and underground networks.

Additionally, some very common traits of the LV distribution networks are the following according to (Jen-Hao, 2003):

- Most commonly they are operated in radial structure. Typically in urban areas, it is common to have link boxes to allow the connection of LV circuits to other feeders due to maintenance or faults. In some specific cases, LV networks might be operated in an interconnected fashion, where two LV distribution substations supply power to the common connected circuit. Yet, there are already pilots projects and prototypes in the UK and Germany that make use of LV switching devices based on power electronics for network reconfiguration (Brewin et al.; Siti et al., 2007). Soft normally open point are being installed to provide the capability to defer network reinforcement (i.e., avoid line congestions), increase capacity and could act to reduce network losses.
- Multi-phase and unbalanced operation, because of the unequal load distribution, untransposed lines and conductors couplings.
- Unbalanced distributed load; the connection type might be single-phase or three phase depending on the type of load to be supplied. The single-phase customers (in Europe up to 10kVA), should always have neutral return conductor, which is commonly provided by the closest earthing point of the secondary winding of the transformer as well as earthed in several poles. Any current injection in one phase provokes a neutral-point shifting that stems from the voltage drop along the neutral conductor and the inverse voltage component. Increased voltage unbalances higher than to 2% (i.e., according to IEC standards) may be resulted either by random load distribution among phases or high integration of single-phase DER.
- Wide-ranging resistance and reactance values according to the type of the grid (city, urban, semi-urban and rural networks). In all cases LV networks are highly resistive ($R/X > 1$) compared to MV network or even transmission networks. Rural networks are also considered to be much more resistive compared to the remainder types.

The large size of LV grids introduces an increased size problem compared to transmission grid

leading to high-dimensional problem, combined with the limitation that there is limited observability of LV network.

2.1.1 Classical view and operation of Low Voltage distribution networks

The safe operation of networks foresees power quality conditions such as admissible nodal voltage magnitudes and acceptable voltage unbalances, as forced by the respective standards. Regarding voltage magnitudes, Distribution System Operators (DSOs) usually adjust the tap positions of the secondary transformer based on seasonal changes of load profiles to avoid excessive voltage drops. From the operational viewpoint, distribution transformers for LV networks are not equipped with On-Load Tap Changer (OLTC). Given that the "typical" domestic load evolution through seasons is well known based on smart meters, transformers with off-load tap changers used to suffice to cope with voltage drops. On the other side, to ensure phase balancing, DSOs have to manually redistribute the consumers' connections, a process that is quite costly and time consuming.

The grid's assets (i.e., lines, transformer) have thermal rating, which is determined by the maximum current-capacity of that component (Trichakis et al., 2008). For the safe operation of the grid, the loading of all equipment has to be below their nominal rating. Typically, distribution lines and transformers on the distribution gird are oversized able to host the expected load growths. However, the recent spreading of single phase DER has violated these assumptions (i.e. resulting in line congestions, voltage issues and phase unbalances), raising the concern for network security and power quality along distribution networks.

The "fit and forget" approach may be the main obstacle for the maximization of renewables and generally green technologies integration (Lopes et al., 2011, 2007). If no measures are undertaken the DSOs might not be capable to host the increasing adoption of DER. Despite extensive grid reinforcement may resolve the security issues, high investment costs are implied. From a technical viewpoint, advanced functionalities for the monitoring and control of distribution network will have to be explored along with an increased installation of sensory devices (e.g., smart meters, intelligent electronic devices etc) and communication infrastructures. The modernization of distribution networks towards the enhancement of their monitoring and observability requires radical effort.

The particular case of secondary distribution networks –i.e., from the MV/LV transformer to the downstream grid– is seen by the DSOs as black boxes, implying that are not monitored nor controlled (Bruno and La Scala, 2017). Another limitation is the fact that most of the LV distribution systems are poorly characterized both in terms of topology and electrical characteristics of distribution lines. Only in some cases there is available knowledge regarding the loads (i.e. capacity and connected phase) connected to each MV/LV transformer (Costa et al., a). The imbalance between load and generation is also underdetermined at the LV level, while its modeling sometimes is challenging, provided the lack of knowledge of location and phase connection of end-users along with any installed microgeneration. For instance, in condominiums end-users are connected to one of the existing phases at the the delivery point following a rotating order. Furthermore, circuit modifications because of faults, maintenance, or even for the connection of new

customers have to accommodated manually by DSOs' staff; any circuit modifications is noted down the changes in the substation level and no update status is sent back at the control center databases. As a matter of fact, analytical circuit information and the LV grid topology may not be available at the centralized level.

2.1.2 Towards the future Low Voltage distribution networks' operation

Few measurements –based on smart meters or Intelligent Electronic Devices (IEDs), current or voltage transformers– are in some cases acquired to represent the state of large segments of distribution grid (e.g., hundreds of nodes including several end-users). According to (James Northcote-Green, 2013), utilities have focused their efforts and investments on improving the performance of the HV and MV networks. However, this practice, particularly in European distribution grids, tends to be gradually insufficient with the integration of PV, since each secondary substation feeds dozens of customers. Therefore, there is a broad range of hardware, nowadays, that is being deployed by several utilities such as Remote Operation of Switchgear, Remote Indication of Switchgear, Voltage Measurement on LV systems and Automatic Changeover for LV distribution Systems.

Particular effort is, still, needed to enhance the monitoring of LV networks not only with efficient placement of sensory devices but also with advanced algorithms capable to assure observability of the distribution networks. Lately, several research works are investigating the exploitation of smart metering devices along with Advanced Metering Infrastructure (AMI) to develop control and monitoring functionalities for LV grids (Silva, 2010; Olivier et al., b). Several challenges arise in LV grid for such functionalities due to the complexity of multi-phase unbalanced networks, the accuracy of distribution state estimation algorithms, given the unsynchronized measurements.

Utilities are in the throes of some phenomenal changes; in distribution, the transformation commenced with the advent of smart grids around the beginning of the millennium, but accelerated greatly the last decade. The distribution network is changing in the following ways:

- The integration of intermittent and less predictable distributed energy resources based on renewable energy clearly results in higher supply variability. Concurrently, the connection of DER brings further complexity and flexibility not only limited to distribution's and customers' level but also at generation and transmission through the provision of ancillary services.
- The utilities are increasingly adopting newer non-wires alternatives (i.e. deferring traditional planning practices) such as different types of energy storage based applications to serve customers at a competitive rate (McCabe, 2019). Those alternatives may, also, leverage energy efficiency, demand response, DER, and other distributed solutions to ensure safe operation of the distribution grid. They may be employed individually (e.g., energy storage at a substation) or in combination (e.g. energy efficiency, demand response, and energy storage), depending upon the system's needs (Grueneich, 2015).
- New sensory devices and control system are connected not only at DSOs' assets (e.g. IED installed at distribution cabinets or the secondary substation) but also at end-users level

such as smart meters and Home-Energy Management System (HEMS), (Heleno, 2016). At the DSOs' level, advanced automation systems provide the capability of functioning in automated manner deploying network monitoring, fault location, isolation and service restoration. At end-users' level several objectives (i.e. technical, economical and end-user comfort level settings) may be optimized towards minimization of costs.

- The deployment of demand response schemes enables end-users participation in energy markets which takes place through the appearance of new entities such as aggregators and retailers. Therefore, customer expectations are changing particularly when they become owners of DER that can be likely coordinated with HEMS to provide active participation on the operation of the grid.
- The evolving behavior of end-users with the introduction of Local Energy Communities (LEC) as well as their interaction amongst them, the aggregators and the utilities.

The aforementioned on-going changes in the landscape of distribution networks clearly affect traditional methods of planning and operation, field services and customer services. Additionally, such changes impart higher complexity in the management of distribution systems, while the so-called smart grid paradigm acts as a key driver to a shared new vision devoted to embrace more flexibility on distribution network operation using advanced concepts and methods. Utilities are currently moving towards the deployment of Advanced Distribution Management Systems (ADMS) as an integrated platform with user interface for supervisory control and acquisition (SCADA), where Distribution Management Systems (DMS) functionalities incorporate the future planning and operational requirements of the upcoming distribution networks. The ADMS applications, substantially, leverage the enhanced observability and controllability level to actively and optimally manage network assets and DER based on advanced analytics (Kotsalos et al., a).

In (Dubey et al., 2020) authors, categorize ADMS application into the following categories based on the time-horizon of deployment:

- Short-term application which are currently at R&D stage and are expected to be adopted within the next years (one to five years). Such applications are: short-term demand and generation forecasting, network topology and state estimation, utility/customer microgrid, optimal DER control and coordination, proactive demand response schemes, resilient restoration with intentional islanding modes. If proper grid observability is obtained, Optimal Power Flow (OPF) algorithms-engines may be deployed for the management of LV operation.
- Long-term applications and enablers, which are expected to be mature enough for deployment by utilities in the next five to ten years. Adaptive protective schemes, proactive crew and mobile restoration resources for resilience, data-driven post-disaster situational awareness and autonomous decision making are amongst them.

ADMS applications that aim to optimize network's operation by coordinating the flexible use of heterogeneous loads and DERs in a unique framework. The core of network-level optimization application is based on OPF algorithms. Further information on a decision-making engine based on a three-phase unbalanced OPF to support the operation and control LV distribution grid is in

Section 2.5.

2.2 Transformer and distribution lines modeling

The lack of monitoring, together with the need of deeply understanding the behavior of LV networks and the consumers connected to them makes it even more challenging to assess the impacts of future (more "active") scenarios. In general the abundance of sensory infrastructures makes more difficult the implementation of advanced control strategies for the LV level. In the direction of complete vision of LV distribution (i.e. can be achieved based on pseudo-measurements), the correct representation and modeling of the distribution network is of substantial importance. Towards the "smartification" of DMS frameworks, efforts are focused to integrate control and monitoring functionalities embedded in DMS. The representation of smart grid may be defined by a four-layer structure, the field composed of physical components (nodes-buses, transformers, distribution lines, capacitor banks, loads etc), the sensory and actuating apparatuses, the deployed ICTs along the system, and the control layer (head-end systems), according to (Santacana et al., 2010; Gottschalk et al., 2017). Therefore, a guideline of the developed models and adaptation based on the literature follow in this section.

2.2.1 Transformer

The distribution transformer (MV/LV) can be represented and included in the Y_{bus} of the network by constant impedances (i.e., for steady state analysis), according to its type i.e., wye–delta, wye–wye, open-wye–open-delta, delta–delta (most common delta–wye grounded in Europe). For each type of transformer's configuration, the admittance matrices for the distribution transformer can be found in the literature, as in (Chen and Chang). Building the admittance matrix of the transformer is commonly known that it is not always invertible other than wye-g-wye-g; hence, an addition of a fictitious small admittance from the isolated transformer sides to the ground remedies the issue (Gorman and Grainger, 1992).

More analytically, a three-phase distribution transformer may be represented by two blocks, a series block modeling the leakage admittance and a shunt block for transformer's core losses, (Bazrafshan and Gatsis, 2018b). For the particular case of $\Delta-\mathrm{Yg}$ distribution transformer the per unit admittance matrix is formulated by Eq. (2.1), assuming that the transformer can be represented by two-port object and each port with three-terminal (i.e. one per phase).

$$\mathbf{Y}_{\mathrm{MV/LV}} = \begin{bmatrix} \mathbf{Y}^{s}_{\mathbf{nm}} & \mathbf{Y}^{m}_{\mathbf{nm}} \\ \mathbf{Y}^{m}_{\mathbf{mn}} & \mathbf{Y}^{s}_{\mathbf{mn}} \end{bmatrix} \tag{2.1}$$

where

$$\mathbf{Y}^{s}_{\mathbf{nm}} = \frac{1}{3}\begin{bmatrix} 2y_t & -y_t & -y_t \\ -y_t & 2y_t & -y_t \\ -y_t & -y_t & 2y_t \end{bmatrix} \qquad \mathbf{Y}^{m}_{\mathbf{nm}} = \frac{1}{\sqrt{3}}\begin{bmatrix} -y_t & 0 & y_t \\ y_t & -y_t & y_t \\ 0 & y_t & -y_t \end{bmatrix}$$

$$\mathbf{Y}^{m}_{\mathbf{mn}} = \frac{1}{\sqrt{3}}\begin{bmatrix} -y_t & y_t & 0 \\ 0 & -y_t & y_t \\ y_t & 0 & -y_t \end{bmatrix} \qquad \mathbf{Y}^{s}_{\mathbf{mn}} = \sqrt{3}\begin{bmatrix} y_t & 0 & 0 \\ 0 & y_t & 0 \\ 0 & 0 & y_t \end{bmatrix}$$

where y_t is the per unit leakage admittance. Note that $\mathbf{Y}^{s}_{\mathbf{nm}}, \mathbf{Y}^{m}_{\mathbf{nm}}, \mathbf{Y}^{m}_{\mathbf{mn}}, \mathbf{Y}^{s}_{\mathbf{mn}}$, are the corresponding nodal admittances, supposing that n-edge is the primary winding Δ-type and the secondary winding is m-edge for grounded star.

For OLTC hardware on the distribution, the variable turn ratio has to be regarded respectively in the admittance matrix. Regarding the control interface and the relevance of the modeling of OLTC analytical information is in Chapter 5.

2.2.2 Distribution lines

In this study the LV distribution network is represented as a three-phase four wire unbalanced network with a multi-earthed neutral; this fact allows the application of the Kron's reduction (Ciric et al., 2003). The representation of the line model as well as the the interconnection of the LV with upstream distribution grid are in Figure 2.1. All nodes of the grid in this study have three terminals, each of which represents the phases a, b, c. The voltage magnitude for node j is given by the real vector $v_j = [v_{j,a}, v_{j,b}, v_{j,c}]^T$, where $\Phi = \{a, b, c\}$ the set of available phases in the distribution grid. Accordingly, the voltage angles by the real vector $\vartheta_j \in \mathbb{R}^3$.

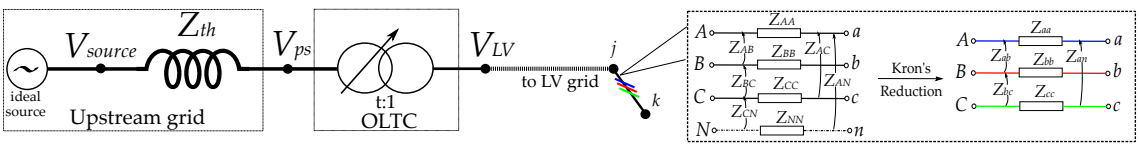

Figure 2.1: Representation of transformer connected with the upstream grid, along with distribution lines' representation -Kron's reduction is illustrated-.

A connection between buses j and k is mathematically represented by a square symmetric matrix $\mathbf{z_{k,m}} \in \mathbb{C}^{\Phi_{k,m} \times \Phi_{k,m}}$ (e.g., Kron's reduction, the analytical form would explicitly include the neutral and the earth conductor), where $\Phi_{k,m}$ the number of phases interconnected nodes k and m. The active conductors (i.e. the three-phases, neutral follows the reduction) present coupling amongst them; hence, the $[z_{k,m}]$ has off-diagonal elements different from 0, as well as the corresponding self-inductances. The admittance matrix ($Y_{bus} \in \mathbb{C}^{3N_b \times 3N_b}$) defines the topological structure and the connectivity among nodes of the distribution network. The line shunt admittances for the distribution lines in LV grid can be neglected (Cheng and Shirmohammadi, 1995)). Consequently, the element $Y_{k_{p_k}, m_{p_m}}$ of $\mathbf{Y_{bus}}$ which refers to the connection between phase p_k of bus

k and phase p_m of m can be expressed as:

$$(Y_{k_{p_k},m_{p_m}}) = \begin{cases} -\frac{1}{(z_{k,m})_{p_k,p_m}} & \text{if } k \neq m, \\ \sum_n \frac{1}{z_{k,n}} & \text{if } k = m. \end{cases} \tag{2.2}$$

The ideal voltage source (i.e. considered as balanced with infinite feed-in capacity) is used to impose constant phase in the slack bus $\underline{/\theta_{source}} = \left[0, \frac{2\pi}{3}, -\frac{2\pi}{3}\right]^T$ as well as to represent a stiff busbar according to its equivalent Thevenin impedance (i.e. calculated by the short-circuit power) placed in series. The V_{source} for power flow applications does represent the slack bus; instead within the proposed modeling it follows the voltage derived by OLTC (V_{ps}).

2.2.3 Loads

The representation of any type of loads at a node has to be represented by two terms the active and the reactive power contribution. In general, residential consumer's load profiles are characterized by very high variability; hence, for the analysis load can be regarded as constant quantity either representing the instant contribution or other statistical metrics such moving average or simply averaged consumption for the examined simulation window. For a node j, the load is stated:

$$s^j_{\text{load}} = p^j_c + jq^j_c \tag{2.3}$$

and accordingly $S_{\text{load}} = P_c + jQ_c$ represents the $n_b \times 1$ vector of complex loads at all buses of the examined network. This consideration follows the constant PQ assertion; still, constant impedance or constant current loads may be regarded for exceptional cases, where a modifications has to be concerned as explained in Section 2.4.3, for the calculation the injected current per node. Controllable loads are described in the section DER modelling (see Section 2.3.4).

Including a brief representation in the developed distribution networks simulation framework, the additional deployed load models, based on the literature (Lindén and Segerqvist, 1992), are:

- Constant current (I) or n-exponential (constant I is for $n = 1$),where powers (P and Q) vary with voltage magnitude ($|V|$):

$$\frac{P}{P_0} = \left(\frac{|V|}{|V_0|}\right)^n, \quad \frac{Q}{Q_0} = \left(\frac{|V|}{|V_0|}\right)^n \tag{2.4}$$

- Constant impedance (Z), where powers (P and Q) vary with the square of voltage magnitude ($|V|$):

$$\frac{P}{P_0} = \left(\frac{|V|}{|V_0|}\right)^2, \quad \frac{Q}{Q_0} = \left(\frac{|V|}{|V_0|}\right)^2 \tag{2.5}$$

- Polynomial (P_0), the power (P and Q) and the voltage magnitude $|V|$ are connected with a polynomial equation:

$$\frac{P}{P_0} = \alpha_0 + \alpha_1 \frac{|V|}{|V_0|} + \alpha_2 \left(\frac{|V|}{|V_0|}\right)^2, \quad \frac{Q}{Q_0} = \beta_0 + \beta_1 \frac{|V|}{|V_0|} + \beta_2 \left(\frac{|V|}{|V_0|}\right)^2 \tag{2.6}$$

where $\alpha_0, \alpha_1, \alpha_2$ and $\beta_0, \beta_1, \beta_2$ are constant parameters of the model respecting the following equations:

$$\alpha_0 + \alpha_1 + \alpha_2 = 1, \quad \beta_0 + \beta_1 + \beta_2 = 1$$

and P_0, Q_0 and V_0 are parameters determined per node in the network.

It should be noted that the ZIP load model provides an approximate representation of the dependencies of nodal injection currents on voltages. More recent studies on voltage dependencies have identified that modern appliances behave on a significantly different manner to those from a decade ago, fact which is related to the prevalence of power electronic and energy efficient loads (Bokhari et al., 2013). More sophisticated models have to be considered even for the steady-state analysis of residential load. Nonetheless, the exponential ZIP model properly tuned can provide an acceptable representation as per (Bazrafshan and Gatsis, 2018a).

2.3 Distributed Energy Resources: modeling and controls

2.3.1 Microgeneration (μG)

The microgeneration, namely Photovoltaics (PVs) installed at rooftops in LV distribution networks, analytical models may be applied. For instance, a PV model may consider analytically the ambient temperature and the tilt angle of the PV. Accordingly, the PV model can be assigned with a solar irradiance model to capture the dependence on realistic weather conditions (e.g. clouds) as in (Pedersen et al.).

The microgeneration in this work is simply considered to be single-phase inverter based installations. In case the DSO desires to incorporate the control of microgeneration as active network management measure, the type of control pertaining the active power through Active Power Curtailment (APC) and/or Reactive Power Control (QR). Regarding the APC, the following settings define the maximum possible curtailed power as a percentage of the instant injected power (i.e., maximum curtailment β=20%), given the following rule in Equation (2.7):

$$\overline{p_{pac}(\tau)} = \begin{cases} \beta \cdot p_{inj}(\tau), & \textbf{if } p_{inj}(\tau) \geq \xi \cdot p_{rated}, \\ 0, & \textbf{else.} \end{cases} \tag{2.7}$$

ξ stands for a parameter which leads to control PV with larger injected power in proportion to their installed power at the instant period. The reactive power control is defined in similar way, though allowing capacitive and inductive operation (i.e., injecting and absorbing reactive power accordingly). Nevertheless, if the option of controlling the PVs in both PAC and QR mode, to avoid the nonlinear constraint inherent to the operation of the inverter; a simpler linear constraint is posed to ensure that the microgenerator's inverter does not exceed its rated power:

$$\begin{aligned} \overline{Q_{QR}(\tau)} &= (p_{rated} - p_{inj}(\tau)) \cdot \tan(\theta_{\min}) \\ \underline{Q_{QR}(\tau)} &= -\overline{Q_{QR}(\tau)}, \end{aligned} \tag{2.8}$$

where $\theta_{\min}$ is given by the minimum power factor ($\mathrm{PF}_{\min}$) applied; $\theta_{\min} = \cos^{-1}(\mathrm{PFmin})$.

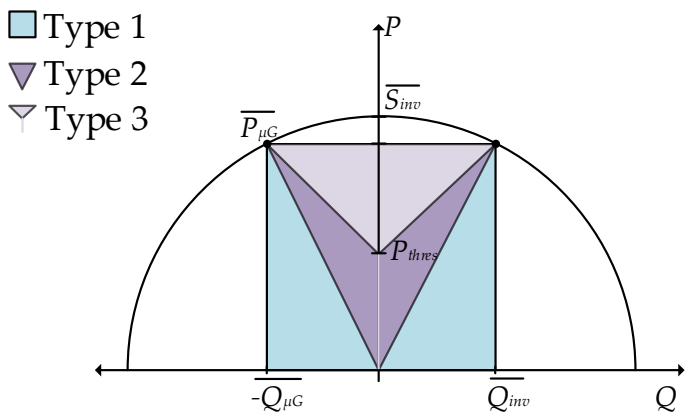

Figure 2.2: Smart inverter's P-Q capability curve.

Note that in practice several droop settings can deployed locally in smart inverters following an intelligent manner of operation to avoid constraints in the grid. As already discussed, the continuous installation of DERs in the distribution networks typically causes power quality issues limiting the hosting capacity for DER, or imply the need for grid expansion. Due to the high R/X branch ratio and the voltage rise increases in more distant nodes from the distribution transformer in radial networks, fact which proportionally occurs in traditional load-dominated grids. Off-line modifications on the distribution transformer is the resolution in some cases, but still time demanding and costly.

Since the last decade local controls are extensively investigated for voltage control applications. Typical droop settings for dispersed generators are to provide reactive power support in proportion to the voltage of point of common coupling ($Q = f(V)$), or based on their active power injection and voltage measurements ($Q = f(P,V)$), (Karagiannopoulos et al., 2017; Kotsampopoulos et al.). Other approaches suggest the adjustment of power factor according to their active power injection ($\cos(\phi) = f(P)$), (Olivier et al., 2016b). Nonetheless, those approaches appear to decide increase flow of reactive power even when no voltage issues exist, leading to increased network losses. In all strategies the capability curves of the inverter have to be respected. This defines the semi-circle rule as illustrated in Figure 2.2. Usually, inverters are oversized by a 5–10% to provide a head-space and allow the injection or consumption of some reactive power (Kotsampopoulos et al.). The grid codes and international standards define the operation of the inverter within a certain area lying within the capability curve. As an example three types of operation are defined in the same Figure, type 1 corresponds to the rectangular (□), type 2 to the triangular (▽) and type 3 to the triangular with an active power injection dead-band. For instance, type 1 allows the reactive power control even at periods with very low generation by the μG, whereas type 2-3 are more restrictive.

Following the above information for the development of the μG model three alternative modes of operation may be adopted for reactive power control; mode 1 where constant power factor is followed (defined by grid codes), mode 2 for the voltage control Q-V and mode 3 the $\cos(\phi) =$

$f(P)$. At each time reactive power output is set as in (2.9):

$$Q_g = \begin{cases} Q_{ref} & \text{if mode 1,} \\ g(\upsilon_{ref}, \upsilon_{pcc}) & \text{if mode 2,} \\ P_g \tan(\cos^{-1}\phi) & \text{if mode 3,} \end{cases} \tag{2.9}$$

where Q_{ref} and $\cos(\phi)$ may be defined by the grid code, υ_{ref} is the reference that shapes the droop curve accordingly and υ_{pcc} the voltage at point of common coupling. The droop function is defined by $g : \mathbb{R}^2 \to \mathbb{R}$ as in (2.10).

$$g(\upsilon_{ref}, \upsilon_{pcc}) = \begin{cases} \frac{-2\overline{S_{inv}}}{\overline{\upsilon}-\underline{\upsilon}}(\upsilon_{pcc} - \upsilon_{ref}) & \text{,if } \underline{\upsilon} \leq \upsilon_{pcc} \leq \underline{DB} \vee \overline{DB} \leq \upsilon_{pcc} \leq \overline{\upsilon} \\ 0 & \text{else} \end{cases} \tag{2.10}$$

where $\underline{DB}, \overline{DB}$ define the upper and lower threshold of the dead-band.

2.3.2 Battery Energy Storage System (BESS)

The BESS's model, essentially, captures its energy state at each time. For the resolution of this work a first-order system is used. Yet, more accurate nonlinear model exist and are well studied in the literature (Yao and Aziz).

In this model, the charging mode increases its required consumption in order to get charged, while it injects power the grid during its discharging mode. The stored energy at the upcoming step will be given by:

$$e_{\tau+1} = \begin{cases} e_\tau + \Delta\tau \cdot \eta_{ch}\, p_t & \text{if } p_t \geq 0, \\ e_\tau + \Delta\tau \cdot \frac{1}{\eta_{dch}} p_t & \text{if } p_t < 0, \end{cases} \tag{2.11}$$

where e_τ is the stored energy at the time step τ, $\Delta\tau$ is the sampling resolution that the system is observed, η_{ch}, η_{dch} correspond to the charging and discharging efficiencies, accordingly. The operational constraints for both operation modes as follows:

$$\underline{e} \leq e_\tau \leq \overline{e} \tag{2.12a}$$

$$\underline{p} \leq p_\tau \leq \overline{p} \tag{2.12b}$$

$$\|p_\tau - p_{\tau-1}\| \leq p_{\text{rate}} \tag{2.12c}$$

where constraint (2.12a) refers to the minimum and maximum energy of the system, (2.12b) poses the minimum and maximum limits of power charging or discharging which can be expressed also as State-of-Charge (SoC), and constraint (2.12c) sets the power consumption or injection rate. Including the power rate constraint, the power consumed or injected at the next (simulation) step is determined as follows:

$$p_\tau = \begin{cases} p_{\tau-1} + \text{sign}(p_\tau - p_{\tau-1})\, p_{rate} & \text{if } |p_\tau - p_{\tau-1}| > p_{\text{rate}} \\ p_\tau & \text{else} \end{cases} \tag{2.13}$$

The BESS can be charged or discharged following two different strategies either following a droop control control proportional to the Point of Common Coupling (PCC) voltage, or depending on its SoC.

$$p_\tau = \begin{cases} \underline{p} & \text{if } 0 < e_t < \overline{e} \wedge p_\xi < \underline{p} \\ \overline{p} & \text{if } 0 < e_t < \overline{e} \wedge p_\xi > \overline{p} \\ p_\xi & \text{if } (e_\tau = 0 \wedge p_\xi \leq 0) \vee (e = \overline{e} \wedge p_\xi \geq \overline{p}) \end{cases} \tag{2.14}$$

where p_ξ allows the option to accept a reference point from centralized scheme such as OPF. Accordingly, the BESS control component may have additional control functionalities for reactive power control equally defined as in Section 2.3.1 for smart inverters.

It should be noted that in the implemented simulation framework, these BESS equations are used for single-phase systems. Any three-phase BESS considered, is simply introduced with three single-phase BESSs by applying also the equality constraint for their active and reactive power set-point at each time. The latter, assures that each module follows the same way of operation.

2.3.3 Electric Vehicle (EV)

In this part, a description of residential EV model takes place, where the EV is considered to charge via residential outlet. The EV model is structured following the same rationale as the one for BESS, along with a mobility model to emulate realistic profiles for their usage and the subsequent charging profiles. Further information about the electric mobility model are in Chapter 4. The electric mobility function is based on notions described by (Pedersen et al.). The availability of EV expresses the periods that owners do not use them for any trip, and considered to be parked at the house premises.

The EV charging, can take place following the same modes that the BESS structure uses, maximum charging power, a power reference signal, or set by a $P-V$ droop function.

Therefore, the EV flexibility can be considered as:

$$P_f^{EV}(t) = a(t) * |[p(t)]| \tag{2.15}$$

where $a(t)$ refers to a vector that represents the availability of EV to get dis/charged, and p(t) is the power. Analytically, the availability is:

$$[a(t)] = \begin{cases} 1 & \text{if EV charges} \\ 0 & \text{if EV is not available} \\ -1 & \text{if EV V2G mode} \end{cases} \tag{2.16}$$

2.3.4 Controllable Loads (CL)

Controllable loads are considered at the residential premises particularly those possibly equipped with HEMS interface. Such hardware may automatically assign bilateral contracts with an aggregator provide flexibility to the operation retaining comfort level of the end-user as well. Therefore, the optimized net-load demand curve is considered; nevertheless an optimize load management for

a residential user might not be a proper hypothesis and the uncertainty implied may be alleviated with the participation –of the end-user– to demand response programs.

Concerning the end-users' flexibility several concerns can be asserted. For simplicity here, the operation of CLs can be shifted in other daily time steps. Therefore, such loads can provide temporally flexible amount of active power as:

$$\begin{aligned} P_t^{\text{flex}} &= P_t + \zeta_t \cdot P_{on-off,j}, \quad -1 \leq \zeta_t \leq 1 \\ &\sum_{t=1}^{24} \zeta_t = 0 \end{aligned} \tag{2.17}$$

where $P_{j,t}$ is the typical (without applying shifts of on-off) consumption, $P_{on-off,t}$ the component of available capacity at time t for upward/downward flexibility. The summation constraint, assures that the energy task of the load is completed within the day. Further and more sophisticated controllable load models optimization schemes are generally proposed (Maharjan et al., 2013). For this particular chapter single period optimization will be only discussed; hence, temporal flexibilities are not analytically regarded. CL can be simply stated with similar formulation as the rest inverter-based DERs, such types of load are namely heat-pumps and generally smart appliances. A great effort towards the engagement of flexible loads is the fact that heat pump manufacturers, equip their units with control boards able to receive signals from DSOs under IEC 61850 protocol for substation automation (Bruno and La Scala, 2017).

2.4 Unbalanced three-phase power flow

2.4.1 A review on unbalanced power flows

Power Flow (PF) is considered to be a fundamental application for the power system analysis, providing insights for both planning and operation of the transmission and distribution network. The resolution of power flow equations provides the knowledge of steady state operating point of the entire network through the assessment of state variables (i.e. voltage and angles at each node). For instance, the characterization of state variables, the power balance and mismatches between generation and consumption as well technical constraints (e.g. voltages, line congestion etc) may be recorded. Traditionally, PF application is extensively used for transmission networks (where the existing measurements make feasible its execution), whilst distribution networks were regarded as lumped loads in single buses. However, the ongoing challenges render PF calculations significant for distribution networks.

From the mathematical and practical (i.e. size and complexity of distribution networks) viewpoint, is no analytical closed-form resolution to address the Alternating Current (AC) PF –that corresponds to exact PF expression–. Linear approximation or iterative numerical methods are widely used in the literature to resolve PF efficiently (Abdi et al., 2017). In the particular case of transmission networks, Gauss-Seidel (GS) (Grainger and Stevenson, 1994) , Newton-Raphson (NR) (Tinney and Hart, 1967) or the fast decoupled load flow (FDLF) (Stott and Alsac, 1974) are

typically used for network operation, control and planning applications. All such approaches rely on the fact that transmission networks have a meshed configuration and low ratios of R/X, which allow the direct decoupling of active power from from the voltage magnitude and the angles from reactive power nodal injections. The latter, resorts to accurate approximations providing a fast and tractable resolution for the power flow equations. In some cases the Newton-Raphson approach is also applied in MV distribution networks for balanced conditions.

LV distribution networks present the several challenges for the PF resolution. The fact that they are radially (i.e. no loops) or weakly meshed operated along with the high branch ratio R/X, clearly reduces the diagonal dominance of the Jacobian matrix. Furthermore, LV distribution grids are characterized by the multi-phase power flow and the unbalanced operation due to the single-phase load and DER. The above features formulate ill-conditioned systems of the non-linear power flow equation that do not allow the application of conventional methodologies (GS, N-R, FDLF). In the literature, these challenges are treated either by applying modifications and advancements of the conventional methodologies; for further reading on N-R extensions proposed research work are (Zhang and Cheng, 1997; da Costa et al., 1999; Abdelaziz et al., 2012). Accordingly, on the decoupling formulation of PQ powers are explored in (Vieira et al., 2004; Sun et al., 2011). For all such methodologies it is essential to make use of the proper choice regarding the coordinates either for the complex power flows or for current injections. Alternatively, Backward-Forward Sweep (BFS) algorithms are well-known and extensively discussed in the literature for the straight-forward formulation and resolution properties(Ciric et al., 2003). BFS methods generally lie on the fact that LV distribution network are radial. The core process is structured in two computational steps the backward (i.e. for current calculation) and forward (i.e. for nodal voltages) sweeps,accordingly.

2.4.2 On the non-convexity and non-linearity of power flow equations

The analytical injected power flow from a bus i may be assessed by Eq. (2.18).

$$\boxed{\begin{aligned} P_i^{\phi} &= \left|V_i^{\phi}\right| \cdot \sum_{k=1}^{3} \sum_{m=1}^{N} \left|V_k^{m}\right| \left[G_{ik}^{pm} \cdot \cos(\theta_{ik}^{pm}) + B_{ik}^{pm} \cdot \sin(\theta_{ik}^{pm})\right] \\ Q_i^{\phi} &= \left|V_i^{\phi}\right| \cdot \sum_{k=1}^{3} \sum_{m=1}^{N} \left|V_k^{m}\right| \left[G_{ik}^{pm} \cdot \sin(\theta_{ik}^{pm}) - B_{ik}^{pm} \cdot \cos(\theta_{ik}^{pm})\right] \end{aligned}} \tag{2.18}$$

where

P_i^{ϕ}	Injected active power in bus i, phase ϕ (W)
V_i^{ϕ}	Voltage magnitude at bus i, phase ϕ (V)
G_{ik}^{pm}	Conductance 3n×3n matrix (S)
θ_{ik}^{pm}	Voltage angle difference between bus i and k, phase ϕ (°)
B_{ik}^{pm}	Susceptance 3n×3n matrix (S)
Q_i^{ϕ}	Injected reactive power in bus i, phase ϕ (var)

To exemplify the non-linearity and non-convexity of power flow formulation, a 2-bus segment of a grid is hereby used as in Figure 2.3. Note that node 1 is considered as a stiff bus with complex

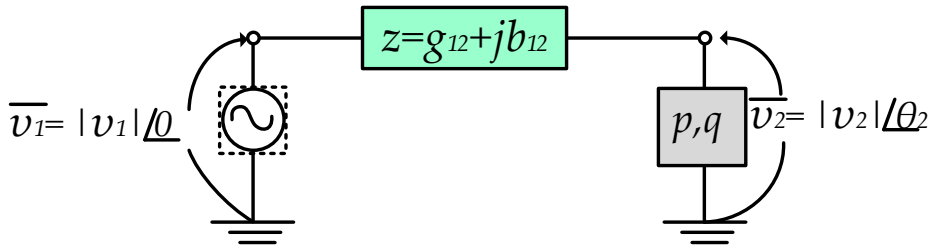

Figure 2.3: Representation of a two-bus segment of grid with variable p,q load consumption. The $\overline{\upsilon_1}$ represents the complex voltage at the considered as firm bus 1, while $\overline{\upsilon_2}$ the one at the load node 2.

voltage $\upsilon_1 = 1\angle 0$p.u. fed by an ideal voltage source. The branch ratio of line $1-2$ is 3.89, indicating the dominance of resistive nature of the conductor. Figure 2.4 illustrates the manifolds among state vectors in relation with the varied p_2, q_2 powers. Additionally, the tangent plane (i.e. this can be used as point of linearizing the PF) at each time is illustrated in all manifolds at point $[\upsilon_2, \theta_2] = [1, 0]$. It should be noted that in this representation the coupling with other phases is not explicitly regarded, since the resolution considers only the single phase power flows –for simplicity–. As it is observed by the group of manifolds it is hard to obtain the exact AC solution. However, towards the formulation of optimization problems such as OPF, it is beneficial to project the exact AC-PF manifolds onto a convex hull, rendering tractable, practical and fast resolutions (Li and Vittal).

2.4.3 Implemented unbalanced power flow algorithm

A three-phase Power Flow (PF) was implemented on MATLAB framework along with DER and grid models as described in Section 2.2–2.3. The PF tool is also incorporated in the overall proposed scheme in 2.5.3, as an algorithmic step, either for the calculation of the initial point of the optimization, or to validate of the set-points yielded by the control scheme. The typical Backward-Forward Sweep (BFS) technique is briefly presented in pseudo-code in algorithm 1. The three-phase power is based on a Backward-Forward Sweep (BFS) technique, where, in the Backward stage, the branch current calculations occur, whilst, in the Forward Sweep stage, the nodal voltage is calculated. This method, unlikely for classical power flow methods, copes with a branch-oriented technique rather than nodal relations.

Note that this power flow algorithm presents quick convergence, i.e., iterations do not exceed 4 for tolerance convergence $\varepsilon_\tau = 1e-4$. The performance can be further accelerated by the valid assertion that the angle displacement in LV distribution networks between adjacent nodes is fairly small (Fortenbacher et al.), i.e., $\Delta\theta$ leads to zero which leads to the conception in Equation (2.19) for the voltage drop:

$$\Delta V_{abc}^{(\kappa+1)} = Re\{Z_\ell \cdot J_{abc}^{(\kappa)}\}, \tag{2.19}$$

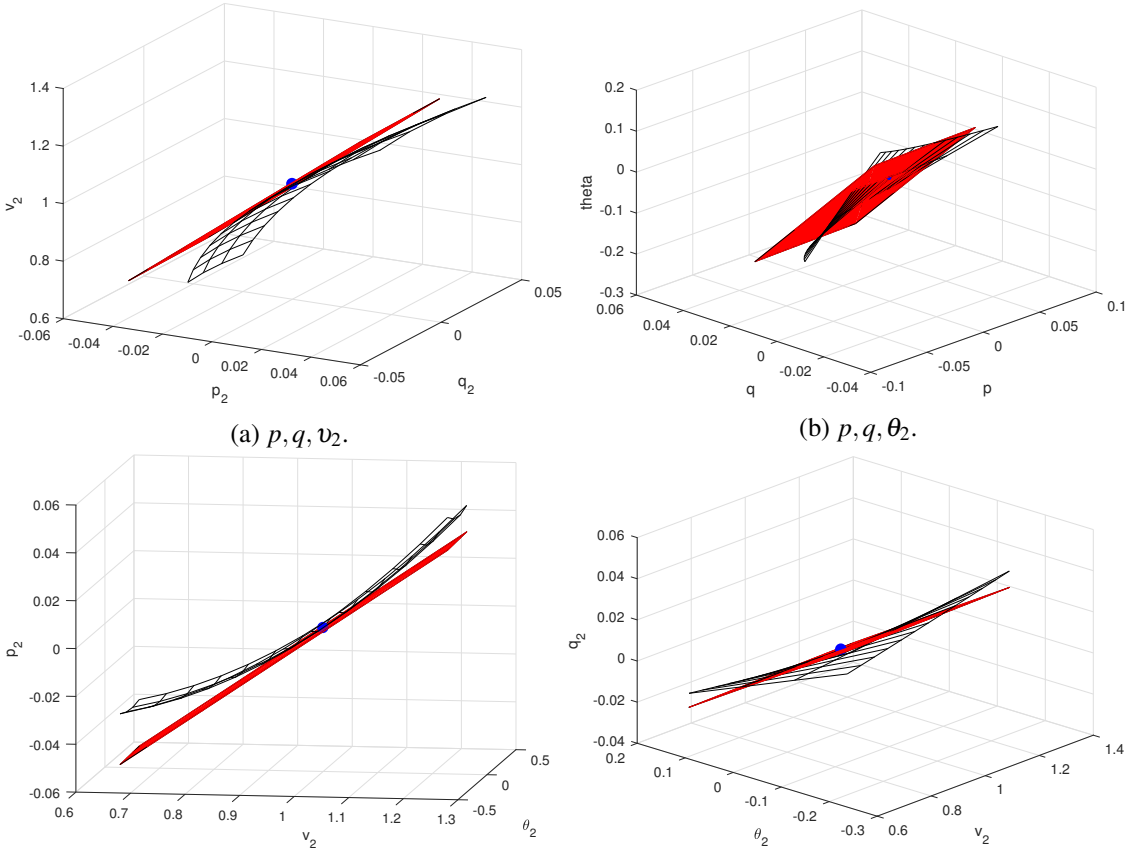

(a) p, q, υ_2.

(b) p, q, θ_2.

(c) p, υ_2, θ_2.

(d) q, θ_2, υ_2.

Figure 2.4: Simulation with 2-generic buses with branch ratio r/x=3.5/0.9. The manifolds of state vectors appear for different load variations, capturing the non-linearity and non-convexity of power flows. v_2, θ_2, p_2, q_2 stand for the voltage magnitude, the voltage angle, the active and reactive power at node 2.

where Z_ℓ is the corresponding impedance among the connected branches and $J_{abc}^{(\kappa)}$ is the vector for the line section currents at iteration κ. Regarding the power flow framework, it is hereby structured in such a way that each load might have a different load model among constant PQ and a constant I or constant Z model. Accordingly, the injection current at node j is given by Equation (2.20):

$$I_{abc}^{j} = (S_{abc} \cdot diag^{-1}(V_{L-L}))^{*} \left\| \frac{V_j}{V} \right\|^{\kappa}, \tag{2.20}$$

where S_{abc} stands for the apparent power consumed at node j, V_{L-L} the line-to-line voltage. The operator $diag(.)$ is settled as an operator that returns a diagonal vector and κ is considered the load model parameter, which is 0 for constant PQ load, 1 for constant current and 2 in case of constant impedance.

Algorithm 1: BFS description, merely based on (Shirmohammadi et al., 1988)

procedure LOAD FEEDER
  Rank nodes, *Node-Order* procedure: Sort m^j
procedure BFS
  initialize $k \leftarrow 1$,
  $V_{j,a}^{(k-1)} = 1\angle 0$, $V_{j,b}^{(k-1)} = 1\angle\frac{2\pi}{3}$, $V_{j,c}^{(k-1)} = 1\angle\frac{-2\pi}{3}$
  do
  Node j Injections : $I_{j,n} = -\sum_{\phi\in\Phi}\left[y_{j,nn}I_{j,\phi}\right]$,
  $I_{j,abc}^{(k)} = \left(\frac{S_{j,abc}}{V_{j,abc}}\right)^{(k-1)^*} - \text{diag}(Y_{j,abc}^{\text{shunt}})\cdot V_{j,abc}^{(k-1)}$
  Backward Sweep- Current Calculation:
  $J_{abc,n}^{(k)} = -I_{j,abcn}^{(k)} + \sum_{m\in M} J_{m_{abc}^j}^{(k)}$
  Forward Sweep Calculation:
  $V_{abc,n}^{(k+1)} = V_{abc,n}^{(k)} - [Z_\ell]\cdot J_{abc,n}^{(k)}$
  $k \leftarrow k+1$
  while max $\left(|V_j^{(k)}| - |V_j^{(k-1)}|\right) \geq \varepsilon_t$
  return $J_{j,abcn}, V_{j,abcn}, j \in \mathcal{N}$

2.4.4 Validation of unbalanced power flow with OpenDSS

The accuracy of the developed BFS-PF algorithm is validated in this section, based on comparison results with OpenDSS environment. OpenDSS is a software-tool that provides analytical modeling of distribution networks and any power delivery equipments, by constructing the explicit $Y-$primitive nodal admittance matrix for each electrical object. Each primitive matrix is then merged into the system's Y-matrix (Dugan, 2016). OpenDSS was, initially, developed to perform harmonic analysis studies; despite, the thorough circuit models that allows multi-phase models makes it reliable for unbalanced PF analysis. In this section, we aim to compare not only the PF developed algorithm but also the implemented models for all the models (transformer –with connection to MV side–, distribution lines and DER).

In Figure 2.5, the fast convergence of BFS-PF (implemented in MATLAB) is presented for the unbalanced case study. It can be observed that for $\varepsilon_t = 1e-4$ (i.e. determined tolerance of algorithm) the maximum number of iterations is four. The assertion of negligible voltage angle displacements between adjacent nodes leads to the accelerated version of the BFS algorithm where two iteration are enough to reach convergence.

The comparative results among OpenDSS and the deployed BFS algorithm are in Figure 2.6, including the different snapshots within a day to capture the accuracy at sunny periods (i.e. when μG is essentially active).The maximum error on absolute voltage magnitudes recorded including simulations with different loading conditions is $\approx 0.15\%$.

2.5 Unbalanced three-phase Optimal Power Flow (OPF)

Power system requires special tool to optimally analyze, monitor and control its planning and operation stages. Most of these tools are different types of optimization formulations. The Optimal

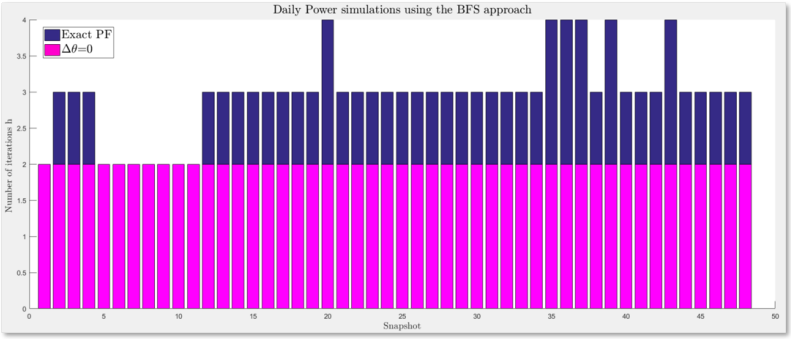

Figure 2.5: Backward-forward sweep unbalanced power flow iterations of convergence for a daily simulation.

Power Flow (OPF) applications are considered to be the backbone of such formulations, that has been thoroughly investigated since the ealy 1960's (Abraham and Das, 2010). OPF algorithms are formulated to optimize power system's operation related subject to physical constraints and technical constraints. OPF problems, are generally a large class of nonlinear, non-convex large-scale optimization problems integrated into DMS applications. For the whole thesis, OPF is considered as any optimization framework that is subjected to the equality constraints of power flow equation (i.e. either the exact formulation of AC or any approximation). This is clarified to segregate OPF from the conventional economic dispatch problem, where power balance poses the sufficient constraint for the operation of the grid.

2.5.1 A review on OPFs

There are several parameters to create a taxonomy on OPFs, such as optimizing term(s), the optimization method it is being handled and the subsequent search algorithms, the type of technical and operational constraints and their nature (e.g. integer, non-linear, linear) as well as the manner PF equations are posed (i.e. exact or approximative). For extensive review and taxonomies on the literature of OPFs one can follow (Momoh et al., 1999; Capitanescu et al., 2011; Frank et al., 2012; Castillo and O'Neill, 2013). A most recent review paper that captures the latest advancements is in (Capitanescu, 2016).

Based on the uncertainty (e.g. forecasts of power and generation profiles) and the likelihood of contingencies occurrence, OPF schemes may be classified as:

- *Deterministic OPF*: OPF is commonly used by utilities for day-ahead operational planning, aim at optimizing e.g. operation costs, ensuring, concurrently, the safe operation (expressed as a group of postulated contingencies) (Lopes et al., 2007). In such cases, control actions, derived from OPF, may be either the preventive security of the system (pre-contigency) or preventive-corrective.
- *Risk-based OPF*: those OPF approaches stem from the fact that deterministic OPF security may suggest actions with unnecessarily high costs as a result of ensuring security for low likely contingencies with possibly low severity impact.

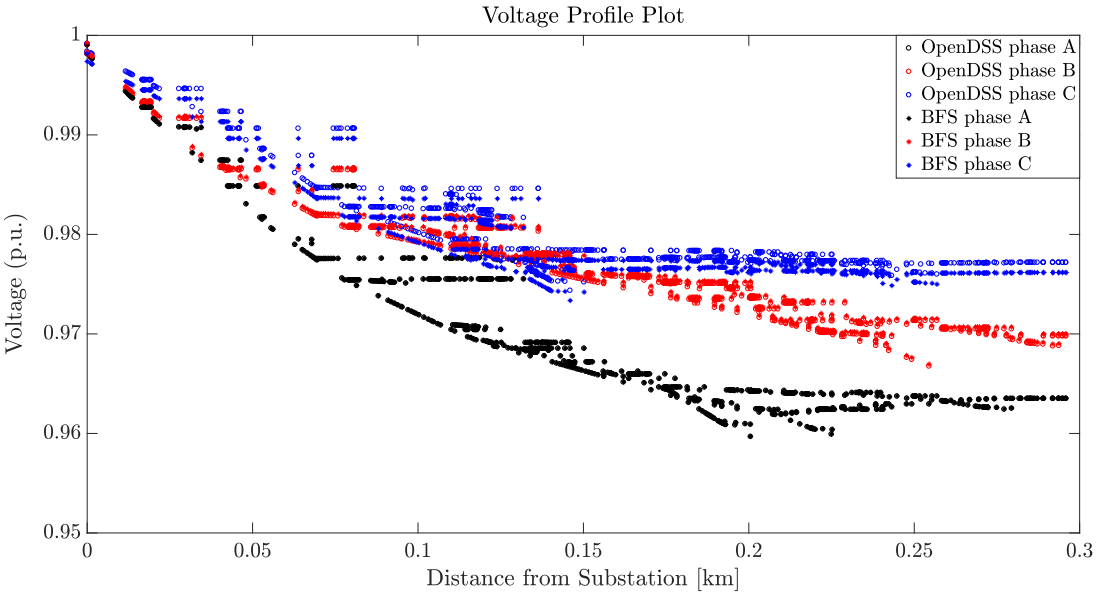

(a) Resolution at $\tau = 18.30$.

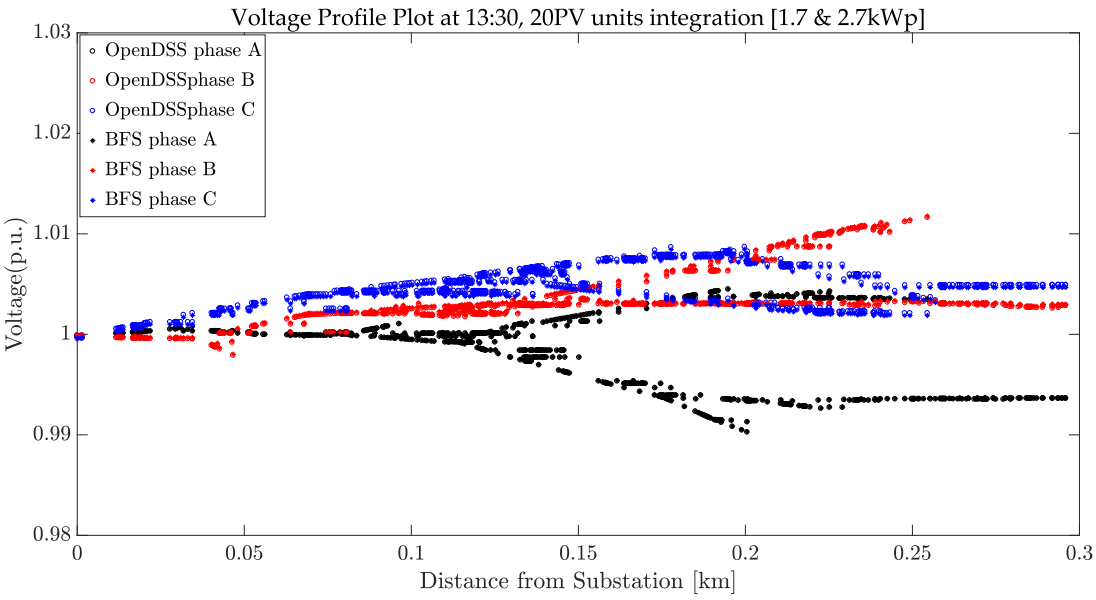

(b) Resolution at $\tau = 13.30$.

Figure 2.6: Resulting voltage profile from unbalanced PF of OpenDSS and the one developed based on BFS notions. The simulated scenario considers 20PVs randomly distributed along end-users.

- *OPF under uncertainty*: this last category emerged from the increasing integration of intermittent renewable generation and the transition to smarter grids, where advantageous flexibility may be enchained by deferrable loads and storage devices among others (Capitanescu, 2016). The two main methods to approach such problems are the chance-constrained and robust optimization.

In this section and generally in this thesis, the focus remains in the deterministic AC-OPF formulations, where further details of the complete proposed operational scheme (operational plan-

ning, corrective actions and real-time operation) are provided in Chapter 4. In this work there is particular focus to address AC OPF in a deterministic manner; the high stochasticity of DER and possible load and generation forecast errors, particularly in LV distribution networks generally arises the need for corrective actions closer to the time of the delivery. However, OPF under uncertainty is capable to limit the constraint violation probability, yet operational costs may be doubly increased according to (Karagiannopoulos et al., c). Therefore, the OPF review continues focusing on the deterministic formulation of the problem.

The generalized formulation of AC-OPF gets hard to be solved due to the non-linear and non-convex properties of power flow equations. In practice, OPF applications derive controls for continuous decision variables such as active or reactive power control set-points for generators or DER, or voltages along the terminal of Series Voltage Regulators (SVR) as well as for discrete controls (e.g. tap-positions of OLTCs, capacitor-banks operation point, EVs' charging decision *etc*). This continuous and discrete control decisions leads in real-life to large-scale non-convex Mixed Integer Non-Linear Programming (MINLP). According to (Sun et al., 2011), current limitations (to be easily deployed in real-life) on state-of-the-art MINLP large scale solvers encourage researchers to explore OPF continuous relaxations towards non-convex Non-Linear Programming (NLP) formulations, by disregarding discrete variables. It should be noted that typical real-life OPF are far too complicated for their resolution, particularly due to the numerous constraints and a range of burdensome solution-seeking and modeling peculiarities, further discussed in (Stott and Alsaç).

In Figure 2.7, a taxonomy and classification is illustrated for different methods to address OPF applications. There are further criteria such as the selection of coordinates for the expression of PF equations or the objective terms; yet, such finer grained criteria are presented in later chapters for the implementation of control and energy management schemes into the frame of smart grids.

2.5.1.1 Convex-relaxation of AC-OPF

As a first-order criteria for the structuring of OPF applications is regarded whether PF equation will formed in their exact AC form or approached through a convex relaxation. One cannot guarantee the global optimality of OPF using a local method due to the non-convexity of PF equations. Nonetheless, convex relaxations may be applied to approach PF equations as characteristically proposed in (Molzahn and Hiskens; Low, 2014). The basic idea of convex relaxation lies on expressing complex voltage with rectangular coordinates, resorting to a quadratic optimization problem; the real and imaginary part of the nodal voltages are both stated as decision variables. This quadratic structure leads to a non-convex feasible space due to the complex voltages. It is commonly discussed in convex relaxation approaches, that voltage variables are expressed by a matrix W converting the problem to a linear form, such that $rank(W) = 1$ and is a semi-definite positive matrix. Presuming that the objective function and any constraints are posed by convex functions, the non-convexity hereby stems entirely from the rank constraint. The most commonly applied relaxation is the Semi-Definite Programming (SDP) that suggests the relaxation of the

rank constraint of W matrix, in the sense that W is also semi-definitive positive. The Second-Orden Cone Programming (SOCP) is another well-known relaxation which proposes the algebraic reformulation of the constraints such that they line in the second-order cone.

Without the loss of generality, convex relaxations may be exact (i.e. the duality gap is zero) meaning that one can assure that solution obtained for the applied relaxation of the problem is globally optimal solution of the –initial– non-convex. For OPF relaxation problems exactness is generally claimed to be satisfied in radial topology networks; yet, only in particular conditions where there is no reversed power according to (Low, 2014). Additionally, as discussed in (Capitanescu, 2016), there are several cases that the global solution cannot be recovered from the convex relaxation due to the non-zero duality gap. The recent advancements and reviews on convexifications discuss that there is a trade-off which has to be addressed between computational effort and convergence's precision (Castillo et al., 2015). It should be also stressed that convex relaxations are of significant importance for the initial NLP problems, since they may provide a lower bound that can be used to interpret the sub-optimality of the local optimizer solution (iff the convex relaxation is tight and accurate). Additionally, the relaxation can provide a certificate of problem infeasibility (Capitanescu and Wehenkel, 2013). To sum up, further computational complexity can be certainly added to the OPF formulation if it is settled for multiple periods leading to multi-period OPF, but this topic will be further explored in Chapter 3.

2.5.1.2 Local AC-OPF methods

The majority of methods addressing NLP constrained are converted to unconstrained optimization problems. Therefore, a brief discussion follows to outline the basic concepts. The classification of local methods based on the two criteria implies the combination among them leading to six possible ways of OPF resolution, as proposed in (Sperstad and Marthinsen, 2016). For instance, based on the manner that PF equations are regarded into the OPF problem, they can be performed in each inner iteration of the optimization. Contrarily, power flows may be resolved explicitly by assessing them for Karush-Kuhn-Tucker (KKT)-optimality. This is done by posing them as a group of equality constraints, which includes them (in the unconstrained formulation) in the Lagrangian function.

The classification of handling the constraints (Figure 2.7) refers particularly for the inequality constraints. The gradient methods propose implicit ways to address inequalities, typically by using heuristics to restrain the next step and ensure that is kept into the feasible space of the problem. The active set methods generally belong to constrained optimization. The majority of optimizers for constrained nonlinear problems that are based on Sequential Linear Programming (SLP) or Sequential Quadratic Programming (SQP), can be regarded as active set algorithms. This is due to the active set of inequality constraints that are handled in the solution of LP or QP subproblems in these methods (Sperstad and Marthinsen, 2016). The identification of active inequality constraints for the optimal solution still remains to be the main weakness of active set methods (Capitanescu et al., 2007). Interior-point (IP) methods or barrier methods are well-known for converting the initial constrained to an unconstrained problem through the augmented

Lagrangian. The Lagrangian contains the a barrier or penalty term to force the decision variables to remain in the interior of the feasible space. The application of IP method on OPF essentially takes place via the resolution KKT equations rather than minimizing the augmented objective function, fact which is further discussed in Chapter 3. The typical formulation of IP methods is commonly referred to primal-dual IP method (PDIPM), where search steps are conducted in the combined space of primal and dual variables while solving the KKT system.

Gradient based methods are superseded by more modern OPF methods. Similarly, Newton-based methods for direct minimization are also superseded apart from cases used for the local solver in more advanced methods. Both active-set methods (based on sequential approximation algorithms, i.e. SLP or SQP) and interior-point methods appear to be more widely deployed both in OPF software tools (Sperstad and Marthinsen, 2016).

2.5.1.3 Global AC-OPF methods

In the previous sections, the local-OPF schemes were briefly described; a complementary category, the so-called global OPF, which in certain conditions converges to the global optimal solution of the exact AC-OPF problem. There are broad algorithms (see Figure 2.7) based on heuristics and meta-heuristics, that target to converge into global optimum rather getting trapped into a local minima. Heuristic methods mainly combine a local search algorithm (e.g. gradient, newton-based, sequential approximation) with random search followed by a heuristic to avoid local optimums.

2.5.2 State-of-the art solvers for exact local OPF

Several utilities already make use of OPF schemes that are based on Sequential Linear Programming (SLP), Sequential Quadratic Programming (SQP) or Newton method, IP optimizers that resort to practically fast resolutions by using high performance computing techniques. As per the academic works discussed in previous sections, those methods have generally reached maturity and are capable enough to solve large instances (Capitanescu, 2016). There are several state-of-the-art general purpose power solvers that can be used as core-engine for solving the NLP form of OPF with KNITRO(Nocedal, 2006) or IPOPT(Biegler and Zavala, 2009). Despite the fact that those local OPF NLP solvers (both general-purpose but also those tailored particularly for OPF resolution) are generally fast enough, they may fail to converge for highly constrained problems (Capitanescu and Wehenkel, 2013). Further conclusions on commercial OPF applications generally resemble the conclusions of academic papers reviewing the state of the art of OPF methods.

2.5.3 Implemented unbalanced OPF algorithm for the operation of LV grid

In this section, the analytical (i.e. exact PF equations) single-period unbalanced AC-OPF is formulated and used as the tool to provide decisions for the operation of LV grid in a centralized manner.

In Figure 2.8, the 3-phase unbalanced OPF scheme is described, which consists of providing an adequate initial point provided by an accelerated (i.e. $\Delta\theta = 0$) BFS-PF performance. If for any

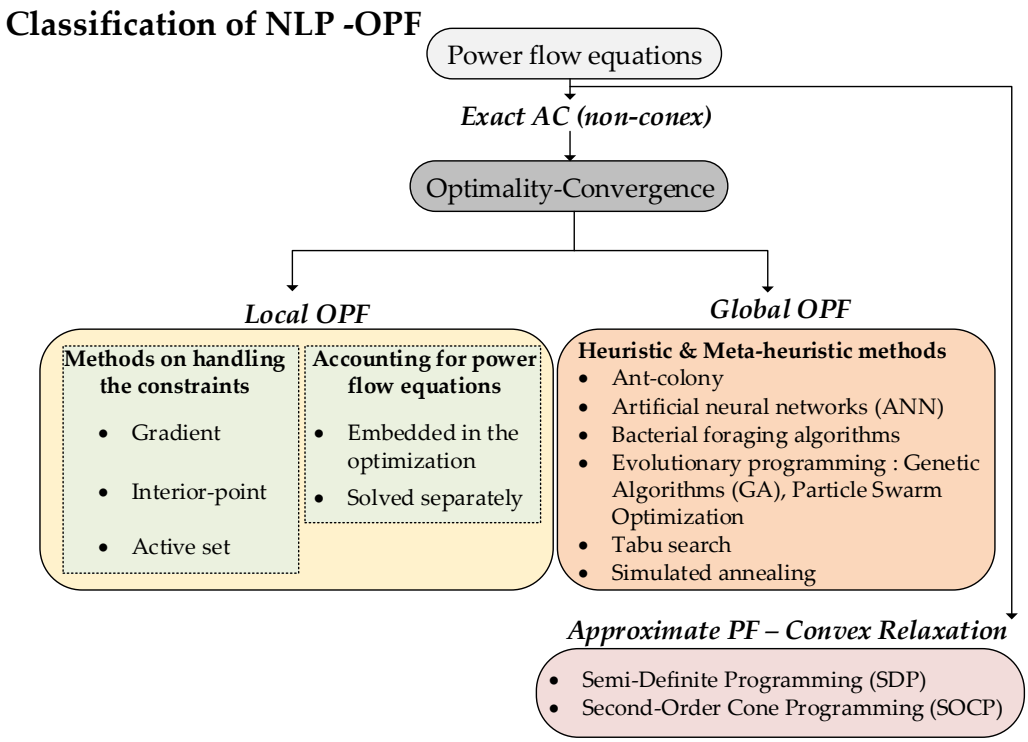

Figure 2.7: A classification of OPF formulations; first-order criterion the formulation of power flow equations; second-order criterion the optimizer's goal; lastly local OPF are further distinguished in the way that constraint are handled and the whether power flows are integrated into the optimizer or resolved in an outer iterative process.

reason there is no convergence of the BFS, as initial input is regarded 1p.u. voltage magnitude and $[0, 2\pi/3, -2\pi/3]$, or initial points from previous occurrences. The objective function aims to minimize the operating costs assigned with all the controllable assets providing their coordination according to their availability at each time. The vector $[x]$ expresses the state vector of the grid (i.e. voltage magnitude and angle -not critical for LV network-). The set of controllable assets $\mathscr{U} := \{1, \ldots, n_c\}$, described by the control vector u, comprised by active and reactive power set points. Therefore, AC-OPF problem is posed by 2.21:

$$\min_u C_{obj}(x_t, u_t) = \min_u \sum_j^{n_b} \left(c_{n_c}^T \cdot u_j\right) \tag{2.21}$$

subjected to

$$F_j(x,u) = 0 \qquad \forall j \in \mathscr{N} \tag{2.22a}$$

$$h_i(x,u) \leq 0 \qquad \forall i \in \mathscr{J} \tag{2.22b}$$

$$V_{\min} \leq V_{j,\phi}(x,i) \leq V_{\max} \qquad \forall i, \phi \in \mathscr{N}, \Phi \tag{2.22c}$$

$$h_\xi(x,u) \leq 0 \qquad \forall \xi \in \mathscr{U} \tag{2.22d}$$

$$g_\xi(x,u) \leq 0 \qquad \forall \xi \in \mathscr{U} \tag{2.22e}$$

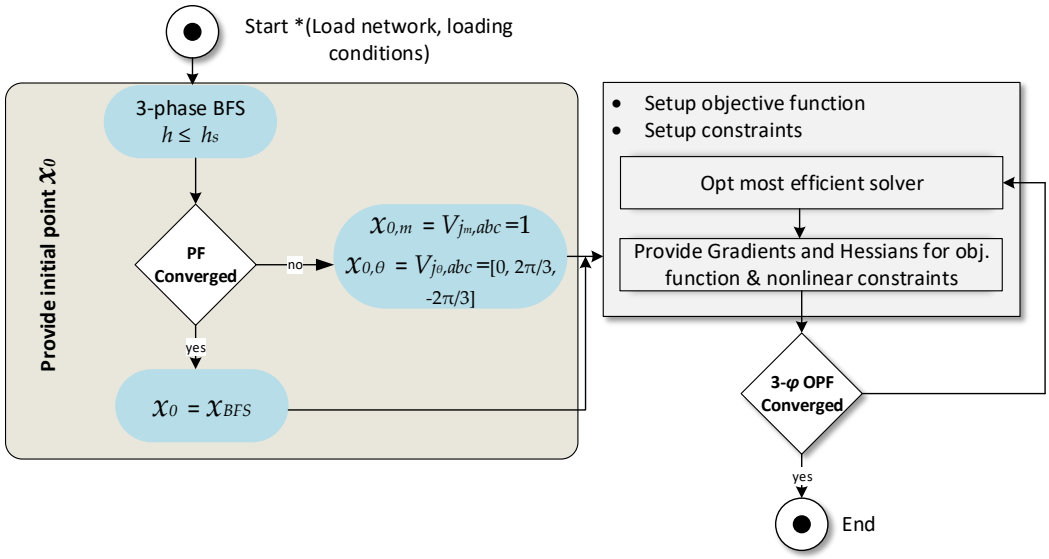

Figure 2.8: Unbalanced optimal power flow solver algorithm.

where the constraints in (2.22a) set the power balances at each bus of the network; the inequality constraint (2.22b) poses the nonlinear constraint for the constrained lines; the constraint in ((2.22c)) to respect all nodal voltages to range strictly within the admissible bounds. The constraints (2.22d)-(2.22e), correspond to the operational limits of the controllable DER. Such equations where analytically discussed in Section 2.3. The formed problem is solved using the following solvers *fmincon* by MATLAB, *MIPS* (Zimmerman and Wang, 2016) and *IPOPT* (Biegler and Zavala, 2009). All solvers present similar performance for the particular case study which is comprised of 141 nodes. The unbalanced modeling leads to $[(3 \cdot 141) \times (3 \cdot 141)]\mathbf{Y}-$ matrix. Based on whether the first and second order gradients of the non-linear constraints can be provided to the optimization solver, the algorithm selects the most efficient optimizer to acquire a solution. If the gradients are not explicitly input, approximative finite-differencing may be used, obtaining slower resolutions. The calculations of the derivatives is analytically presented in the Appendix A.2. In Figure 2.9, the algorithmic steps of the centralized sequential scheme to operate the LV grid. As inputs forecasts of load profiles and generation of μG are used to asses future grid states and identify possible constraint violation. If such inputs are missing or is erroneous the local controller with the complementary local databased (including historical information) tries to reconstruct it as proposed in (Kotsalos et al., a). For each forthcoming $(h+1)$ resolution of the OPF scheme, the previous decision variables of $h-$resolution are exploited as initial point for the faster convergence. Note that local OPF methods are impacted by a satisfying initial point not only in the time of convergence but for quality of the solution.

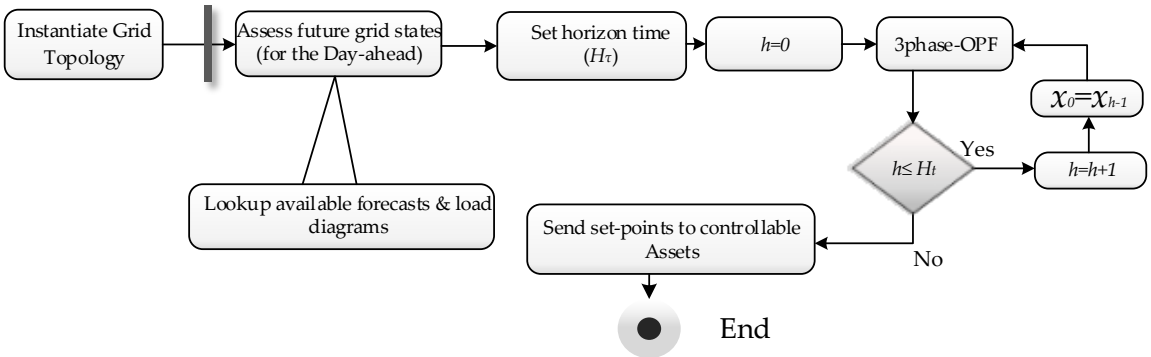

Figure 2.9: Sequential centralized scheme for the operation of LV distribution network.

2.6 Case Study: A centralized OPF scheme versus local scheme for the operation of LV grids

The presented case study compares the previously defined scheme (Section 2.5.3) with local droop controls applied on the μG, that is published in (Kotsalos et al., b). Several different case scenarios (defined in Table 2.1) are considered in this section to identify possible technical bottlenecks due to the integration of PV installations and EVs, both owned by residential users. The phase of connection of loads follow the benchmark IEEE grid (see more details in Appendix A.1), while the PVs and EVs are installed in the same phase of the corresponding customer. Note that both PVs and EVs –and their technical characteristics–, are randomly distributed along the end-users. More information regarding the grid and point of connection of PVs and EVs can be found in Appendix A.1, where the list of the first 20 PV/EV units correspond to each scenario.

In all scenarios, a three-phase centralized BESS is assumed to be connected at node 101 (Figure 4.11). The BESS capacity is 90 kWh and the maximum charging and discharging rate is 45 kW. This BESS is assumed to have an initial SoC of 0.40 with $\underline{SoC} = 0.1$ and, at the end of the optimization horizon, it has to be equal to the initial, $SoC_{H\tau} = 0.40$. The power factor of BESS_{101} is considered as unitary for all the simulated cases and its charging and discharging efficiency is η_{ch}, η_{dch} =0.95, (Palizban and Kauhaniemi, 2016). The simulation day corresponds to a representative summer week day where typically peak loading conditions occur, where the load and generation profiles are illustrated in Figures 2.10a–2.10b, accordingly.

Table 2.1: Definition of scenarios.

Scenario	Number of PV units	Number of EVs
c1	0	0
c2	20	0
c3	0	20
c4	20	20

Table 2.2: Results on scenarios c1–c4 among no controls, local based control and the proposed centralized scheme based on OPF.

Applied Strategy	DER Scenario	min (Vphase)[p.u]	max (Vphase)	Emergy Curtailed [kWh]	Reactive Energy [kVAh]	Voltage Unbalances [%]
No controls	**c1**	0.965	1	-	-	1.41
	c2	0.958	1.059	-	-	1.95
	c3	0.941	1	-	-	1.72
	c4	0.942	1.054	-	-	1.98
Local Controls (droop based rules)	**c2**	0.958	1.05	1.4	17.3	1.84
	c4	0.942	1.049	0	14.1	1.87
Local Controls cos ϕ=0.9	**c2**	0.958	1.05	0	80.5	1,65
	c4	0.942	1.049	0	80.5	1,71
Centralized scheme (OPF-based)	**c2**	0.951	1.049	0.9	9	1.82
	c3	0.95	1.029	0	6	1.92
	c4	0.952	1.019	0	4	1.9

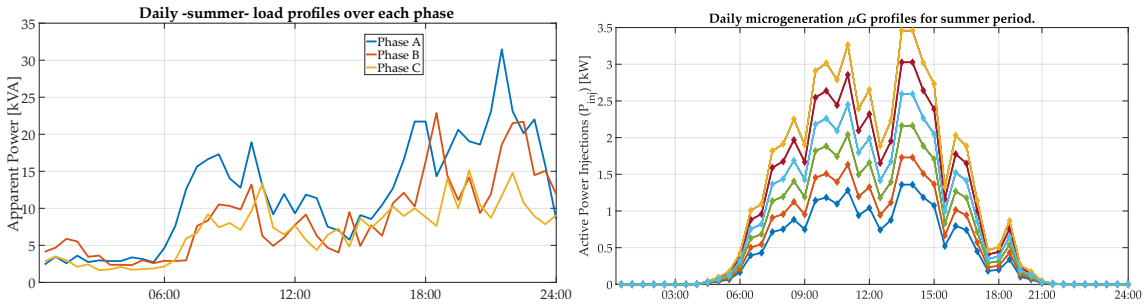

(a) (b)

Figure 2.10: Data profiles: **(a)** load profiles; and **(b)** micro-generation profiles using seasonal (e.g., summer profiles) and regional data.

In Table 2.2, the results are collectively given, for the maximum and minimum voltage magnitudes, the maximum Voltage Unbalance Factor (VUF[%]) (i.e. the ratio of the negative to the positive sequence component), the total curtailed energy and the dispatched reactive energy along the daily analysis. According to the standards of EN50160, under normal operation conditions, at all nodes should kept below 2% for 95% of the week. The nodal voltages, should be limited within +10%, -15% for a 10min mean rms value. Therefore, for the proposed scheme any input data (and the control outputs) used correspond averaged 30min resolution, the voltage limits are set in [0.95, 1.05] p.u.values. All scenarios (c1)-(c4) are initially examined without any controls, where it is obvious that the c1 scenario –without DER integration– does not appear any technical issues neither on the voltage magnitudes nor in the voltage unbalances which is limited to 1.41%.

Two local strategies are considered one with droop based controls (active and reactive power control, prioritizing the reactive dispatch) to prevent overvoltages, and one that foresees constant

power factor set to 0.9. In both scenarios c2 and c4, the local controls mitigate overvoltages by consuming reactive power at the site of μG's inverter combined in some cases with some active power curtailment. It can be observed from Table 2.2, that local droop controls provide a more efficient control scheme compared to constant power factor due to the reduced use of reactive power. The latter can be an important remark for the operation of distribution network, where the overuse of reactive power compensation may lead to increased network power losses. The installation of μG brings an increase on phase unbalances up to 1.95%. Note that for the same PV integration but in higher-grained resolution (e.g. 10-minutes) voltage magnitudes and phase unbalances may be more aggravating.

The centralized scheme (for scenario c2) is able to address the overvoltages by deriving the optimal active energy curtailment and reactive energy consumption 0.9kWh and 9kVAh accordingly, compared to 80.5kVAh when constant power factor considered, or 1.4kWh curtailed energy and 17.3 KVah reactive power consumption for the droop based rules. As a result, for scenario c2 the centralized schemes performs 35% less PV curtailment and 48% reactive energy usage than in the local droop case. In c4 the fact that some EVs occur to charge during sunny periods (10:00-16:00) results to less intensive overvoltages only 4 kVAh for the centralized scheme while the local Q-V control in total 14.1KVAh (72% reduction using the centralized scheme). The voltage drops occur at the peak periods due to the integration of EV that most likely charge at late hours as explained in section 2.3.3. The EVs are most likely considered to be available for smart charging when parked at the house premises. Therefore, in the centralized OPF scheme certain decision can be made to coordinate the charging slots and avoid the voltage drops, lower than 0.95p.u. –which is the settled lower voltage bound in this study–. Nonetheless, the expression of EV flexibility cannot be formulated successfully for single period OPF due to the daily energy fulfillment which has to be expressed with inter-temporal constraints. Furthermore, the flexibility of BESS and CL has to follow the same notions to optimally manage their flexibility. For instance, the application of phase balancing constraints on an operational optimization scheme may be addressed by redistributing the load demand (i.e. flexible EVs, CLs) along different slots possibly when excessive injection occurs by PV integration.

The centralized scheme can be deployed only by the subsequent communication technologies, together with forecasting data, power flow-state estimation tools. The incorporation of further assets, as well as multi-period extension will be described in Chapter 3.

2.7 Final remarks

There is an increasing integration of green energy technologies and generally DERs in the distribution networks. However, a considerable amount of energy produced by μG may need to be curtailed or self-consumed due to technical constraints in the network. DER such as BESS, EVs and CLs may be optimally used to decrease curtailments and other grid constraints (i.e. mainly lines congestion and phase unbalances) and consequently improve the operation of the grid, by delivering, also, profits to them. However, such DER types introduce dynamic terms (expressed

by inter-temporal constraints) into the problem of OPF resembling to scheduling frameworks. Other considerations is that both active and reactive power contribution DER with flexible operation strategies may be enabled, as well as concerns on maximizing the lifetime of batteries (i.e. for BESS and EVs) further increases the complexity of OPF problem. Furthermore, the stochastic and intermittent behavior of DER brings novel challanges in operation and planning stages of distribution networks. Hence, DSOs have to harmonize the operational strategies correspondingly. Advanced functionalities and management strategies could be based on near to 'real-time' optimization aiming at determining the coordination of several DSO's asset and DER technologies ensuring safe grid operation. ADMS applications need to be equipped with -close to- real-time multi-period active-reactive OPF problem to ensure tractable optimality and feasibility for distribution network's operation.

As analyzed in this chapter the explicit modeling of the LV distribution network may be of significant importance particularly for phase balancing constraints which in turn have direct impact to the network losses. The on-going integration of residential EV charging points in addition to single-phase μG will spur the effort for the deployment of advanced monitoring and observability functionalities which are key drivers for the optimal active management of DER.

Chapter 3

Towards unbalanced multi-period AC-OPF

In recent years, the installation of residential Distributed Energy Resources (DER) which produce (mainly rooftop photovoltaics usually bundled with battery system) or consume (electric heat pumps, controllable loads, electric vehicles) electric power, is continuously increasing in Low Voltage (LV) distribution networks. Several technical challenges may arise through the massive integration of DER, which have to be addressed by the distribution grid operator. Yet, DER can provide certain degree of flexibility to the operation of distribution grids, which is generally performed with temporal shifting of energy to be consumed or injected. This chapter proposes a horizon optimization control framework which aims to efficiently schedule hours-ahead the LV network's operation by coordinating multiple DER. The main objectives of the proposed control is to ensure secure LV grid operation in the sense of admissible voltage bounds and rated loading conditions for the secondary transformer. The proposed methodology leans on a multi-period three phase Optimal Power Flow (OPF) addressed as a nonlinear optimization problem. The resulting horizon control scheme is validated within a LV distribution network through multiple case scenarios with high microgeneration and electric vehicle integration providing admissible voltage limits and avoiding unnecessary active power curtailments.

3.1 Introduction

Nowadays, an increasing number of small-scale units, typically referred to Distributed Energy Resources (DER), is connected along the Low Voltage (LV) distribution networks posing several technical challenges, whilst bringing novel and diverse opportunities. Most commonly there is already a large share of injected power at the distribution level by the renewable energy merely based on solar energy through Photovoltaic (PV). The connection of such resources at the LV grid and end-users' premises is foreseen to increase substantially in the close future with small rooftop installation usually coupled with Battery Storage System (BESS), controllable loads (e.g. Electric Water Heaters) and Electric Vehicles (EV). Therefore, it shall be critical to exploit the DER controllability and active participation through demand response schemes in order to support or even optimize the network operation (Eid et al., 2016).

Traditionally, LV networks used to be the most passive circuits within the power systems, since power flows were solely headed from distribution transformers to consumers without the operation of automation elements (Ochoa and Mancarella). In particular, the entire segment from the secondary substation and its downstream connected LV networks is very often not monitored nor controlled (Bruno and La Scala, 2017). Analytical information on the conventional LV operation and on-going operational trends may be found in Chapter 2.

The Distribution System Operators (DSOs) address such technical challenges by increasing the observability and controllability of the grids, envisioning the active management of the DERs for ancillary services, throughout new operation stages Karagiannopoulos et al. (c). Such attributes of advanced control and monitoring techniques do typically refer to Advanced Distribution Management Systems (A-DMS) Bruno et al. (2011). The active management of distribution networks through the engagement of DERs in the operation of the grid is regarded to occur with the provision of flexibilities services such as active and reactive power control (i.e. inverter based control). The smart grid deployment, as an alternative paradigm for the operation of distribution networks, envisions the active management of DER taking advantage of advanced control infrastructures and communications through demand side management schemes. Advanced control methodologies need to be implemented to determine control actions related to controllable DER, that can techno-economically improve distribution networks' operation delivering benefits to residential users.

3.2 Literature review on multi-period OPF

A particular concern in recent research works regards the potential DER flexibility to address grid constraints Costa et al. (b); Olival et al. (2017). In the past years research was focused in active power curtailment following local droop based rules or even combined with reactive control (Tonkoski et al., 2011; Weckx et al., 2014; Demirok et al., 2011). Moreover, self-consumption is commonly imposed by regulation and legislation lately, to address voltage rise effects during the peak period of PV generation. In several European countries residential PV self-consumption

measures based on net metering schemes target at matching the endogenously generated power with local consumption (Heleno et al.). On the contrary, Portugal and Germany promote lower remuneration for energy produced by microgeneration, thus attracting instantaneous consumption. Towards the path to maximize renewable generation into distribution networks, the focus in research remains in controlling the microgeneration itself. A distributed scheme with more sophisticated rules to mitigate overvoltages due to large integration of PVs was proposed in (Olivier et al., 2016b). Besides, real-world LV four-wire distribution networks are in practice fairly unbalanced, since single-phase grid elements (e.g. end-users, micro-generation and EVs) do impact the voltage, not only of the connected phase, but also of the other two phases due to the neutral-point shifting phenomenon (Degroote et al.). Consequently, local droop based controls via single-phase PVs might be insufficient for voltage regulation in unbalanced grids; hence, the deployment of centralized optimization method can deliver optimal and cost-effective solutions (Olivier et al., 2016b; Weckx et al., 2014).

Interest has been also attended for the efficient integration and exploitation of distributed BESS (Miranda et al., 2016; Fortenbacher et al.). Recently, BESS has been introduced by electric utilities to accommodate the increased generated power by solar energy in LV grids. Though the deployment of residential BESSs has been limited up to the previous years, due to the relatively high capital cost of such devices. Lately, the continuous reducing cost of batteries in addition to the rising electricity costs and incentives for investments in storage Hoppmann et al. (2014). According to Directive 2009/72/EC (Union, 2009), the utilization of energy storage systems by grid operators is very limited presently; meanwhile, unbundling requirements for DSOs under EU directives do not allow energy storage units to be directly owned, or controlled by them. Concurrently, the growing number of BESS owned by residential consumers is likely to undermine the current business model of the electric utilities (Efkarpidis et al., 2016a). The latter, aims to maximize the revenue brought to the consumer in particular when home energy management systems are utilized to optimize the local generation and consumption.

Other research works have proposed advanced controlling more DER types such as EV and controllable loads (CL) for the mitigation of overvoltages or line congestions by (Costa et al., b; Olival et al., 2017; Madureira et al., a; Connell et al., 2014; Campos et al.). A centralized control scheme for the voltage regulation and the mitigation of high unbalance instances, is proposed (Efkarpidis et al., 2016b) the efficiency of which is compared with typical local control droops. An extension of the same authors provide a framework for the coordination of an On Load Tap Changer (OLTC), installed at the secondary substation, with BESS and controllable microgeneration (Efkarpidis et al., 2016a).

Optimal Power Flow (OPF) is widely applied as a tool within DMS application for the planning and operation of the power systems. Clearly, OPF problems are deemed challenging since they require solving of non-convex problems. Nonconvexity stems from the nonlinear relationship between voltages and the complex powers consumed or injected at each node (Sperstad and Marthinsen, 2016). Further adaptations and assertions have to regarded for power flow equations in particular for LV grids as they present purely unbalanced loading conditions and mainly re-

sistive line characteristics. The widely used DC power flow methodologies in transmission grid studies, but cannot be applied due to the higher R/X ratios (Sereeter et al., 2017). The application of non-convex and non-linear AC power flows in an OPF framework, possibly leads to computationally complex according to (Karagiannopoulos et al., a). Therefore, in literature convex relaxations are settled, based on e.g. semidefinite relaxations (Christakou et al., 2017; Jabr, 2008); such approaches, explore solutions that are globally optimal for the original problem in many practical cases. The recent advancements and reviews on convexifications discuss that there is a trade-off which has to be addressed between computational effort and convergence's precision (Castillo et al., 2015). It should be also stressed that convex relaxations are of significant importance for the initial NLP problems, since they may provide a lower bound that can be used to interpret the sub-optimality of the local optimizer solution (iff the convex relaxation is tight and accurate). Additionally, the relaxation can provide a certificate of problem infeasibility (Capitanescu and Wehenkel, 2013). Without the loss of generality, convex relaxations may be exact (i.e. the duality gap is zero) meaning that one can assure that solution obtained for the applied relaxation of the problem is globally optimal solution of the –initial– non-convex. For OPF relaxation problems exactness is generally claimed to be satisfied in radial topology networks; yet, only in particular conditions where there is no reversed power according to (Low, 2014). Further computational complexity can be certainly added to the OPF formulation if it is settled for multiple periods (multi-period OPF).

Recent works have dealt with proposing efficient linearizations to resort tractable multi-period OPF (Karagiannopoulos et al., c; Fortenbacher et al.). For instance, authors in (Fortenbacher et al.) take advantage of the linearization to reduce the time of convergence and utilize it for planning of the distribution network. In (Karagiannopoulos et al., c), the author advance the multi-period OPF framework incorporating uncertainties brought by forecasts through chance constrained optimization. Nevertheless, both works do not address the three-phase nature and the subsequent unbalances may arise in LV distribution networks. In this work a three-phase multi-period OPF based on the exact (i.e. non-linear) AC power flows is proposed, incorporating multiple DER within the operation of the distribution grid.

3.3 Proposed advancements on unbalanced three-phase AC-OPF

This Chapter's contributions can be summarized as follows:

- A decision tool which provides support to the DSO for the minimization of the operational costs based on the coordinated operation of multiple DER. The tool is capable to mitigate nodal voltages minimizing curtailments of active power by the microgeneration, ensuring nominal rated power for the secondary transformer (MV/LV) for all time instances. Multiple active measures are posed based on different DER technologies.
- A three phase multi-period OPF framework based on the exact formulation of the AC power flow equations. The overall problem is resolved through a nonlinear optimization problem

addressed interior-point method where efficient explicit calculation for the gradients of the constraints and the Hessian of the Lagragian are proposed leaning on sparsities.

- Analytical inter-temporal constraints (i.e. providing the limitations of each type of DER) and the counterpart inter-temporal cost dependencies are discussed with their subsequent burdens. In particular a technique is proposed to address singularity of Jacobian matrix (i.e. of the nonlinear problem) induced by the inter-temporal constraints.

3.4 Proposed unbalanced multi-period AC-OPF

3.4.1 Problem statement

The centralized coordinated management of the DER is discussed in this section through a multi-period three phase AC-Optimal Power Flow (MACOPF) where the different periods $\tau \in \mathscr{T}$ are coupled with inter-temporal costs and the DER are assigned with inter-temporal technical constraints accordingly.

The MACOPF is stated for an horizon of operational planning H_t. All subsequent time steps belong to the set $\mathscr{T} := \{1, \ldots, H_\tau\}$. The main objective (i.e. $\mathscr{O}_1$) of the scheme is to minimize the operating costs assigned with all the controllable assets providing their coordination given their availability. Penalty costs assigned to auxiliary variables described with the term Φ_p. Such penalty costs refer to relaxation of voltage bounds to ensure feasibility and thus, convergence, as well as penalties to avert simultaneous charging and discharging or even auxiliary variables. A graphical abstract of the optimization framework of MACOPF is illustrated in Figure 3.1.

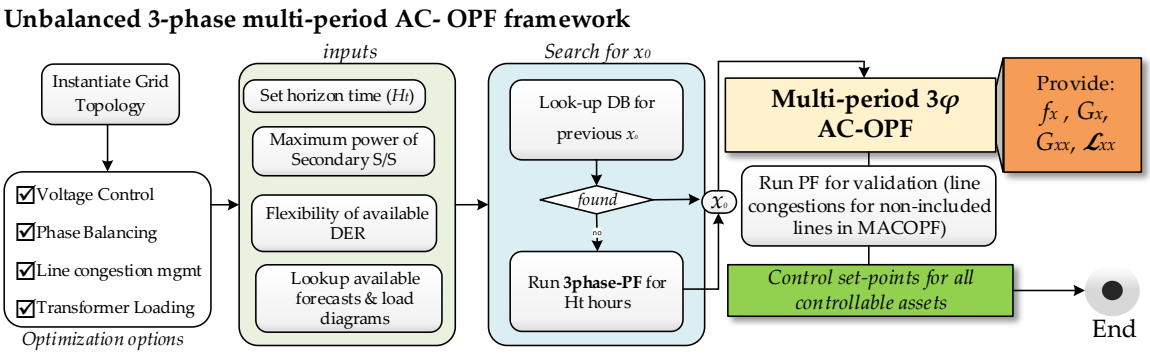

Figure 3.1: Graphical abstract of three-phase multi-period AC OPF application.

Assuming that the state vector $(x_{g,\tau})$ at the time instant τ is given by (3.1) and the set of decision variables τ correspond to the vector u_τ comprised of active and reactive power of each controllable DER as shown in (3.2) as well as auxiliary variables (3.3). The voltage angles can be omitted to reduce the scale of the optimization problem, since the angle displacement between adjacent nodes in LV grids is typically less than 10° (Fortenbacher et al.). Nonetheless, angles are

included for completeness.

$$x_{g,\tau} = \begin{bmatrix} \Theta \\ \mathscr{V} \end{bmatrix}_\tau, \forall \tau \in \mathscr{T}, x_\tau \in \mathbb{R}^{(2*3N_b)} \tag{3.1}$$

$$u_\tau = \begin{bmatrix} P_c \\ Q_c \end{bmatrix}_\tau, \forall \tau \in \mathscr{T}, u_\tau \in \mathbb{R}^{(2*n_c)} \tag{3.2}$$

$$y_\tau = \begin{bmatrix} p_{ch} \\ p_{dch} \\ y_{\pi,ch} \\ y_{\pi,dch} \\ \varepsilon_V \\ \varepsilon_{sub} \\ y_{trip} \end{bmatrix}_\tau, \forall \tau \in \mathscr{T}, y_\tau \in \mathbb{R}^{\ell_y} \tag{3.3}$$

where N_b refer to the number of buses and N_c the number controllable units and $\ell_y = (4*N_{BESS}) + 3*N_b + N_{ev} + 3$ with n_{BESS} the number of BESS and n_{EV} the number of EVs. The real vector $\mathscr{V} = [v_1, v_2, \ldots, v_{N_b}]_\tau^T$ corresponds to the voltage magnitudes for each bus (each bus has three terminals) at each time instant τ, and respectively Θ to the voltage magnitudes. The sets $\mathscr{N}$, $\mathscr{J}$, $\mathscr{T}$, denote the buses (N_b), branches and the horizon of the multi-period scheme.

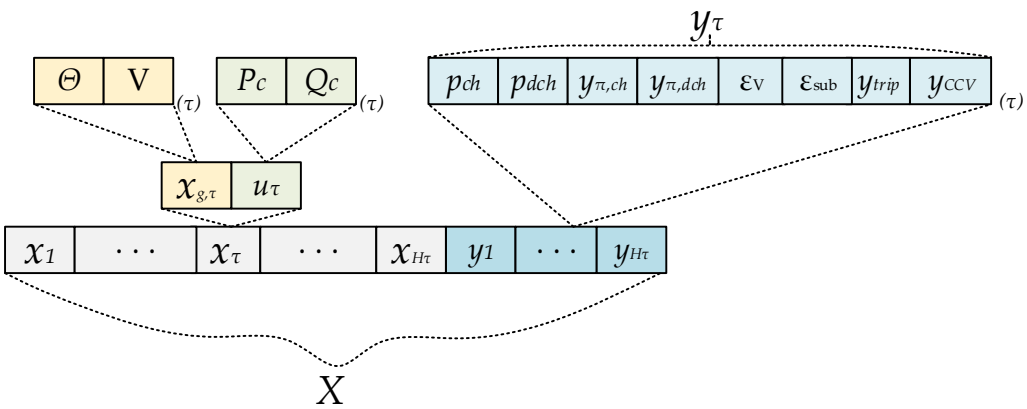

Figure 3.2: Structure of optimization variables; discriminated by state vector, control variables and the auxiliary variables per each time step.

Let for the optimization problem the state vector and the decision variables correspond to the respective matrices $X = [x_1, \ldots, x_{H\tau}]^T$ and $\mathscr{U} = [u_1, \ldots, u_{H\tau}]^T$, essentially defined as stacked vectors of each subsequent time period. For the sake of comprehension, Figure 3.2 presents the described structure of the optimization variables. The fact that the auxiliary variables (y_τ) are appended as last elements of vector X eases the extension of the stated problem. Additional objective terms might be assigned in the current formulation unless no dependence or conflicting interest upon the aforementioned objective.

The overall control scheme can be described by the set of equations (3.4).

$$\min_{u} \sum_{\tau=1}^{H_t} \left\{ \underbrace{\sum_{k}^{N_b} \left([c_k(\tau)]^T \cdot u_{k,\tau} \right)}_{\mathscr{O}_1} \right\} \Delta\tau + \Phi_p \tag{3.4}$$

subjected to

$$G_j(x_\tau, u_\tau, y_\tau) = 0 \qquad \forall j, \tau \in \mathscr{N}, \mathscr{T} \tag{3.4a}$$

$$H_{Sub}(x_\tau, u_\tau, y_\tau) + \varepsilon_{sub} \leq 0 \qquad \forall i, \tau \in \mathscr{J}, \mathscr{T} \tag{3.4b}$$

$$V_{\min} - \varepsilon_{\mathscr{V}} \leq v_j(x_\tau) \leq V_{\max} + \varepsilon_{\mathscr{V}} \qquad \forall i, \tau \in \mathscr{N}, \mathscr{T} \tag{3.4c}$$

$$h_\xi(x_\tau, u_\tau, y_\tau) = 0 \qquad \forall \xi, \tau \in \mathscr{U}, \mathscr{T} \tag{3.4d}$$

$$g_\xi(x_\tau, u_\tau, y_\tau) \leq 0 \qquad \forall \xi, \tau \in \mathscr{U}, \mathscr{T} \tag{3.4e}$$

where vector $[c_k(\tau)]^T$ includes the price of each controllable unit per time step τ in €/kWh or €/kVARh. The constraints in (3.4a) set the nonlinear power flow equation at each bus of the network; inequality constraint (3.4b) poses the technical constraint for the MV/LV transformer; the boxed constraints in (3.4c) to respect all nodal voltages to range strictly within the admissible bounds. The additional positive variable $\varepsilon_{\mathscr{V}}$ is used to relax the voltage constraints and avoid infeasibility. The latter is applicable substantially when the active measures are not adequate to address voltage problems. Accordingly, since a transformer is capable to be operated in full load conditions or slightly higher for certain short interval, an auxiliary variable is also applied to turn these constraints less tight. The constraints (3.4d)-(3.4e), correspond to the operational limits of the controllable DER.

In the following subsection, the resolution of the optimal control problem is analytically discussed through the optimization techniques used to address it efficiently. The proposed control scheme evidently deals with a large number of decision variables -$X \in \mathbb{R}^{N_X}$, where

$$N_X = \{(2 \times 3N_b + 2 \times N_c + 2 \times N_{BESS} + 2 \times N_{ev} + 3) \times H_\tau\}$$

Accordingly, the power flow through the non-linear equations are accounted $N_{nonlin} = 2 \times 3 \times N_b$. Such large optimization problems where the structure of the Jacobian of the nonlinear constraints present very sparse blocks should possibly reveal particular framing of the problem re-structuring it and inherently leading to improved computational efficiency. In Kourounis et al. (2018), the authors restructure the multi-period OPF, to a tailored approach revising the Karush-Kuhn-Tucker conditions. Hereby, particular techniques are proposed to speedup the size of the non-linear optimal control programming. The explicit calculation of the Jacobian and the Hessian are proposed taking advantage of the sparsities, as well as slight pivotal elements to the Jacobian address any singularities met by the inter-temporal constraints. The initial point X_0 for the optimizer is either obtained through a local database which has stored previous occurrences or by running sequen-

tially (H_τ) power flows. Additionally, if load and weather forecasts are not available or cannot be obtained, in a worst case, they can be surpassed by utilizing historical data.

3.4.2 DER incorporation on multi-period AC OPF

3.4.2.1 Battery Energy Storage System (BESS)

The BESS model is based on a first order battery model. Two distinct auxiliary variables are settled as power injections. The positive term refers to the discharging mode of operation $p_{dch} \geq 0$, $p_{dch} \in \mathbb{R}_+$, while the charging of the storage unit is negative $p_{ch} \leq 0$,$p_{ch} \in R_-$. This model captures the losses during charging and discharging modes, through the corresponding efficiencies (η_{ch}, η_{dch}). As $\mathscr{E}_0$ is considered the initial (i.e. τ=0) stored energy of the BESS. The available energy capacity of a BESS at time step τ can calculated by equation (3.5), which bundles the instant energy state with the former one:

$$\mathscr{E}(\tau) = \mathscr{E}(\tau - 1) - \Delta\tau \begin{bmatrix} \eta_{ch} & \frac{1}{\eta_{dch}} \end{bmatrix} p(\tau) \tag{3.5}$$

where

$$p(\tau) = \begin{bmatrix} p_{ch}(\tau) \\ p_{dch}(\tau) \end{bmatrix}$$

The energy state for the BESS for the last step will be accordingly defined as a linear combination with the previous states of its energy. As it will be presented in section 3.4.6 such intertemporal couplings lead to problematic conditions for the resolution of an optimal control, hence special treatment is proposed. In the proposed optimization framework, as primary decision variable for each BESS is considered its power injection P_{BESS}, which should be subjected to the equality constraint (3.6a) for each instant τ, followed by some operational constraints for both operation modes as follows:

$$P_{BESS}(\tau) = p_{ch}(\tau) + p_{ch}(\tau) \tag{3.6a}$$

$$\overline{p_{ch}} \leq p_{ch}(\tau) \leq 0 \tag{3.6b}$$

$$0 \leq p_{dch}(\tau) \leq \overline{p_{dch}} \tag{3.6c}$$

$$\underline{SoC} \leq SoC(\tau) \leq \overline{SoC} \tag{3.6d}$$

$$SOC(\tau) = \frac{\mathscr{E}(\tau)}{\mathscr{E}_{rated}} \tag{3.6e}$$

(3.6a)– (3.6e) are posed $\forall\tau \in \mathscr{T}, \mathscr{T} := \{1, \ldots, H_\tau\}$ and H_τ the last instant defining the horizon of the optimization. The constraints (3.6a)– (3.6e) pose the technical constraints for the BESS charging and discharging power. Accordingly, the State of the Charge (SoC) –defined in equation (3.6e) – is constrained based on the BESS's characteristics. To avert simultaneous charging and discharging of the BESS, a penalty cost is assigned with each auxiliary decision variables p_{ch}, p_{dch} both of which should greater -at least one order-than the use of the BESS (c_{BESS}) itself, i.e. P_{BESS}.

As additional note, any three-phase BESS is hereby considered that the different phases follow the same mode of operation, therefore the mathematical expression is comprised of three single-batteries installed in the different phases, coupled with the equality constraints for their active and reactive power injections as in (3.7).

$$\begin{array}{rclcl} P^A_{BESS}(\tau) & = & P^B_{BESS}(\tau) & = & P^C_{BESS}(\tau) \\ Q^A_{BESS}(\tau) & = & Q^B_{BESS}(\tau) & = & Q^C_{BESS}(\tau) \end{array} \quad \forall \tau \in \mathscr{T} \tag{3.7}$$

3.4.2.2 Electric Vehicles (EVs)

The EVs are structured following the same rationale as the BESS model. In this study the EVs are considered as flexible DER according, certainly, to their availability each time. Their provided flexibility is essentially regarded to be the intervals when they are parked to their owner's house premises. Being in this state (i.e. parked) if there is need for charge this will be decided by the proposed control following the coordinated smart charging scheme. When the owner of an EV desires to provide a signal of flexibility, the time interval when the estimated trip will occur together with the estimated consumed energy should be dispatched to the DSO. These two signals are captured for each controllable (i.e. willing to be charged in concordance to the smart charging scheme) with $[y_{trip}]$ that is added to discharge the EV and E_{tr}, where n_{tr} corresponds to the number of trips for an EV. The fictitious variable $[y_{trip}]_{n_{tr}\times H_\tau}$ is added to discharge the EVs during their trips.

The Vehicle-to-Grid (V2G), where the EV injects power to the grid, operation is also incorporated within the proposed EV model. Whenever the V2G mode of operation is not deemed to be followed, simply the p_{dch} is constrained to zero.

One can define the energy state for each instant for one EV given by the vector $\mathscr{E}_{EV} \in \mathbb{R}^{H_\tau}$ recasting equation (5.22), which infers to a linear combination of preceding instances inherent to the controllability that its flexibility allows, and the initial stored energy $\mathscr{E}_0$. The energy storage for one EV at instant τ can be calculated by (3.8).

$$\mathscr{E}(\tau) = \mathscr{E}_0 + \underbrace{\Delta\tau[\mathrm{diag}\{n_{dch}\}\ \mathrm{diag}\{1/n_{ch}\}]}_{\Lambda} \cdot \underbrace{\begin{bmatrix} p_{dch} \\ p_{ch} \end{bmatrix}}_{p_{\mathrm{EV}}(\tau)} - y_{\mathrm{trip}}(\tau) \cdot E_{\mathrm{tr}}(\tau) \tag{3.8}$$

For one EV, let it j, connected along the distribution network, the energy state function (3.8) can be rewritten in a compact matrix format capturing both operating modes where the energy stored to each EV towards the time evolution H_τ can expressed as the vector $\mathbf{E}^j_{\mathrm{EV}} = [E^j_{\mathbf{EV}}(0), \ldots, E^j_{\mathrm{EV}}(H_\tau)]^T$:

$$\mathbf{E}^j_{\mathrm{EV}} = \begin{bmatrix} I \\ \vdots \\ I \end{bmatrix} \mathscr{E}^j_0 + \begin{bmatrix} \Lambda & & \mathbf{0} \\ \vdots & \ddots & \\ \Lambda & \ldots & \Lambda \end{bmatrix} \begin{bmatrix} p^j_{\mathrm{EV}}(1) \\ \vdots \\ p^j_{\mathrm{EV}}(H_\tau) \end{bmatrix} - \mathbf{y}^j_{\mathrm{trip}} \cdot \mathbf{E}^j_{\mathrm{tr}} \tag{3.9}$$

3.4.2.3 Microgeneration (μG)

The microgeneration in this work is considered to be single phase inverter based installations. In case the DSO desires to incorporate the control of microgeneration in the control, the type of control pertaining the active power through Active Power Curtailment (APC) or Reactive Power Control (QR) have to be opted. Regarding the APC the following settings define the maximum possible curtailed power as a percentage of the instant injected power (i.e. maximum curtailment β=20%). The same modeling equations as presented in Chapter 2 are applied with ξ (in this study ξ=0.5), which stands for a parameter which leads to control PV with larger injected power in proportion to their installed power at the instant period.

The reactive power control is defined in similar way, though allowing capacitive and inductive operation (i.e. injecting and absorbing reactive power accordingly). Nevertheless, if the option of controlling the PVs in both PAC and QR mode, to avoid the nonlinear constraint inherent to the operation of the inverter; a simpler linear constraint is posed to ensure that the microgenerator's inverter does not exceed its rated power.

$$\begin{aligned} \overline{Q_{QR}(\tau)} &= (p_{rated} - p_{inj}(\tau)) \cdot \tan(\theta_{\min}), \\ \underline{Q_{QR}(\tau)} &= -\overline{Q_{QR}(\tau)}, \end{aligned} \tag{3.10}$$

where $\theta_{\min}$ is given by the minimum power factor ($\mathrm{PF}_{\min}$) applied; $\theta_{\min} = \cos^{-1}(\mathrm{PF}_{\min})$. There might be inter-temporal costs for μG deployed within MACOPF framework as it is explained in Section 3.4.7.

3.4.3 Non-linear programming based on primal-dual algorithm

The proposed control scheme based on the MACOPF is stated with the set of equations (5.4). Hereby a discussion will follow based on interior-point (IP) method which following the above form of the previous section, will involve lengthy and complicated notation. To ease the description the control problem is reformulated in a more compact manner (i.e. grouping the equalities and inequality constraints) as proposed in the literature (Nocedal and Wright, 2006; Zhu, 2015b; Wachter, 2003). Note that vector form is implied by bold notation. The decision variables and state vectors are simply represented by one vector $\mathbf{x}$:

$$\min_{\mathbf{x}} f(\mathbf{x}) \tag{3.11}$$

subject to

$$g_E(\mathbf{x}) = \mathbf{0} \tag{3.11a}$$

$$h_I(\mathbf{x}) \leq \mathbf{0} \tag{3.11b}$$

$$\boldsymbol{x}_{\min} \leq \mathbf{x} \leq \boldsymbol{x}_{\max} \tag{3.11c}$$

where $g_E(\mathbf{x})$ contains any type of equality constraint (i.e. linear and non-linear) and h_I any type of inequality constraint. The inequalities constraints can be introduced as equality constraints by the addition of slack variables s_j, such that $h_I(\mathbf{x}) - \mathbf{s} = \mathbf{0}$. Then a *penalty function* introduces a new form to the initial objective function as follows

$$\min_{\mathbf{x}} f_p = f(\mathbf{x}) - \mu^{(k)} \sum_{j=1}^{N_x} \ell n(x_j - x_{j,\min}) - \mu^{(k)} \sum_{j=1}^{N_x} \ell n(x_{j,\max} - x_j) - \mu^{(k)} \sum_{j=1}^{N_{ineq}} \ell n(s_j) \tag{3.12}$$

subject to

$$\begin{aligned} g_E(\mathbf{x}) &= 0 \\ h_I(\mathbf{x}) + \mathbf{s} &= 0 \\ \mathbf{x}, \mathbf{s} &\geq \mathbf{0} \end{aligned} \tag{3.13}$$

where $\mu^{(k)}$ is the logarithmic barrier parameter for iteration k which essentially reduces monotonically to 0 as iteration progresses. The non-negativity conditions at (3.13) are handled by incorporating them into logarithmic barrier terms. The Lagrangian ($\mathscr{L}_p$) of the f_p can be defined as:

$$\begin{aligned} \mathscr{L}_p(\mathbf{x}, \boldsymbol{\lambda}, \boldsymbol{\sigma}, \mathbf{s}) &:= f_p(\mathbf{x}) - \boldsymbol{\lambda}^T g_E(\mathbf{x}) - \boldsymbol{\sigma}^T (h_I(\mathbf{x}) + \mathbf{s}) \Leftrightarrow \\ \mathscr{L}_p(\mathbf{x}, \boldsymbol{\lambda}, \boldsymbol{\sigma}, \mathbf{s}) &= f(\mathbf{x}) - \mu^{(k)} \sum_{j=1}^{N_x} \ell n(x_j - x_{j,\min}) - \mu^{(k)} \sum_{j=1}^{N_x} \ell n(x_{j,\max} - x_j) - \\ &\quad \mu^{(k)} \sum_{j=1}^{N_{ineq}} \ell n(s_j) - \boldsymbol{\lambda}^T g_E(\mathbf{x}) - \boldsymbol{\sigma}^T (h_I(\mathbf{x}) + \mathbf{s}) \end{aligned} \tag{3.14}$$

where vectors $\boldsymbol{\lambda}$, $\boldsymbol{\sigma}$ are the Lagrange multipliers for the corresponding equality and inequality constraints. The first-order KKT condition (**iff** g_E, h_I are first order differentiable) for a local optimum point $p^* = (\mathbf{x}^*, \boldsymbol{\lambda}^*, \boldsymbol{\sigma}^*, \mathbf{s}^*)$ are the following:

$$\begin{aligned} \nabla_x \mathscr{L}_p(\mathbf{x}^*, \boldsymbol{\lambda}^*, \boldsymbol{\sigma}^*, \mathbf{s}^*) &= \nabla_x f_p(x) - \boldsymbol{\lambda} \nabla_x g_E(\mathbf{x})^T - \boldsymbol{\sigma} \nabla_x h_I(\mathbf{x})^T - \mathscr{D} &= \mathbf{0} \\ \nabla_\mu \mathscr{L}_p &= \mu[\mathbf{s}]^{-1} e - \lambda &= \mathbf{0} \\ \nabla_\lambda \mathscr{L}_p &= g_E(\mathbf{x}^*) &= \mathbf{0} \\ \nabla_\sigma \mathscr{L}_p &= h_I(\mathbf{x}^*) - \mathbf{s}^* &= \mathbf{0} \\ \mathscr{D} = \boldsymbol{\mu}[\mathbf{x} - \mathbf{x}_{\min}]^{-1} \mathbf{e} + \boldsymbol{\mu}[\mathbf{x}_{\max} - \mathbf{x}]^{-1} \mathbf{e} \end{aligned}$$

(3.15a)

where **e** appropriate size vector with all entries equal to one.

The first-order Karush-Kuhn-Tucker (KKT) conditions are necessary and sufficient for global optimality for convex problem when Linear Constraint Qualification (LICQ) holds (Hauswirth et al., 2018). In the proposed control scheme, the non-convex nature of the -exact- non-linear power flow necessitates the verification second-order KKT conditions to certify the local optimal-

ity of p^* . The second-order conditions can be found analytically in the literature (Nocedal and Wright, 2006), since here the first-order will be analytically discussed due to the examination of linear dependence of the inter-temporal constraints introduced by DER.

The IP algorithm at iteration k requires the solution of the following nonlinear system:

$$\begin{bmatrix} \nabla_x^2 \mathscr{L}_p & \nabla_x g_E(\mathbf{x}) & \nabla_x h_I(\mathbf{x}) & 0 \\ \nabla_x g_E(\mathbf{x})^T & 0 & 0 & 0 \\ \nabla_x h_I(\mathbf{x})^T & 0 & 0 & I \\ 0 & 0 & I & \nabla_s^2 \mathscr{L}_p \end{bmatrix} \begin{bmatrix} \Delta\mathbf{x} \\ \Delta\boldsymbol{\lambda} \\ \Delta\boldsymbol{\sigma} \\ \Delta\mathbf{s} \end{bmatrix} = - \begin{bmatrix} \nabla_x f_p(x) - \boldsymbol{\lambda}\nabla_x g_E(\mathbf{x})^T - \boldsymbol{\sigma}\nabla_x h_I(\mathbf{x})^T \\ \mu[\mathbf{s}]^{-1}e - \boldsymbol{\lambda} \\ g_E(\mathbf{x}) \\ h_I(\mathbf{x}) - \mathbf{s} \\ [\mathbf{z}]\mathbf{x} - \mu\mathbf{e} \end{bmatrix} \tag{3.16}$$

The KKT system in (3.16) is nonlinear and its solution most commonly in the literature (Torres and Quintana, 1998) is addressed by applying the Newton's method. In the proposed control scheme the gradients for the nonlinear constraints and the Hessian of the Lagrangian are explicitly calculated. In case where these derivations are not provided, approximations based on finite differences are typically applied (Wächter and Biegler, 2006; Coleman et al., 1999).

3.4.4 Gradients of nonlinear constraints and Hessian of Lagrangian

The gradient of the objective function, the Jacobian of nonlinear constraints and Hessian of the Lagrangian are implicitly provided to the optimizer, by expanding the calculations presented in Zimmerman (2010). On this point it is important to state that voltage vectors are expressed using polar coordinates: expressing voltage in rectangular coordinates eliminates trigonometric functions from the PF equations (Frank and Rebennack, 2016). Nevertheless, in (Torres and Quintana, 1998; Wood et al.) a benchmarked comparison of both types of coordinates present same order of computational performance as well as equivalent number of iterations for convergence for a typical OPF. From one hand, rectangular coordinates can ease the process of first and second order gradients leading to quadratic and constant forms; both types, cannot avoid the nonlinear equalities (and inequality) constraints and form a convex region. Concurrently, rectangular coordinates may provide slightly faster evaluation of particular gradients and Hessian, but the voltage bounds are handled as functional bounds in many OPF problems.

Therefore, the complex voltage vector might be denoted by $V \in \mathbb{R}^{3N_b}$. The element at bus j at phase a is $\upsilon_{j,a} = |\upsilon_{j,a}|e^{j\theta_{j,a}}$. The derivation with the state vectors for instant period τ follows,- obviously for the other periods are 0 entries-:

$$V_{\Theta_\tau} = \frac{\partial V_\tau}{\partial \Theta_\tau} = j[V_\tau] \quad V_{\mathscr{V}_\tau} = \frac{\partial V_\tau}{\partial \mathscr{V}_\tau} = [V_\tau][V_\tau]^{-1} := [E] \tag{3.17}$$

The analytical AC power flow equations over all periods of the horizon window can be derived by the resolution of equation (3.18). The operator $\odot$ is used for element-wise matrix product. Complex number equations are not addressed by state-of-the art optimizers and only in few cases yield to faster solutions (Gilbert and Josz, 2017). Thus, a segregation is proposed-as shown in equation (3.19)- which introduces the power flows through the vector $G(X)$, due to their complex nature which essentially cannot be posed at the optimization stage.

$$\begin{aligned} G_c(X) &= S_{bus}(V) + S_d - C_g S_g \quad , G_c : \mathbb{C}^{n_b} \rightarrow \mathbb{C}^{n_b} \\ S^{\tau}_{bus}(V_\tau) &= V_\tau \odot (I^{\tau}_{inj})^* = V_\tau \odot (Y_{bus} \cdot V_\tau)^* \end{aligned} \tag{3.18}$$

$$G(X) = \begin{bmatrix} \Re\{G_c(X)\} \\ \Im\{G_c(X)\} \end{bmatrix} \quad , G : \mathbb{R}^{2n_b} \rightarrow \mathbb{R}^{2n_b} \tag{3.19}$$

The current bus injection I_{inj} appear in the power flow equations (3.18). It would be useful for the power flow expressions derivation to present the corresponding for the current injections.

$$\begin{aligned} \frac{\partial I^{\tau}_{inj}}{\partial x_\tau} &= \begin{bmatrix} \frac{\partial I^{\tau}_{inj}}{\partial \Theta_\tau} & \frac{\partial I^{\tau}_{inj}}{\partial \mathscr{V}_\tau} & 0 & 0 \end{bmatrix} \\ \frac{\partial I^{\tau}_{inj}}{\partial \Theta_\tau} = Y_{bus} \frac{\partial V_\tau}{\partial \Theta_\tau} &\overset{(3.17)}{=} jY_{bus}[V_\tau], \quad \frac{\partial I^{\tau}_{inj}}{\partial \mathscr{V}_\tau} = Y_{bus} \frac{\partial V_\tau}{\partial \mathscr{V}_\tau} \overset{(3.17)}{=} Y_{bus}[E] \end{aligned} \tag{3.20}$$

The first and second derivatives for the non-linear constraints, which substantially refer to the power flow equation will be based on the introduced vector $G_c(X)$.

$$G_X = \frac{\partial G}{\partial X} = \begin{bmatrix} \frac{\partial \Re\{G_c(X)\}}{\partial X} \\ \frac{\partial \Im\{G_c(X)\}}{\partial X} \end{bmatrix} = \begin{bmatrix} \frac{\partial G}{\partial x_1} & \frac{\partial G}{\partial x_2} & \cdots & \boxed{\frac{\partial G}{\partial x_{H_t}}} & \cdots & \frac{\partial G}{\partial x_{H_t}} & \frac{\partial G}{\partial y_1} & \cdots & \frac{\partial G}{\partial y_{H_t}} \end{bmatrix} \tag{3.21}$$

$$\frac{\partial G}{\partial x_\tau} = \begin{bmatrix} G_{\Theta_\tau} & G_{v_\tau} & G_{Pg_\tau} & G_{Qg_\tau} \end{bmatrix} \tag{3.22}$$

The first order partial derivatives are presented for the defined G_c, which can thereafter appended in the equation (3.22).

$$G_{c,\Theta_\tau} = \frac{\partial S_{bus}(V_\tau)}{\partial \Theta_\tau} = [I^{\tau}_{inj}] \frac{\partial V_\tau}{\partial \Theta_\tau} + [V_\tau] \frac{\partial (I^{\tau}_{inj})^*}{\partial \Theta_\tau} \overset{(3.17)}{=} j[V_\tau] \left([I^{\tau}_{inj}] - Y_{bus}[V_\tau] \right)^* \tag{3.23}$$

$$G_{c,\mathscr{V}_\tau} = \frac{\partial S_{bus}(V_\tau)}{\partial \mathscr{V}_\tau} = [I^{\tau}_{inj}] \frac{\partial V_\tau}{\partial \mathscr{V}_\tau} + [V_\tau] \frac{\partial (I^{\tau}_{inj})^*}{\partial \mathscr{V}_\tau} \overset{(3.17)}{=} [V_\tau] \left([I^{\tau}_{inj}] + Y_{bus}[V_\tau] \right)^* [\mathscr{V}_\tau]^{-1} \tag{3.24}$$

$$G_{c,P^{\tau}_g} = -C_g, \quad G_{c,Q^{\tau}_g} = -jC_g \tag{3.25}$$

where $(C_g)_{N_b \times N_c}$ stands for the injection connectivity matrix that each element (i, j) is one if at bus i_{th} controllable asset j_{th} is connected, else the element is zero. It is obvious that the partial derivatives of $G_c(x_\tau)$ with respect to other $x_{g,\tau_2}, u_{g,\tau_2}$ -with $\tau_2 \neq \tau$- results to zero entries.The G_X is therefore formed by two stacked matrices which present sparse block diagonalities. The

corresponding partial derivatives with respect to the auxiliary variables will be zero entries as well.

The second derivatives for the complex power injections are necessary only for the assessment of the Hessian of the Lagrangian which appears in iteration of the KKT-system –equation (3.15)-. As it can be observed the Hessian matrix of the Lagrangian can be given by equation (3.26).

$$\mathscr{H}_p(\mathbf{x},) = \nabla_{XX} L_p = \nabla_{XX} f(X) + \nabla_{XX} g_E(\lambda) + \nabla_{XX} H(X) \tag{3.26}$$

The second order derivatives for the complex power flows are calculated in proportion to the instant λ. The derivative is provided discretized in two parts

$$\begin{aligned} \frac{\partial^2 G_c \lambda}{\partial x_\tau^2} &= \frac{\partial}{\partial x_\tau}\left(\boldsymbol{\lambda} G_{c,x_\tau}^T(X)\right) \\ &= \begin{bmatrix} G_{c,\Theta_\tau\Theta_\tau} & G_{c,\Theta_\tau\mathscr{V}_\tau} & 0 & 0 \\ G_{c,\mathscr{V}_\tau\Theta_\tau} & G_{c,\mathscr{V}_\tau\mathscr{V}_\tau} & 0 & 0 \\ 0 & 0 & 0 & 0 \\ 0 & 0 & 0 & 0 \end{bmatrix} \end{aligned} \tag{3.27}$$

A brief presentation of all the subsequent expressions follows:

$$\begin{aligned} G_{c,\Theta_\tau\Theta_\tau} &= \frac{\partial}{\partial \Theta_\tau}\left(j\left([I_{inj}^\tau] - [V_\tau] Y_{bus}^T\right)^* [V_\tau]\boldsymbol{\lambda}_\tau\right) \\ &= \underbrace{[V_\tau]^*\left((Y_{bus}^*)^T [V_\tau][\boldsymbol{\lambda}_\tau] - [(Y_{bus})^*[V_\tau]\boldsymbol{\lambda}_\tau]\right)}_{A_1} + \underbrace{\mathscr{C}_2\left(Y_{bus}^*[V_\tau]^* - [I_{bus}]^*\right)}_{A_2} \end{aligned} \tag{3.28}$$

Accordingly, the $G_{c,\mathscr{V}_\tau\Theta_\tau}$ can be calculated as:

$$G_{c,\mathscr{V}_\tau\Theta_\tau} = j\mathscr{B}(A_1 - A_2) = (G_{c,\Theta_\tau\mathscr{V}_\tau})^T \tag{3.29}$$

$$G_{c,\mathscr{V}\mathscr{V}_\tau} = \mathscr{B}(\mathscr{C} + \mathscr{C}^T)\mathscr{B} \tag{3.30}$$

where

$$\begin{aligned} \mathscr{B} &= [V_\tau]^{-1} \\ \mathscr{C}_2 &= [\lambda_\tau][V_\tau] \\ \mathscr{C} &= \mathscr{C}_2(Y_{bus}[V_\tau])^* \end{aligned}$$

The overall assessment of the second order gradient can be induced to a simple routine reducing computational effort and memory allocation by saving certain matrices presented above.

The subsequent gradients of the objective functions can be assessed for the proposed scheme since the $f(X) = \sum_{\tau\in\mathscr{T}} f(x_\tau)$, substantially corresponds to a linear combination of convex functions. The first-order gradient of the objective will be comprised by constant and null entries since the costs are linear functions, as described in subsection 3.4.7. By extension, the second-order derivatives of the objective function will be a null matrix.

If a solution of the barrier problem satisfies the primal-dual equations (3.16) of the non-linear KKT system, its solution may be approximated by an iteration of Newton's method. The search direction can be obtained as a solution of the linearization of the KKT system which is presented in the next subsection 3.4.5.

3.4.5 Solution of Karush-Kuhn-Tucker equations

Hereby for the barrier solution is presented for the optimal control problem (3.11), assuming that the decision variables x are positive (i.e. to avoid lengthy notation). The dual variables can be introduced as:

$$z_i := \frac{\mu}{x_i} \tag{3.31}$$

$$\begin{bmatrix} \mathscr{H} & \mathbf{0} & -J_E^T & -J_I^T & -I \\ \mathbf{0} & [\boldsymbol{\lambda}] & \mathbf{0} & [\mathbf{s}] & \mathbf{0} \\ J_E & 0 & \mathbf{0} & \mathbf{0} & \mathbf{0} \\ J_I & -I & \mathbf{0} & \mathbf{0} & \mathbf{0} \\ [\mathbf{z}] & \mathbf{0} & \mathbf{0} & \mathbf{0} & [\mathbf{x}] \end{bmatrix}^{(k)} \begin{bmatrix} \Delta\mathbf{x} \\ \Delta\mathbf{s} \\ \Delta\boldsymbol{\lambda} \\ \Delta\boldsymbol{\sigma} \\ \Delta\mathbf{z} \end{bmatrix}^{(k)} = - \begin{bmatrix} \nabla_x \mathscr{L}_p \\ \nabla_\lambda \mathscr{L}_p \\ \nabla_\sigma \mathscr{L}_p \\ \nabla_s \mathscr{L}_p \end{bmatrix}, \tag{3.32}$$

where $\mathscr{H} = \nabla_{xx}\mathscr{L}_p$, $J_E = \nabla_x g_E(\mathbf{x})$ and $J_I = \nabla_x h_I(\mathbf{x})$. The system (3.32) can be further simplified -based on Gaussian elimination- by eliminating the last row. Therefore, with this elimination it will be:

$$\begin{bmatrix} \hat{\mathscr{H}} & \mathbf{0} & -J_E^T & J_I^T \\ \mathbf{0} & [\hat{\boldsymbol{\lambda}}] & \mathbf{0} & -I \\ J_E & \mathbf{0} & \mathbf{0} & \mathbf{0} \\ J_I & -I & \mathbf{0} & \mathbf{0} \end{bmatrix}^{(k)} \begin{bmatrix} \Delta\mathbf{x} \\ \Delta\mathbf{s} \\ \Delta\boldsymbol{\lambda} \\ \Delta\boldsymbol{\sigma} \end{bmatrix}^{(k)} = - \begin{bmatrix} \nabla_x \mathscr{L}_p + [\mathbf{x}]^{-1} g_E(\mathbf{x}) \\ [\mathbf{s}]^{-1}(-\mu\mathbf{e} + \mathbf{s}\boldsymbol{\lambda}) \\ -g_E(\mathbf{x}) \\ -h_I(\mathbf{x}) \end{bmatrix}, \tag{3.33}$$

where $\hat{\mathscr{H}} = -\mathscr{H}^k - [\mathbf{x}^k]^{-1}[\mathbf{z}^k]$ and the diagonal matrix $[\hat{\boldsymbol{\lambda}}] = -(\mathbf{s}^k)[\boldsymbol{\lambda}]$. The updates for the dual variables can be obtained from the equation (3.34).

$$\Delta\mathbf{z}^k = [\mathbf{x}^k]^{-1}(\mu\mathbf{e} - [\mathbf{z}^k]\Delta\mathbf{x}^k) - \mathbf{z}^k \tag{3.34}$$

The overall resolution of the KKT system provides the search direction set for each subsequent iteration. An important condition for the Netwon step is that the Jacobian J_E is a non-singular matrix. The latter implies properties which are assigned with the constraint qualification (CQ). The QP is a critical condition that needs to be assessed along with the KKT conditions. More analytically, the LICQ necessitates that the gradients of the equality constraints and any active bound constraints (i.e. binding constraints) which are linearly independent. If this does not hold the KKT system cannot be resolved.In (Hauswirth et al., 2018), the authors show that for any local optimizer the KKT conditions with LICQ satisfied can ensure the generic existence of the Lagrangian multipliers. The inter-temporal couplings among different periods τ in some cases lead to singularities for the Jacobian of the nonlinear equalities. The following section 3.4.6 thoroughly discusses an efficient manner to avert such issues.

3.4.6 On the treatment of singularity of Jacobian matrix

The Jacobian matrix that stems from the first-order KKT optimality conditions is being updated in each Newton-Raphson iteration step towards optimality. In certain cases, the Jacobian is singular at neighborhoods close to optimality due to binding inter-temporal constraints. Therefore, this particularity arises the numerical conflict of the non-invertibility which can result in the non-convergence or convergence to an erroneous solution. Convergence to erroneous solution may occur if the Jacobian is singular or close to singular; typically, the assessment the invertible of a matrix takes place either by applying LU factorization or LDL decomposition, and the resolution of linear system provides the inverse matrix. For a Jacobian matrix close to singular the solution of the LU system is not exact or accurate.The causes of such singularities are mainly rooted with inter-temporal technical constraints posed for DER such as BESS and EVs.

3.4.6.1 Mathematical analysis of inter-temporal constraints

Assume the generalized NLP formulation of (3.11). According to LICQ, the gradients of all the binding constraints must be linearly independent at the optimal solution (x^*), which essentially implies that there is no unique solution for the Lagrange multipliers (Hauswirth et al., 2018; Baker et al., b). The LICQ also provides certificate that even if KKT conditions are fulfilled, there is no unique solution for the instant set of Lagrange multipliers that corresponds to the dependent binding constraints. Analyzing such linear dependences the Jacobian matrix of the KKT system (3.33) has to be explored, particularly focusing on the following rows:

$$\begin{bmatrix} \mathbf{0} & [\hat{\boldsymbol{\lambda}}] & \mathbf{0} & -I \\ J_E & \mathbf{0} & \mathbf{0} & \mathbf{0} \\ J_I & -I & \mathbf{0} & \mathbf{0} \end{bmatrix}. \tag{3.35}$$

When the gradients J_E, J_I of both equality and inequality constraints are linearly dependent and the constraints are binding, then the entire matrix block of (3.35) has dependent rows.

Focusing particularly for the case related to a BESS or an EV for two subsequent time steps $(\tau, \Delta\tau)$, let the variable vector $\mathbf{x} = [S(\tau) \;\; u_1(\tau) \;\; u_2(\tau) \;\; S(\tau+1)]$.

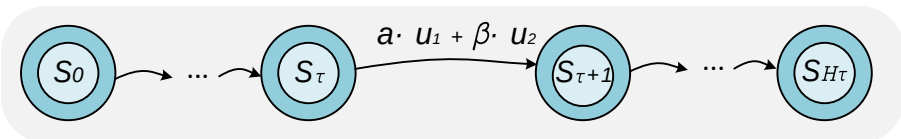

Figure 3.3: Generalized transition state model for BESS, EV and CL.

Presuming the generalized constraints for the model present in Figure 3.3 as:

$$S(\tau+1) = S(\tau) + \alpha \cdot u_1 + \beta \cdot u_2, \tag{3.36a}$$

$$\underline{S} \leq S(\tau) \leq \overline{S}, \tag{3.36b}$$

$$\underline{S} \leq S(\tau+1) \leq \overline{S}, \tag{3.36c}$$

$$0 \leq u_1 \leq \overline{u_1}, \tag{3.36d}$$

$$\underline{u_2} \leq u_2 \leq 0. \tag{3.36e}$$

The generalized constraints (3.36a)–(3.36e), couple the different states between the successive steps and possible technical constraints on the decision variables. Presuming the optimal solution is $\mathbf{x}^* = [\underline{S} \;\; 0 \;\; 0 \;\; \overline{S}]$, which essentially implies that the system's state for the consecutive time slots is equal to the lower bound, the gradient of the active constraints (3.36a)–(3.36e) is given by the matrix (3.37).

$$\begin{bmatrix} 0 & \dots & 0 & 1 & \alpha & \beta & -1 & 0 & \dots & 0 \\ 0 & \dots & 0 & 1 & 0 & 0 & 0 & 0 & \dots & 0 \\ 0 & \dots & 0 & 0 & 0 & 0 & 1 & 0 & \dots & 0 \\ 0 & \dots & 0 & 0 & 1 & 0 & 0 & 0 & \dots & 0 \\ 0 & \dots & 0 & 0 & 0 & 1 & 0 & 0 & \dots & 0 \end{bmatrix} \begin{array}{c} \text{for (3.36a)} \\ \hline \text{for (3.36b)} \\ \hline \text{for (3.36c)} \\ \hline \text{for (3.36d)} \\ \hline \text{for (3.36e)} \end{array} \tag{3.37}$$

It is clear that the matrix (3.37) that contains the gradients of the constraints has linear dependent rows; hence, LICQ does not hold which results to singular Jacobian matrix.

3.4.6.2 Computational techniques to remedy singularity

In the proposed multi-period OPF the inclusion of inter-temporal constraints (e.g. mainly due to BESS and EVs) in most cases lead to the singularity of Jacobian matrix (J_E). Whenever the gradients of the active constraints are linearly dependent the consequence is that Jacobian matrix for the first-order optimality conditions will be singular. This can be observed for the presented KKT systems (3.33) when there are some -assuming a set of j- binding constraints (from the h_I inequalities) $\mathbf{s_j} = 0$, while $\boldsymbol{\sigma}_j \neq 0$. Therefore, if additionally there gradients of the respective gradients $\nabla g_E, \nabla h_I$ are dependent when constraints are active the last three rows of the iteration matrix (3.33) will have dependent rows. An additional problematic condition might appear whether the binding conditions are linearly dependent, then the Jacobian matrix is again singular according to (Baker et al., a).

The singularity issue to some extent occur due to the structure of the control scheme which essentially has no unique set of Lagrange multipliers corresponding to the dependent binding constraints. The particular case of BESS and the subsequent problems are analytically discussed in (Baker et al., a,b). In these works techniques are proposed to address the singularities; in (Baker et al., a) the authors simply suggest the elimination of the linearly dependent binding constraint once the Jacobian matrix is singular. Nonetheless, none can guarantee that the no constraint violation will take place and meanwhile it is tailored to mitigate certain singularities. The same authors

propose further methods based on either on Moore-Penrose pseudoinverse of the Jacobian or by adding the standby losses.

Hereby a simple technique will be presented which is model-free which aims to correct the singularity introducing pivotal changes within the Jacobian matrix based on notions presented in (Nocedal and Wright, 2006). To avoid the failure of singularity small pivot element (i.e. blue elements) might be added whenever the issue arises

$$\begin{bmatrix} \hat{\mathscr{H}} & \mathbf{0} & -J_E^T & J_I^T \\ \mathbf{0} & [\hat{\boldsymbol{\lambda}}] & \mathbf{0} & -I \\ J_E & \mathbf{0} & \delta_\pi \cdot I & \mathbf{0} \\ J_I & -I & \mathbf{0} & \mathbf{0} \end{bmatrix}^{(k)} \begin{bmatrix} \Delta\mathbf{x} \\ \Delta\mathbf{s} \\ \Delta\boldsymbol{\lambda} \\ \Delta\boldsymbol{\sigma} \end{bmatrix}^{(k)} = - \begin{bmatrix} \nabla_x \mathscr{L}_p + [\mathbf{x}]^{-1} g_E(\mathbf{x}) \\ [\mathbf{s}]^{-1}(-\mu\mathbf{e} + \mathbf{s}\boldsymbol{\lambda}) \\ -g_E(\mathbf{x}) - \delta_\pi \cdot \lambda \\ -h_I(\mathbf{x}) \end{bmatrix}, \tag{3.38}$$

where δ_π stands for a fairly small positive number. The latter correction takes place in each iteration that the Jacobian is tracked as rank-deficient, which implies the linear dependency among constraints.

3.4.7 Inter-temporal Costs

Inter-temporal costs have to be incorporated to ensure that transitions from one operating point to the next are feasible (i.e. managing flexibilities provided by the DER) and economical. These costs do apply independently to DER or assets while spanning multiple periods in particular if multiple tariff are defined along the horizon.

The costs for the controllable resources such as BESS and μG follow a conditional operation regarding their mode of operation. The cost function, for instance, of charging a BESS is expressed by a linear convex function depending of the quantity of energy consumed -see Figure 3.4(a) scenario when charging and discharging are equally priced-. At any time step (e.g. charging or discharging) a Cost Constrained Variable (CCV) is posed to represent the proper cost. For instance, the piecewise linear cost function $c_{BESS}(x)$ –for a BESS owned by the DSO– is represented by the red line on Figure 3.4(a)- is substituted by an auxiliary variable y_{BESS} and a set of linear constraints. These linear constraints form a convex region with the $c_{BESS}(x)$, setting the y_{BESS} always to lie in the epigraph of the cost function. This auxiliary variable is onwards reflected to the objective function.

$$c_{BESS}(x) = \begin{cases} \pi_{BESS} \cdot x & \textbf{if } x \geq 0 \quad \text{(discharging)} \\ -\pi_{BESS} \cdot x & \textbf{else } x < 0 \quad \text{(charging)} \end{cases} \tag{3.39}$$

where π_{BESS} corresponds to price of utilizing the BESS either for charging or discharging. The necessary linear constraints for the auxiliary variable are the following:

$$\begin{aligned} y_{BESS} &\geq \pi_{BESS} \cdot x \\ y_{BESS} &\geq -\pi_{BESS} \cdot x \end{aligned} \tag{3.40}$$

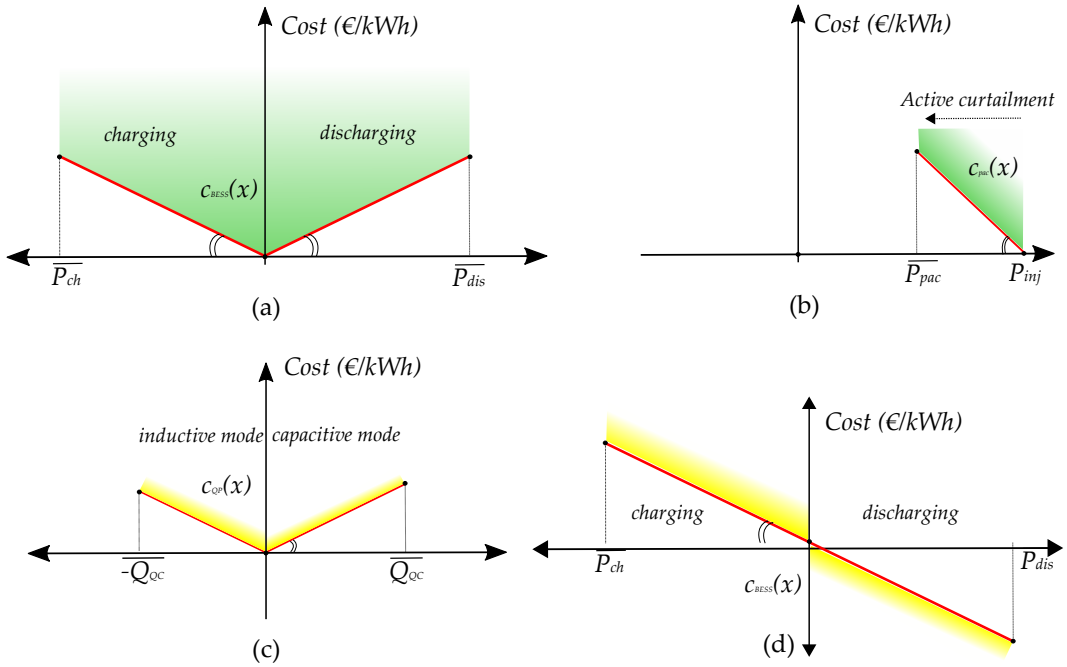

Figure 3.4: Cost function functions. (**a**) Cost function for utilizing a BESS-owned by the DSO-. (**b**) Cost of active power curtailment. (**c**) Cost function of reactive power control for microgeneration. (**d**) Cost function of an EV with V2G operation.

Accordingly, the cost functions and their subsequent auxiliary variables are defined. Note that for EV or domestic BESS their cost function can have an arbitrage regime, in the sense that charging has a cost reduction for the owner and a cost for discharging mode of operation –Figure 3.4(d)–. Note that all Figures 3.4 are indicative for a particular period τ; different functions might be regarded for different time steps implementing demand response schemes based on variable pricing schemes.

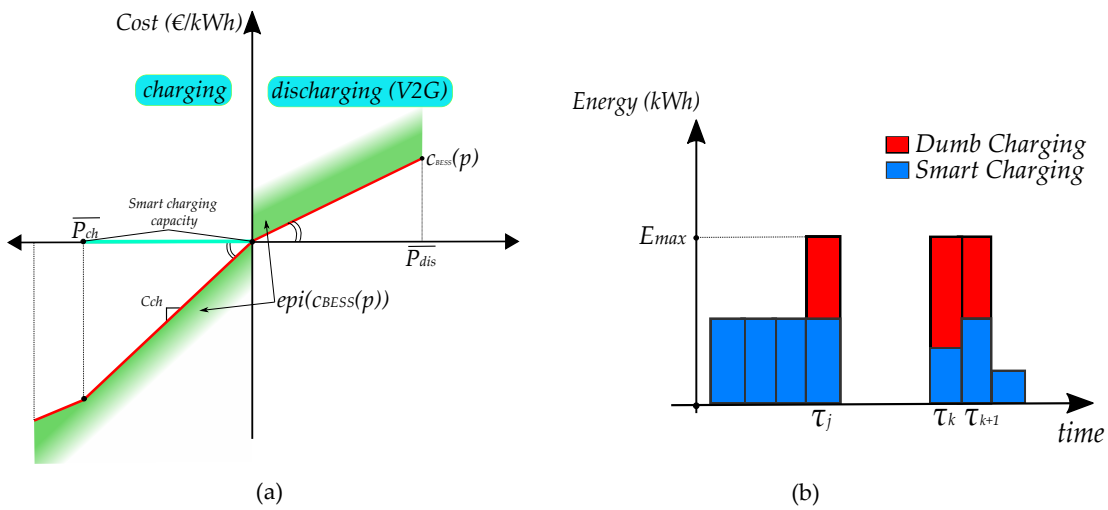

Figure 3.5: (**a**) cost function assignment for smart charging; (**b**) example of smart charging operation.

The flexible use of smart charging operation is, alternatively, illustrated in Figure 3.5b, where some charging energy slots are shifted at later hours. In Figure 3.5a, the cost function definition is illustrated, where the dumb charging is added on the objective function as a negative cost (i.e., profit), whereas the decision to use smart charging decreases proportionally this profit. The cost function is deployed as a piecewise linear function with a CCV. Note that, for periods when no dumb charging does occur, a V (not purely symmetric since use of V2G is considered more expensive) cost function is considered with its vertex at (0,0). Other definitions, may arise to account for the flexibility DER models and the manner that should be regarded on DMS applications. There could be direct contracts of the DSO with prosumers or with intermediate player such as aggregators. For instance, if there is a certain load profile selected by an end-user (e.g. derived from a HEMS local optimizer), a further request of the DSO for flexibility may take place under advanced demand response scheme; hence, the presented cost functions in Figure 3.4 may have different slopes per time step.

3.4.8 Lagrangian multipliers and sensitivity analysis

The analytical resolution of the control scheme (3.11) is presented in this section. Without the loss of generality, assume an NLP as described by equation (3.41).

$$\begin{aligned} \min \quad & f(x) \\ \text{s.t.} \quad & g(x) = 0 \end{aligned} \tag{3.41}$$

The Lagrangian multipliers can be exploited to quantify the change in the optimal solution of (3.41) if some constraints are slightly perturbed. Obviously, the Lagrangian function of problem (3.41) is:

$$\mathscr{L}(x) = f(x) - g(x)^T \lambda \tag{3.42}$$

where $\lambda : M \to \mathbb{R}^m$ Let as $p(\xi)$ as:

$$p(\xi) = \min\{f(x) : g(x) = \xi\} \tag{3.43}$$

where $f : \mathbb{R}^n \to \mathbb{R}$, $x \in \mathbb{R}^n$ and the constraints represented by $g : \mathbb{R}^n \to \mathbb{R}^m$, with $m < n$ are efficiently smooth. Let a x^*, a non-singular local optima; the function is defined on a close region M of 0 in $\mathbb{R}^m$. There exist smooth functions $x : M \to \mathbb{R}^n$ and $\lambda : N \to \mathbb{R}^m$ such that $x(u)$ is the a unique local solution of (3.41). The latter can be proved by applying the implicit function theorem to the KKT-system (3.44)

$$\begin{cases} \nabla f(x) + \nabla g(x)\lambda & = & 0 \\ g(x) - u & = & 0 \end{cases} \tag{3.44}$$

Therefore, from the latter it is:

$$p(u) = f(x(u)) \tag{3.45}$$

and

$$g(x(u)) = u. \tag{3.46}$$

By applying the operator ∇ to equation (3.45) and (3.46), accordingly to obtain their differentiation:

$$\begin{aligned} \nabla p(u) &= \nabla x(u) \nabla f(x(u)) \\ \nabla x(u) \nabla g(x(u)) &= I. \end{aligned}$$

Replacing those equations:

$$\begin{aligned} \nabla p(u) &= \nabla x(u) \nabla f(x(u)) \\ \nabla x(u) \nabla g(x(u)) &= I. \end{aligned}$$

Due to $\nabla f(x^*) = \nabla g(x^*)\lambda^*$, it can be replaced in the previous equation leading:

$$\begin{aligned} \nabla p(0) &= \nabla x(0)(\nabla g(x^*)\lambda^*) \\ &= (\nabla x(0) \nabla g(x^*))\lambda^* \\ &= I\lambda^* \\ &= \lambda^* \end{aligned}$$

Reaching to the result that:

$$\nabla p(0) = \lambda^* \tag{3.47}$$

The result of equation (3.47), essentially, can be interpreted that if the settled constraints $g(x) = 0$ are slightly perturbed such that $g(x) = u, (u \to 0)$, the optimal value of the objective can be approximated by equation (3.48).

$$\nabla p(0) \cdot u = \lambda^* \cdot u = \sum_{j=1}^{m} \lambda_j^* u_j. \tag{3.48}$$

3.5 Case study on incremental PV integration

The network selected for the case study is the one presented in Section A.1. In all scenarios, a three-phase centralized BESS is assumed to be connected at node 101 (Figure 3.6). The technical characteristics of BESS are in Table 3.1, selected from (Palizban and Kauhaniemi, 2016). This BESS is assumed to have an initial SoC of 0.40 equal also with the one at the end of the optimization horizon it has to be equal to the initial, $SoC_{H\tau}$=0.40.

Table 3.1: Technical characteristics of BESS_{101} placed at node 101.

Energy capacity [kWh]	Power Rate [kW]	c-rating	Minimum SoC [%]	Charging efficiency	Discharging efficiency
90	45	0.5	10	0.95	0.95

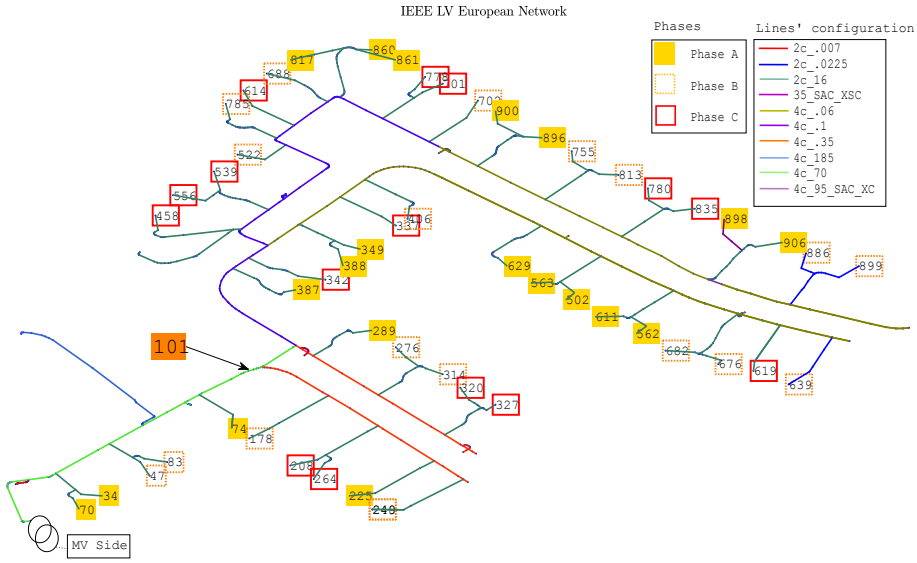

Figure 3.6: The IEEE European LV benchmark network. 55 consumers are connected to this case network; the position of the placed BESS_{101} is indicated.

The load and the microgeneration profiles used correspond to daily data for a summer period, which are extrapolated from realistic data pool provided for the benchmarked grid, which can be found in (Espinosa, 2015). All the microgeneration units are considered as single-phase PV rooftop installations which are connected to the same phase as the respective residential user. The simulation is for a representative summer week day where typically peak loading conditions occur.

Table 3.2: Electric Vehicles models and characteristics.

EV Model	Battery Capacity [kWh]	Charging Power [kW]	Driving Efficiency (km/kWh)	End-user owner
Nissan Leaf	24	4	6.7	249.2/861.1/264.3/522.2
Chevrolet Volt	16	3.75	3.75	327.3/755.2/886.2/906.3/780.3/ 619.3/899.2/337.3/701.3
BMW i3	22	11	7.2	785.2/225.1/314.2/320.3/ 817.3/702.2/178.2/73.1/342.3
Tesla S	60	11	6.7	563.1/47.2/208.3/682.2/406.2/ 248.2/458.3/83.2/349.1/289.1

Four EV models considered are based on four different EV models Nissan Leaf, Chevrolet Volt, BMW i3, Tesla S which present different technical features regarding the Battery Capacity and charging power, as well as their driving efficiency are considered from (Osório et al., 2018). Their characteristics are listed in Table 3.2, where $x.1, x.2, x.3$ implies connection at node x on phase a, b, c, accordingly. All Tesla S and BMW i3 models are charged with Efacec HomeCharger 7.4kVA, while the rest EVs are charged through an Efacec HomeCharger 3.4kVA (Efacec, 2018). Therefore, the maximum charging power of each EV is limited and driven by the home charger used.

Concerning the EV usage, a routine is built to emulate credible scenarios which is fed with public statistical data by (Survey). This routine aims to capture patterns pertaining the EV usage

upon different trip purposes as well as the trip duration (minutes) and length (km). The resulting data reflects a realistic response for the EV behavior during a day of operation, standing on the assertion that EVs charge exclusively at home. Nonetheless, the available statistical data do not explicitly provide information if the trip is from or to a destination. Therefore, the data as suggested in (Pedersen et al.) are split into starting a trip and ending a trip, and it is assumed that a driver starts and ends every trip at home. To assess the SoC change per each EV model used, averaged values for the purpose of each trip is used and correlated with each EV model's driving efficiency (Table 3.2).

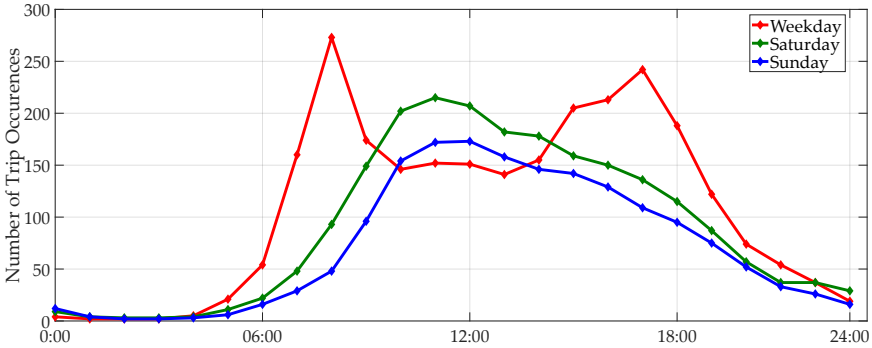

(a)

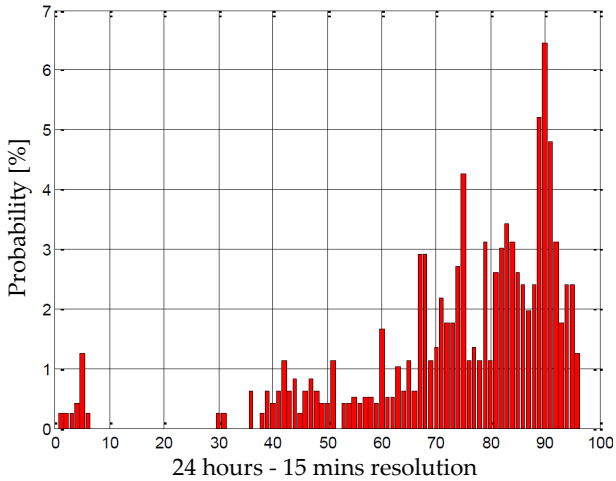

(b)

Figure 3.7: Data profiles: (a) Trips in progress along a week. and (b) probability density function for EV charging demand, used for the dumb charging scenarios (source: (Richardson et al., 2013)).

The following assumptions are also regarded for the EV:

- Initial SoC for all EV models is SoC_0=0.5 which is meant to be the same at the end of the horizon $SoC_{H\tau} = SoC_0$.
- The charging efficiency and discharging -when V2G- efficiency are considered 85% for all EV models.

Two EV charging strategies are considered in this study:

- "Dumb" charging or uncontrolled charging where the EVs are not incorporated within the proposed operational scheme.
- "Smart" charging, where the EV owner communicates relevant data (i.e. flexibility as defined above) regarding their commute and accordingly its availability to be charged according to the proposed tool. The V2G mode services enables the option to utilize the EV essentially for grid services. These constraints are automatically incorporated in the multi-period-OPF scheme as the generalized set of equations (5.4f)-(5.4g), whenever the availability of the EV allows it. The availability of the EV to charge is considered along the day during their idle periods (i.e. parked at the owner's house).

Concerning the case where EVs follow the dumb charging, their charging occurs based on the distribution function given by (Richardson et al., 2013). The time departure and arrival as well as the daily distance traveled by each are randomly selected for a summer week day.

According to the standard EN-50160, the 10 min mean r.m.s voltages shall not exceed the statutory limits during 95% of the week. Meanwhile, all 10 min mean r.m.s voltages shall not exceed the range of the Vn% + 10% and Vn%–15% (which corresponds to 253 V and 195.5 V for most European grids). Given the fact that the proposed control scheme uses 30-min averaged data resolution, the voltage limits are set in [0.95, 1.05] p.u.values (Masetti).

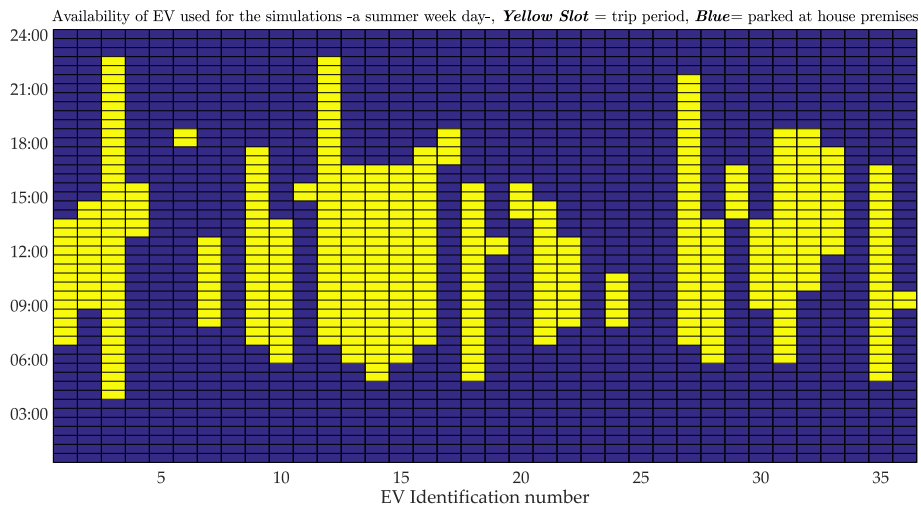

Figure 3.8: State of trip for Electric Vehicles used along simulation period. Profiles extracted for a summer week day.

The percentage of PV and EV integration refers to the proportion of end users that own such units. For instance, 35% of EV penetration (i.e. 30 EVs), where the charging point of the EV are indicated on last column of Table 3.2.

The use of DER is prioritized through the weighted terms $c_k(\tau)$, in the sense that the operational tool attempts to manage the flexibilities by addressing any voltage issues and respect secondary transformer's rated power with the controllable DER assigned with the more economical combination of $c_k(\tau)$. These $c_k(\tau)$ can be attributed with real operational cost values to reflect

monetary values for the use of flexibility. For this study the weighted terms for the use of flexibility for each type of DER derive a merit order scheme settled as $c_{BESS} < c_{EV} < c_{V2G} < c_{QR} < c_{APC}$, which present respectively the price of using the BESS, incorporating an EV in the coordinated charging, the use of V2G mode and finally the use of reactive and active power by the microgeneration. In this way the tool prioritizes the use of the centralized BESS which is owned by the DSO; avoids excessive active power curtailments and the presence of the EVs restrain the dispatch of reactive power by the PVs which is rather not effective for addressing voltage issues in LV grids (i.e. $R > X$). Note that in this study the V2G operation is set slightly cheaper than any control of the microgeneration (i.e. APC or QR), meaning that it is the last active measure to be used.

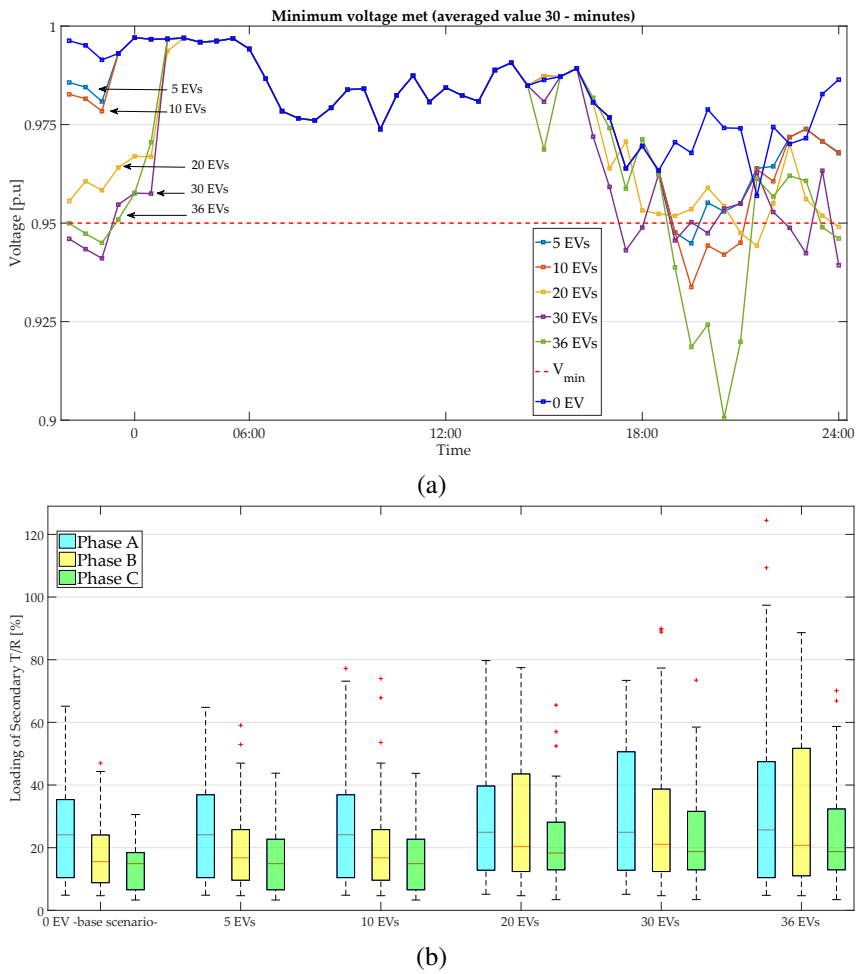

Figure 3.9: Incremental integration of EV scenarios: (a) Minimum voltage range over all phases and buses. and (b) Secondary transformer loading for each case of EV integration (the increase in loading is observed up to 120%).

Prior to the presentation of the results within the proposed control approach, an exploration of discrete incremental integrations of PV and EV are given. For both cases no control were deployed. In Figure 3.9a, the impact in voltage magnitudes is depicted; notable voltage drops can be observed for an EV integration about 35% (i.e. 20EVs). Higher EV integration of 55-65%

present severe voltage drops as well as overloaded condition for the secondary substations (see Figure 3.9b). In Figure 3.10a, the analogous scenario for PV integration is presented. Overvoltages appear in scenarios with more than 35% of PV integration, where the reverse power flow towards the secondary substation can be also viewed through Figure 3.10b. One can notice that in a mixed scenario with PVs and EVs overvoltages will typically appear during morning and evening hours, whereas voltage drops will arise at late hours when most regularly charging of EVs occur (see Figure 3.7a).

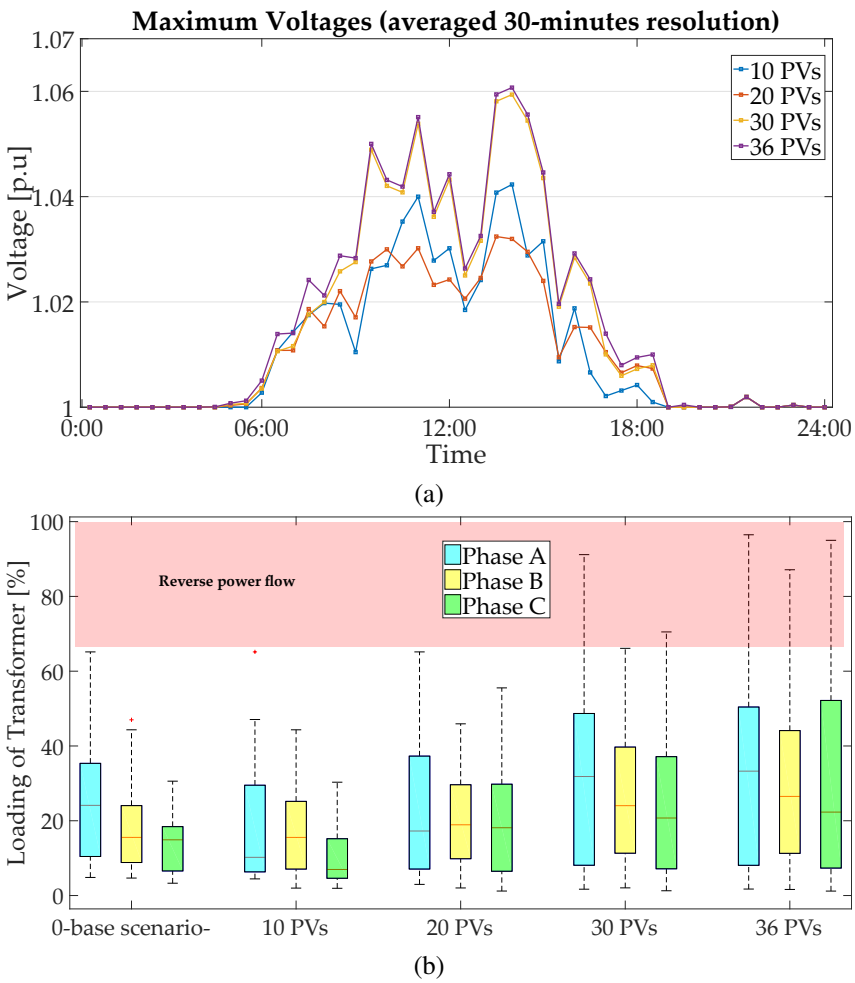

Figure 3.10: Incremental integration of EV scenarios: (a) Minimum voltage range over all phases and buses. and (b) Secondary transformer loading for each case of EV integration (the increase in loading is observable up to 120%).

The explored scenarios in which the proposed control scheme is validated are defined in Table 3.3. Analytical information regarding the points of connection for the micro-generation and EVs are given in the Appendix A.2. The scenarios are selected in order to validate that the MACOPF could allow high integration of microgeneration avoiding overvoltages and overloading of the transformer; secondly mixed scenarios of DER integration including EVs are assessed by the coordinated control amongst them.

Table 3.3: Scenarios description.

Scenario	Case 01 (C1)	Case 02 (C2)	Case 03 (C3)	Case 04 (C4)	Case 05 (C5)	Case 06 (C6)
EV [%]	0	0	0	35	55	65
PV [%]	55	73	85	0	0	35
BESS 101	✓	✓	✓	✓	✓	✓

3.6 Results

The assessment of proposed control framework takes places in all the scenarios for a day-ahead deterministic planning of operation with a time-step of $\Delta\tau$ =30 minutes, (i.e. 48 time steps). The available active measures for operational purposes are active power control of the centralized three-phase BESS, the coordinated charging of the EVs in addition to V2G mode of operation where both are considered once the EV is available (i.e. parked at house premises), and the control active and reactive power of the microgeneration. The setup for the controller considers minimum power factor for microgeneration 0.9 and maximum allowed curtailment 15% of the injected power by each unit.

3.6.1 Cases C01-C03

In scenario C01, with 65% (36 PV units) overvoltages (up to 1.062p.u) do arise along the grid due to notable active power injections. Additionally, reversed power flow is also present increasing the loading conditions of the secondary transformer up to about 90%. In Figure 3.11a, the actions taken along the horizon period are illustrated. Among the decisions, BESS_{101} is essentially charged during sunny periods, reducing the reversed flows to the substation and restraining the voltages. Ultimately, the voltages issues are addressed in coordination with reactive power dispatch by the microgeneration (Figure 3.11a). Note that the for the same PV integration scenario considering solely the use APC the total curtailments obtained through MACOPF are 5.3kWh, which corresponds to minimum curtailments since the controller is centralized (Figure 3.11b); hence, dealing with local P-V droop control would lead to higher curtailments since there would no topological confluence regarded among PV and the decisions are merely based on the voltage at the point of connection of the inverter. The coordinated control actions of BESS and reactive power dispatch are presented in Figure 3.11a. The BESS energy schedule can be observed with the green surface, where it is noticed that the BESS is discharging along morning hours up to 11.00 o'clock. At 11.30, the first overvoltages are detected and BESS 101 charges consuming close to 20kWh mitigating the voltage issue.

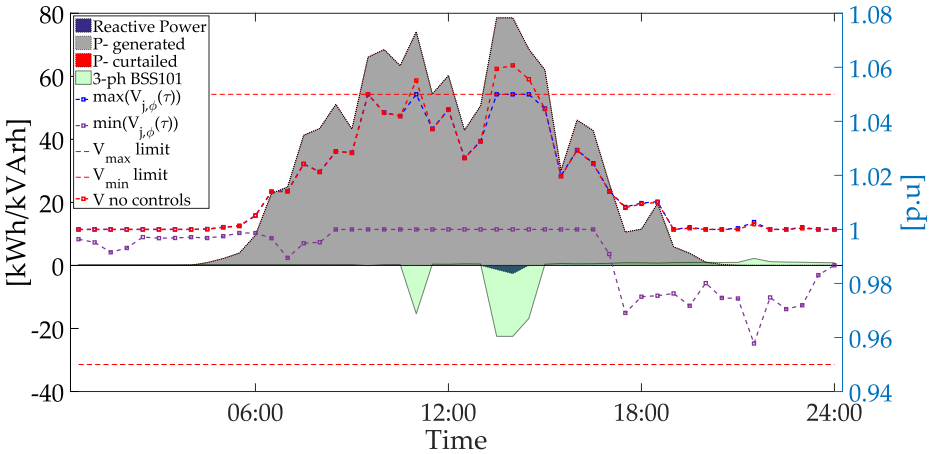

(a)

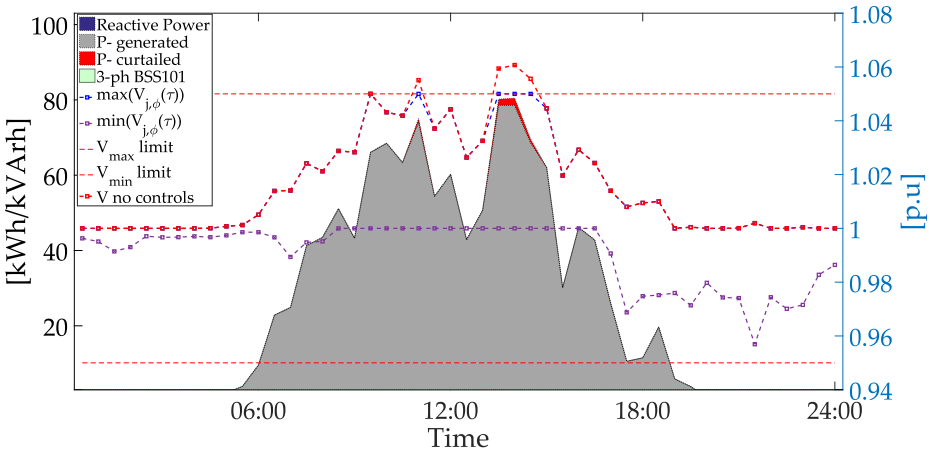

(b)

Figure 3.11: Incremental integration of PV: (a) Case 01.(b) Case 01, solely APC was selected within the controller.

The scenario 02 refers to the point of PV integration where overvoltages and secondary substation are within admissible bounds without curtailing any active power by the PV units. The subsequent controls derived in this case refer to the coordinated operation of the centralized BESS with reactive power dispatch of a set of microgeneration units. Maximum overvoltages without any controls reach 1.06 per unit in this case while the reversed power flow due to excessive PV production, arise the loading of the secondary transformer at about 110% of its rating. The coordinated operation of BESS and smart inverters reduce MV/LV loading to 90%, substantially, by reducing reversed power flows at the secondary substation level.

A higher integration is considered on C03. In this sceratio, given the following selected options for the controller (i.e. minimum PF=0.9 and maximum APC 15%), the proposed control is capable to mitigate overvoltages and ensuring rated power for the secondary substation up to 85% of PV integration. Analytically, the actions taken for this scenario are illustrated in Figure 3.12b. One can notice that BESS 101 is not adequate to regulate high overvoltage that reach 1.08 per unit. Therefore, MACOPF decides the coordination of active and reactive power support from the smart

inverters.

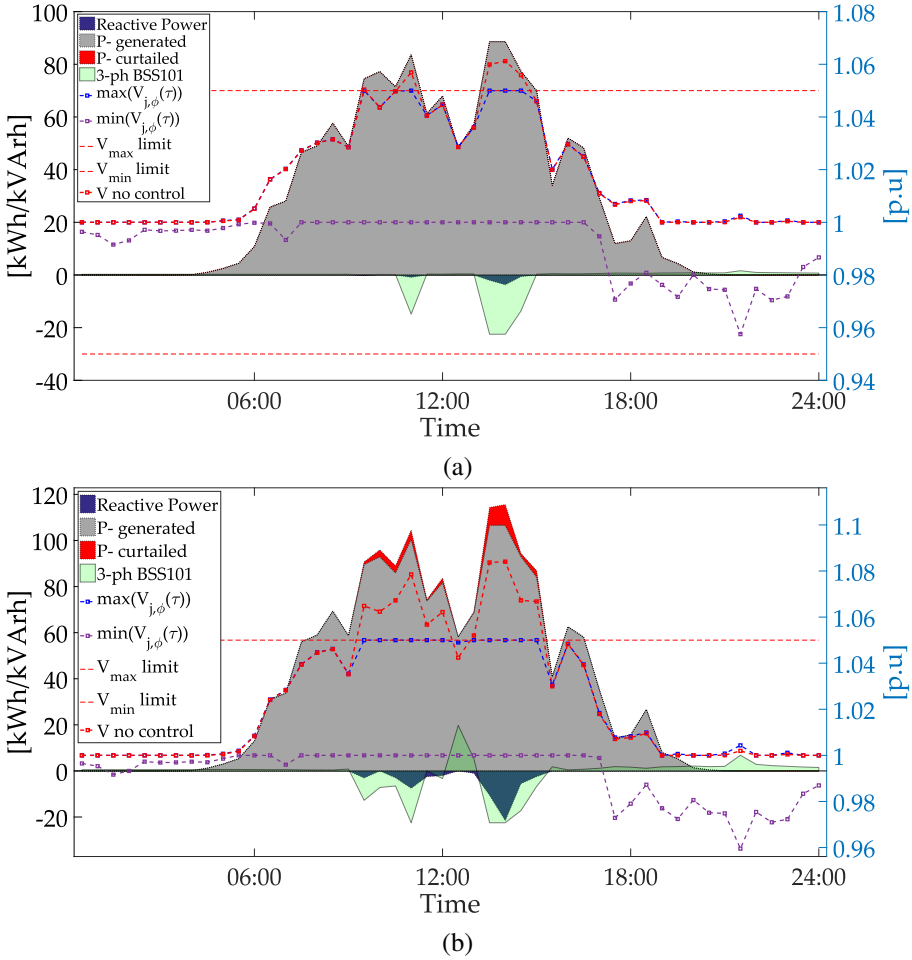

Figure 3.12: Incremental integration of PV, Cases 02-03:(a) Case 02. (b) Case 03.

In Figures 3.13a–3.13c, the derived control set-points are illustrated for scenarios 01-03. In all cases, it is observed that the BESS scheduled operation discharges during the beginning of the simulation (early hours) until the first overvoltages appear (i.e. at 11:30). In scenarios 01 and 02 almost the same BESS schedule is determined by MACOPF, obtaining charging slots for the BESS between 11.30 – 15.00, to mitigate the overvoltages provoked by the excessive PV generation. It should be reminded that among the BESS's constraints, the SoC at final slot should be kept equal to the initial one at $\tau = 0$. For this reason, the BESS is discharging, once there are no voltage constraints occurring, aiming at reaching $\text{SoC}_{H\tau} = 0.4$. On the other hand, the very intense overvoltages in Scenario 03 –due to the higher integration of PV–, the MACOPF foresees the expected overvoltages and discharges BESS even on sunny periods, yet when solar irradiance is lower and no overvoltages appear (12.30–13.30). During this interval the SoC decreases from about 60% to 30%. These actions target to allocate time slots when voltages issues arise, which apparently occurs between 13.30–15.00. At this period, the BESS charges at its maximum power rate 45kW mitigating all voltage issues, resulting to 100% at 15:00 o'clock.

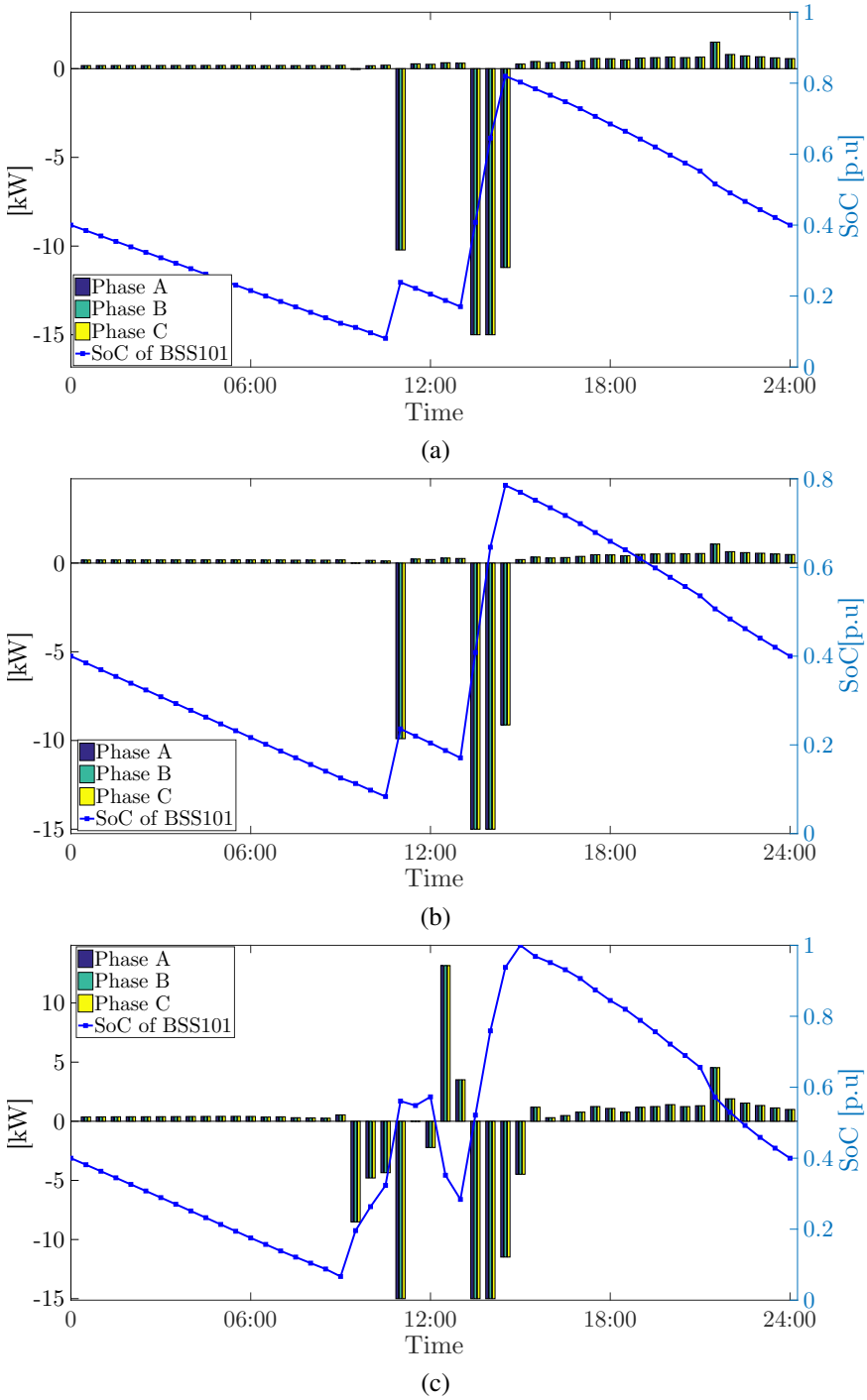

Figure 3.13: Control set-points and SoC derived by the MACOPF for centralized three phase $BESS_{101}$ for:(a) Case 01.(b) Case 02.(c) Case 03.

Figure 3.14, presents all cases C1-C3 and the corresponding transformer loading conditions if the decision derived by the MACOPF are followed. It is noted that in all cases the MACOPF delivers actions which restrain the reversed power to the secondary substation. Only in scenario C3 there a slight relaxation of the respective constraint since the all active measures have been optimally utilized. Table 3.4 presents the anticipated curtailed power and dispatch reactive power

within the day of operation for C1-C3.

Table 3.4: Resulting curtailed active power and dispatched reactive power for the microgeneration units.

Scenario	Curtailed Energy [kWh]	Reactive Energy [kVArh]
Case 01	0	3.94
Case 02	0	7.43
Case 03	34.5	59.3

Excessive active power curtailment may indirectly mean high compensation costs for the DSO. The installation of a BESS can reduce the need of APC as shown in scenarios 01-03. In particular, scenario 01 presented that solely based on APC 5.3kWh at least would be curtailed with local P-V droop based control. This fact may justify the investment from the DSO side when high integration of PV prevails.

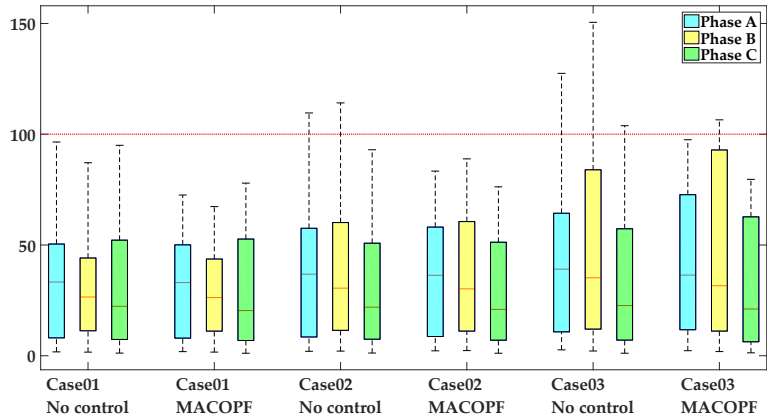

Figure 3.14: Secondary transformer loading conditions for Case 01-03, overloaded conditions are noticed due to reversed power injected by microgeneration units; admissible conditions are obtained applying the proposed coordinated operation.

As a remark, the current analysis is performed averaged values of 30-minutes resolution; therefore, notable overvoltages may appear in higher resolution analysis for less PV integration. The latter justifies the tight limits posed for the voltage magnitudes for the purpose of this study. Concurrently, the importance of coordinated actions will be observable even in scenarios with less PV integration.

3.6.2 Cases C04-C06

In this part of the study the EV integration is introduced within the LV grid. Initially, cases 04-05 examine the integration of 20 and 30 EV accordingly. The EV are randomly distributed along the end-consumers, only following the assumption that no more than one EV can be connected at each consumer. The point of connections for each scenario are given at Appendix A.2.

Case 04 presents voltage drops along the early hours (00:30 to 04:00) but most significantly and below the posed lower limits at late hours where the peak load is met (21:00-22:00). In this scenario the MACOPF derives an optimal scheduling (Figure 3.15b) of the DSO's BESS in order to address the undervoltages at late hours. The coordinated charging for the current case is not deemed to be needed according to the proposed control. Nonetheless, it can be seen from Figure 3.15a that a slight increase of the peak load (i.e. hereby 18:30 to 23:00) might arise critical voltage sags and possible transformer loading conditions. It should be stressed that the 35% integration of EV, following dumb charging, leads to an increase of 22% of the peak load compared to the base case.

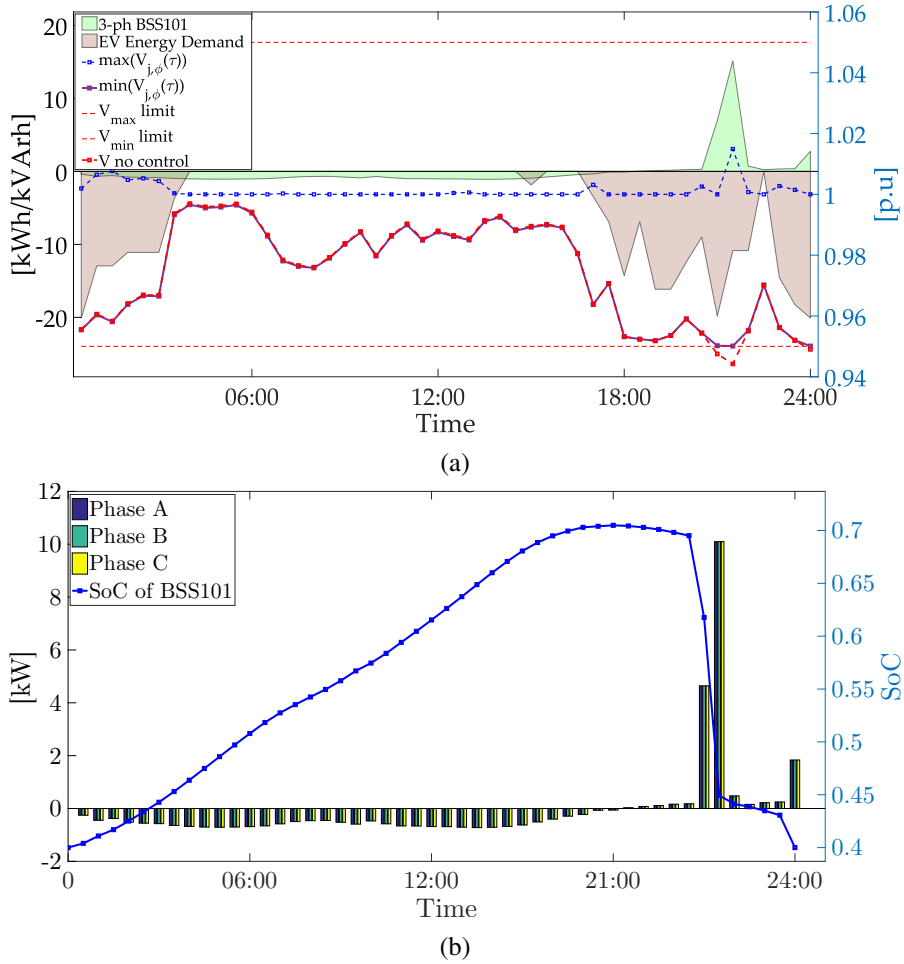

Figure 3.15: Case 04: (a) Resulting voltage ranges and actions yielded for $BESS_{101}$.(b) Control set-points and SoC for $BESS_{101}$.

The following scenario C4 emulates a case with 55% of EV integration. In this case the importance of multiple DER coordination is stressed since critical voltage sags can be noticed if EVs follow the dumb charging operation. The MACOPF yields a scheduling for the $BESS_{101}$ which essentially supports during the late hours (i.e. 20.00-21.30) in addition to some EVs that are decided to operate at V2G mode. The peak load conditions along this interval is deteriorated

due to the EVs that are added to consumption while returning from their trips. The coordinated charging during the early hours avoids the voltage drop along the distribution feeder which would be noticed in the uncoordinated charging (Figure 3.16a).

The centralized $BESS_{101}$ is not adequate to entirely mitigate voltage problems due to the fact that some of the EV are connected to ending point of the feeder. Therefore, V2G mode of operation (i.e. for EVs that are willing to provide it) and coordinated charging efficiently added to the coordinated operation to maintain the voltages within the bounds. The SoC for all EVs are illustrated in Figure 3.16b. The V2G mode of operation comprises generally an effective measure to address undervoltages in LV grids due to the fact that active power is purely injected ($R > X$). Nevertheless, proper spatial and temporal distribution of the available EVs to provide such service is necessary. The spatial distribution refers to the bus and the phase of connection of the EV, whereas the temporal distribution to the availability along the horizon.

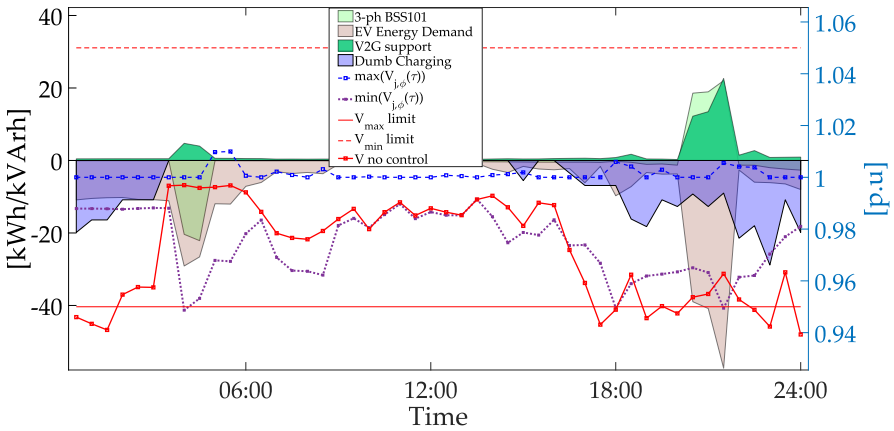

(a)

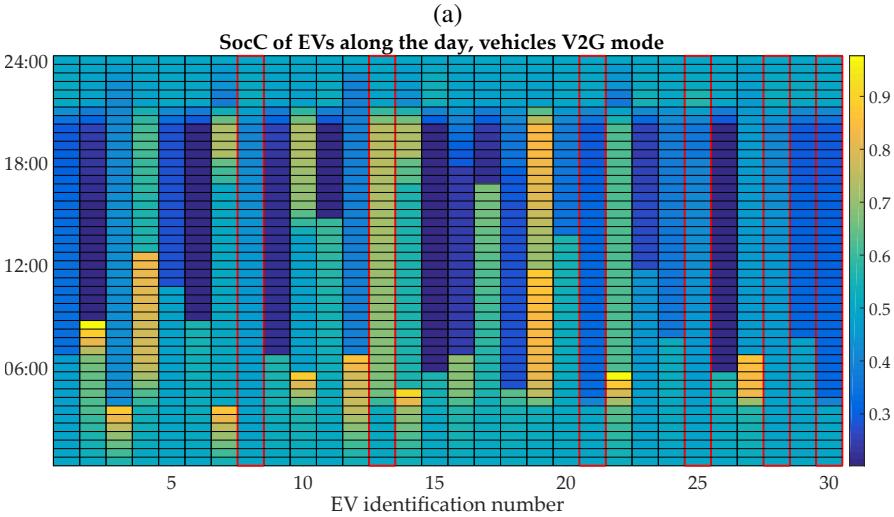

(b)

Figure 3.16: Case 05: (a) Resulting voltage ranges, coordinated charging in comparison with dumb charging; $BESS_{101}$ scheduling of operation and V2G actions.(b) SoC for all EVs; circled by red line correspond to V2G mode of operation.

The following scenario C06 presents a case with increase PV and EV integration (i.e. both

55% and 65% respectively). The presence of PV installation injects notable active power during the sunny period (10:00 to 15:00), whereas at the rest of time slots voltage drops are observed due to the dumb charging. Notice that in the current study, the PVs and EVs are randomly distributed, in the sense that a PV installation is not necessarily connected at a point were an EV is placed (see Table A.1 and A.2). In addition, the fact that the majority of EVs are on trip progress along the sunny hours, essentially implies that only a few could be available to be shifted for charging at this time slots. The subsequent results for this case are illustrated in Figure 3.17a. In this scenario as it can be seen from the SoC of EVs in Figure 3.17b, the EVs are charged within a coordinated way during the 00:00 to 05:00 where light loading conditions prevail in the grid avoiding the undervoltages which are present within the dumb charging. Nonetheless, due to increased charging demand, idle EVs provide support at the slot 05:30 as well as at 17:00 to 18:00, maintaining the voltages within the bounds. Accordingly, during sunny periods shifted EV charging can be noticed as well.

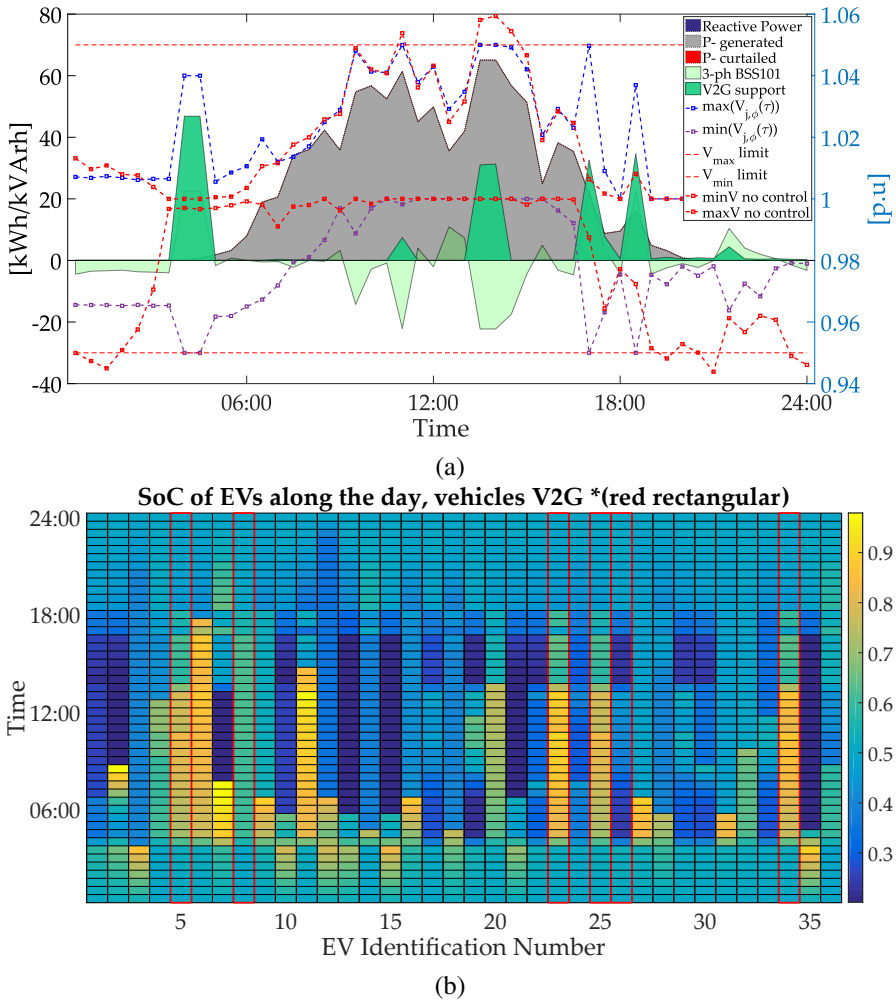

Figure 3.17: Case 06: (a) Resulting voltage ranges, coordinated charging in comparison with dumb charging; $BESS_{101}$ scheduling of operation and V2G actions.(b) SoC for all EVs; circled by red line correspond to V2G mode of operation.

3.7 Final remarks

This chapter presented a tool which is capable of providing support to the DSO decision for the operation of LV three-phase distribution grids with increased integration of DER. The computational techniques proposed based on the explicit calculation of the first and second order derivatives (i.e. Jacobian and Hessian of the Lagrangian and the objective function) in addition to pivotal adjustments in the Jacobian, ensure a tractable optimal control based on the exact AC power flows.

The proposed centralized scheme ensures admissible voltage profiles by minimizing the active power curtailments of microgeneration through the efficient coordination of DER; maximizing, in this sense the integration of microgeneration. The coordinated operation among the DER units reassures in the presented study up to 73% integration of microgeneration avoiding any curtailment brought by PV units. The EV integration can be also maximized if coordinated charging is adopted within the MACOPF which essentially can ensure admissible voltages and normal loading condition for the transformer. The V2G mode of operation can regarded important when high integration of EV takes places with increased peak load conditions in the grid.

For all simulated cases, one can conclude that the radial configuration of LV networks present overvoltage issues particularly in buses -electrically- furthest from the substation since the high resistance of the lines leads to the aggravation of them. In addition, distant nodes at ending point might face significant voltage drops (i.e. if EVs are present) or even overvoltages (i.e. if PVs are present). Therefore, the placement of a BESS in proper location (i.e. adjacent to nodes with voltage issues) along the grid is rather crucial since the installation adjacent to the secondary substation provides mainly reduced loading for the transformer rather than voltage support to the furthest points. Nonetheless, the assessment of this Chapter does not regard line ratings; such constraint is explored in the following Chapters, where there are scenarios detected with line congestions being the most severely binding constraint.

The proposed control scheme is based on deterministic analysis for the planning in day-ahead scale the operation of the grid. Meanwhile, the scheme can be deployed only by the subsequent communication technologies (for online implementation), together with forecasted data and power flow-state estimation tools (i.e. if topology is not known).

The MACOPF framework is capable to coordinate several DER and DSO asset and propose their optimal coordination to schedule the safe LV grid operation; yet, corrective control actions closer to the time of the delivery are necessary to deal with uncertainties and stochasticity (e.g. forecast errors, stochastic behavior of loads and EVs *etc*). Such advancements of MACOPF will be discussed in the following chapters, along with the incorporation of OLTC as well as extension of the presented problem to a multi-objective one.

Chapter 4

An active network management operational framework for unbalanced LV grids

The ever-increasing integration of multiple types of Distributed Energy Resources (DER) raises the concerns for the modernization of operation and planning strategies of distribution networks. Distribution System Operators have to harmonize the grids 'operation ensuring safe and cost-effective energy delivery addressing the complexity and any technical challenges provoked by extensive DER integration. This chapter proposes a substation centered scheme and architecture for the safe operation of unbalanced Low Voltage (LV) distribution networks with increased DER integration. A planning algorithm is proposed for sizing and the placement of battery storage system extending the multi-period AC optimal power flow scheme. The substation centered active network management framework is comprised of three temporal operational stages: the scheduling of operation, the intra-day corrective actions and real-time local controls. The first two stages are based on the proposed optimization multi-period AC optimal power flow framework stated in the Chapter 3. Forecasting errors of microgeneration (μG) and load profiles are handled by refreshing the scheduled actions with event-triggered second stage; hence, the likelihood of insecure operation is restrained. Close to real-time local actions deal with the high stochasticity of residential loads along with the intermittent Photovoltaic generation. A case study is presented for the particular case of high integration of Electric Vehicles in an unbalanced LV distribution network, demonstrating the importance of coordinated smart changing which may be derived by scheduled actions.

4.1 Literature review on distribution management applications for LV grid operation

In the literature there focus attended for advanced active network management controls for all types of DER met as well as manners of coordinating them with DSO assets. There is a plethora of research works that propose control schemes for multiple types of DER in order to mitigate technical bottlenecks on the LV networks, or even to optimize some technical or economical objectives. A taxonomy of such works is presented in this chapter. Firstly, an exploration of pilot projects that have proposed conceptual frameworks for control and management architectures for distribution networks (MV and LV). Towards the modernization of distribution networks' operation from classical vertical and centralized management to decentralized multi-agent based system, the main theme and rationale will be highlighted. Following, the review focuses particularly, on works that have been proposed for the LV distribution grid.

4.1.1 Alternative Control & Management architecture for the LV operation

The large-scale integration of renewable-based Distributed Generation (DG) –particularly micro-generation at the LV level– may brings technical problems to distribution systems as discussed in previous Chapters. These may be tackled either reinforcing the network (e.g. additional distribution lines), or by enabling the DER as flexible resources which can provide control functionalities for the grid operation (Löf, 2013).

In the previous decade, the utilities commenced mitigating such technical challenges through the implementation of Demand Response (DR) schemes or self-consumption practices. The DR may occur on shifting load either to the periods when Renewable Energy Sources (RES) are available or from peak hours to valley hours, granting better prices for consumers and facilitating secure grid operation (Bai, 2016). A very common approach in the direction to compensate the intermittency of RES, is the installation of storage devices, which basically provide a surplus of stored energy available to be injected on the grid when the DG is not available –particularly if DG plays the role primary source–(Miranda et al.). Nevertheless, the extensive integration of several DER technologies, should be concerned as an active appendage of the grid participating on the grid operation rather than being a bottleneck from technical and economic standpoint. In (Eid et al., 2016), it is stated that the deployment of DER has to follow an active approach, since these sources could bring a significant amount of flexibility capacity for operating purposes.

The deployment of DER in distribution networks – including mDG and μDG units, loads under DR, EV or stationary storage systems – requires a change from a traditionally passive approach into a fully active approach. In this context, active network management can be regarded as a way to achieve cost-effective solutions following DER integration in distribution grids at both the planning and operation stages of the distribution system (Djapic et al., 2007).

4.1.2 Conceptual control frameworks

Active control actions over multiple DER technologies are essential to overcome technical problems that may arise (such as poor voltage profiles or branch congestion). Yet, network control is a rather complex issue that requires the development of specific and dedicated solutions (Matos et al., 2016). Notwithstanding, the control and operation of traditional electricity grid is organized in a purely centralized way. Future distribution networks require novel planning schemes for novel decentralized network architectures able to incorporate all these new grid elements, including the need for new design and planning tools that rely on heuristics, probabilistic approaches and multi-scenario analyses (Madureira et al., 2009).

Economics are moving the utility resource mix from traditional generation to central station and distributed renewables. This fact, will lead to a new way of operating the system and to a new utility business model. In the literature the operation of distribution networks is addressed with several different control architectures tracing the transition from passive to smart by taking advantage of the IEDs and high-performance ICT (Evangelopoulos et al., 2016). The discrimination of the control architectures can be organized as follows:

- *Centralized control architectures:* decision of control actions is made at DMS and SCADA system levels, through Power Applications. Centralized approaches require critical investments in communication infrastructure of utilities, since several metering data has to be aggregated on the control centers. Such architectures have been pushed back with the evolving changes in the generating technologies as well as the distributed automation along the grid, signifying the necessity to transit to less centralized planning and operation, approaches possibly with additional layers of control.
- *Decentralized control architectures:* this approach considers that along the grid exist components (such as DER, Shunt Capacitors, OLTC) capable to act as individual agent (local intelligence) with limited communication exchange. Decentralized control architectures are usually settled into two-way communication technologies the so-called Control Net Protocol (CNP) or based in Multi-Agent System (MAS) technologies which provide peer-to-peer or distributed control.

  There several works in the literature dedicated on this approach as in the pilot European project INCREASE, where the multi-agent based system (MAS) is set for the Smart Grid implementation. In this approach the MAS was used as the top hierarchical layer of the control structure (Andreas Tuerk, 2017), as part of the discrimination featuring Local Control, Overlaying Control and Scheduling Control. A middleware layer, is used to perform agent-aggregator architecture, with two types of software based agents the grid agent and the DER agent. The above multi-level control strategies target in mitigating voltages in LV networks with possibility of coordinating assets/agents, and avoiding branch congestion through scheduling units participate in DR.
- *Hierarchical control architectures:* it is based in multi-level strategy, that usually, has at least one controller along each hierarchical level. Each of them has a certain degree of autonomy

as well as the ability to communicate with other controller or layers in order to make decision for control actions. A typical implementation of this control strategy is the microgrid and multi-microgrids concept. Several pilot projects as the *MICROGRIDS* project, where the microgrid is introduced as an LV modular compartment of the main grid, to which other electrical and micro generation units are connected. On the same pilot project, a very first hierarchical level was envisaged at the level of the MV/LV substation, entitled MicroGrid Central Controller (MGCC), which is responsible to host control and management functionalities as well as a point of interface with the main grid (upstream) (Madureira et al., 2011). A second hierarchical level follows, which is refers to local controllers for the loads called Load Controller (LC), and microsource controller (MC) for each microgenerator unit. Several advanced control algorithms have been proposed in the literature for this particular control strategy, in order to optimize the economic operation of the microgrid (Dimeas and Hatziargyriou, 2005; Hatziargyriou, 2014; Zakariazadeh et al., 2014), perform advanced control for LV grid control (Olival et al., 2017) or even algorithms for the islanded operation (Gouveia et al., 2014). Further projets on that direction extended the microgrid concept to the multi-microgrids where an additional upper hierarchical layer added to the HV/MV primary substation called Central Autonomous Management Controller (CAMC), caters for coordinated operation of the microgrids and manages the MV network ().

In the InovGrid project a purely hierarchical structure was selected, where each level of control fits to each corresponding voltage level, (Matos et al.). According to (Silva, 2010), one control layer is accommodated at the primary substation (i.e. HV/MV), where is encompassed a control called Smart Secondary Substation Controller (SSC), where control functionalities for the MV are being performed. Another control layer is regarded for the management of LV network, which is regarded as each secondary substation (i.e MV/LV) equipped with a Distribution Transformer Controller (DTC). A SCADA/DMS system is considered for the overall supervisory control, data acquisition and event logging.

In a more recent project DREAM (Kamphuis et al.), the proposed architecture is based on a "hierarchical" or heterarchical approach, which has the particularity that changes configuration according to the current operating status of the grid. This is accomplished through agent-based Virtual Power Plants' (VPPs) configuration, which can switched if any congestions occurred. In project SuSTAINABLE, a hybrid architecture was designated that leverages hierarchical (each voltage level comprise a control layer) and distributed control functions (project, 2012).

There is much discussion exploring the potential among the above presented operational architectures. From the one hand, according to (Dimeas and Hatziargyriou, 2005), a decentralized architecture with MAS presents the great potential that the amount of data processed at each node is less, comparing to a centralized one where several data has to flow up to the central controller. The latter implies that less communication infrastructures are needed in the decentralized approach since only a local network is sufficient to support the interaction of agents.

Comparing the aforementioned framework approaches, there are several advantages and disadvantages that namely refer to communication infrastructures, reliability, scalability and complexity of the system, which are analytically discussed in (Matos et al., 2016). In this research project, the secondary substation will be responsible for the LV distribution grid operation, possessing a layer of control which will certainly has notions of interactions with the upstream levels.

4.2 Advanced control strategies for the LV network operation

The interconnection of DER in the LV networks, arise the notion to treat these resources in such way to supply anciallary services for grid operation and accept on-line requests from the utility. In this section a literature overview takes place in order to map the most influential proposed works, as well as to identify the research gaps oriented to the coordinated use of DER at the level of LV.

The state-of-the-art on operation schemes for LV network are organized as follows. The studies are analytically organized by the type of the control strategy used, and the objectives of each case as well. As it is depicted in Figure 4.2, the synthesis of the problem is comprised of several structural particularities of the optimization problem (i.e. objective terms, control variables, constraints, DER types). In Figure 4.1, a further discrimination is used according to the framework architecture, the types of DER used and any capabilities of coordinating other DSO assets.

Accordingly, in the literature there are different alternatives to cope with the several objectives such as optimizing the economic operation of the grid which is accomplished by minimizing power losses or cost of use of the assets, or to manage the operation of the network by minimizing voltage deviations. Following these discriminations table 4.3, includes some of the most influential studies that were found.

In recent work (Evangelopoulos et al., 2016), the authors introduce a relevant taxonomy of models and optimization methods that are applied to resort to optimal operation of MV distribution networks with extensive integration of DERs, under several objectives. In this section, we further expand this approach focusing on advanced strategies which lead to controls for DER in order to optimize technical (e.g. optimize LV operation) or economical (i.e. DSO or end-user perspective) objectives.

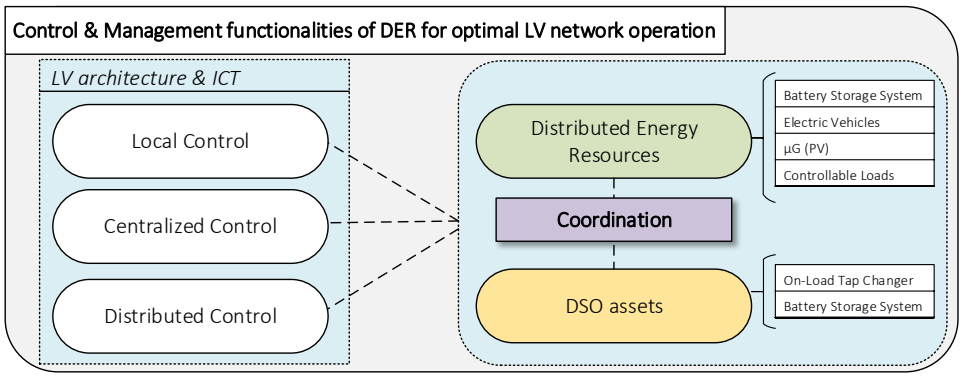

Figure 4.1: Control and management functionalities of DER.

4.2.1 Problem synthesis

In the exploration of the literature, the management and control of DER is posed as the problem to determine the optimal values of control variables subject to technical (e.g. minimum cosφ value) and operation constraints (e.g. voltage limits), provided the type of DER specification and the reliability of power system. Several approaches address the management of DER by setting an Optimal Power Flow (OPF) technique; depending on the mathematical model chosen, the opted objective function and the mixture of control variables (i.e. continuous or discrete), the problem might be discriminated in linear problem, non-linear problem, mixed-integer linear or mixed-integer nonlinear optimization problem (Zhu, 2015a).

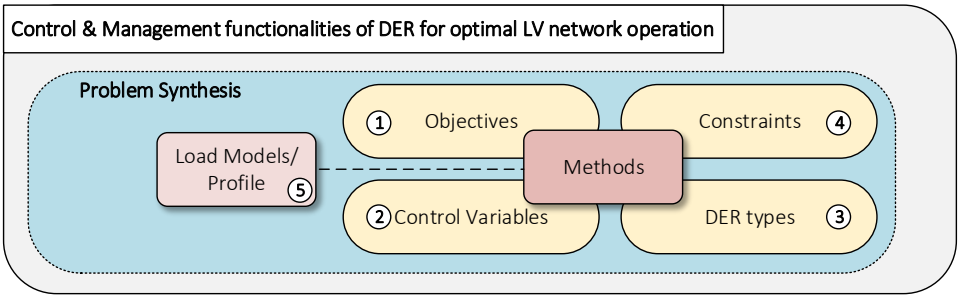

Figure 4.2: Problem Synthesis: Optimal LV network operation through DER management.

4.2.2 Objectives

The main objective functions found are addressing the (1) minimization of power losses, (2) minimization of micro-DG curtailment (3) minimization of operational costs (4) maximization of total profit of either DSO or consumer, (5) maximization of consumer's benefit and (6) minimization of voltage deviations. It is plausible that the main objectives are techno-economically dependent on the stakeholders' benefits (i.e. DSO, end-user and aggregator). Other objectives may be related to indirect operational cost such as the minimization of DER flexibility activation costs or energy costs.

4.2.3 DER types

The DER might be segregated into μG/mG, Battery Storage System, EV as well as flexible demand (e.g. controllable loads) under a demand response scheme. In the literature, most work are addressing the management of one DER at each time, while only in (Costa et al., b) consider the coordination of them for network operational purposes.

4.2.4 Constraints :Operational requirements & Technical constraints

In the frame of LV distribution network operation, there are several constraints that have to be posed regarding the controllable assets (e.g. On-Load-Tap Changer step changes), technical limits of controllable DER (e.g. active and reactive power generation) as well as limits for the grid

itself (e.g. branch congestion, nodal voltages). Regarding the limits of controllable DER there are implications that they are additionally undergone to the regulatory framework set forth. Furthermore, constraints related to DER operation are not limited to technicalities (e.g. for a BESS the consideration of maximum power rate), but also associated with the strategy of operation considered. For instance, constraints related to EV charging operation should clearly state if Vehicle-to-Grid (V2G) mode is regarded or minimum SoC at the end of the horizon and other suchlike inter-temporal constraints possibly associated with pricing scheme applied. The grid operating constraints (i.e. admissible voltage magnitudes and voltage unbalances, branch congestions) have to be respected so as to ensure the secure operation of the network.

4.2.5 Type of control architecture

Several advancements are taking place concerning smart metering apparatus, advanced automation (e.g. IED, controllers) as well as several communication technologies ICTs towards smart grid implementation. Some of the schemes proposed in the literature might be classified as centralized, since the control actions are computed by a central entity which caters for gathering information about the network, processing them according to some optimization objectives and constraints, and sending the set-points back to the actuators. In such schemes, the decision of control actions often relies on optimal power flow (OPF) formulations of the problem and require extended communication infrastructure along with the need of an accurate network model. In centralized schemes, simplified local controller may be additionally deployed for droop-based voltage control strategies or load balancing (Weckx and Driesen, 2015b).

Following, a second category of schemes refers to distributed: the controllable units along the grid are controlled in a distributed fashion without the existence of a centralized control entity. The distributed controllers often use local information to adjust each unit individually; hence, in most cases are grid agnostic.

A last category of control schemes, relies on the combination of centralized and distributed schemes, usually decentralized. More specifically, they are composed of local controllers and a centralized entity which computes the control set-point to be sent to them, so local communication is always needed.

4.2.6 Load and DER models

The load data models might vary from case to case, according to the control strategy under consideration. In table 4.1, a categorization of load models is suggested depending on deterministic and stochastic analysis. As aforementioned, most DER are, generally, characterized by their intermittent and stochastic nature, fact which impacts on the operation of the distribution grids (Zangs et al., 2016). Therefore, a methodological assessment of a control strategy, might consider different load model depending on the optimization approach and the assumptions made (Evangelopoulos et al., 2016).

In (Navarro et al., b), it is stressed that an adequate assessment to consider the stochasticity of DER, should follow a Monte-Carlo based technique in order to introduce the uncertainties. Nevertheless, analysis of load and generation may follow hourly resolution data as was carried out in (Widén et al., 2010), where it is stated that a time step of one-hour is efficient enough to estimate network voltages. Undoubtedly, an analytical quantification of the DER impact on the grid should follow a non deterministic approach, possibly through a Monte-Carlo (Navarro et al., a) or through probabilistic density functions for the data of DER behavior (Zangs et al., 2016).

In case of long term evaluations (i.e. one year), simplification can be made to reduce the computational burden, by clustering data for certain periods. The authors in (O'Connell et al., 2014), address an unbalanced load flow and a rolling optimization data using multi-period analysis for the day ahead operation. More simplified approaches (e.g. deterministic and/or snapshot) of uncontrolled DERs that do not concern the random nature of these resources (e.g. the randomness of -uncontrolled- charging of EV) are presented. For instance, (Quirós-Tortós et al.), a probabilistic impact assessment of realistic uncontrolled charging is accomplished, focusing on highlighting the uncertainties associated with household demand. In (Ochoa and Mancarella) the EV charging behavior is analytically introduced by using probability distribution function for starting an EV trip at a certain hour.

Table 4.1: Load model segregation.

Stochastic	**Deterministic**
Probability density	Time series Analysis • daily load profile • multi-period (cluster) load profiles
Monte Carlo Simulation	Snapshot Analysis

4.2.7 Optimization Methods

Among relevant research works several methods were noticed in the literature to resolve the optimization problems to achieve the optimal operation of the LV distribution networks towards different objective terms. These methods may be divided as shown in table 4.1. In this part, the discussion does not focus to compare each programming formulation from the computation viewpoint; the target is to explore the most common formulations for operational purposes, the DER active management as well as the objective terms. It should be also noted that the majority of the cited research works included in the taxonomy, implicitly include the power flow calculations either through their exact formulation or based on linear or convex approximations.

4.2.7.1 Numerical Methods

Linear Programming The Linear Programming (LP) based optimization techniques typically lie on the equivalent linearized power system problems (e.g. an OPF) (Zhu, 2015b). An optimal LV network operation is proposed in (Bertani et al.), where the two-stage scheme includes several

Table 4.2: Categorization of methods explored in the literature incorporating DER for LV grid operation.

Numerical Methods	Heuristic Methods
Linear Programming (LP)	Evolutionary algorithm (EA)
Non-linear Programming (NLP)	Stochastic algorithms (SA) {fuzzy sets}
Interior point (IP)	
Quadratic programming (QP)	
Sequential Linear-Quadratic programming (SQLP)	

DER to participate,targeting to match techno-economic constraints with the objectives posed by the co-generation. Only the second stage of this problem targets to propose corrective control actions, through a LP.

In (Richardson et al., 2012), an optimal charging of EVs based on LP targets to maximize the total power that can be delivered to the vehicles while operating within network limits. This approach requires advanced ICT, but provides only efficient control actions that benefit a very narrow objective. (Olivier et al., a), proposes a centralized approach that uses voltage sensitivity factors (i.e. derived by linearizing the power flow equation) Forward Backward Sweep OPF ((Fortenbacher et al.)) which targets to increase the generated power by distributed resources, mitigating any overvoltages, but merely proposing curtailments of PV generation. Another distributed control scheme is also developed on the same work which is shown to lead partially to an optimal solution. The operation of those distributed controllers follows a machine learning technique which adopts a learning process from the decision making patterns derived by the centralized solution. A tractable multi-period OPF is proposed in (Fortenbacher et al.), for the coordination several DER. Linearized approximations of the power flow equation are proposed allowing the exploitation of this framework for planning (i.e. optimal sizing and siting of BESS) and operation stages; yet, dealing only with balanced networks.

In the same category of LP, the Mixed-Integer LP (MILP) may be classified, which essentially provides the flexibility to apply integer decision variables as well. A centralized co-optimization operation and planning control scheme for balanced LV distribution networks is proposed by (Karagiannopoulos et al., a). This approach advances the scheme of (Fortenbacher et al.), by incorporating controllable and OLTC as well as by introducing an iterative process for the calculation of state vectors. At the end of each optimization's iteration, authors propose the analytical computation of the voltages and currents after each OPF solution, which can improve the convergence of the BFS-OPF, particularly when the current operating point is away from the optimum or close to the stability limits and a single BFS iteration would not give a good approximate of the values. The same authors, propose a decentralized control scheme which is based on machine learning techniques to obtain close-to optimal control actions in (Karagiannopoulos et al., 2019). The local controllers are tuned properly based on the optimal results derived from the centralized multiperiod OPF. Subsequently, the droop functions of local controllers are trained with machine learning techniques to follow the predetermined patterns. Any suggested control and management

framework may need to be harmonized with concepts under deployment such as local energy communities, and subsequent AMI.

Non-linear Programming Generally, the power system problems (e.g. power flows) are non linear (Zhu, 2015b);hence, non-linear programming (NLP) based techniques can address this sort of complexity. The authors in (Acha et al.), propose a time coordinated optimal power flow, aiming at a minimization of active power losses by efficiently controlling the PHEVs (including Vehicle-to grid operation) and an OLTC transformer. This work leans on a piecewise NLP based problem that uses a weighted linear objective function that thrives to reduce power losses throughout network with the least number of tap changes, considering Electric Vehicles charging and V2G approach. Nevertheless, this control scheme mainly relies on the optimal operation of the EVs. Lately, researchers' focus has been attended on compact multiperiod OPF formulation addressed as a NLP class. For instance, (Costa et al., b) propose an AC multi-period OPF for LV distribution networks resolved with interior point algorithm, extending essentially the scheme proposed by (Tavares et al.) which in turn was applied in MV networks. Yet, authors do not provide analytical discussion concerning the inter-temporal constraints. A very recent work proposes an efficient distributed framework for the resolution of NLP multiperiod OPF. The resolution of the initial problem in a distribution fashion allows the fast convergence and resolution, but also makes it compatible for the orchestration of local energy communities' operation.

In (Efkarpidis et al., 2016a), an optimization scheme is proposed that controls both the magnitude of nodal voltages and the voltage unbalances of an LV network, by coordinating the OLTC of the distribution transformer with PV and BESS. This optimization control is formed with mixed-integer variables (i.e. decision variables the tap positions, $x_t \in \mathbb{Z}$), in order to minimize the distribution system's cost in addition to domestic consumers' cost; thus, it is classified as a mixed-integer non-linear programming (MINLP). Nonetheless, this multi-objective control scheme, does not provide fairness criteria between DER, resulting to excessive use of OLTC. From the standpoint of resolving this category of optimization problems, it is suggested to introduce the relaxation of integer variables and resolve the equivalent NLP one (Nocedal and Wright, 2006). A MILNP is additionally used in (Madureira et al., b; Costa et al., a) to solve an optimal three-phase power flow, which targets to regulate the nodal voltages of the LV grid by enabling larger deployment of DER. This approach presents interesting considerations according to the degree of observability of the grid at the level of the substation. Nevertheless, these approaches do not extend the operation of DER to provide flexible resources or further techno-economic optimization on the operation of the grid, since local set-points are used to only mitigate overvoltages.

Table 4.3: Overall mapping of the review literature.

Reference	Control Arch	Optimization	DER	Objective
(Acha et al.)	Centralized	LP (TCOPF)	PHEV	$min\{$Power Losses$\}$
(Bertani et al.)	Centralized*	IP & LP (multi-stage)	Multiple DER	$min\{$Operating Costs$\}$
(Richardson et al., 2012)	Centralized	LP	EV	$max\{$Energy EVs at charg. period$\}$
(Olivier et al., a)	Centralized	LP (FBS-OPF)	PV	$max\{$host DG in LV network$\}$
2-Techniques	Distributed	Machine Learning	PV	$max\{$host DG in LV network$\}$
(Efkarpidis et al., 2016a)	Centralized	NLP	PV	$min\begin{bmatrix}\text{Power Losses, OLTC operation}\\ \text{Reactive Power, BESS Operation}\end{bmatrix}$
(Madureira et al., b)	Centralized	NLP	multiple DER	$min\begin{bmatrix}\text{Power Losses}\\ \text{RES curtailments}\end{bmatrix}$
(Costa et al., a)	Centralized	NLP (OPF)	multiple DER	$min\{$Deviation Actual-Exp. Net-load$\}$
(Tavares et al.)	Centralized	IP (OPF)	multiple-DER	$min\{$Oper.Cost$\}$+$max\{$RES$\}$
(Costa et al., b)	Centralized	IP (OPF)	multiple-DER	$min\begin{bmatrix}\text{Power Losses}\\ \text{Dev. Actual-Exp. Net-load}\end{bmatrix}$
(Connell et al., 2014)	Centralized	SQP	EV	$min\{$Cost of Charging$\}$
(Weckx and Driesen, 2015b)	Centralized	SQP	PV	$min\{$Curtailed P$\}$
(Reponen et al.)	Centralized	SQP	PV	$min\begin{bmatrix}\text{Power Losses, RES curtailments}\\ \text{OLTC operation, } \Delta V^2\end{bmatrix}$
(Su et al., 2014)	Centralized	SQP (OPF)	PV	$min\{$Power Losses+Generations Costs$\}$
(Balram et al.)	Centralized	SQLP (MPC)	BESS & PV	$min\begin{bmatrix}\Delta V\\ \text{controls: BESS+ OLTC}\end{bmatrix}$
(Bidgoli and Cutsem, 2017)	Centralized+Local	SQPLP (MPC)	DG	$min\{$multiple objectives proposed$\}$
(Olival et al., 2017)	Centralized	EPSO	BESS, μDG, Loads	$min\{$Volt Control actions+ ENS$\}$
(Zakariazadeh et al., 2014)	Centralized	Stochastic	BESS, μDG	$min\{$Total Expected costs$\}$
(Kourounis et al., 2018)	Centralized	IP (adapted)	BESS	$min\{$Total Expected costs$\}$
(Fortenbacher et al.)	Centralized	LP (approximative)	BESS	$min\begin{bmatrix}\text{Operating costs}\\ \text{sizing of BESS}\end{bmatrix}$
(Karagiannopoulos et al., a)	Centralized (hybrid)	MILP	OLTC, BESS, CL	$min\begin{bmatrix}\text{Operating costs}\\ \text{planning costs}\end{bmatrix}$
(Karagiannopoulos et al., 2019)	Decentralized (data-driven)	MILP along with ML	OLTC, BESS, CL	$min\begin{bmatrix}\text{Operating costs, Power Losses}\end{bmatrix}$
(Pinto et al., 2020)	Centralized (hybrid)	MILP	OLTC, BESS, CL	$min\begin{bmatrix}\text{Cost of generation\& prosumers' flex.,}\\ \text{kVWh exchange with maingrid}\end{bmatrix}$

Interior Point The interior-point (IP) based techniques, are usually selected to address classic OPF algorithms as found in the literature that will be presented hereby. This subcategory could be also classified under the NLP problems. Usually, the IP method is selected since they present faster convergence (Zhu, 2015b). (Bertani et al.), propose a multi-stage control scheme that is comprised by two consecutive optimization problems. In the first stage, an IP-based technique aims at determining the optimal scheduling of several dispatchable units, in order to minimize overall costs. The second-stage of this work was composed by an intra-day LP based technique which is performed every 15 minutes, to update the initial set-points by considering the current improved data of short-term forecasts and state estimation. An IP-based approach is also used in (Tavares et al.) to address a multi-temporal OPF which includes BESS, EVs, Controllable loads and miro-generation. The main target of that work was to assess the potential of the demand flexibility of the aforementioned DER, as to solve operation problems such as branch loading and voltage violations, but by particularly offering these services for the MV network operation.

Following relevant considerations are made by (Costa et al., b), who proposes a multi-temporal three-phase OPF scheme that manages efficiently BESS's and demand flexibility for optimize the LV grid operation. More specifically, the main objective of this approach is to minimize the deviation between the actual and expected net load profile, in addition to minimizing power losses, respecting the technical constraints of the network as well as concerning future states of the grid.

Sequential Quadratic Programming The Sequential Quadratic Programming (SQP), is one of the most effective methods within the nonlinearly constrained optimization, which is resolved in steps of quadratic subproblems. In the literature a rolling multi-period optimization based on an SQP was found, that manages the charging of EVs (Connell et al., 2014). In particular, the objective of this work is to minimize the cost of charging EVs over all phases, nodes and time steps subjected to network constraints. Furthermore, the schemes aims to encourage the consumer to get engaged to centrally controlled charging; hence, any voltage deviations and overloading of equipment are avoided. The contributions of this work are related to the restrain to of unpredictability of each individual consumer behavior. Accordingly, the rolling nature of the scheme leads to updated decisions closer to the time of delivery. Another recent work (Weckx and Driesen, 2015a), proposes a coordinated EV charging strategy with load balancing by PV inverters and EV chargers, which targets to mitigate grids unbalances, resulting indirectly to reduced system losses. The latter is accomplished by setting a convex optimization problem on the minimization of load variance in all phases. In (Su et al., 2014), a multi-objective optimal power flow towards the certification of admissible voltage magnitudes and balanced voltage profiles, while minimizing network losses and generation costs. The multi-objective OPF is converted into an aggregated single-objective OPF problem using weighted summation method, and then addressed as global SQP. Nevertheless, the multi-objective optimization problem with conflicting objective cannot reach to a global optimum, so the authors make use of Pareto optimality. A coordinated voltage control scheme is proposed by (Reponen et al.), which is addressed a non-linear objective function that aim to minimize network losses and curtailed production, in addition to a cost parameter for load control,

cost for tap changer operations as well as a term to penalize the voltage difference from nominal at each node. The optimization is solved as series of approximates of the original nonlinear problem (i.e. SQP).

Sequential Linear-Quadratic programming (SQLP) The SQP methods as discussed above require the solution of a general (inequality constrained) quadratic problem at each iteration. The cost of solving each subproblem imposes a limit on the size of problems that can be solved in practice.The sequential linear-quadratic programming (SLQP) method attempts to overcome these concerns by computing the step in two stages, each of which scales well with the number of variables. (Balram et al.), propose a predictive voltage control Model Predictive Approach (MPC) based scheme, which suggests the minimization of control actions by coordinating BESS and OLTC, in close to real time response. This indirectly, brings minimized operating costs for the voltage regulation and is finally addressed by a multi-step optimization problem, and resolved as SQLP. However, this scheme does not provide control actions for the optimal operation of the LV grid, since only predictive actions are decided, presenting insightful results for the minimization of tap positioning. Relative works have been applied to the MV level by coordinating more DER such as (Bidgoli and Cutsem, 2017).

4.2.7.2 Heuristic Methods

Evolutionary algorithms In recent work of (Olival et al., 2017), an advanced voltage control scheme is proposed for the coordination of several DER such as BESS, controllable loads and microgeneration units. The main objective of this study is the minimization of voltage control actions, which implies that the least possible power of controllable resources is used to ensure admissible voltage values respecting technical limits. The scheme follows an Evolutionary Particle Swarm Optimization approach, while it is being cyclically performed each hour and compared with the baseline scenario (day-ahead analysis), to lead to final decision for the set-points of controllable units.

Stochastic optimization The stochastic optimization problems offers the capability of including, uncertainties that come from RES, where the model of the problem to be optimized is not completely known. A stochastic optimization framework that considers a stochastic energy and reserve scheduling method for microgrids, including all types of loads into various demand response programs, is discussed in (Zakariazadeh et al., 2014). The goal of this study is to reduce the total operating costs of the particular case that represents a microgrid case .

This category might be further extended to account for uncertainties in information, and therefore, to goals related to multiple and usually conflicting objectives (e.g. Pareto needs Decision making properties), the use of probability theory, fuzzy set theory or even analytic hierarchy process. For instance, (Chaouachi et al., 2013), propose an energy management and allocation of DER resources accounting the uncertainty of forecasting which is tackled by using the fuzzy theory.

4.2.8 Provision of DER flexibility for operational purposes

Amid the smart grid paradigm, the major expected evolution is the active participation of DER, including users participation through DR programs, in energy markets and network's operation by providing different types of flexibility capacities. The benefits from better price condition, in the sense of dynamic tariff schemes, is foreseen to be implemented, fact which may contribute to higher operational efficiency for the grid along with the maximization of integration of RES. According to the EU Directive 2009/72/EC, it is stated that electricity markets have to be based on the real possibility of choice for all consumers and access to new business opportunities for all. Nonetheless, in Europe, such efforts for DR deployed has been following a tardy pace (see Figure 4.3) comparing with United States status, as stated in (Coalition, 2014).

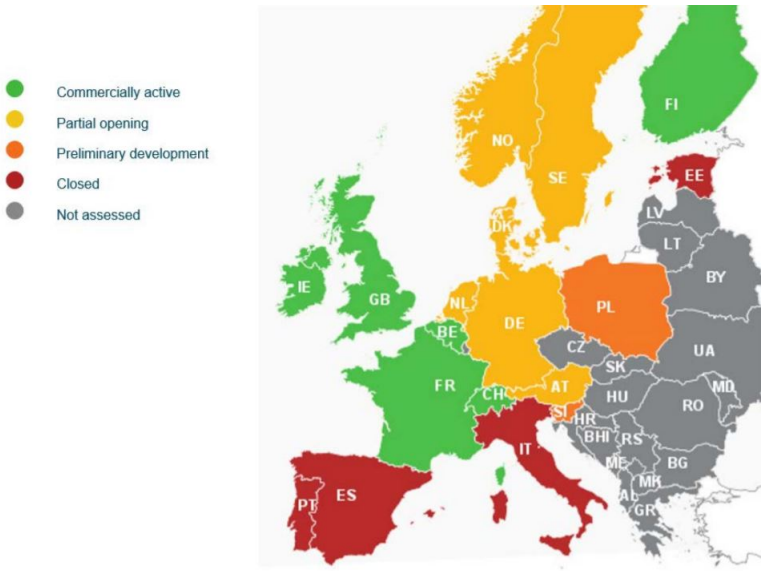

Figure 4.3: Mapping of demand response programs' status in Europe up to 2017 (Coalition, 2017).

Higher concern is gained in recent works regarding the potential flexibility provided by the DER installed in along the distribution networks, down to LV level (Tavares et al.; Olival et al., 2017). The connection of DER at the LV grid is envisaged to increase substantially in the close future, with small sized domestic BESS, small rooftop PV installations or controllable loads (i.e. Electric Water Heaters (EWH) or Combined Heat and Power (CHP) units) (Heleno et al.). Accordingly, it may be important to explore the management of this sort of flexibilities through DR response programs or other types of remuneration mechanisms defined in market framework, in order to support or even optimize network's operation. More specifically, exploiting the DER flexibility could support stressful operation periods, voltage support, or to create operational conditions that maximize DER, bringing concurrently profits to the consumers (Eid et al., 2016).

The emerging DER are attributed with different types of flexibility, which can be further grouped by an aggregator. The aggregator can be responsible to manage these multiple types of DER flexibility and create an added value to the grid and the electricity market, possibly, in dedicated sessions. Several studies are addressing the procedure of aggregating these flexibilities

at aggregators or DSO level, so that they can use it for market participation or for network support, respectively. In the literature there are models developed for the monitoring of Home Energy Management System (HEMS) flexibility models, which are capturing the multi-period flexibility of DER like Thermostatically Controlled Loads (TCL), Electric Water Heat Pumps (EWHP) or BESS, incorporating also the high uncertainty of net-load forecasts. The multi-period flexibility is generally used as the ability of a HEMS to deviate from the expected net-load profile for a specific period of time (Pinto et al., 2017a). Such tools may be used to enhance DER control and management strategies, by reducing the existing uncertainties of net-load forecasting as well as the stochasticity of certain flexibilities such as EVs and controllable loads.

Recent studies have examined the provision of reserve services through DR programs within the SG context (Heleno et al., 2016). For instance, (Iria et al.) proposes a method through HEMS to engage several household loads to participate in DR schemes in quasi real-time. This indirectly targets to achieve reduced electricity costs. Several recent works regard the DER flexibility to be involved in ancillary services as frequency response (Samarakoon et al., 2012), or even in larger time frames contingency management (Shayesteh et al.) or replacement management. A review by (Eid et al., 2016) presents a classification of existing DER as flexibility providers and a breakdown of trading platforms for DER flexibility in electricity markets, as well as relevant current flexibility deployments and gaps on the regulatory framework.

Other DER flexibility concepts have been used in the context of electric vehicle charging for primary frequency control so as to contribute to the system's dynamic behavior (Lopes et al., 2011). (Sundstrom and Binding, 2012), use the energy stored in the EV fleet and the bounds of this energy to optimize the charging schedules at the aggregator-fleet level, avoiding on that way distribution grid congestion. A step further was proposed by (Harbo and Biegel) to define flexibility services contracted between players where the aggregator manages a portfolio with flexible consumers with low marginal flexibility costs. For this purpose is developed a core framework to evolve such contractual relationships. There is a clear focus from the research field to the utilities to enable the DER flexibility within the smart grid context providing several benefits to all through the improved operation of distribution networks.

The effective use of flexibility from DER requires a strict analysis of their technical characteristics, as well as the analytical breakdown of trading platforms for DER flexibility in electricity markets. From the technical standpoint, it is required to identify insights for cost-efficient flexibility coordination that supports technical system needs. The regulation and policies generally have delayed such developments (Eid et al., 2016), which basically implies that yet have to expect alignments from the market models and policies to the DER transactions.

4.3 Proposed operational control framework for LV distribution networks

In this part, an overall technical and control architecture is discussed. The proposed framework aims to describe substation centered approach which is able to interact with prosumers and provide

optimal coordinated operation under several objectives for unbalanced LV distribution networks with high integration of DER.

4.3.1 Conceptual technical architecture

The proposed architecture (Figure 4.5 & 4.7) aims to equip the LV grid with information and devices to automate grid management and reduce operating costs by taking full advantage of DER connected along the grid. This targets to decentralize up to a certain level control and management functionalities, reducing unnecessary data flows from and to the control center. Introducing a central controller (i.e. Distribution Transformer Controller (DTC)) at the level of Secondary Substation. The DTC will be namely responsible not only to coordinate the operation of LV distribution network, but also act as data aggregator (i.e. data collected from IEDs and smart meter, current or voltage transformers *etc*). The latter eases complexity brought by the proliferation of gradually extended observability (i.e. smart metering) of the LV grid to the Control Centers. A local database at DTC level can be exploited to take advantage of historical smart metering data. The input data will have to be processed –before locally stored into the histrorical data-base– using advanced analytics. Based on these post-processing inductive decision may be derived for the improvement of the LV networks' characterization (e.g. phase identification) and its observability in real-time, with reduced real-time monitoring requirements as proposed by (Kotsalos et al., 2019b; Campos et al., 2017). Such procedures render the deployment of a range of DMS applications for LV distribution networks (e.g. the proposed multi-period AC OPF) feasible.

The functionalities that may be accommodated at DTC level are thoroughly discussed in (Campos et al., 2017; Kotsalos et al., 2019b, a). In these research works, the Data Management and Processing module is analytically defined that is, essentially, responsible for the processing and storing of an incoming data-measurement at the DTC based database. As schematically presented in Figure 4.4, once a new batch of data is available for processing, the Data Management and Processing (functional) module accesses the Historical Data Database; following, the module accesses the configuration file provided by the user that determines the type of measurements to be analysed, a bandwidth of acceptable variation, and the method used for filling the missing (or erroneous) data. The processed data is stored in the Historical Data Database along with a log of all the actions made. Any changes are implied in case erroneous data are discarded and reconstructed accordingly. In case data is discarded, it will be reconstructed based on previous occurrences archived, lying on similar grid operating points. This latter functionality is illustrated in Figure 4.4, as the second step, where the interrogated archived data is combined with current forecast to detect closest similar operating point. As presented in (Maniatopoulos et al., 2017), other functional blocks on the enhancement of LV observability and controllability deploying functionalities for the phase identification, network model builder and state estimation.

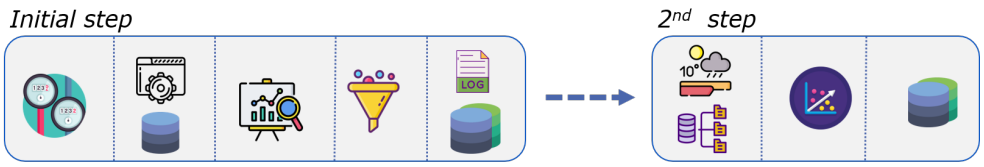

Figure 4.4: Data Management and Processing module: Local data aggregation, processing and management.

4.3.1.1 Actors and Key Components

In the upper level (i.e. gray layer) of Figure 4.5 are illustrated possible external inputs for the DTC that may comprise inputs for the control and management functionalities. This upper level of the framework is not the main concern of this work and thus will not be analytically described; nevertheless, some notions according to the literature exploration will be expressed about ongoing trends on such formations. The relevance of this upper level with this work is the interaction with the DTC level, which will be accordingly accordingly accommodated to the DMS applications. The analytical definition of such conceptual frameworks for the market setup with the existence of aggregators as well as the overall interaction among them, has been approached by projects as in *ADDRESS*, (Belhomme et al.; Peeters et al.).

The DSO is illustrated, who is mainly responsible to ensure secure and efficient operation of the distribution network through supervision and control mechanisms, based on SCADA and DMS systems. The interaction of DSO with TSO is vital to reassure the secure network operation. The Market Operator (MO) is as typically responsible to perform market procedures and commercial agreements among the power system's participants. This entity can be further disaggregated to different products and services.

The aggregator on this architecture stands as third party to the grid business, that essentially bundles demand response and generally DER flexibilities from customers at their own expense, and offer these for grid services. Analytical breakdown research works present further information pertaining the trading processes for several flexibility services provided by DER in the distribution networks (Eid et al., 2016).The aggregator as a market player intends to optimize his own profits, by assigning agreements with the end-users. Typically, due to the scale of economies, the aggregators engage industrial and generally large commercial customers, albeit some specialize in residential customers. The aggregator communicates with its customers through two-way communication to gather the information, conducting the preparation of the portfolio services that will participate on the market. Therefore, it is assumed that the aggregator is capable of assigning contracts with the majority of customers of participating on such demand response programs. In the findings of (Belhomme et al.) the distinction and interaction of technical and commercial frame is further traced out. From the one hand the commercial processes deals with the negotiations (e.g. requests or offers) and agreement within the participants. The technical frame deals with the activations, interactions of the participants and their services.

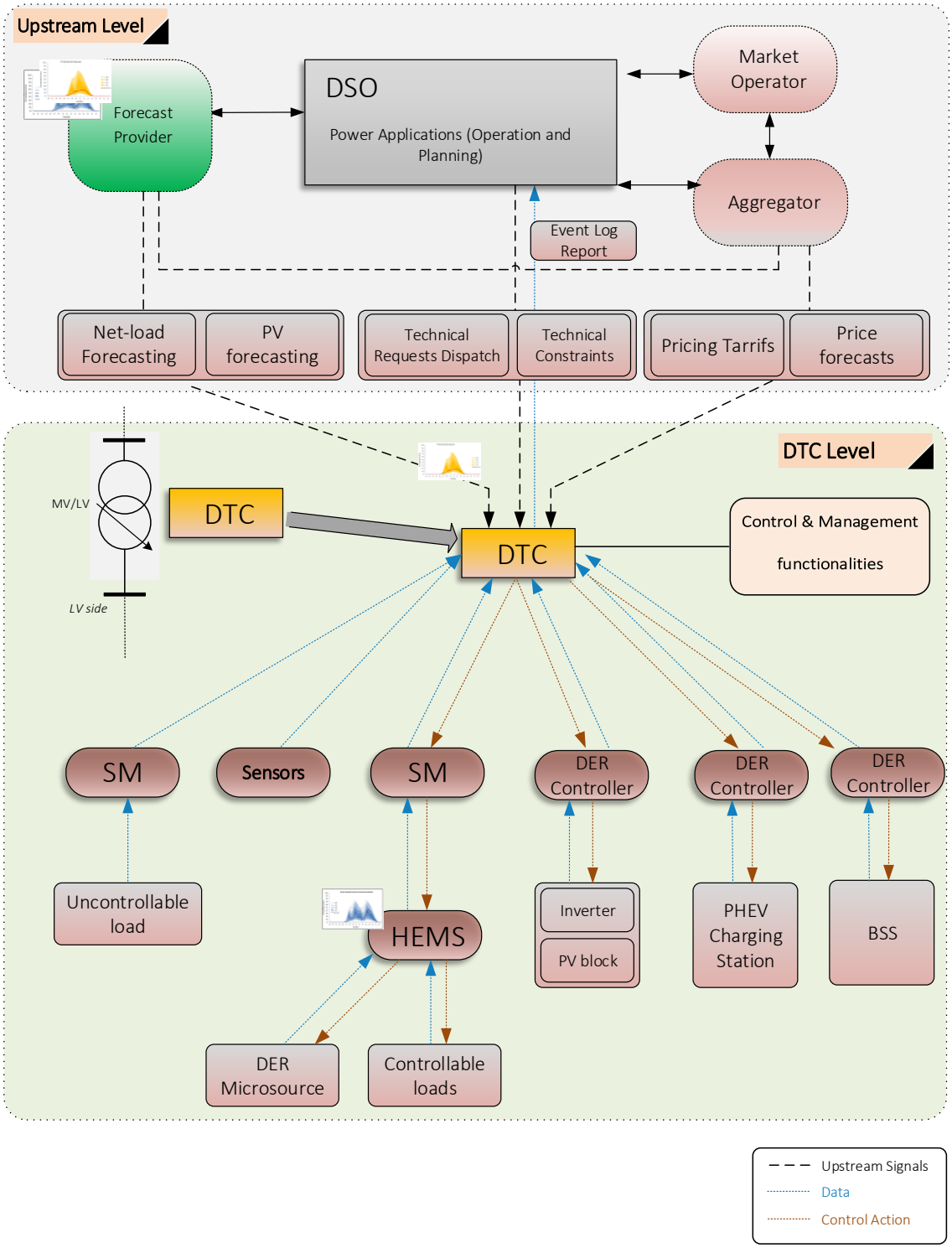

Figure 4.5: Conceptual architecture framework. Upstream Level - Substation Level - Grid Components.

The Forecast Provider intends to provide data analytics and forecast profiles for short term periods up to 24 hours regarding the consumption of end consumers as well as the production of the micro-generation. Such services might be directly calculated at the level of Secondary

Substation or even at the level of smart meters, by acquiring only Weather Forecasts (Bessa et al., 2016).

The DTC placed on the Secondary Substation, will facilitate the operational control and management tools for the LV grid operation. This level of control located at the MV/LV is assumed to be responsible for a single LV network. The DTC will be also responsible for the aggregation of measurements from the smart meters in order to monitor the current state of the downstream grid. This configuration intends to incorporate advanced control functionalities in order to consistently address the technical challenges may occurred on the LV operation, by communicating set points to the several smart meters or corresponding DERs through their controllers.

In the frame of consumers smart metering devices will tender the accurate tracing and recording of load and generation profiles, in addition to their capability to integrate multiple commercial processes (e.g. multiple-tariff, real-time pricing etc.). Only some of the end-users are expected to include a Home Energy Management System (HEMS), which will be substantially in charge to manage optimally the household smart appliances and microgeneration units (i.e. Photovoltaic roof top panel and storage devices) as illustrated in Figure 4.6.

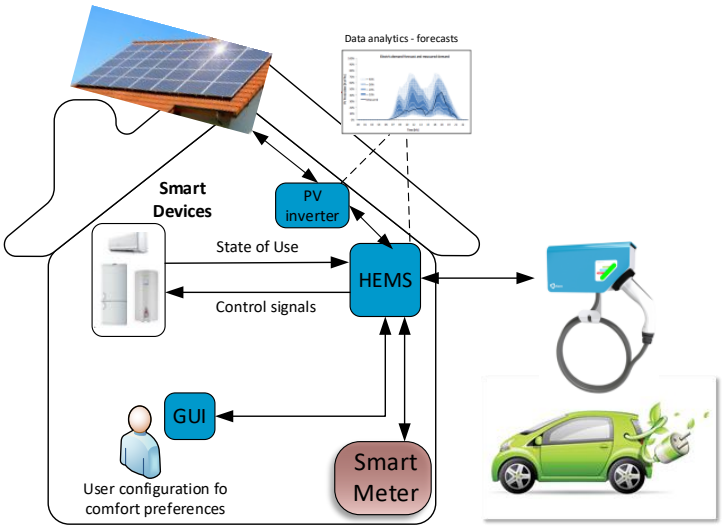

Figure 4.6: End-user equipped with Home Energy Management System (HEMS).

The HEMS is basically interconnected with the Smart Meter to the DTC, releasing the capability to accept set-points to participate in Demand Integration Management schemes via agreed contacts with the aggregator, receiving incentives or activation fees. The HEMS intends to provide certain degree of distributed intelligence (i.e. local optimization see (Heleno et al., 2016; Heleno et al.)), capable to control and coordinate appliances and loads according to end-user's preferences.

The Table 4.4 gives the definition and the role of each actor of the framework. An overall mapping of actors and key components within the SGAM architecture (CEN-CENELEC-ETSI, 2015) is portrayed in Figure 4.7. Generally, the identification of UCs should steered on the SGAM toolbox, since it intends to consolidate novel smart grid architecture to a common field; thus, resulting in the identification of possible standardization gaps (i.e. to the architecture itself or even

the current standards and protocols), and provide a foundation for communication about it to other domains which need to interoperate. Therefore, the actors and components have been placed in an abstractive way (i.e. not detailed interaction), along the layers of the SGAM architecture.

Table 4.4: Actors Description.

Actor Name	Description of Actor
DSO	Responsible for executing the network planning and operation of the distribution system at each time, making use of SCADA system and subsystems (e.g. DMS, OMS and GIS). The DSO owns several assets among the distribution network and several distribution and substation automation units. Particularly, for LV grid the DSO caters for the optimal operation managing the DER.
Forecast and Service Provider	This actor is responsible to supply forecasts for the electric demand and the PV production. • Demand forecast: Weather forecasts combined with historical measurements which are recorded by Smart Meters. Several dynamic inputs required historical measures for electrical demand comfort (transmitted by HEMS) and weather forecasts. Generally, necessary static inputs are the geographical coordinates of the consumers and their rated power. • PV production: Weather forecasts and historical measurements are combined to produce probabilistic forecasts. The appropriate dynamic inputs refer to the solar irradiation measured, whilst typical static inputs are the geographical coordinates of the DER source and their installed capacity.
Market Operator	Responsible to seamlessly organize the performance of the market clearing the wholesale market prices. On the proposed architecture, the aggregators actively bid on the wholesale market their flexibility services to pursue their benefits. The aggregators will act a turnkey demand response resource to vertical integrated utilities, since typically they participate directly on the wholesale market bypassing the retail utility.
DTC	The DTC refers to the Distribution Transformer Controller, which is housed in the Secondary Substation. The DTC act as the LV Network Controller and Data aggregator. Besides the integrated communication with the Smart Meters, the DTC will facilitate hereby the underdeveloped control and management tools for the LV operation.

Client, end-user (Prosumers)	This actor presents some enhanced notions since DER will be installed at some residential level premises, in addition to the fact that Some may have installed Home Energy Management System (HEMS).

Table 4.5: Key components.

Component Name	**Component Property**	**Component Description**
DER	DSO or Client/end-user	Represents distributed electrical sources connected to the public distribution grid, applying small-scale generation or storage of whatever form. At the low voltage networks premises of typical DER types met are merely Photovoltaic Panel (PV), controllable loads, Battery Storage Systems and Plug-in Hybrid/Electrical Vehicles (PHEV) etc.
Intelligent Electronic Device (IED)	DSO – Retailer prosumers	The Intelligent Electronic Devices are essentially installed to the grid to provide monitor, control or protection to a specific area of the network. IEDs acquire field measurements by using sensing devices; thus, enabling the capability to apply control actions trough actuators. In the current framework, a major category of IEDs -owned by DSO- is the Smart Metering infrastructures, reasonably placed in some end-users. Control actions decided within the proposed management tools on the DTC are transmitted either to SMs directly or the DER controllers.
HEMS	Client-end user	The HEMS represents the central device responsible to receive data from the Forecast provider and the Energy Provider. This data is combined with local models of the building appliances. The provision of a balancing power (flexibility) is identified through controllable loads that can be shifted for a certain period, in exchange of a profit. In general, types of loads that can be shifted are electrical and thermal loads. The HEMS shall be in direct contact with the aggregator.

DER Controller	DSO or Client (end user)	A smart inverter essentially comprises the DER controller. It is capable to receive set-points commands to adjust its operating point in the proper point (i.e. adjusting its power factor). There are several other options that can be implemented on a smart inverter such as configuring droop parameters.
Provision of Flexibility Services	DSO or Client (end user)	Flexibility or availability for Load Management refers to the capability of particular controllable loads under Demand Response programs, to be shifted contributing essentially in the operation of LVDN. Hence, the residential users or microgeneration, transmit to the DTC their own flexibility for each hour for the day ahead. Each HEMS or DER controller calculate the day ahead flexibility profile for each controllable household. The DTC will aggregate these profiles (i.e. upward and downward signal with respective amounts) and then will decide which of them needs to be purchased, informing afterwards the aggregator. Therefore, the flexibility for a particular interval is P_{rated}, if P_{rated} is positive then it is referred to an upward flexibility, conversely a downward flexibility.
On-Load Tap Changer (OLTC)	DSO	The On-Load Tap Changer is accommodated on the secondary substation to provide an additional voltage control asset.
Sensors	DSO or Client (end user)	The sensing devices may appear in the grid in several types such as solar irradiation (PIR sensors), temperature, humidity etc.

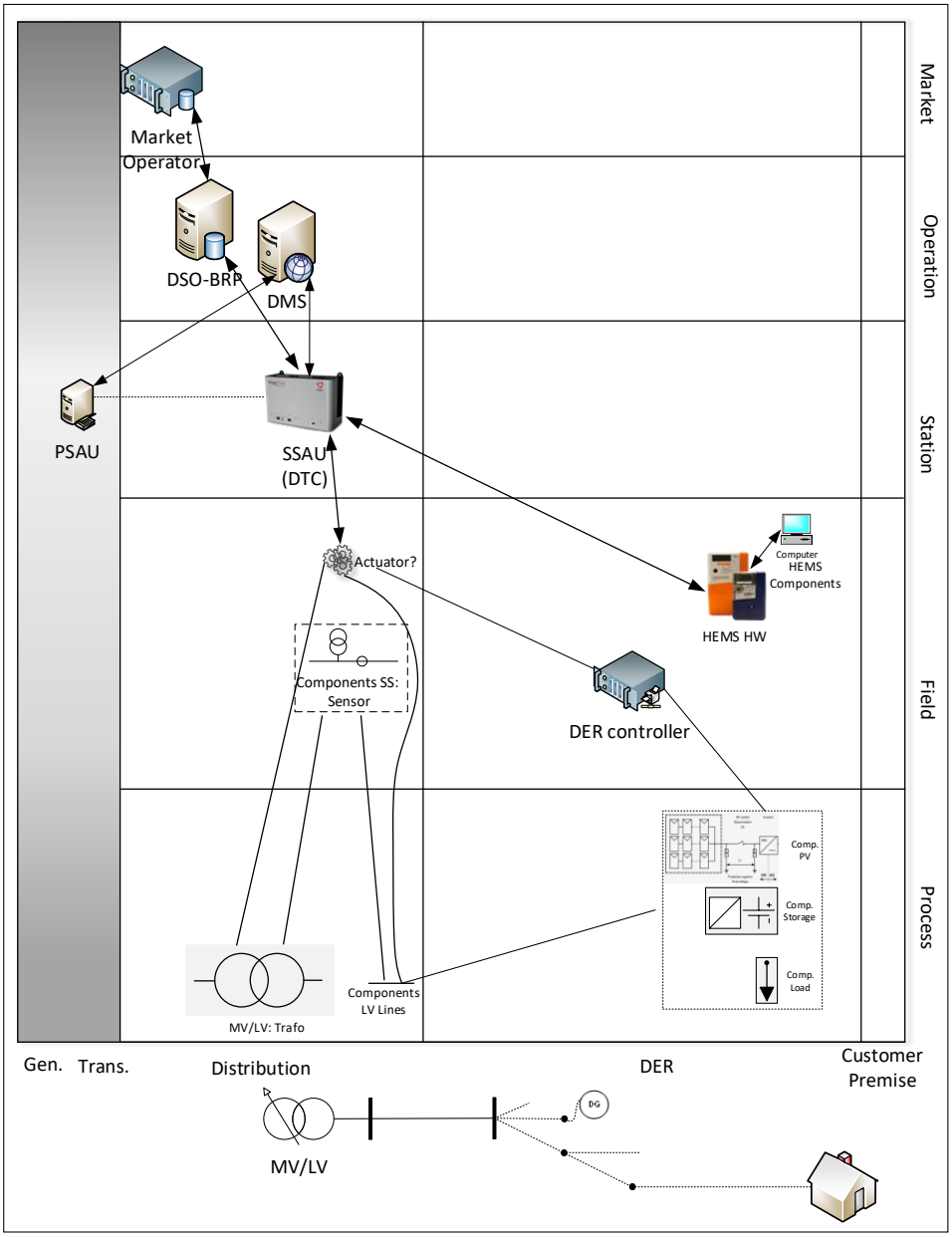

Figure 4.7: Mapping of Actors and key components on the SGAM model.

4.4 Control algorithms

In this section, the proposed control and management framework which is used to facilitate the planning and operation of LV distribution networks, is presented. The overall scheme has as core algorithm the mathematical framework proposed in Chapter 3 and based on the unbalanced three-phase multi-period AC-OPF. The developed scheme can be described by four temporal stages. The first one is stated for planning purposes, which utilizes synthetic data-profiles to provide insights for efficient investments (i.e. BESS or installation of new distribution lines) for the upcoming years, by co-optimizing the planning and operation of the grid. The following three stages are

purely designated to steer the operation of LV grids with increased integration of DER, based on the substation centered technical architecture discussed in Section 4.3. One stage deals with operational planning of operation, while the subsequent one provides refreshed control actions to ensure safe operation, mitigating any uncertainties detected.

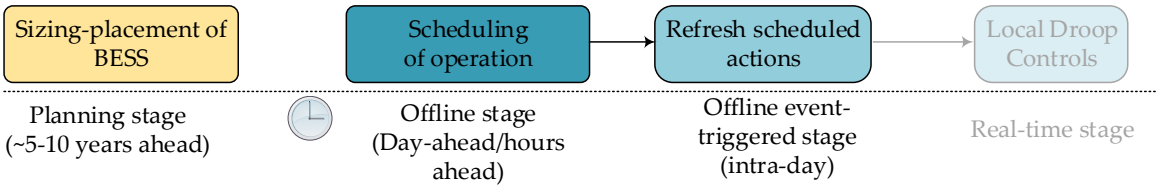

Figure 4.8: Analytical control scheme accommodated in DTC.

4.4.1 Planning stage: Efficient sizing and placement of BESS

The power system's planning used to take place considering an expected load growth term combined with worst-case scenarios (e.g. high load simultaneity, low probability contingencies etc). Such strategies, aligned with "fit-and-forget", appear to be rather conservative and inefficient due to the installation of multiple DER (Pilo et al., 2014). The increased integration of DER in the grid rises the concern for their active participation in the operation of the grid. Such active measures in the operation stage should be also regarded in the planning stage. In this sense, hybrid planing may arise such as the co-optimization of planning and operation, where in the operation stage active measures are contributing in the respect of technical constraints as in (Karagiannopoulos et al., 2017; Grover-Silva et al., 2018).

The optimal sizing and placement of the BESS is hereby derived using an extended formulation of MACOPF as presented in (4.1):

$$\min_{u,z_j} (w_1 \cdot O_1 + w_2 \cdot O_2) + w_{\text{plan}} \cdot \sum_{j \in \mathscr{D}} z_j \tag{4.1}$$

subject to:

$$\begin{array}{lll} k \cdot z_j & \leq p_{ch}(\tau) & \leq 0, \\ 0 & \leq p_{dch}(\tau) & \leq k \cdot z_j, \\ \underline{\eta} \frac{\mathscr{E}_j(\tau)}{z_j} & \leq SoC(\tau) & \leq \overline{\eta} \frac{\mathscr{E}_j(\tau)}{z_j}. \end{array} \tag{4.2}$$

Objectives O_1, O_2 correspond to operational terms to be minimized. Variable $z_j$is added referring to the sizing of the BESS to be installed and the set $\mathscr{D}$ contains all candidate nodes for the investment of a single BESS owned by the DSO. Accordingly, the cost associated with the investment is added on the objective function. The c-rating of the BESS is denoted with k, and the under investment BESS is considered to be a three-phase system. The parameters $\underline{\eta}, \overline{\eta}$ define the technical parameters for the minimum and maximum SoC for the technology of the BESS to be invested.

The same formulation can be extended to add the alternative of investing on grid reinforcement. The additional objective might be posed as:

$$\begin{aligned} & w_L \cdot \textstyle\sum_{i \in \mathscr{Y}} I_{d,i} - I_{n,i}, \\ & \text{s.t.} \\ & I_{d,i} \geq I_{n,i}, \forall i \in \mathscr{Y} \end{aligned} \tag{4.3}$$

where is $w_L(\frac{€}{A})$ is the overall cost (including installation) of investing on distribution lines, $I_{d,i}$ is the decision variable for the necessary amperage of the new distribution line, $I_{n,i}$ the nominal amperage of the existing distribution line and $\mathscr{Y}$ the set of branch lines to explore for grid reinforcement.

In this planning problem, the major challenge stems from the need to include large data-sets (i.e. to capture expected load growth, connection of new clients and DER). This fact, may lead high computational burden and increased needs for memory allocation. This challenge is addressed by constructing representative yearly synthetic profiles; thus, the characteristics of the large data-set may be reflected.

A data-set has been created for this study case to emulate and induct the results for yearly analysis. A data-pool of yearly load profiles (found in repository (Pedersen et al.)) is statistically processed by using a k-means algorithm. Several sets of load profiles are aggregated and normalized to represent MV/LV substation's profiles. This data are then properly clustered into seasons, weekends and weekdays. Regarding the clustering a distance metric that is utilized for minimization, is considered as the component-wise median of that cluster, let it c_i as the centroid and x_i each datapoint. Each datapoint is accordingly clustered in Equation (4.4):

$$d(x,c) = \sum_{i=1}^{n_t} |c_i - x_i|. \tag{4.4}$$

For this application eight cluster have been selected in order to obtain an aggregation of the aggregated substation profiles into weekdays/weekends and accordingly into seasons. The representative data-set is thereafter composed of eight days, two per season (one representing weekdays and another one for weekends). Each of those is selected based on the centroid metric derived by k-means. To reproduce the load profiles, the inversed cumulative Gaussian distribution function (Φ^{-1}) is set with maximum standard deviation $\sigma = 0.08$ and median the value of the centroid at each datapoint. Therefore, each point of the load profile i at instant τ is calculated from Equation (4.5):

$$P_i(\tau) = \Phi^{-1}(c_i(\tau), \sigma) \cdot P_{i,\text{rated}}, \tag{4.5}$$

where $P_{i,\text{rated}}$, refers to the installed capacity of residential user i. The Gaussian copula method is used to generate N temporal scenarios PV solar profiles, encapsulating the seasonal dependence as proposed in (Pinto et al., 2017b).

Building upon synthetic profiles may be a very helpful practice particularly to reduce the

complexity of large datasets. Nonetheless, to create synthetic profiles that replicate statistical behaviour of larger period can be a quite demanding task and may need careful exploitation of sampled historic data and seasonal interdependencies (Alarcon-Rodriguez et al., 2009).

4.4.2 Scheduling of operation (Operational Planning)

The stage of scheduling aims at exploiting the generation units and flexible DER on the basis of their availability(i.e. temporal availability based on technical also constraints such as ramp-up/down) and production costs. The scheduling of operation is aligned with the market operation closure. Therefore, hereby it is assumed that aggregator is assigned with an amount of LV end-users and participates at the market closure (possibly in dedicated sessions). The DER flexibility services are in fact part of Demand Response services; a further activation of them by the DSO (through the proposed scheduling of operation), may lead to higher compensation fees to the end-users.

The scheduling of operation is formulated with the three-phase unbalanced multi-period AC-OPF (MACOPF). The optimizer targets to minimize operating costs coordinating multiple DER types and DSO's assets. The scheduling of operation derives decisions for entire day of operation. As it is schematically presented in Figure 4.9, the expected forecast error (for generation and loads) for later hours are higher. Such deviations may provoke technical issues which are mitigated by the intra-day corrective actions.

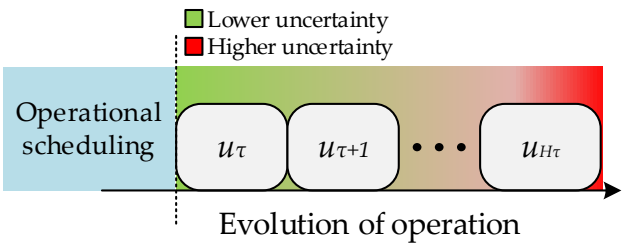

Figure 4.9: Analytical control scheme.

To sum up, this stage will be responsible to provide schedules to all flexible DER (e.g. EVs, BESS, μG) and any DSO assets (e.g. OLTC, BESS), for the determined horizon period.

4.4.3 Intra-day corrective control actions

This stage is settled to provide refreshed control actions, are necessary to avoid insecure deviations from the scheduled actions, due to possible forecast estimate errors or intense load deviations. Thus, this scheme is triggered once at DTC an event is detected. An event is defined as:

- By the acquirement of a group new measurements from IEDs or Smart Meters. It should be noted, the concept of Send On Data (SoD) may be used for the measurement aggregation at the DTC level to alleviate high communication traffic. Therefore, a measurement update may be send to the DTC only if it is larger than δ. This type of event based sampling,

defines an event once a crossing of the signal $x(\tau)$ from a one dimensional region bounded by δ. *(Type I)*

- If updated forecasts regarding generation (i.e. PV) or aggregated load appear a large deviation ($\hat{\varepsilon_f}1, \hat{\varepsilon_f}1$, accordingly) compared to the initial guess. *(Type II)*

The event time instants $\tau_n, \in \mathbb{Z}, n \in \mathbb{Z}$ are defined as:

$$\tau_n = \begin{cases} \min\{\tau > \tau_{n-1},\ \ |x(\tau) - x(\tau_{n-1})| > \delta)\}, & \textbf{if } \textit{Type I} \\ \min\{|P^{new}_{\mu G}(\tau) - P_{\mu G}(\tau)| > \hat{\varepsilon_{f1}},\ \ P^{new}_{\text{Load}}(\tau) - P_{\text{Load}}(\tau)| > \hat{\varepsilon_{f2}}\}, & \textbf{if } \textit{Type II}. \end{cases} \tag{4.6}$$

The generation of events will trigger the process to refresh the scheduled operation, by takings more accurate decisions based on the newly calculated/arrived forecasts. As it is schematically presented in Figure 4.10, closer to the time of the delivery new actions are decided to mitigate the uncertainties, once an event is recorded.

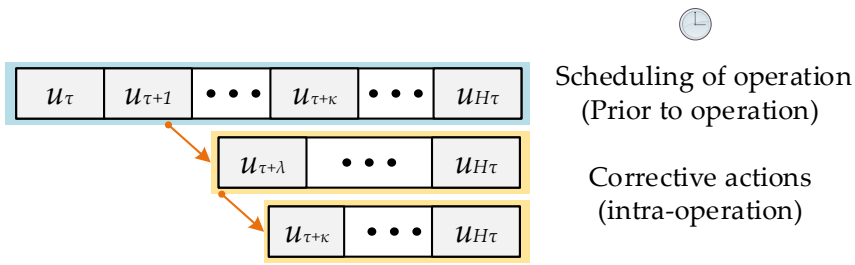

Figure 4.10

4.4.4 Quasi-real time droop controls

In the overall scheme, one subsequent objective is to ensure safe grid operation by maximizing integration of μG in the LV distribution network. The latter is accomplished, by prioritizing the use of other DSO assets or DER and only if it is necessary reactive power dispatch and/or active power curtailment is determined. In this way, there is clear potential to exploit the capability curves of smart inverters in real time by applying droop based rules as discussed in section 2.3.1. The selection of local control schemes for "close-to" real-time operation eliminates essentially the need of communication; thus, the remainder control stages can be employed with the establishment of high latency ICT.

4.5 Case study on Coordinated EV Smart Charging Operation

The presented coordinated DER operation through MACOPF is validated on IEEE LV benchmark network (Espinosa, 2015) (Fig. 4.11), where slight modifications are regarded solely for the transformer characteristics 150kVA, 20/0.4kV.

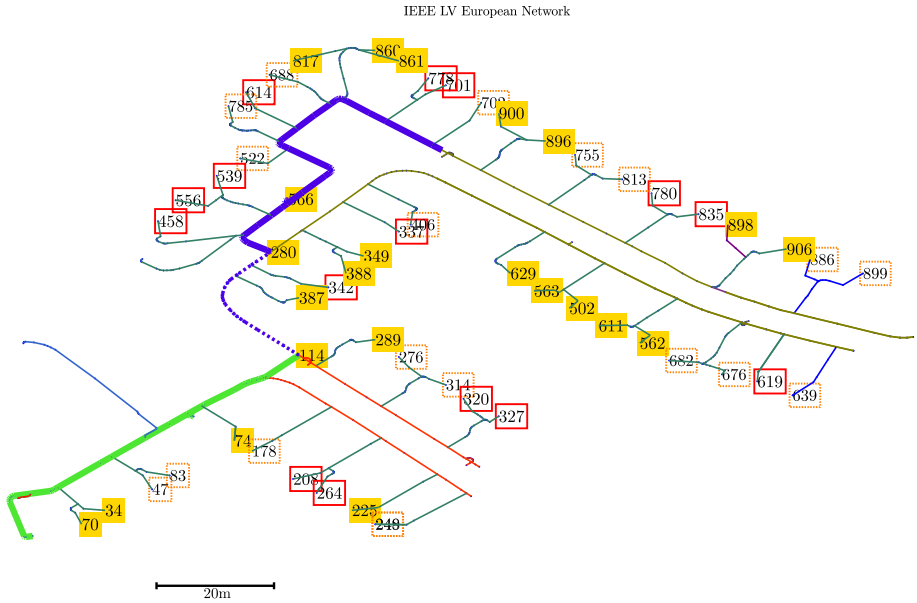

Figure 4.11: The IEEE European LV benchmark network. 55 consumers are connected to this case network.

One three-phase BESS is considered at node 566, the capacity of which is 90kWh, the maximum charging and discharging rate is 45kW, while its initial SoC is 0.40 with minimum allowed $\underline{SoC} = 0.1$. An additional constraint imposes equal SoC for the last instant of the horizon and the initial one, $SoC_{H\tau}$=0.40.

The definition of the examined scenarios is presented in Table 4.6. The integration of PV and EV as a percentage, implies to be proportional to the share of end-consumers that possess such units. For instance, 65% of EV penetration corresponds to 47 EVs. Analytical information regarding the point of connections and the characteristics of DER can be found in (Kotsalos et al., 2019a).

Each scenario (of EV and PV) is performed 4 times 1) no control applied 2) only EVs coordinated flexibility within MACOPF –denoted as caseXa– 3) with BESS_{566} –owned by DSO– coordinated with flexibility brought by EV charging -denoted as caseXb– 4) replacing distribution line branch $114-280$ (illustrated on Fig. 4.11 with dashed line) of 37 meters from 4core$\times 10^2$ to a 4 core$\times$16 mm^2 –denoted as caseXc–.

Table 4.6: Scenarios Definition & Resulted EV flexibility capacity allocated

Scenario	C1	C1a	C1b	C1c	C2	C2a	C2b	C2c	C3	C3a	C3b	C3c	C4	C4a	C4b	C4c
EV [%]	65	65	65	65	65	65	65	65	85	85	85	85	85	85	85	85
PV [%]	0	0	0	0	55	55	55	55	0	0	0	0	55	55	55	55
BESS_{566}	×	×	✓	×	×	×	✓	×	×	×	✓	×	×	×	✓	×
Line 4c_.16 [**114 – 280**]	×	×	×	✓	×	×	×	✓	×	×	×	✓	×	×	×	✓
Necessary % of engaged EV Charging flexibility	–	50	40	20	–	50	10	10	–	85	75	25	–	85	60	40
max **VUF** [%] ($\leq 2\%$)	1.94	1.16	1.17	1.43	1.94	1.11	1.66	1.72	3.29	1.22	1.74	1.81	3.21	1.16	1.78	1.54

The controllable DER are prioritized analogously to the price terms $c_k(\tau)$. Such c_k might be associated with real monetary cost values; nonetheless, in this study a merit order scheme

Table 4.7: Line characteristics for considered constrained lines

Line Name	**Nominal Area of conductor** [**nr of cores** $\times$ **mm**^{2}]	**Rated Current** [**A**]
4c_.1	4×10	92.0
4c_70	4×70	245.0
4c_.16	4×16	115.0

as follows $c_{BESS} < c_{EV} < c_{V2G}$, setting the BESS as the cheapest action, the coordinated EV charging as the next one to follow, and lastly the use of V2G mode, accordingly. Hence, MACOPF prioritizes the use of the BESS –when installed– which is owned by the DSO, or the coordinated smart charging, avoiding unnecessary curtailments on microgeneration units.

In the case study network, the thick illustrated distribution lines –in Fig. 4.11– are particularly included within the MACOPF with current flow constraints. Nonetheless, all distribution lines' rated thermal loading conditions are verified by performing power flow analysis. The characteristics of the constrained lines are given in Table 4.7.

4.5.1 Results

Assessing, initially, the cases where no control is applied (i.e. C1, C2, C3 & C4), critical voltage drops are observed especially during evening hours (17:00 to 23:00) since the installed EVs are charging. Accordingly, in scenarios C2 and C4 overvoltages up to 1.065 p.u. appear due to notable active power injections by PV during increased solar irradiance (14:30–15:00). Regarding, the VUF parameter in scenarios C1–C2 is closely to 2%, yet, below the threshold. Nonetheless, in scenarios C3–C4 where higher EV integration is considered, the VUF reaches up to 3.21%. All the VUF indexes are recorded on the last row of Table 4.6. The increased demand raised by the EVs integration leads to the overload of the secondary substation up to 118% of its rated power (C4), while the most congested branch of the grid is thermally overloaded reaches up to 1.5p.u. (C1 & C2) and 1.8 p.u. (C3 & C4). The latter clearly signifies that such capacities of EV integration (65 – 85%) cannot be accommodated in the examined LV grid, without taking actions either by investing on grid reinforcement (e.g. distribution lines with higher rated power), or alternatively, by taking advantage of DER and exploiting active network management such as the MACOPF tool to address the aforementioned technical issues.

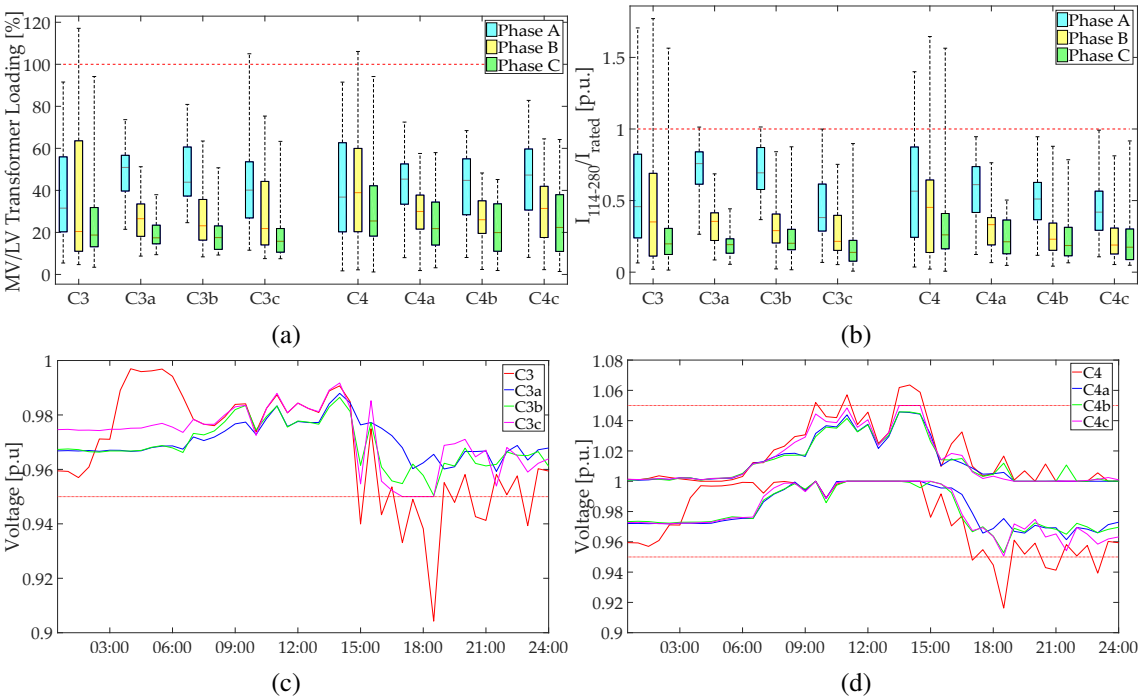

Figure 4.13: Simulation results for scenarios C3-4 and the subsequent subcases. (a) Transformer loading conditions.(b) Branch currents 114-280.(c)Minimum Voltages met for C3a-c. (d) Minimum and maximum Voltages met for C4a-c.

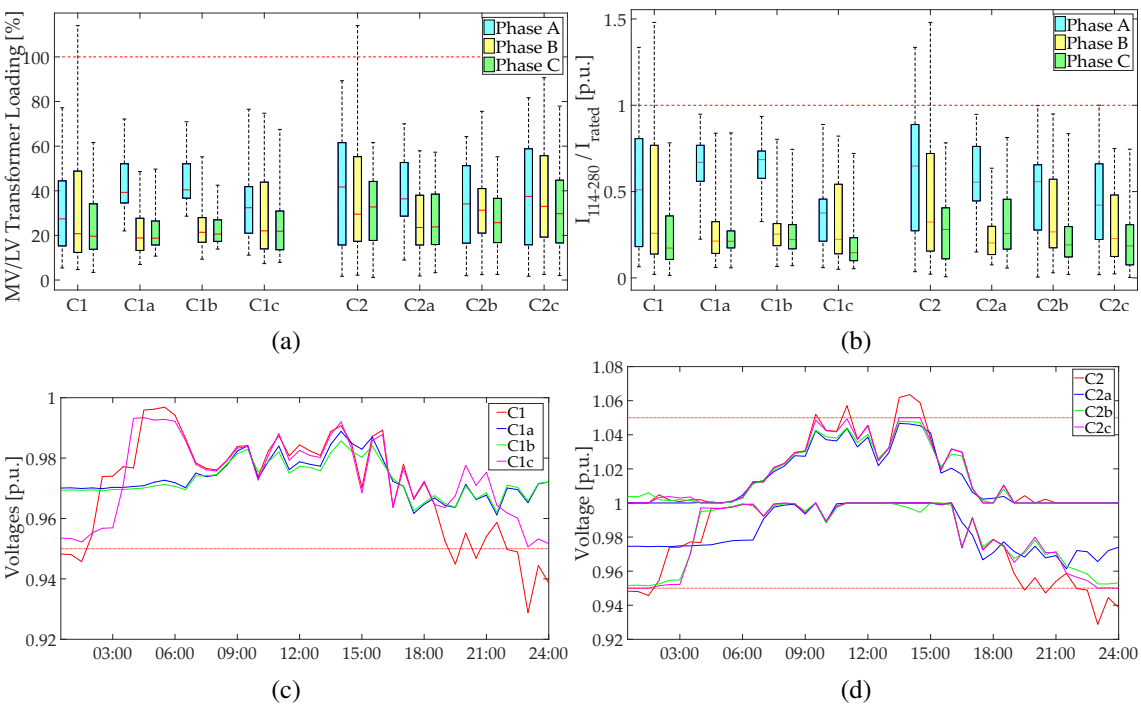

Figure 4.12: Simulation results for scenarios C1-2 and the subsequent subcases. (a) Transformer loading conditions.(b) Branch currents 114-280.(c)Minimum Voltages met for C1a-c. (d) Minimum and maximum Voltages met for C2a-c.

Following the proposed scheme based on MACOPF, the most cost-efficient control actions will be derived to operate the grid under all the technical constraints. It is noted that for such high EVs (55% and 65%) share a minimum 50% and 85% out of total EVs, accordingly, need to follow the coordinated charging as per Table 4.6. The inferred scheduling by MACOPF may assure that all the technical issues are properly addressed as it can be seen in Fig. 4.12a-4.12d and Fig. 4.13a-4.13d. The high level of EV charging coordination is capable to efficiently avoid any line congestions as well; this occurs by averting simultaneous EV charging, as well as by shifting the available and parked at house premises EVs during periods with high solar irradiance (C2 & C4). The latter leads to the mitigation of overvoltages arose by active power injections from the PVs.

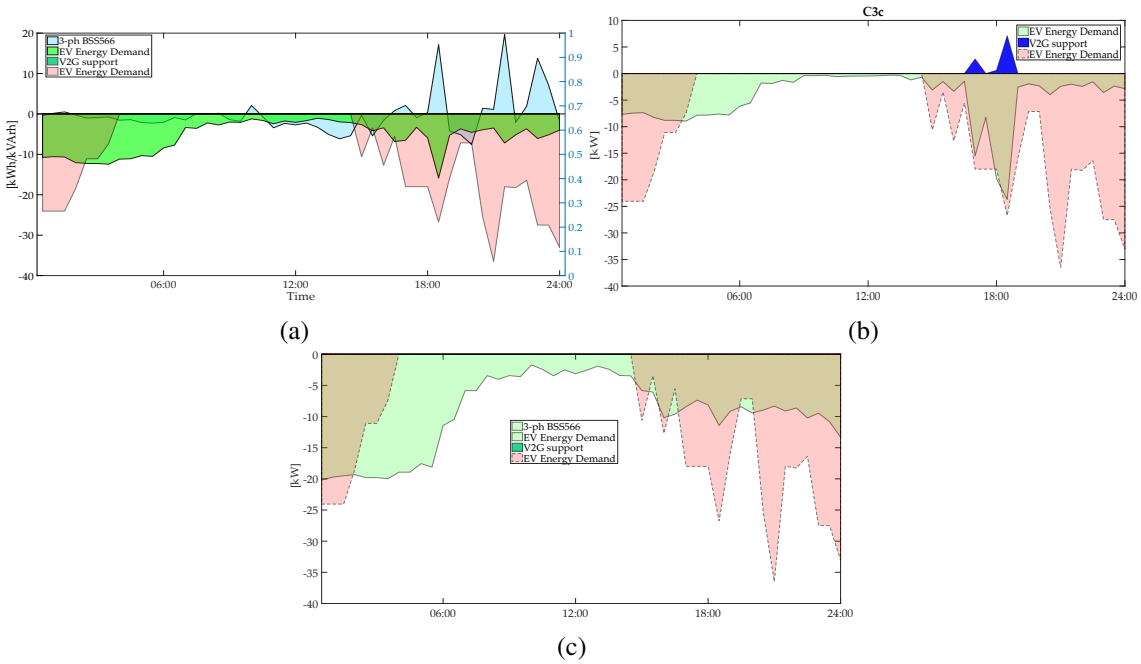

Figure 4.14: Simulation results for scenarios C3-4 and the subsequent subcases. (a) Transformer loading conditions.(b) Branch currents 114-280.(c)Minimum Voltages met for C3a-c.

The connection of $BESS_{566}$ close to the most congested distribution line 114–280 is also assessed in this study in coordination flexible EVs. The connection of the BESS, clearly, reduces the necessary amount EV flexibility that has to be engaged by the DSO to 10% (C2b) compared to 50% needed for C2a&C2c. The BESS is merely utilized to absorb the excess PV generation and restrain voltages within the admissible bounds. It should be noted that the installation of a BESS might be supportive in intra-day operation when forecasts error and deviations from the scheduled controls appear; thus to deal with such mismatches.

The replacement of branch 114–280 line with a larger cross-section one, apparently allows the high EV integration among the examined cases with a reduced amount of EV engaged flexibility to respect all the technical constraints. For instance, a significant reduction of 65% on the need of EV coordination is observed particularly in scenario C3c, which corresponds to the higher EV

integration case examined in this study. The difference on the EV flexibility engaged between C3c–C4c is due to the shifted EVs (in C4c) that address subsequent overvoltages by excessive solar generation. The energy management for smart charging mode as per MACOPF is illustrated in Figure 4.14a–4.14c for all modes of operation in C3. It should be noted that the smart charging concept here considers that each controllable (i.e. available to participate in the scheme) is considered rather flexible within its periods of availability; thus, the tool may create a much different charging profile compared to the dumb profile. Whereas, in Chapter 5, the EV flexibility is further advanced by regarding the initial dumb profile as a pre-assigned schedule of the EV owner (possibly with an aggregator), and any EV flexibility engagement determined by MACOPF tool can be an additional compensation for them. Therefore, the tool shifts such charging profiles only if technical issues are identified. The mathematical formulation of this EV flexibility concept is defined in Section 5.3.4.3.

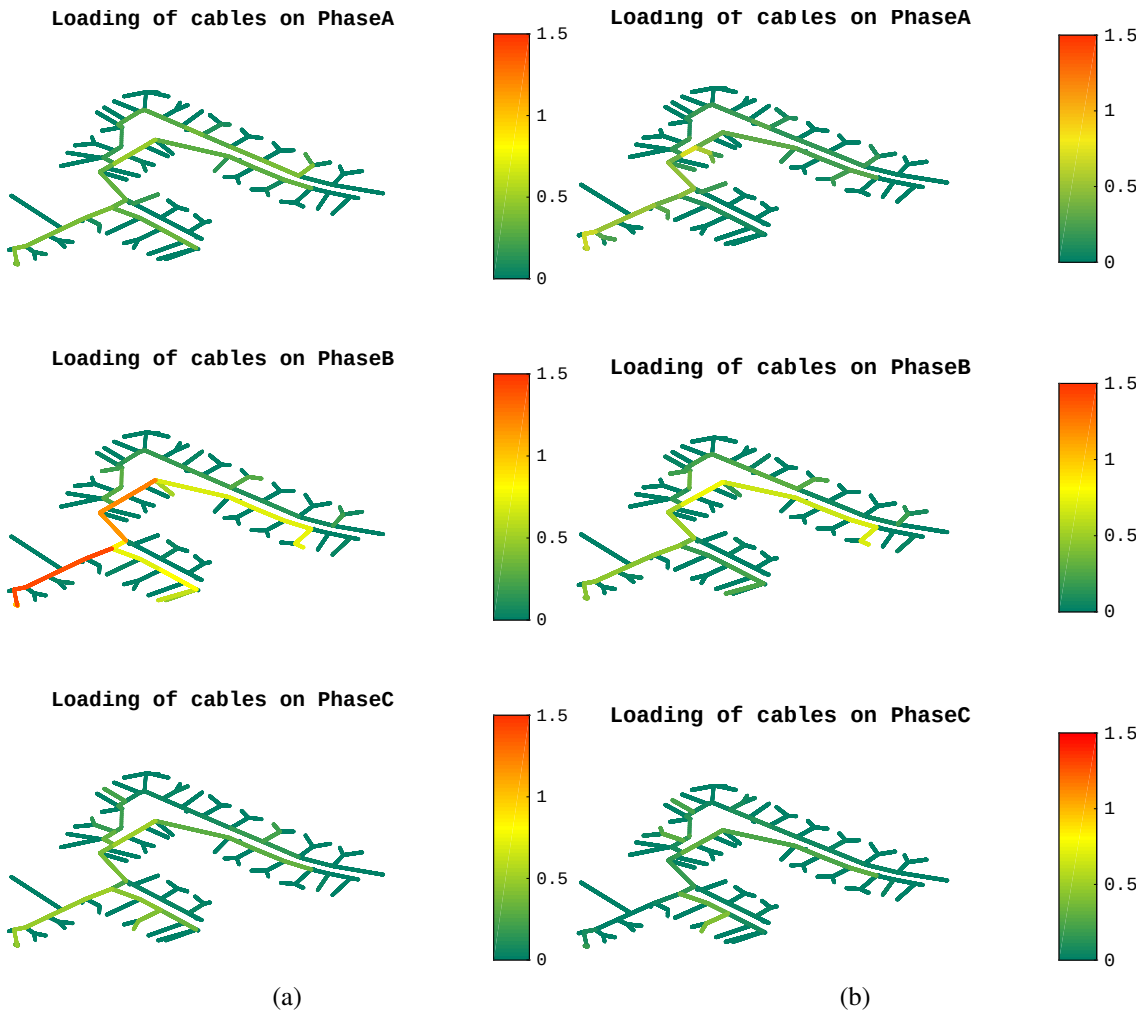

Figure 4.15: Loading of cables at 18:30 in p.u. per nominal current of each type for: (a) C3b: No controls applied.(b) C3b: BESS operation coordinated with EV flexibility.

The overall results of the necessary EV flexibility (i.e. day-ahed basis) on each scenario is

illustrated in Figure 4.16. A general remark that applies to all the examined cases, during particular intervals the line congestion is merely an active binding constraint in MACOPF and the projection to the feasible area leads to lower loading level of the transformer (i.e. values much less than 100%). An analogous phenomenon is observed for voltage unbalances which presents a maximum values lesser than 2% in all cases when MACOPF is used, implying the dependence with the voltage magnitude constraints.

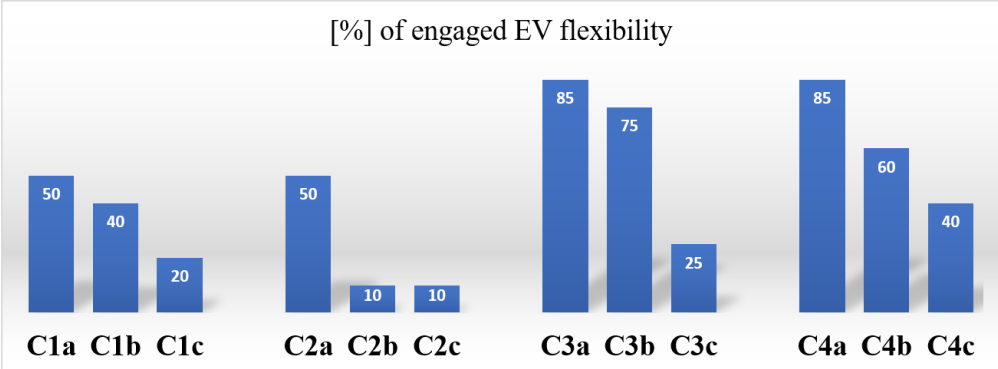

Figure 4.16: Percentage of engaged EV flexibility in day-ahead planning of operation, along all cases explored.

4.6 Final remarks

This chapter discussed an analytical substation centered technical architecture for the operation of unbalanced four-wire LV distribution networks. The control framework that developed to facilitate the operation is also presented. This is an optimization framework based on a three-phase unbalanced multi-period AC-OPF, which is capable to manage multiple types of DER to ensure safe operation in a microgrid or LV distribution grid. The proposed tool derives a cost-efficient coordination of DER, supporting the safe operation of the LV distribution grid maintaining admissible voltages and voltage unbalances within 2% as well as avoiding thermal overloading of the MV/LV transformer and distribution lines even on conditions of increased DER integration.

Through the presented scenarios, the high integration of EVs raises the concern that coordinated charging is deemed vital to maintain all the aforementioned technical constraints. The installation of BESS at the proximity of most congested branch manages to reduce the need of EV flexibility engagement from 10–40% for the examined cases. Accordingly, the replacement of the most loaded line with larger cross-section one reduces the need of EV coordinated to levels of 20 to 60%. Finally, it should be noted that in all the scenarios no active power curtailment is derived to address the voltage effects by the microgeneration.

As a general remark, coordinated operation schemes –as the one presented in this study– along with the active management of DER can be key-drivers towards the smart grid deployment. Results of this chapter show that efficient coordination of DER flexibilities can assure safe grid operation even on conditions with increased penetration of EV and microgeneration.

Chapter 5

A techno-economical assessment of OLTC/BESS investment for the coordinated operation with DER

The large number of small scale Distributed Energy Resources (DER) such as Electric Vehicles (EVs), rooftop photovoltaic installations and Battery Energy Storage Systems (BESS), installed along distribution networks, poses several challenges related to power quality, efficiency, and reliability. Concurrently, the connection of DER may provide substantial flexibility to the operation of distribution grids and market players such as aggregators. This Chapter proposes an optimization framework for the energy management and scheduling of operation for Low Voltage (LV) networks assuring both admissible voltage magnitudes and minimized line congestion and voltage unbalances. The proposed tool allows the utilization and coordination of On-Load Tap Changer (OLTC) distribution transformers, BESS, and flexibilities provided by DER. The methodology is framed with a multi-objective three phase unbalanced multi-period AC Optimal Power Flow (MACOPF) solved as a nonlinear optimization problem. The performance of the resulting control scheme is validated on a LV distribution network through multiple case scenarios with high microgeneration and EV integration. The usefulness of the proposed scheme is additionally demonstrated by deriving the most efficient placement and sizing BESS solution based on yearly synthetic load and generation data-set. A techno-economical analysis is also conducted to identify optimal coordination among assets and DER for several objectives.

5.1 Introduction

Low Voltage (LV) distribution networks used to be a passive segment of the power system, mainly for the supply of consumers; thus, power flows were heading from the bulk transmission points to the distribution grid. Accordingly, from the secondary substation and the downstream connected LV grid, there used to be very limited or an absence of automation for its monitoring and control (Bruno and La Scala, 2017). In the last decade, there has been a large number of small-scale

units, commonly referred to as Distributed Energy Resources (DER), that are getting connected along distribution grids. Several types of DER may be connected such as domestic rooftop Photovoltaics (PV) or generally microgeneration (μG) in some cases coupled with Battery Storage Systems (BESS), controllable loads (e.g., Electric Heat Pumps or other smart domestic appliances), and Electric Vehicles (EVs). The extensive integration of DER in the grid may cause several technical challenges on the operation of distribution networks such as voltage problems, branch congestions, and phase unbalances. Despite these technical bottlenecks, DER may be utilized in favor of the grid operation, providing ancillary services and supporting the bulk transmission system and distribution networks (Hatziargyriou et al., 2017; Razavi et al., 2019).

The Distribution System Operators (DSOs) are currently adopting practices to enhance the observability and controllability of the distribution grids throughout Advanced Distribution Management Systems (A-DMS), (Bruno et al., 2011). The active involvement of DER and generally prosumers in the operation of the network is generally referred to active network management, which is regarded to take place utilizing their flexibility. Sources of flexibility may come from several types of DERs that are enabled with temporal shifting of active or reactive power to be consumed or injected into the grid. Such strategies of active participation of consumers in the grid's operation have gained the interest of utilities for the past few decades by engaging, mainly, industrial consumers through demand side management schemes (Lotfi et al.). Several research works have discussed recently about the Smart Transformers (STs) envisioned as a key element for the controllability of distribution networks in a future context of DER massification (Rodrigues et al., 2020). For the smart grid development, more novel advanced control schemes have to be implemented towards the active involvement of DER.

5.2 Related Works and Contributions

The operational control schemes and energy management applications could be generally classified into several categories according to the communication infrastructure and the data requirement (i.e., deemed necessary to be used). Based on the latter, centralized schemes usually look for solutions not only to resolve technical grid constraints but also to optimize the economical operation of the grid (Karagiannopoulos et al., b; Borghetti et al., 2010; Et-Taoussi et al., 2019); local control (or decentralized) techniques may be applied merely relying on droop based rules (Olivier et al., 2016a; Karagiannopoulos et al., 2019) and distributed strategies which are in line with the deployment of local energy communities and transactive energy concepts (Lilla et al., 2019; Karambelkar et al.; Karfopoulos et al., 2016).

In LV distribution networks, voltage regulation and phase balancing are managed by the DSOs, typically by manual adjustments (offline) of the MV/LV—secondary—transformer which may happen once or twice a year, depending on the seasonal changes in the loads (Efkarpidis et al., 2016c). Alternatively, DSOs act by investing on grid reinforcement measures such as line replacement (i.e., when branch congestions) and manual phase redistribution for phase balancing (Shahnia et al., 2011; Degroote et al.). Considering the stochasticity of both load and generation, the

aforementioned practices of manual configuration of tap-positions and grid reconstruction may be inadequate in many cases (Efkarpidis et al., 2016b). Manual controls and simple local controls may be insufficient due to the intermittent nature of μG and the stochastic behavior of EV charging. On the other hand, the grid reinforcement may be considered quite effective but still a costly measure for the DSO.

The possibility of utilizing droop capabilities (for active and reactive power control –$P = f(V)$, $Q = f(V)$, accordingly) with a smart PV inverter particularly for voltage regulation has extensively been studied in the literature (Demirok et al., 2011; Olivier et al., 2016a; Cagnano et al., 2011). The reactive power control is generally a less efficient solution in the LV grid for voltage control due to the high branch ratio R/X (i.e., rather resistive nature of LV distribution lines) compared to Medium Voltage (MV) distribution networks or transmission. Self-consumption is commonly imposed by regulation and legislation lately, to address voltage rise effects during the peak period of PV generation. In several European countries (e.g., Belgium, Denmark, the Netherlands and Greece), residential PV self-consumption measures based on net metering schemes aim at matching the endogenously generated power with local demand (Heleno et al.). In Germany, there is a cap for active power feed-in at 70% of the installed capacity for all the prosumers with a capacity of less than 30 kWp (Stetz et al., 2012). Nevertheless, Active Power Curtailment (APC) might not be an economically attractive solution for both DSOs and the prosumers. Therefore, more sophisticated control schemes are proposed exploiting the coordination of μG with DSO assets to improve the network's power quality (Su et al., 2016; Samadi et al., 2014).

Several applications have focused their interest on introducing the control of other DER, such as BESS or EVs. Most research applications refer to the coupling of BESS systems with μG to firm-up the dispatched power produced from PVs by reducing the mismatches between generation-demand (Heleno et al.; Petrou et al., 2019). The increased cost of investment has been the main limitation for the extensive deployment of BESS, a fact that is likely expected to change in the current decade according to (Tsiropoulos et al., 2018). Concurrently, several works have lately proposed the utilization of BESS by DSOs—i.e., owned and controlled by the DSO—(Aghaei et al., 2019; Miranda et al., 2016) to deliver operational flexibility operation as well as to increase hosting capacity of DER into the grids. Nonetheless, there is very limited BESS utilization by DSO currently due to the in force Directive 2009/72/EC (Union, 2009), where the unbundling requirements for DSOs do not allow BESS directly owned and controlled by them. As a result, the ever growing number of domestic BESS may undermine the current business model of the electric utilities (Efkarpidis et al., 2016a). The following trend aims to maximize the revenue brought by "smart" consumers that utilize home energy management systems to optimize the local generation and consumption.

The large-scale penetration of EVs that is expected in the current decade will notably increase electricity consumption, during charging periods. Therefore, power flows—including Vehicle-to-Grid (V2G)—grid losses, and voltage profile patterns and generally power quality along the grid will change significantly (Lopes et al., 2010). These effects may arise the need to reinforce the grid in some locations. Based on the EV charging strategy to be adopted, grid reinforcement may

be deterred. Several schemes have been proposed to derive smart charging schedules to ensure safe grid operation (Sharma et al., 2014; Richardson et al., 2012; García-Villalobos et al., 2016; Connell et al., 2014), while some of those dealing with phase unbalances may be provoked by EVs in the grid. None of the aforementioned works, however, propose any possible coordination of DER amongst them or with DSO assets to optimize cost objectives or the technical operation.

Several industrial prototypes for secondary transformers (Efacec, Reinhausen, Siemens) are equipped with the capability of On-Load Tap Changer (OLTC) (Jiricka et al., 2017) for MV/LV transformers. There is relatively limited work dealing with the coordinated operation of OLTC with DER in (Liu et al., 2012; Maniatopoulos et al., 2017; Kulmala et al., 2014; Efkarpidis et al., 2016a). In spite of the fact that these works provide the optimal coordination of OLTC with DER, there is no insight for the temporal flexibility that may be delivered by DER between subsequent time slots. Authors in (Karagiannopoulos et al., b) propose a framework for the optimal coordination among several DER and the OLTC, dealing also with the phase balancing constraint. In this work, authors propose efficient linearizations to resort tractable multi-period OPF extending the problem statement in (Fortenbacher et al.). On the contrary, a three-phase multi-period OPF based on the exact (i.e., nonlinear) AC power flows is proposed in this work, incorporating multiple DER within the operation of the distribution grid.

This Chapter essentially advances previous Chapter 3. The main contributions of this part may be outlined as follows:

- Advances an analytical DMS framework for the energy management and scheduling of operation of unbalanced distribution networks with increased integration of DERs. The tool is capable of deriving control actions and schedules for flexible DER and the OLTC subjected to multiple operational constraints such as congestion management, phase balancing, and voltage regulation. Furthermore, optional objective terms might be opted among the minimization of operational costs or minimization of flexibility activation costs and minimization of active power losses.
- An analytical study is conducted to compare the alternatives among OLTC, BESS, active network management, or their coordinated operation for scenarios with increased DER integration.
- A sensitivity analysis for coordinated operation between BESS and EVs exploring variable base pricing for the BESS investment and the variable price of EV flexibility.

5.3 Extended formulation of Coordinated Active Network Management Tool

This section details the statement of the proposed multi-objective unbalanced Multi-period AC-OPF (MACOPF). The formulation provides a flexible DMS framework for LV unbalanced networks. The main focus is to minimize the DSO/grid's operation cost; hence, it is essential to minimize DER flexibility activation costs (e.g., minimize the engagement of DER on the operation), the overuse of any DSO assets (e.g., BESS, OLTC), minimize the grid losses as well as

to minimize the energy costs by means of the energy imported by the upstream grid. Based on the strategy applied for each type of DER/asset, the optimization strategy (i.e., dispatchable μG, definition of EV flexibility, V2G, etc.) may be formulated respectively.

In this study, the LV distribution network is represented as a three-phase four wire unbalanced network with a multi-earthed neutral; this fact allows the application of the Kron's reduction (Ciric et al., 2003). More analytical information on the modeling of lines and the transformer may be found in Chapter 2. Each time slot is denoted by $\tau \in \mathscr{T}$, where the length of set $\mathscr{T}$ is the horizon of the desired scheduling of operation H_τ. Let $x_{g,\tau}$ be the state vector for time slot τ represented by Equation (5.1), containing the instant angles and voltage for each bus ($j \in \{1,\ldots N_b\}$) and phase ($\phi \in \Phi$). The vector of decision variables u_τ consists of active and reactive power for each of the controllable DER ($k \in \{1,\ldots N_c\}$) as shown in (5.2). The voltage angles displacement between adjacent nodes may be considered as constant (commonly less than 10° (Fortenbacher et al.)); thus, the scale of the optimization problem can be reduced significantly. However, angles are analytically defined in this work due to the need of assessing phase balancing constraints:

$$x_{g,\tau} = \begin{bmatrix} \Theta \\ \mathscr{V} \end{bmatrix}_\tau \forall \tau \in \mathscr{T}, x_\tau \in \mathbb{R}^{(2*3N_b)}, \tag{5.1}$$

$$u_\tau = \begin{bmatrix} P_c \\ Q_c \end{bmatrix}_\tau \forall \tau \in \mathscr{T}, u_\tau \in \mathbb{R}^{(2*N_c)}, \tag{5.2}$$

$$y_\tau = \begin{bmatrix} p_{ch} & p_{dch} & y_{\pi,ch} & y_{\pi,dch} & y_{\text{trip}} & y_{\text{tap}} & \varepsilon_{j,\text{con}} \end{bmatrix}_\tau \tag{5.3}$$

All of the auxiliary variables, for τ, are contained in the y_τ; such variables are involved in the DER or OLTC modeling as well as slackness variables to relax constraints and ensure convergence for any resolution. The sets $\mathscr{N}$ and $\mathscr{J}$ stand for the nodes (each bus has three nodes, one per phase) and the branches of the grid. Let X be the vector that contains stacked the state vectors, the decision variables, and any auxiliary variables defined as $X = [x_1,\ldots,x_{H\tau},y_1,\ldots,y_{H\tau}]^T$. As explained also in Chapter 3, the auxiliary variables are intentionally appended as last elements of vector X to allow the flexible configurations of the stated problems (i.e., eases the calculation of derivatives and the data logging of initial points). To avoid lengthy notation on the problem statement, a symbolic variable $\mathscr{X}_\tau = (x_{g,\tau}, u_\tau, y_\tau)$ is defined. The MACOPF is stated in Equation (5.4a):

$$\min_u \sum_{\tau=1}^{H_t} \left[\{w_1 \cdot \Pi_\tau + w_2 \cdot \mathbf{P_L}_\tau\}\Delta\tau + w_3 \cdot \mathbf{U}_{\text{OLTC}\boldsymbol{\tau}} + w_4 \cdot \mathbf{Tap}_{\boldsymbol{\tau}} + \Phi_{p,\boldsymbol{\tau}}\right], \tag{5.4a}$$

subjected to

$$G_j(\mathscr{X}_\tau) = 0, \qquad \forall j, \tau \in \mathscr{N}, \mathscr{T}, \tag{5.4b}$$

$$H_{Sub}(\mathscr{X}_\tau) \leq S_{rated} - \varepsilon_{sub}, \qquad \forall \tau \in \mathscr{T}, \tag{5.4c}$$

$$VUF_j(\mathscr{X}_\tau) \leq \overline{\text{VUF}} - \varepsilon_{\text{VUF}}, \qquad \forall i, \tau \in \mathscr{N}, \mathscr{T}, \tag{5.4d}$$

$$V_{\min} - \varepsilon_{\mathscr{V}_{j,\tau}} \leq v_j \leq V_{\max} + \varepsilon_{\mathscr{V}_{j,\tau}}, \qquad j, \tau \in \mathscr{N}, \mathscr{T}, \tag{5.4e}$$

$$h_\xi(\mathscr{X}_\tau) = 0, \qquad \forall \xi, \tau \in \mathscr{U}, \mathscr{T}, \tag{5.4f}$$

$$g_\xi(\mathscr{X}_\tau) \leq 0, \qquad \forall \xi, \tau \in \mathscr{U}, \mathscr{T}, \tag{5.4g}$$

where the analytical expression of the objective is the following:

$\Pi_\tau = \sum_k^{N_b} \left([c_k(\tau)]^T \cdot u_{k,\tau}\right)$	$\mathscr{O}_1$:	flexibility activation costs
$\mathbf{P_L}_\tau = \sum_{\phi\in\Phi} \sum_{i\in\mathscr{B}} \frac{\left(\Delta V_{\varphi,ij}\right)^2}{R_{\varphi,ij}}$	$\mathscr{O}_2$:	Apparent power losses
$\mathbf{U}_{\text{OLTC}\boldsymbol{\tau}} = \sum_{\phi\in\Phi} \left(V_{\phi,ps}(\tau) - V_{\phi,ps}(\tau-1)\right)^2$	$\mathscr{O}_3$:	Penalize fast transitions of primary winding voltage
$\mathbf{Tap}_{\boldsymbol{\tau}} = \sum_{\phi\in\Phi} \left(t_{c_\phi}(\tau) - t_{c_\phi}(\tau-1)\right)^2$	$\mathscr{O}_4$:	Cost of tap operations

and vector $c_k(\tau)$ assigns a price for the utilization of controllable DER or asset k at τ in €/kWh or €/kVArh. Multiple pricing schemes may be defined, enabling demand–response schemes. The exact form of nonlinear power flow equations is encapsulated with the nonlinear equality constraints in (5.4b); inequality constraints (5.4c) is posed to ensure that the MV/LV transformer is not loaded more than the nominal, or may provide a power cap for the LV grid energy management; (5.4d) inequality constraints stand for the phase balancing requirements; the boxed constraints in (5.4e) to maintain all nodal voltage within the preset limits. The slackness variables ε in (5.4c)–(5.4e) are applied to slightly relax the constraints and reassure the convergence of the optimizer even when the available active measures cannot strictly provide a solution into the feasible space (thus, it is enlarged). The last equality and inequality constraints (5.4f)–(5.4g) describe a generalized form pertaining to operational constraints of all controllable assets and DER.

In the objective function in Equation (5.4a), the term $\Phi_{p,\boldsymbol{\tau}}$ assigns to some of the auxiliary variables a penalty cost. Such penalty costs may be for the relaxation parameters ε, as well as some penalties to prohibit the concurrence of charging and discharging as explained more analytically in the BESS model.

The mathematical form of the objective function is a combination of linear (F_L) and quadratic (F_Q) cost functions. All the quadratic terms in the objective function are encapsulated by the following Equation (5.5):

$$F(X) = \sum_{\tau\in\mathscr{T}} f(\mathscr{X}_\tau) = F_L + F_Q = c^T \cdot w + \frac{1}{2} w^T \cdot H \cdot w, \tag{5.5}$$

where w contains all variables of the stated problem, including the auxiliary variables of problem statement (5.4a). Variable w can be defined in the following steps, by primarily considering an additional variable u as proposed in (Zimmerman and Murillo-Sánchez, 2016). This u variable can be formed by applying a linear transformation N_T and a shift $\hat{r}$ to the extended set of the optimization variables:

$$r = N_T \cdot X, \tag{5.6}$$

$$u = r - \hat{r}, \tag{5.7}$$

To enable flexible extension of such costs able to handle scaled linear and quadratic costs as in Equation (5.4a), each element of the optimizer full set of variables X (let x_i) is input as:

$$w_i = \begin{cases} m_i f_a(u_i + z_i), & w_i < -z_i, \\ 0, & -z_i \leq x_i \leq w_i, \\ m_i f_a(u_i - z_i), & x_i > w_i, \end{cases} \tag{5.8}$$

and

$$f_a = \begin{cases} \alpha, & \text{if } d_i = 1, \\ \alpha^2, & \text{if } d_i = 2, \end{cases} \tag{5.9}$$

where z_i provides the option to shift the cost function, m_i scales the variable x_i accordingly, and, according to the specified input d_i, the cost function may be shaped as linear (i.e. $d_i = 1$) or quadratic (i.e. $d_i = 2$). This formulation is used to structure all the cost functions. The quadratic terms refer to the loss minimization as well as the operational cost functions for OLTC. For instance, the cost formulation: BESS, EV, μG, is a piece-wise linear(PWL) function that is incorporated in the optimization framework through cost constrained variables. Further details regarding this mathematical formulation are given in Chapter 3.

5.3.1 Interior-Point Algorithm

The stated MACOPF is addressed using the Interior-Point (IP) primal-dual algorithm. Assume the compact formulation for the stated MACOPF by the set of equations (5.10), where the set of variables is denoted by $\mathbf{x}$:

$$\min_{\mathbf{x}} f(\mathbf{x}), \tag{5.10a}$$

subject to

$$g_E(\mathbf{x}) = \mathbf{0}, \tag{5.10b}$$

$$h_I(\mathbf{x}) \leq \mathbf{0}, \tag{5.10c}$$

$$\boldsymbol{x}_{\min} \leq \mathbf{x} \leq \boldsymbol{x}_{\max}, \tag{5.10d}$$

The corresponding Lagrangian function is given by Equation (5.11):

$$\mathscr{L}_p(\mathbf{x},\boldsymbol{\lambda},\boldsymbol{\sigma},\mathbf{s}) := f_p(\mathbf{x}) - \boldsymbol{\lambda}^T g_E(\mathbf{x}) - \boldsymbol{\sigma}^T(h_I(\mathbf{x})+\mathbf{s}) \tag{5.11}$$

where vectors $\boldsymbol{\lambda}$, $\boldsymbol{\sigma}$ are the Lagrange multipliers for the corresponding equality ($g_E(\mathbf{x})$) and inequality constraints h_I which can be regarded also as equality constraints by the addition of slack variables s, such that $h_I(\mathbf{x}) - \mathbf{s} = \mathbf{0}$. Thereafter, the augmented objective function for the unconstrained problem (*penalty function*) $f_p(\mathbf{x})$ is defined by Equation (5.12):

$$\begin{aligned} \mathscr{L}_p(\mathbf{x},\boldsymbol{\lambda},\boldsymbol{\sigma},\mathbf{s}) := f_p(\mathbf{x}) - \boldsymbol{\lambda}^T g_E(\mathbf{x}) - \boldsymbol{\sigma}^T(h_I(\mathbf{x})+\mathbf{s}) \Leftrightarrow \\ \mathscr{L}_p(\mathbf{x},\boldsymbol{\lambda},\boldsymbol{\sigma},\mathbf{s}) = f(\mathbf{x}) - \mu^{(k)}\sum_{j=1}^{N_x}\ell n(x_j - x_{j,\min}) - \mu^{(k)}\sum_{j=1}^{N_x}\ell n(x_{j,\max} - x_j) - \\ \mu^{(k)}\sum_{j=1}^{N_{ineq}}\ell n(s_j) - \boldsymbol{\lambda}^T g_E(\mathbf{x}) - \boldsymbol{\sigma}^T(h_I(\mathbf{x})+\mathbf{s}), \end{aligned} \tag{5.12}$$

where $\mu^{(k)}$ stands for the logarithmic barrier parameter per iteration k. The latter is forced to monotonically reduce to 0 as iteration progresses by the minimizer.

The exact formulation of the non-convex nonlinear power flow equality constraints inflicts the certification of the second-order KKT conditions regarding local optimality of one point-solution p^*. An analytical description for the first and second order KKT conditions may be found in (Nocedal and Wright, 2006). As per (Kotsalos et al., 2019a), particular computational techniques are proposed to remedy the singularities of the Jacobian matrix (caused by the inter-temporal dependencies of DER) which is necessary to be assessed along with the Hessian one, for the iterative process of the IP algorithm. Based on the MACOPF structure, efficient explicit calculations (exploiting sparsities) of the Jacobian and Hessian matrices are input in the optimizer not only to accelerate the convergence, but also to avoid faulty solution due to the singular Jacobian. A database is used to procure initial points (X_0) to the optimizer from past resolutions of the problem, as well as to acquire historical data regarding load and weather forecasts if they are not currently available.

5.3.2 Multi-Objective MACOPF Treated with a Weighted Sum Method

As presented in the problem statement, MACOPF is clearly a multi-objective optimization problem. The discipline of Pareto needs to be introduced hereby, which is posed to ensure that none of the objectives can be further improved in the search space without any major impact on the objective function. There exist several methods to support the decision maker, but, in practice, the most commonly used one is the weighted sum method; this recommends the scaling (i.e., ψ_i) and the multiplication of all the objectives with a weighting factor (i.e., w_i) as follows:

$$F(X) = \sum_i^k w_i \cdot O_i(X)\frac{1}{\psi_i}, \text{ such that } \begin{cases} \sum_i^k w_i = 1,\ \mathbf{w} \geq \mathbf{0},\ \mathbf{w} = [w_1,\ldots,w_k]^T \\ \psi_i = \max(O_i) \end{cases} \tag{5.13}$$

The scaling of each objective term is critical to balance their impact by balancing their order of magnitude on the aggregated objective function but is often disregarded leading to mistaken and overestimated efficient points.

5.3.3 Grid Constraints

5.3.3.1 Power Flows

The nonlinear power flows equations, at time instant τ, are formed by Equation (5.14), expressed as a function of phasor nodal voltage, injection from loads and the DER injection in complex form; essentially imposing that the mismatch between nodal injections and the injection from loads and DER is zero:

$$\begin{aligned} G(\mathscr{X}_\tau) = S_{\text{nodal}}(\mathscr{X}_\tau) + S_{\text{load}}(\mathscr{X}_\tau) - C_p \cdot S_{\text{DER}}(\mathscr{X}_\tau) = \mathbf{0} \\ S_{\text{nodal}}(\mathscr{X}_\tau) = [V_\tau] Y_{\text{bus}} V_\tau^* \end{aligned} \tag{5.14}$$

where the $S_{\text{load}} \in \mathbb{C}^{3N_b}$ vector contains the complex loads for all buses of the system; $S_{\text{DER}} \in \mathbb{C}^{N_c}$ the DER injections or consumptions. The sparse matrix $C_p \in \mathbb{N}^{3N_b \times N_c}$ is defined to map the DER net injections to the $3N_b$ nodes. Any (i, j) element of C_p is zero, whereas it is one if generator j is located in bus i.

5.3.3.2 Voltage Unbalances

It is important to account for voltage unbalances particularly in LV grids, which inherently present unbalance nature. The integration of single phase DER may lead to much higher unbalances. The Voltage Unbalance Factor (VUF) has several definitions; however, EN 50160 standards make use of the sequence components as in Equation (5.15), (Efkarpidis et al., 2016b):

$$\text{VUF}_j[\%] = \frac{|\upsilon_{2,j}|}{|\upsilon_{1,j}|} \cdot 100\% \approx |\upsilon_{2,j}| \cdot 100\%, \tag{5.15}$$

where $\upsilon_{1,j}, \upsilon_{2,j}$ are positive and negative sequence components, respectively. Obviously, the technical constraints for unbalances present a non-convex nature. Nonetheless, the phase balancing constraint can be easily convexified by the accurate approximation that the magnitude of positive sequence components are closely to 1 p.u. as per (Wang, 2001). For a node j, the phase balancing constraint is given by Equation (5.16):

$$\text{VUF}_{j,\tau} - \varepsilon_{\text{VUF}_j} \leq 2\% \quad \forall j \in \mathscr{N}, \tau \in \mathscr{T}, \tag{5.16}$$

$\varepsilon_{\text{VUF}_j} \leq 0$ is an auxiliary variable relaxing the balancing constraint and ensure convergence of MACOPF.

5.3.3.3 Line Congestion Management

The connection of several EVs along the distribution feeder may increase the peak load profile leading to line congestions. The technical constraint to manage the branch currents is applied at

each phase. Let $I_b(\tau) \in \mathbb{C}^{3\cdot 3\cdot N_b}$ represent the line currents for τ slot. Exploiting the definition of the Bus-Injection to Branch-Current (BIBC) matrix as proposed in (Jen-Hao, 2003), the phase currents at each branch can be derived from Equation (5.17):

$$\begin{aligned} I_{b_\tau} &= \mathbf{BIBC} \cdot I_\tau \quad \Leftrightarrow \\ &= \mathbf{BIBC} \cdot (Y_{bus} V_\tau) \quad \Leftrightarrow \\ &= Y_m \cdot V_\tau, \end{aligned} \tag{5.17}$$

where Y_m represents the modified admittance matrix that maps the nodal current injection vector to the respective branch current injection. The group of nonlinear inequality constraints provided in (5.18) are posed to ensure line congestion management. The analytical contribution of these constraints into the Jacobian and Hessian is input to the optimizer and is indicatively formulated in Appendix A.2.1:

$$\mathrm{I}_{j,\tau} - \varepsilon_{\mathrm{L}} \leq \overline{I_j}, \quad \forall j \in \mathscr{J}, \tau \in \mathscr{T}. \tag{5.18}$$

5.3.4 OLTC and DER Operational Model

5.3.4.1 On-Load Tap Changer (OLTC) Model

The OLTC mechanism is considered to be connected at the primary winding of the MV/LV transformer. The primary side is connected through a branch line to the slack bus through a fictitious line impedance (i.e., Z-Thevenin) representing this way the upstream connected MV distribution network, as represented in Figure 5.1. The incorporation of the OLTC introduces discrete decision variables to determine the tap-positioning at each time step of the horizon. This would resort the MACOPF's formulation to a Mixed-Integer Nonlinear (MINLP), which is generally classified as an NP-hard problem. The MINLP—especially non-convex problems—are characterized by the challenge of handling the nonlinearities in addition to the combinatorial nature posed by integer decision variables (Zhu, 2015b). The continuous relaxation of non-convex MINLP is itself a global optimization problem, thus likely to be NP-hard (Burer and Letchford, 2012). In the literature, some approaches have been proposed to treat the discrete nature of tap positions by introducing continuous decision variables as in (Timbus et al., 2009; Kulmala et al., 2014; Maniatopoulos et al., 2017). Nevertheless, none of these works couple the stages among them and subsequent time slots (i.e., multi-period optimization) or provide the option to follow any technical limitations as a maximum number of tap changes.

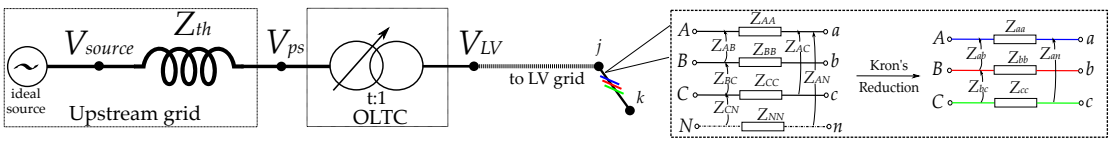

Figure 5.1: Representation of OLTC connected with the upstream grid.

A three-stage resolution is hereby proposed to avoid the introduction of integer variables. In the first stage, the tap changer decision variables are treated as a continuous set $[\underline{t_{p_a}}, \overline{t_{p_a}}]$.

Those decision variables are tracked with heuristic variables that follow the tangent between two-subsequent time slots. The algorithmic diagram of the proposed scheme for the OLTC is illustrated in Figure 5.2. The corresponding mathematical expressions that connect the tap-positioning decision variables with primary and secondary winding voltage are in Equation (5.19):

$$V_{LV} = V_{ps} - \Delta s \cdot t_{p_\phi}, \quad \forall \tau, \phi \in \mathscr{T}, \Phi \tag{5.19}$$

where V_{LV}, V_{ps} are the voltage magnitudes on secondary and primary winding accordingly and Δs is the % resolution of tap-step t_{p_ϕ}. The constraints have to be applied to all phases since many OLTC provide the option to have different tap-position per phase, yet their control is mechanically coupled to shift them all simultaneously.

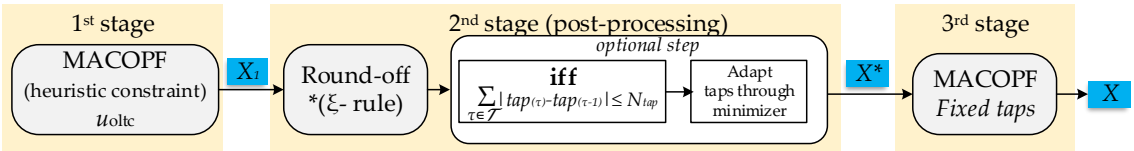

Figure 5.2: Proposed optimization scheme for the OLTC.

The post-processing routine on the second stage lies on the round-off rule described in Algorithm 2. According to this algorithm, the continuous tap-position set is projected to the closest integer variable, whereas a tangent rule is used to enhance the algorithm and avoid excessive tap changes.

Algorithm 2: OLTC round-off ξ—rule based on (Timbus et al., 2009); in this study, $\xi = 0.5$.

Data: $X_{1,c} = [t_{c,1}, \ldots, t_{c,H_\tau}]$—continuous tap-positions from 1st stage—
Result: $[tap_1, \ldots, tap_{H_\tau}]$ discrete tap-positions.
begin
  for $j \in H_\tau$ **do**
    $d \longleftarrow \left| t_{c,j} - \overline{t_{c,j}} \right|$; where $\overline{t_{c,j}}$ defines the nearest to $t_{c,j} \in H_\tau$ admissible tap value
    if $d \geq \xi \cdot \Delta s$ **then**
      $tap_j = \overline{t_{c,j}}$
    else
      $tap_j =$ maintain tap-position

An optional scheme is included within the second stage relying on a minimizer to adapt the decision taken regarding the tap-position in case of particular technical limitations regarding the daily number of tap changes. This optimizer is set in Equation (5.20) and (5.21):

$$\min_{u_d} \sum_{\tau} (u_d(\tau) - tap_\tau)^2 \tag{5.20}$$

such that

$$\sum_{\tau} \|u_d(\tau) - u_d(\tau - 1)\| \leq \overline{\Delta tap}. \tag{5.21}$$

The optimizer targets to reduce the distance between vectors $u_d(\tau)$ and tap_τ, such that the maximum number of tap-positioning posed for the horizon of the optimization—$\overline{\Delta tap}$. This formulation clearly presents a quadratic function with non-convex constraints. The problem is resolved by using a state-of-the art optimizer called NOMADS (Le Digabel, 2011). This solver implements a Mesh Adaptive Direct Search algorithm (MADS), which is capable of dealing with non-smooth objective functions and constraints since it resorts to black-box optimization, avoiding the evaluation of costly derivatives.

The post-processing of second stage outputs the discrete tap-positions, which compose inputs for the third stage. The final operational decisions are decided in the third stage where any additional control actions may be determined. The vector X^* contains control actions derived from the first stage extracting the OLTC decision variables, and this is then used as an initial point for the last MACOPF resolution.

The characteristics of the OLTC equipment used for this case study are given in Table 5.1. This equipment may be installed to retrofit an existing transformer, adding the OLTC capability.

Table 5.1: On-Load Tap Changer technical and economical parameters (Efkarpidis et al., 2016a).

Investment cost (€)	c_{inv}	7.000
Step Voltage (%)	Δs	(up to 3) hereby constant at 2
Min/Max tap-position	$\underline{tap}/\overline{tap}$	(up to ± 9)± 2
Min/Max voltage (p.u.)	$\underline{V_{ps}}/\overline{V_{ps}}$	1.1/0.9
Maintanance-free operations	$\overline{N_{oltc}}$	700.000
Approximated Cost per Tap (€)	c_{tap}	0.01

5.3.4.2 Battery Energy Storage System (BESS)

The BESS model is a first order model, where two distinct auxiliary variables participate in the BESS state equations and operational constraints—one for the discharging $p_{dch} \geq 0$, $p_{dch} \in \mathbb{R}_+$, while the charging mode $p_{ch} \leq 0$,$p_{ch} \in \mathbb{R}_-$. Any losses occur in each mode of operation are associated with charging and discharging efficiencies (η_{ch}, η_{dch}). $\mathscr{E}_0$ is defined the initial (i.e., $\tau =$ 0) stored energy at the BESS. The remaining stored energy of a BESS at one time step τ can be calculated by Equation (5.22), which clearly bundles the instant energy state with the former one:

$$\mathscr{E}(\tau) = \mathscr{E}(\tau - 1) - \Delta\tau \begin{bmatrix} \eta_{ch} & \frac{1}{\eta_{dch}} \end{bmatrix} p(\tau), \quad \text{where} p(\tau) = \begin{bmatrix} p_{ch}(\tau) \\ p_{dch}(\tau) \end{bmatrix}. \tag{5.22}$$

Within the proposed optimization framework and the subsequent participation of BESSs in the power flow equations (i.e., in S_{DER}), a primary decision variable per BESS defines the scalar

variable for active power injections P_{BESS}:

$$P_{BESS}(\tau) = p_{ch}(\tau) + p_{ch}(\tau), \tag{5.23a}$$

$$\overline{p_{ch}} \leq p_{ch}(\tau) \leq 0, \tag{5.23b}$$

$$0 \leq p_{dch}(\tau) \leq \overline{p_{dch}}, \tag{5.23c}$$

$$\underline{SoC} \leq SoC(\tau) \leq \overline{SoC}, \tag{5.23d}$$

$$SOC(\tau) = \frac{\mathscr{E}(\tau)}{\mathscr{E}_{rated}} \tag{5.23e}$$

$$\mathscr{E}(0) = \mathscr{E}(H_\tau). \tag{5.23f}$$

The constraints (5.23a)–(5.23e) are settled $\forall \tau \in \mathscr{T}$. The constraints (5.23b)–(5.23d) limit the maximum charging and discharging power as well as the minimum and maximum State-of-Charge (SoC)—defined in Equation (5.23e)— according to the BESS's technology and characteristics. The last constraint (5.23f) imposes that BESS's ending energy state should be equal to the initial stored energy; thus, the BESS does not get fully discharged.

To avoid simultaneous charging and discharging of the BESS, a penalty cost is assigned with each auxiliary decision variables p_{ch}, p_{dch}, both of which should be greater—at least one order—than the cost of use of BESS (c_{BESS}) itself, i.e., P_{BESS}.

Based on the European Commission's study in (Tsiropoulos et al., 2018), where several scenarios for Li-ion BESS costs are concerned depending on different market growth indexes, Table 5.2 presents the selected characteristics for BESS used in this study. A base price is selected for the year 2025, assuming a moderate adoption of Li-ion BESS by the market. The Levelized Cost of Energy (LCOE) for BESS is also calculated to assign it with the operational costs.

Table 5.2: BESS technical consideration based on the data presented on (Tsiropoulos et al., 2018) for energy-designed BESS.

	2025 (reference year)
Price (€/kWh) *(includes costs of investment)	290
Cycles DoD at 80% in lifetime	5000
LCOE calculation (€/kWh)	0.0725

5.3.4.3 Electric Vehicles

The same mathematical formulations as the BESS's are settled to simulate the EV operation and technical constraints, with the difference that, in the energy state Equation (5.22), a term $A_\tau = y_{\text{trip}}(\tau) \cdot E_{\text{tr}}(\tau)$ is deducted whenever there is a trip occurrence. The variable $[y_{trip}]_{n_{tr} \times H_\tau}$ captures the temporal occurrence of a trip combined with the energy consumed E_{tr} along that period. The variable n_{tr} simply refers to the expected number of trips per EV. The combination of those variables creates a mapping of flexibilities (i.e., to charge or discharge based on EVs' availability,

when not used). The Vehicle-to-Grid (V2G) may be considered as an additional mode of operation for the EVs, described by the discharging decision variable.

One can define the energy state of an EV at time period τ through $\mathscr{E}_{EV}(\cdot) \in \mathbb{R}$ that is temporally coupled with the prior period's energy state and the decision of charging/discharging set-point. For one EV_j, the energy state equation (5.22) can be recasted in a matrix format (Equation (5.24)) towards evolution of time as a linear combination of the initial stored energy $\mathbf{E}^j_{\text{EV}} = [\mathscr{E}^j_{EV}(0), \ldots, \mathscr{E}^j_{EV}(H_\tau)]^T$, representing all energy states:

$$\mathbf{E}^j_{\text{EV}} = \begin{bmatrix} I \\ \vdots \\ I \end{bmatrix} \mathscr{E}^j_0 + \begin{bmatrix} \Lambda & & \mathbf{0} \\ \vdots & \ddots & \\ \Lambda & \ldots & \Lambda \end{bmatrix} \begin{bmatrix} p^j_{\text{EV}}(1) \\ \vdots \\ p^j_{\text{EV}}(H_\tau) \end{bmatrix} - \mathbf{y}^j_{\text{trip}} \cdot \mathbf{E}^j_{\text{tr}}, \tag{5.24}$$

where $\Lambda = [\text{diag}\{n_{dch}\}\ \text{diag}\{1/n_{ch}\}] \cdot \Delta\tau$.

The EVs are modeled to emulate realistic behavior, using a mobility routine as explained analytically in Chapter 3. Further assumptions and details about the EVs are given in Section 5.4, particularly in regard to the consideration of mobility model and habit of trips. The flexible use of smart charging operation is illustrated in Figure 5.3b, where some charging energy slots are shifted at later hours. In Figure 5.3a, the cost function definition is illustrated, where the dumb charging is added on the objective function as a negative cost (i.e., profit), whereas the decision to use smart charging decreases proportionally this profit. The cost function is deployed as a piecewise linear function with a CCV. Note that, for periods when no dumb charging does occur, a V (not purely symmetric since use of V2G is considered more expensive) cost function is considered with its vertex at (0,0).

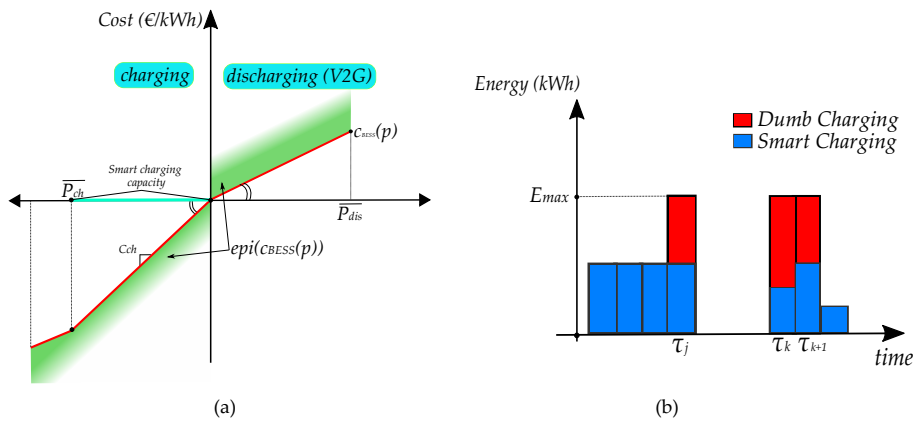

Figure 5.3: (**a**) cost function assignment for smart charging; (**b**) example of smart charging operation.

5.4 Case Study Synopsis

The validation of the proposed coordinated control of LV operation takes place for an IEEE LV benchmark network (Espinosa, 2015). This LV grid—in Figure 4.11—presents the same technical characteristics with the benchmark with the difference that the MV/LV transformer 250kVA, 20/0.4kV, since only one feeder is regarded.

The MACOPF formulation is used to obtain the most suitable placement and sizing of the BESS for the examined grid. The results obtained, given the requirement of an energy BESS application—c-Rating 0.5—suggest the installation of a 90 kWh (round-trip efficiency considered to be 0.8) at node 460, and alternatively for distributed BESS solution one additional placed at node 666. The optimal sizing and placement problem performed co-optimizing the planning and operational services of the BESS (i.e., without the coordination with other assets or DER) for the 8-day dataset in 1-hour resolution (i.e., 384 time slots) for the mixed DER integration scenario 02; the same sizing and placement obtained are also used for all scenarios. In this particular planning stage, the BESS solution is used as the sole option to resolve the issues.

The definition of the examined scenarios is in Table 5.3. The PV and EV integration refer as a percentage proportional to the number of units installed out of the total 55 consumers. Note that all DER are connected to the grid as single-phase units connected in the same phase as the respective end-user. Analytical information regarding the point of connections and the characteristics of DER can be found in Appendix A.1. It should be stressed that an assumption is made in this case study that residential chargers provide the capability for V2G operation with an efficiency 5% lesser than their charging efficiency. In practice latest surveys report that round-trip efficiency during charging and discharging of EVs are approximately 70% (Apostolaki-Iosifidou et al., 2018).

Table 5.3: Definition of examined scenarios.

	Case 01	**Case 02**	**Case 03**	**Case 04**
PV [nr of PV units]	30	30	0	20
EV [nr of EVs]	0	30	30	35

A data-set has been created for this study case to emulate and induct the results for yearly analysis. A data-pool of yearly load profiles (found in repository (Pedersen et al.)) is statistically processed by using a k-means algorithm. Several sets of load profiles are aggregated and normalized to represent MV/LV substation's profiles. The process of the synthetic data-set constructions is described in Section 4.4.1.

The representative data-set is thereafter composed of eight days, two per season (one representing weekdays and another one for weekends). Each of those is selected based on the centroid metric derived by k-means. The normalized aggregated at the substation level profiles are illustrated in Figure 5.4. To reproduce the load profiles, the inversed cumulative Gaussian distribution function (Φ^{-1}) is set with maximum standard deviation $\sigma = 0.08$ and median the value of the centroid at each datapoint. Therefore, each point of the load profile i at instant τ is calculated from

Equation (5.25):

$$P_i(\tau) = \Phi^{-1}(c_i(\tau), \sigma) \cdot P_{i,\text{rated}}. \tag{5.25}$$

The Gaussian copula method is used to generate N temporal scenarios PV solar profiles, encapsulating the seasonal dependence as proposed in (Pinto et al., 2017b).

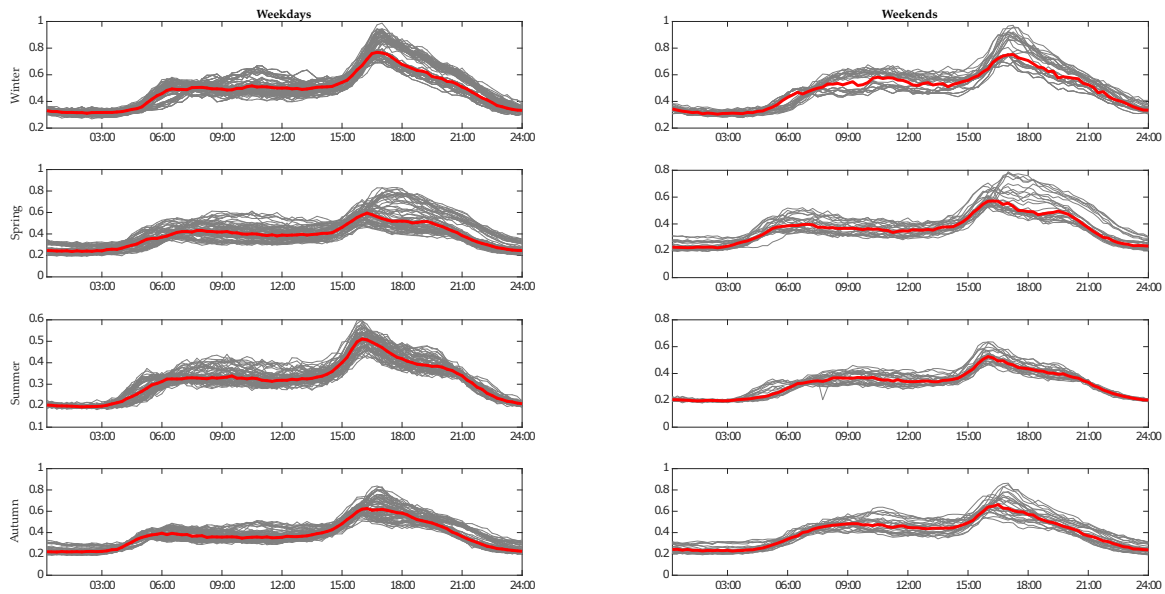

Figure 5.4: Classification of aggregated normalized loads (at the secondary substation level). The red line represents the centroid of the k-means.

Prior to the presentation of the analytical case study, an assessment of incremental DER integration (EVs and PV) on operational grid constraints is conducted. In this part of the study, no controls are deployed; though any voltage issues, voltage unbalances, and any line congestions are recorded along the yearly data-set. For the following analysis, it should be noted that, for each scenario of DER integration, five days of the same season and type of day (i.e., weekday or weekend) are considered, and the resulting metrics (i.e., voltage magnitudes and unbalances) are averaged. The collected information is exported by sequential three-phase unbalanced power flow for averaged 30-minutes profiles. Obviously, the impact of DER in higher resolutions (e.g., order of minutes) may be more intensive (i.e., leading to more severe technical problems) particularly for phase unbalances and voltage issues. All the subsequent Figures 5.5–5.7 represent the per season impact of integrating residential PV and EV. For all the incremental scenarios, random values of PV units (1.7, 2.7, 3.7kW) and EVs (charging power outlet of 3.7 and 7.4 kW) are assigned accordingly.

The evolution of maximum and minimum voltage magnitudes met in the grid for integration of PV and EV appear in Figures 5.5a,b, respectively. One can notice the impact of inversed power flows due to microgeneration which lifts up both maximum and minimum voltage magnitudes. During summer periods, higher overvoltage are faced; meanwhile, higher overvoltage are more

common during weekdays, since the loading conditions are lighter during sunny hours (see Figure 5.8a). In Figure 5.5a, the upper x-axis describes the PV integration correlated with the peak load as a percentage. For the considered load profiles, significant voltage increase (up to 1.07 p.u.) effects close to 50% of PV integration. In higher time resolution, voltage may experience, instantaneously, values higher than 1.1 p.u.; however, this study examines only a 30-minute average profile to determine maximum and minimum voltage limits as well to identify other technical bottlenecks on the safe operation of the grid. Regarding the EV integration, the minimum voltage up to 0.915 p.u. voltage appear with a number 40 EVs along the end-users. During weekends, due to lesser EV mileage, the demand for charging appears to be more limited compared to the weekdays. Furthermore, the simultaneity of charging at late evening hours (where daily peak load appears) leads to significant voltage drops.

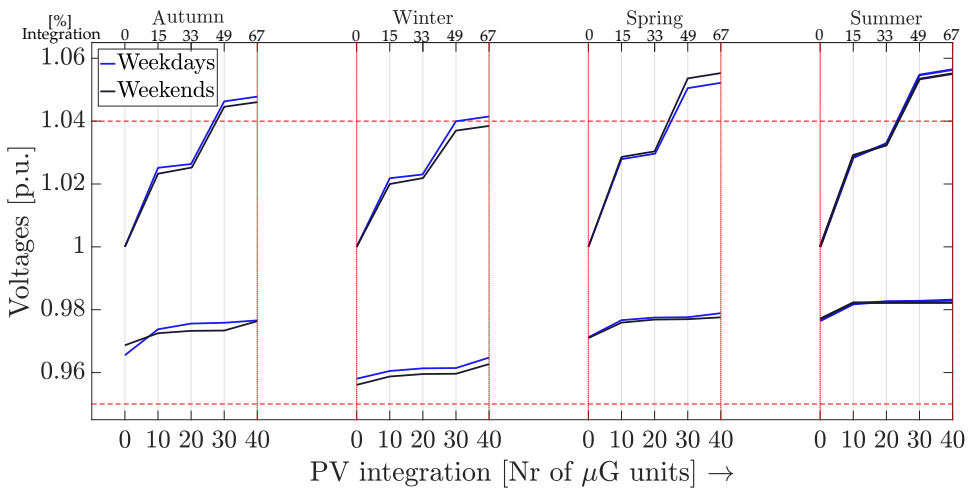

(a)

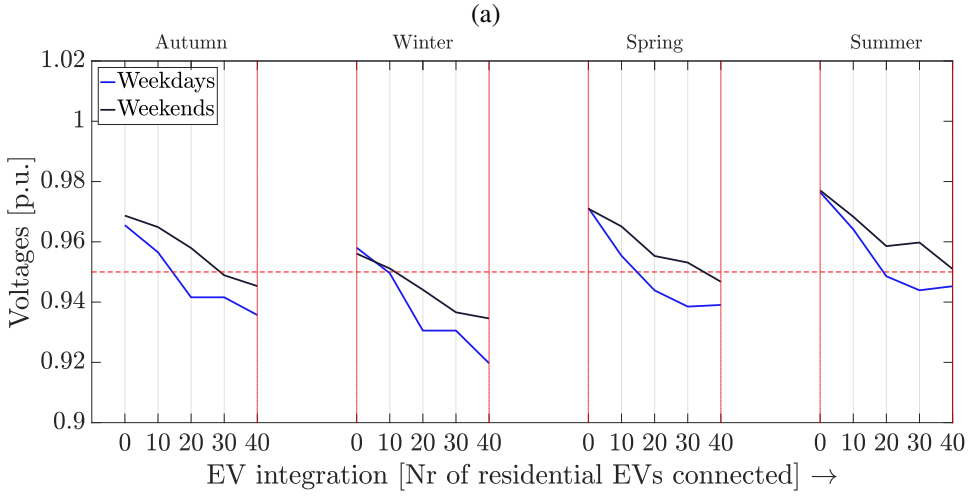

(b)

Figure 5.5: Minimum and maximum voltage according to the seasonal data over: **(a)** incremental PV integration; and **(b)** incremental EV integration seasonal (e.g., summer profiles) and regional data.

The impact of connecting single phase DER on VUF is presented in Figure 5.6a,b. In all cases

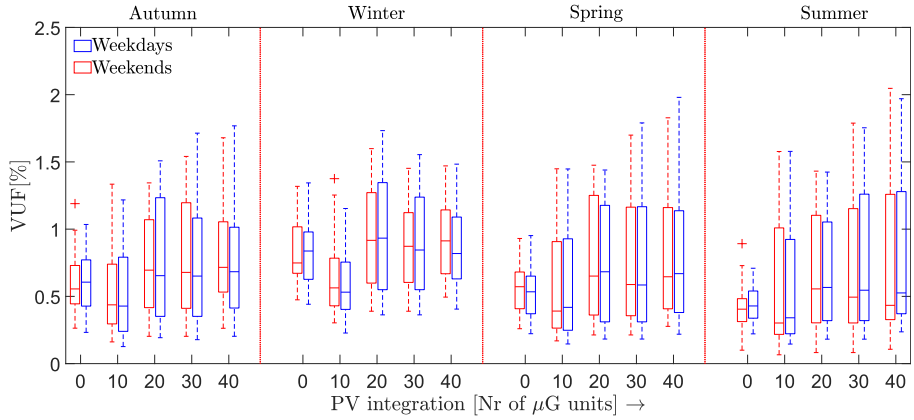

(a)

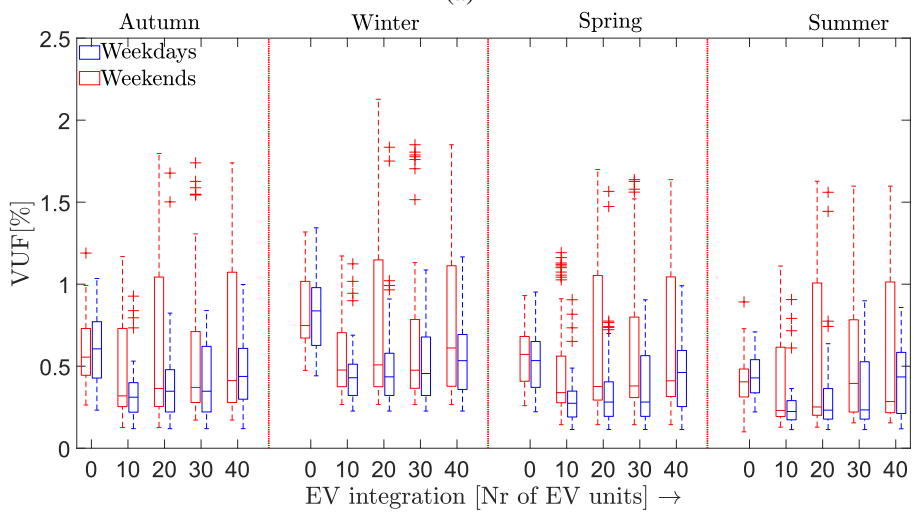

(b)

Figure 5.6: The range of maximum voltage unbalances according to the seasonal data over: (**a**) incremental PV integration; and (**b**) incremental EV integration seasonal (e.g., summer profiles) and regional data.

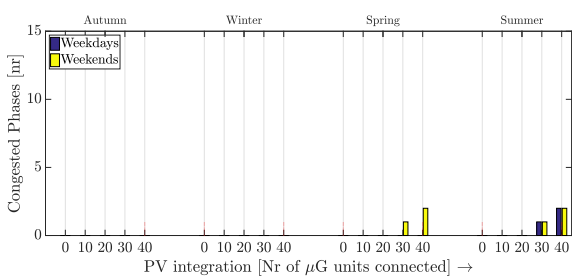

(a)

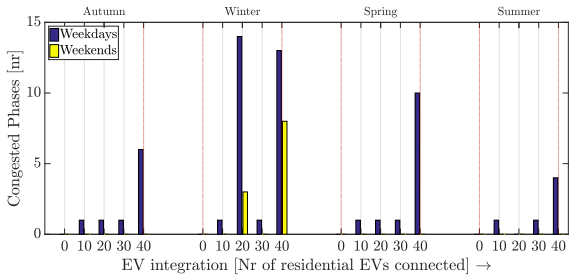

(b)

Figure 5.7: The total number of congested phases on the seasonal data over: (**a**) incremental PV integration and (**b**) incremental EV integration seasonal (e.g., summer profiles) and regional data.

where no DER is installed, there are quite balanced conditions only up to 1.3%. The installation of microgeneration leads to an increase of VUF up to 2.1% during summer periods, which is justified due to lighter load conditions and higher PV generation. The connection of EVs increases a high amount of imbalance particularly in winter periods, where the loading conditions are intensive reaching up to 2.2%. The increasing integration of EV obviously leads to more severe phase unbalancing conditions. Being in accordance with IEC standards necessitates that VUF has to be less than 2% for 95% of the week (Masetti); hence, for this presented analysis—that is performed for 30-minute time slots—the VUF threshold is considered at 1.8%.

The connection of multiple PV units does not arise any line congestions up to 33% of their integration. Higher PV integration, though, results in excessive reversed power along the upstream grid, particularly overloading line 280–566 up to 0.98 p.u. of line currents. The line loading conditions are much more severe concerning the EV integration as illustrated in Figure 5.7b, where line congestions may reach up to 1.5 p.u. particularly in winter periods.

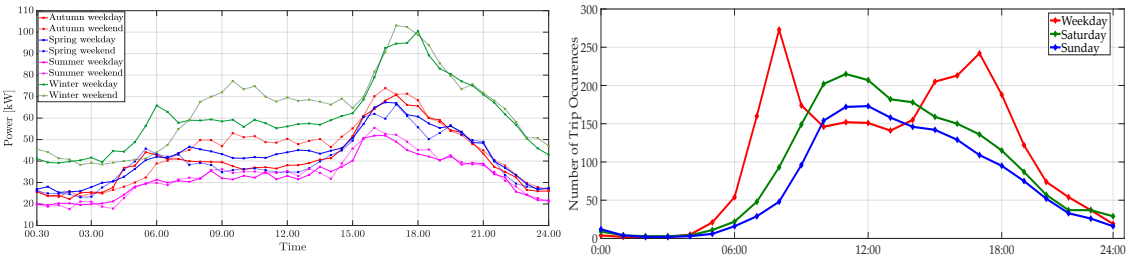

(a) (b)

Figure 5.8: (**a**) Seasonal load demand at secondary substation and (**b**) trips in progress during a week.

5.4.1 Results

This section demonstrates the techno-economical results for the examined cases of Table 5.3 performed with the proposed MACOPF scheme, among several modes of operation as defined in Table 5.4. Note that the conventional mode of operation m_0, applies for controls with no particular intelligence. Such controls in this study are derived by executing sequential three-phase power flows to identify technical bottlenecks (i.e., line congestions or voltage issues). Based on an iterative process for every node with overvoltage, 5% of the produced energy is curtailed until the issue is resolved. Accordingly, EVs' charging process is shed at the overloaded branches iteratively. The mode of operation m_1 refers to the sole coordination of all types of DER orchestrated by the MACOPF. It should be mentioned that, for this section, all EVs are considered available to provide grid support (i.e., through smart-charging), once they are parked at the house premises. Modes of operation m_2 and m_3 extend the aforementioned coordination with the utilization of one and two BESS—owned by the DSO—installed at nodes 460 and 666, accordingly. The last mode of operation stands for the coordinated operation of the OLTC with available DER for grid support.

Table 5.4: Definition of MACOPF setup along different modes of operation.

Operational Mode	Conventional Operation –No Smart Controls Applied– (m_0)	DER Optimal Coordination (m_1)	BESS Coordinated with DER (m_2)	Distributed BESS Coordinated with DER (m_3)	Coordination of OLTC with DER
OLTC	x	x	x	✓	✓
BESS	x	x	✓	x	✓
Smart Charging	x	✓	✓	✓	✓
Vehicle to Grid	x	✓	✓	✓	✓
μG Active Power Curtailment	✓	✓	✓	✓	✓
μG Reactive Power Dispatch	x	✓	✓	x	x
Load Shedding	✓	x	x	x	x

The assigned costs for the utilization of each of the DER's flexibility for this analysis are presented in Table 5.5. Note that the active power curtailment is considered about three times larger than the price of selling the energy produced by residential μG in Portugal. The main concern of the proposed scheme is to maximize the integration of microgeneration by exploiting other sources of flexibility, at the stage of the scheduling of operation. Concurrently, closer to the time of the delivery, APC may be used by typical droop control functions, ensuring safe grid operation. The cost of energy not supplied is set according to reports in (dos Serviços Energéticos, 2014). The respective costs for the OLTC and BESS investment as well as the corresponding cost (summarized in Tables 5.1–5.2) of their utilization are discussed in the previous sections together with their models. Concerning the OLTC investment, it is considered that the transformer's remaining lifetime—and subsequently the OLTC investment lifetime—is 15 years.

Table 5.5: Cost assumption for the case study.

		Cost (€/kWrh-kVArh)
Cost of Active Power Curtailment	c_{apc}	0.30
Cost Smart Charging	c_{apc}	0.15
Cost of V2G	c_{V2G}	0.35
Cost of Energy Not Supplied Lines	c_{ENS}	3

The yearly operational costs for all modes of operation are illustrated in Figure 5.9a, while a breakdown of seasonal cost analysis appears in Figure 5.9b. One can notice that, in most scenarios, m_0 leads to higher operational costs than any coordinated operational scheme, apart from case 01 (i.e., where all modes are comparable). The increased connection of EVs in scenarios 02 and 04 leads to very high operational costs for m_0, due to the need for EV shedding in order to avoid branch congestions.

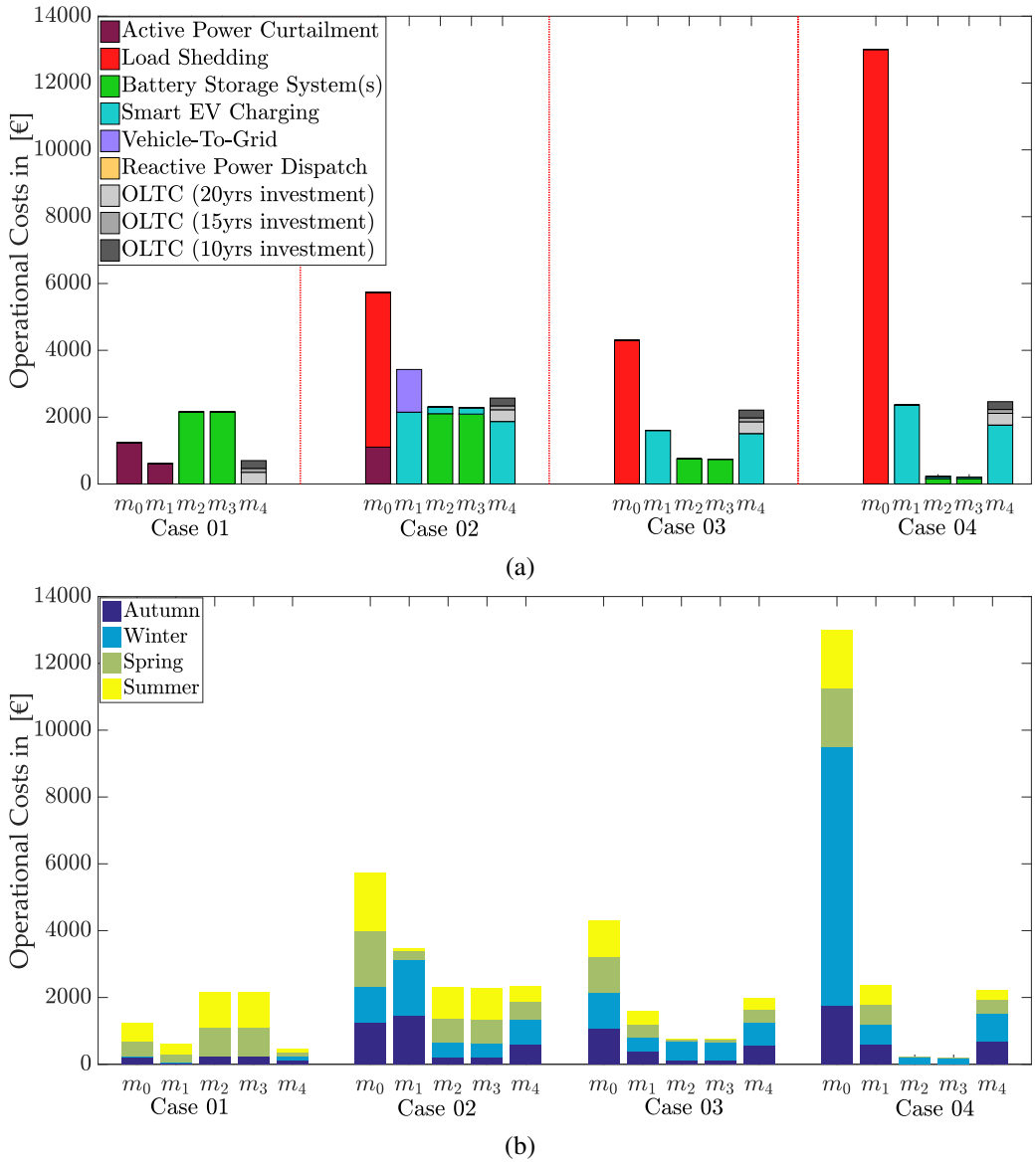

Figure 5.9: Annual DSO operational costs for all modes of operation $m_0 - m_4$: (**a**) over the examined scenarios; and (**b**) seasonal breakdown annual costs.

Commenting on case 01, where solely PV integration is regarded, one can notice that the cheapest operational modes of operation appear to be either the coordinated curtailment of PVs or the investment of OLTC. The curtailment of μG should be followed by a compelling compensation fee as applied hereby; otherwise, such schemes should adopt fairness strategies. In this particular case, MACOPF on m_1 provides the optimal dispatch of active and reactive power leading to lower costs than in m_0. Indicatively, the curtailed energy for case 01 is in Figure 5.10a. Both cases $m_2 - m_3$ lead to higher operational costs due to the topological distance of the BESS from the most problematic nodes (i.e., with overvoltage). Additionally, the BESS constraint for cyclic charging substantially increases the operational cost of BESS's usage, since the absorbed energy—during sunny periods—will have to be consumed in other time slots, whether it is needed

or not. For instance, BESS can be incorporated in MACOPF for extended energy management applications, where BESS are allowed to participate in the electricity market. In that case, grid operational costs for BESS usage would be more encouraging results, since the overall coordination of grid operation would follow the market price accordingly. More distributed BESS solutions may treat overvoltage by μG more efficiently, depending on their spatial distribution along the grid. Nonetheless, the economical results between m_3–m_4 are closely equivalent since the tool decides the utilization of BESS placed at node 460 in both cases. Clearly, the OLTC presents very low annual operation costs in the vicinity of 350–700 € (i.e., depending on the remaining lifetime of the retrofitted transformer) for case 01, where solely PV are installed.

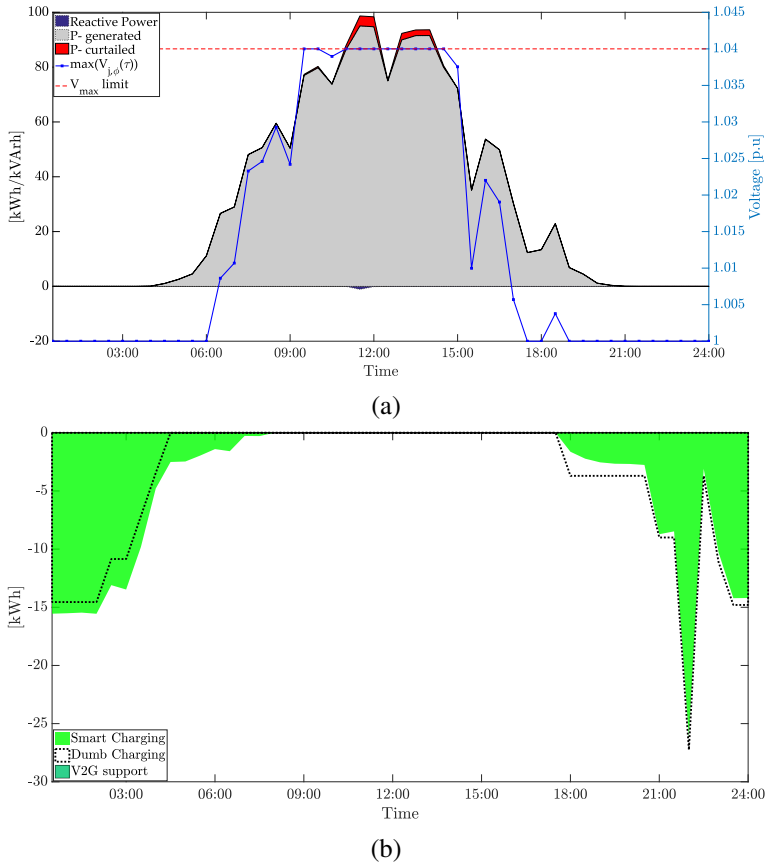

Figure 5.10: Control actions derived for case 01 (m_1) and case 03 m_3: **(a)** active power curtailments and reactive power dispatch to regulate voltage; and **(b)** smart EV charging schedules to avoid voltage drops and lines overloading.

The installation of EVs in scenario 03 (no PVs) is followed by undervoltage and line congestions as analyzed previously. The yearly estimated operational costs due to the shedding of loads (m_0) reach up to 4.3 k€. The coordinated smart charging presents a much cheaper alternative of 1.6 k€. This price may slightly fluctuate considering the uncertainty of EV users that are willing to charge under this regime. It should be reminded that smart-charging hereby is strictly regarded when EVs are not in trip progress and refers to any deviation from the expected–dumb charging profile. An example from a typical winter day used in the simulations is in Figure 5.10b. The dumb

charging profile for case 03 results in overloaded lines up to 1.09 p.u., a fact that is addressed with the coordinated smart charging in m_1. It can be observed that some charging profiles are shifted in slots with lesser loading conditions for the grid, which is the early morning hours as it appears in Figure 5.10b. In the same Figure, it can be noticed that there is no V2G participation since the high EV availability concerned is capable of addressing the technical issues. In this scenario, the BESS coordinated operation presents much lower grid operational costs close to 750€ and about 700€ for m_2 and m_3, accordingly. The OLTC in this scenario—considering the 15 years lifetime of the transformer—presents annual costs close to 1.9 k€, due to the need for coordination with smart charging which pertains to 80% of this cost. Therefore, it is observed that the OLTC can only reduce the lines' overload by lowering its taps; thus, the transformer's secondary winding voltage is lifted up reducing the line currents analogously. This branch current reduction in this case of 5% (i.e., 1.09 p.u. reduced to 1.037 p.u.) on the most congested branch. From Figure 5.9b, it can be observed that the highest share of the operational costs comes from winter and autumn period, when the used data-set appears to have the peak demands.

Both scenarios 02 and 04 examine the integration of mixed DERs, considering extensive integration of PV and EV units. Case 02 is a PV rich scenario with the 30 single phase μG, which corresponds to 49% of the peak demand of the grid. The last scenario 04 refers to a higher EV integration (35 EVs) and a 33% of the peak demand installed PV units. In both cases, the m_0 leads to high operational costs due to the need of EV shedding as well as an amount of 1.1 k€—case 02—for APC. Indicatively, Figure 5.11 presents analytically the control decisions derived from MACOPF for each mode of operation. It can be observed that along m_1, smart charging schedules shift some of the EVs during sunny period hours (i.e., 10.00–14.00), while some other EVs are further charged in the beginning of the day before the trip occurrences. The V2G mode of operation takes place not only to reduce line currents, but also to create available charging slots to be used during sunny periods with expected overvoltage. All EVs are constrained to keep their SoC at the end of the day equal to the one at the beginning of the simulation. Therefore, EVs that are parked at home all day present high availability, which is observed to be used in this way (i.e., charge during periods with high solar irradiance and discharge to avoid line congestions). Regarding OLTC operation, as illustrated in Figure 5.11d, it ends during the end of each day at tap –2, which is due to the loss minimization term. The OLTC acts in such way to increase the secondary winding voltage in order to avoid any voltage drops and minimize the active power losses as well. Obviously, the addition of some more EVs (case 04) results in a very abrupt increase of operational costs for m_0, a fact that is connected to the extensive line congestions that occur.

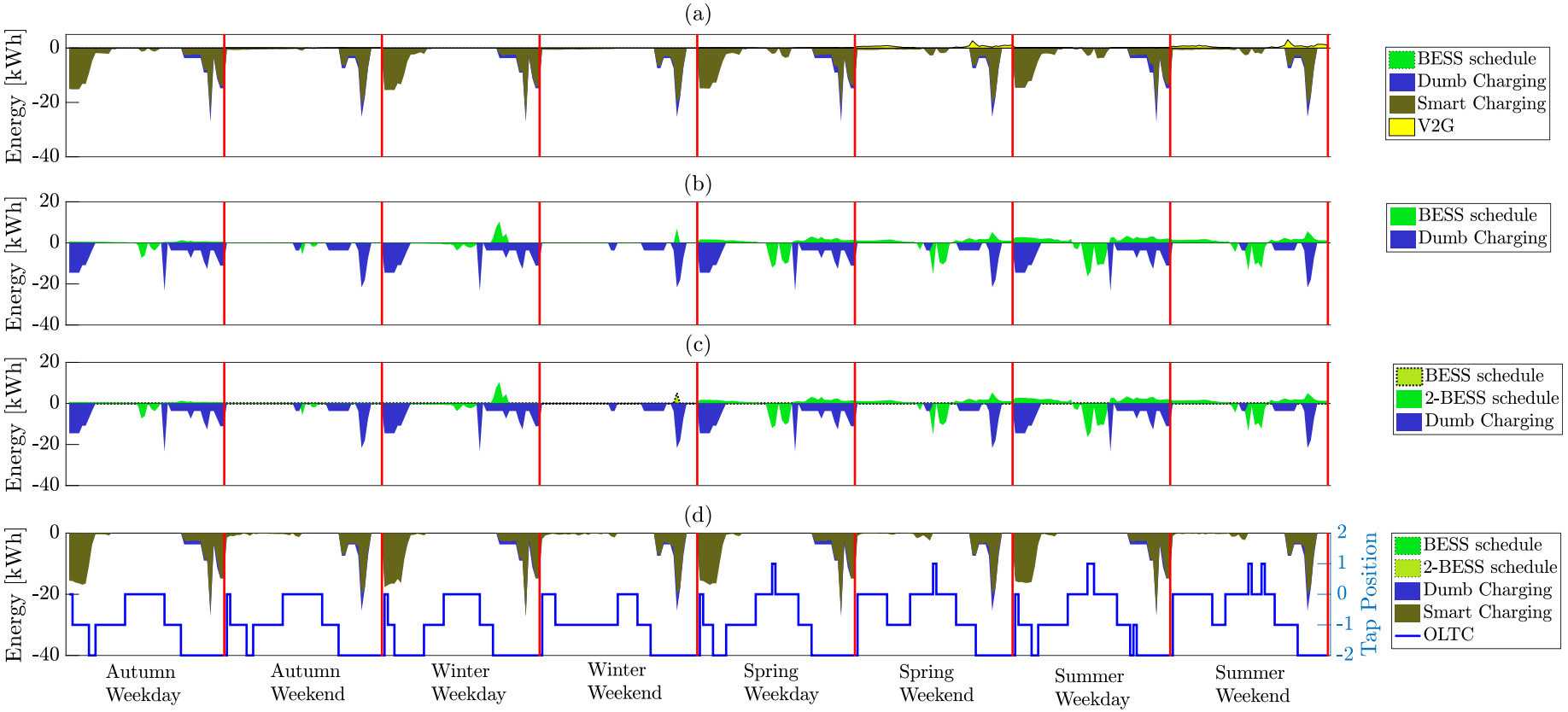

Figure 5.11: Control actions derived from MACOPF for case 02 along the examined modes of operation: (**a**) m_1; (**b**) m_2; (**c**) m_3; and (**d**) m_4.

The proposed OLTC equipment is allowed to be set offline in different tap positions per phase to treat unbalances. The performed analysis considers 30-minute data resolution, a fact that may underestimate the real-time conditions regarding phase unbalances. Therefore, the OLTC may need further engagement with flexible DER to deal with phase unbalances; hence, higher operational costs may be foreseen in such a case.

5.4.1.1 Minimization of Active Power Losses

The annual active power losses without DER integration are estimated to be 1.5 to 2.5%, calculated through sequential power flow executions. From Figure 5.12, it can be observed that there is an increase in line losses due to the extensive DER integration, particularly when EVs are considered. The charging of the EVs does most likely occur during peak load period in the afternoon, increasing notably the loading along the distribution lines and to some extent the line losses (see Figure 5.12 reaching close to 6%).

In all cases and the subsequent modes of operation towards the resolution of technical bottlenecks (i.e., voltage magnitudes, voltage unbalances, and line congestions) line losses are also reduced compared to the scenario where no controls are applied. Particularly, modes m_1–m_4 based on the proposed MACOPF control framework do further reduce the line losses due to the involved objective term. The coordinated operation of the OLTC with DER appears to perform the most efficient measure in the direction of losses minimization. Additionally, experimenting (i.e., by assigning higher values to w_2) with the weighted terms among the objective terms in modes m_1–m_3 does not impact significantly the control decisions and the losses. The latter can be justified due to the fact that further minimization of active power losses, substantially, precedes more engagement of DER flexibility. Nonetheless, involving more flexibility in the scheduling of operation for the losses minimization cannot be justified economically.

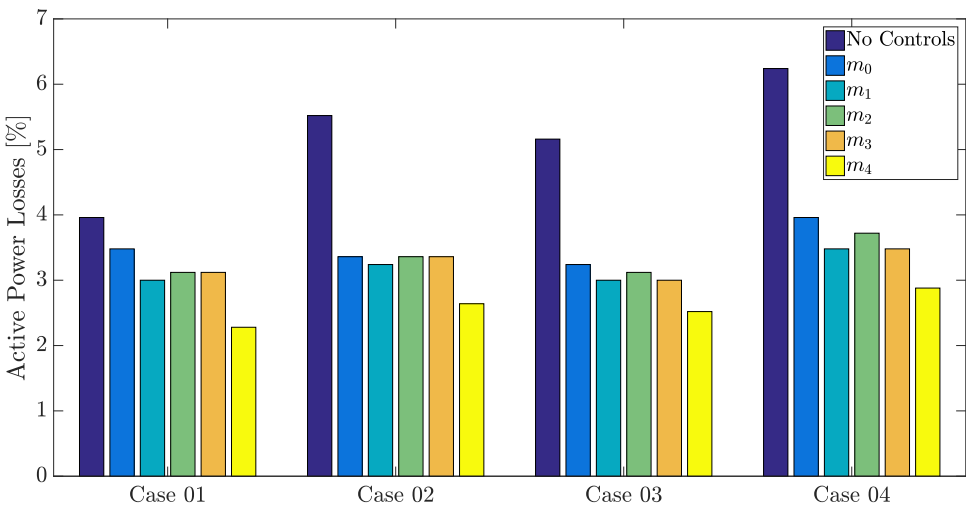

Figure 5.12: Annual active power losses for each scenario and each mode of operation.

The exploitation of the OLTC brings greater benefit to the objective, particularly for the minimization of active power losses, since the low cost per tap operation allows the optimizer to derive taps-down, lifting the primary side to higher voltage.On the other hand, the combination of BESS or smart charging cannot justify their excessive usage towards further minimization of losses at the same order of reduction compared to the OLTC.

5.4.1.2 Sensitivity Analysis on BESS and Smart-Charging Coordination

A sensitivity analysis is presented hereby to observe the evolution of the estimated DSO annual operational costs for different prices of smart charging and different LCOE for the BESS. This section provides a comprehensive comparative analysis not only in the reflection of the pricing of EV flexibility—i.e., EV available for smart charging—and the BESS, into the DSO equivalent annual cost of operation, but also signifies the importance of enabling EV smart charging towards the reduction of operational costs. Furthermore, one scenario concerns the V2G mode of operation in the sensitivity analysis. Along the evolution of BESS and EV pricing and their availability (i.e., spatio-temporal), the resulting coordination is recorded through the proposed control scheme.

In each case, the range of BESS prices lies within [200–380]€/kWh (i.e., corresponding LCOE [0.05, 0.0925] €/kWh) according to the study in (Tsiropoulos et al., 2018), for base year 2025. For the purpose of this study, scenario 02 is considered regarding the integration of DER. The cost of utilizing EV flexibility is considered in the range [0.05, 0.25] €for each kWh of shifted charging slot.

On the data-points in Figure 5.13, the coordination of EV and BESS is displayed as a share of the annual DSO operation costs. As BESS price increases, the EVs' flexibility is further used following a quasi-linear dependence and vice versa. Note that, particularly in Figure 5.13a, where only 20% of the connected EVs are considered as flexible, even when BESS cost is higher than the EV flexibility, the limited EV availability forces the resolution of technical bottlenecks mainly with the use of BESS. On the other hand, one can notice that, in Figure 5.13b, the higher availability of EVs—60%–(which implies better spatio-temporal distribution) leads to reduced DSO costs in most cases (see data-points in Figure 5.13b). The fact that EVs are distributed along the grid is foreseen to be very efficient to address any technical bottlenecks arising from PV and EV integration. The latter can be further observed when all EVs are considered as flexible in Figure 5.13c, where the effect on the cost reduction is more intensive since the plane follows—an affine—curvature. The last sensitivity analysis considers V2G in constant pricing at 0.35€/kWh, combined with 100% EV availability for smart charging. The fact that V2G is considered in the framework essentially allows the utilization of EVs that do not proceed with a trip (i.e., and then they have to get charged, since they are constrained to recharge in the simulation day at least the energy used). The effective coordination of the BESS, EV smart charging, and V2G leads to notably lesser grid operational costs compared to other cases. Note that the maximum cost observed when BESS and EV are assigned with the highest price values is 1.6k€, when the resulting maximum cost in the other planes reaches close to 2.5k€.

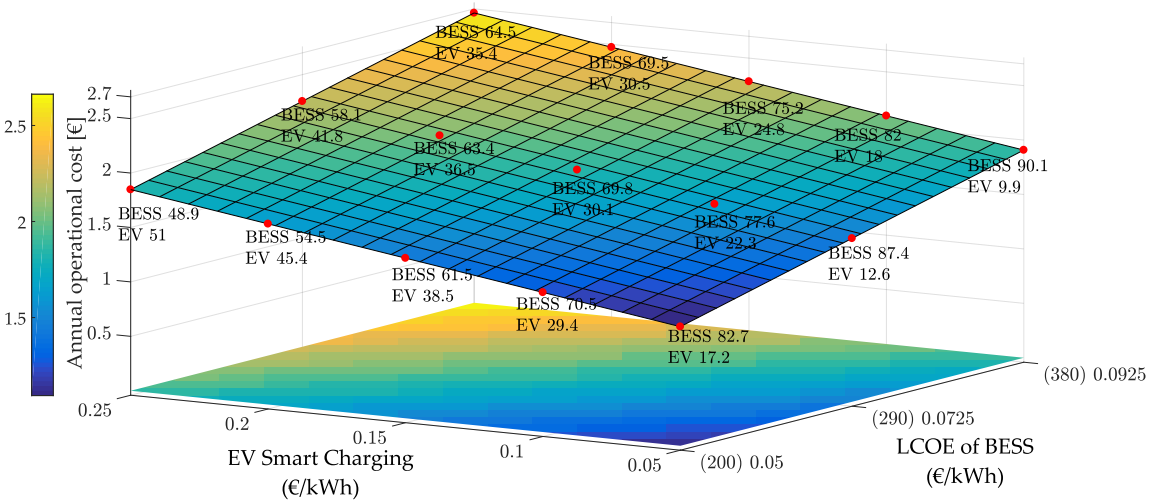

(a)

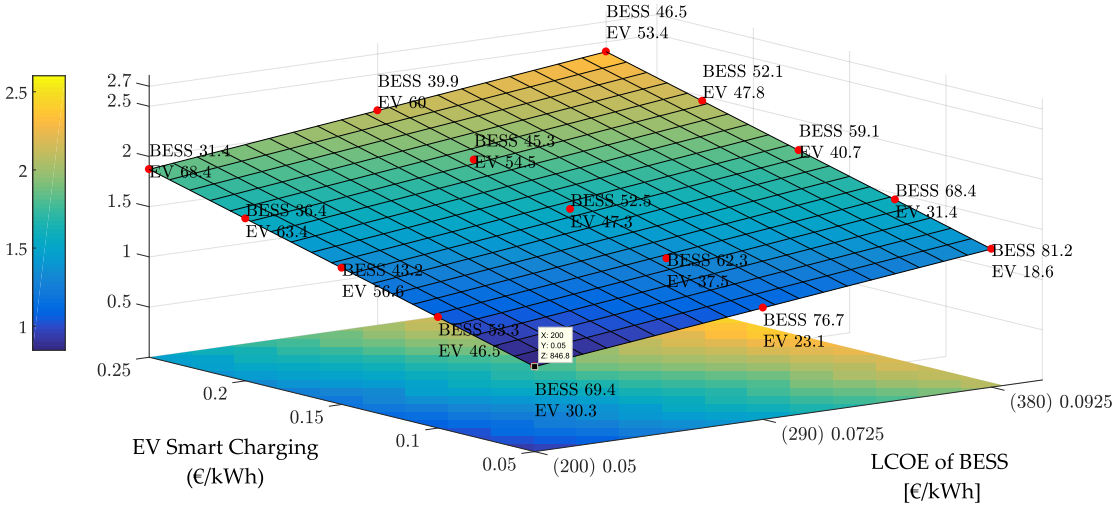

(b)

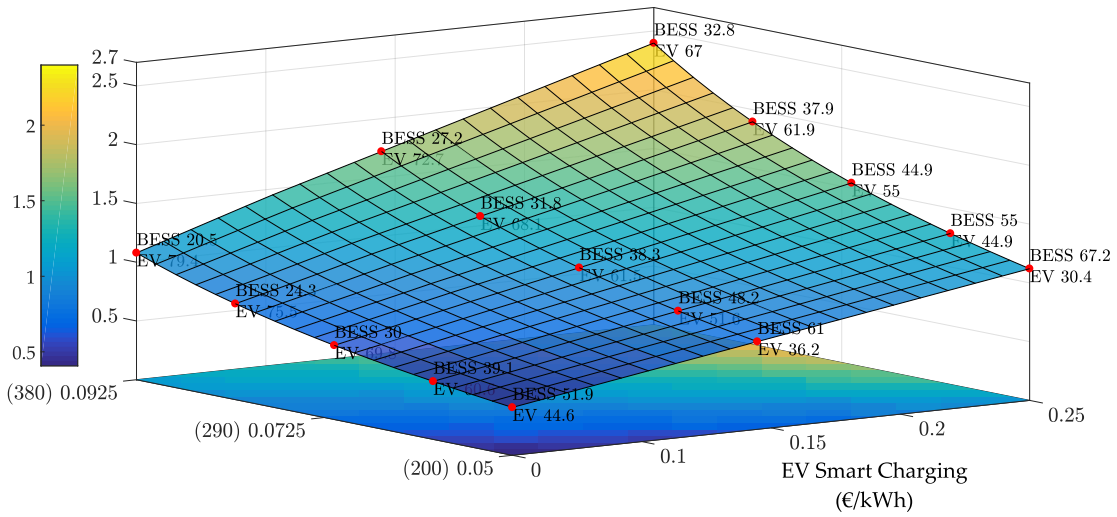

(c)

Figure 5.13: Annual operational costs for different shares of EV willing to participate in smart charging: (**a**) 20% flexible EVs; (**b**) 60% flexible EVs;(**c**)100% flexible EVs.

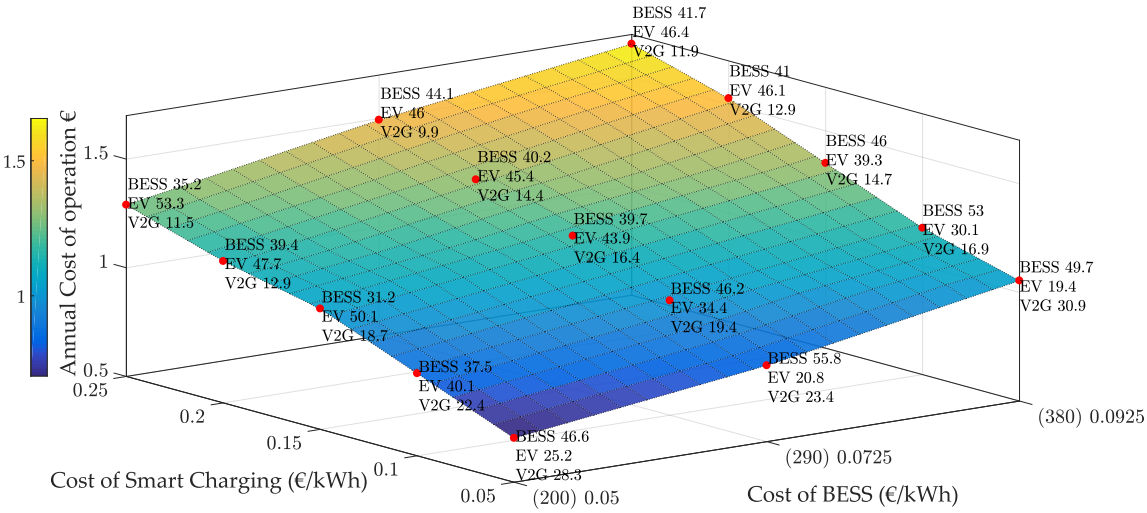

(a)

Figure 5.14: Annual operational costs for different shares of EV willing to participate in smart charging: 100% flexible EVs and V2G mode of operation are also available.

5.4.1.3 Efficient sizing of BESS: co-optimization of planning and operation stage

In this part, the selected site for BESS investment is node 460 as explained in the case study synopsis. The co-optimization of the planning and operation stages is explored here to identify the size of BESS for different cost of operational EV flexibility usage. The considered range of cost for EV operational flexibility is from 0.05–0.25 €/kWh. Two cases are examined one with 20% and another with 40% of the EVs share willing to be coordinated by the MACOPF. The considered scenario for this investigation is the case 02.

The results for both cases of EV participation on the control scheme are presented in Figure 5.15. When no participation of EV flexibility the sizing of BESS is 90kWh as explained in case study synopsis. One can notice, that for the lowest cost (0.05 €/kWh) of EV flexibility there is a reduction of 12.2% and 27.8%, accordingly, for 20% and 40% EV availability, on the selected size of BESS compared with the scenario with no EV participation. For the moderate cost of EV flexibility (0.15 €/kWh), the reduction on BESS size falls at 3% and 20% reduction of size from the 90kWh, for 20% and 40% EV availability, respectively. Once the EV flexibility is set to 0.25 €/kWh the BESS capacity is closely to 90kWh.

These results essentially show that the sizing of a BESS and generally the planning of distribution network were active measures are regarded can be rather complicated. In the explored scenario, the active participation of EV, through their coordinated charging, can reduce the necessary capacity of BESS to be installed. The cost assignment of EV operational flexibility has a clear impact on the BESS investment. In the examined case for 0.05€/kWh cost of EV flexibility, the MACOPF identifies the coordinated EV charging as a cost-efficient measure to resolve grid constraints; thus, the necessary capacity of BESS falls at 65kWh when 40% of EV share is available.

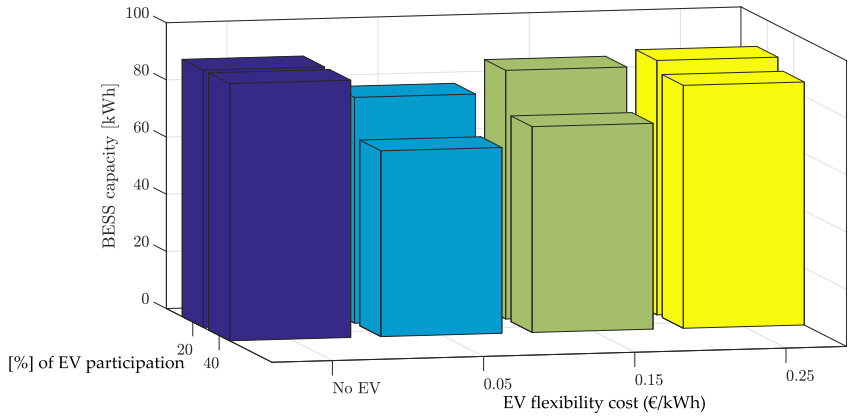

Figure 5.15: Sizing of BESS at node 460, with co-optimization of planing and operation stage considering EV operational flexibility.

5.5 Final remarks

In this chapter the control framework is further advanced to derive the coordinated management for multiple DSO assets and DER, in a way to ensure safe grid operation pertaining admissible voltage magnitudes, phase balancing, and avoiding line congestions. The overall scheme is formulated as a nonlinear multi-objective program resolved with a primal-dual interior point algorithm. A three-stage technique is proposed to incorporate the OLTC in the decision-making process. The control framework is used to obtain efficient decisions for the placement and sizing of BESS.

The study shows that OLTC appears to be the most efficient option to treat overvoltage when high PV integration is encountered, considering loss minimization. Nonetheless, phase unbalances may occur that could be treated by coordinating with other DER, or the installation of BESS. It was concluded that, for long-term phase imbalances, the OLTC can be also setup in offline mode to proper tap positions per winding—hence reducing the unbalances and the need of coordination with other assets or DER. The extensive integration of EVs (more than 20 EVs in the examined case) cannot be accommodated only by the optimal operation of the OLTC. In the presented study the OLTC is capable of reducing the overloading to 25–32% of the most congested branches; however, coordination with EVs is deemed necessary to respect all technical constraints. Depending on the selected OLTC technology and whether the transformer can be retrofitted—as examined in this study—the OLTC is foreseen to be most efficient to address reversed power flows effects and the subsequent overvoltage. On the other hand, BESS's solution is very dependent on the expected costs along the evolution in the next decade. Considering a moderate BESS cost (i.e., regarding the expected adoption of BESS in the market) presents comparable results—or better results in some cases—with OLTC. In mixed DER scenarios (i.e., PV and EV), BESS coordinated with DER outperforms the compared modes of operation, presenting the lowest DSO annual equivalent operational costs.

A sensitivity analysis demonstrated the DSO's annual costs of operation considering different costs for BESS and EV flexibility utilization. The main outcome of this sensitivity study

shows the importance, due to their spatio-temporal distribution, of the active participation of DER (i.e., mainly for EVs with V2G hereby) in the grid operation and the significant reflection on cost reduction.

Chapter 6

Conclusions

The scope of this last chapter is threefold. The content of the thesis is summarized, capturing the proposed methodologies and explored case studies. Secondly, it draws the conclusions based on the outcomes of each chapter. Finally, some suggested directions on future work and advancements, are highlighted.

6.1 Summary of Thesis

The thesis explored and developed optimization-based methods for the control and active management of Low Voltage (LV) distribution networks, focusing on a substation-centered architecture. An overall mapping of the Thesis is given on Figure 6.1.

An introduction on the classical view and operation of Low Voltage (LV) was covered in Chapter 2. The mathematical modeling of grid components and different types of Distributed Energy Resources (DER) were discussed in this part, along with a discussion on the non-nonvexity of power flow equations. A literature review on unbalanced Power Flow and Optimal Power applications for LV distribution grids takes place in Chapter 2, while a step further on a comparison study between a centralized single period control scheme and local droop based functions is addressed.

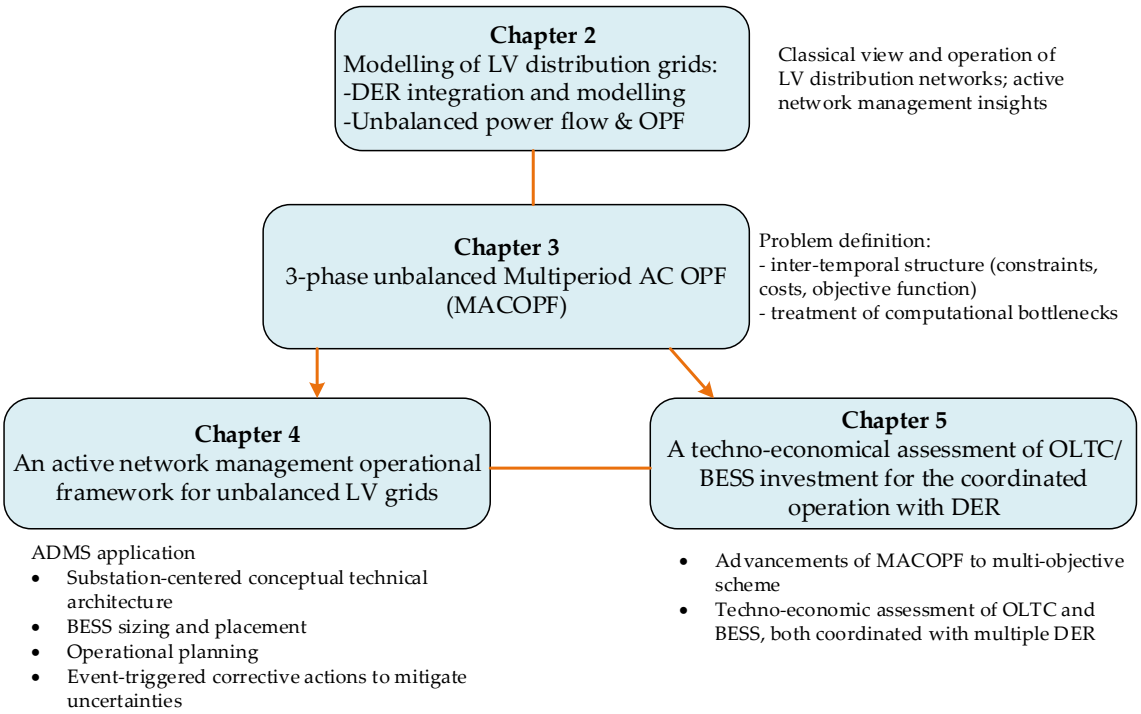

Figure 6.1: Mapping of Thesis content.

Chapter 3 proposed the formulation of a three-phase multi-period AC OPF (MACOPF), where several computational suggestions for the exact power flow equations and their subsequent first and second-order derivatives. The treatment of Jacobian matrix (i.e. the one of primal-dual method) singularity, provoked by inter-temporal constraints, is addressed with pivotal elements once needed assuring convergence of the problem. A case study examines cases with increased integration of DER where the proposed methodology ensures admissible voltage profiles by minimizing the active power curtailments of microgeneration through the efficient coordination of DER, maximizing in this sense the integration of microgeneration.

Chapter 4 commences with the description of a substation centered approach based on Distribution Transformer Controller (DTC) placed at the secondary substation field. A three-phase un-

balanced Multi-period AC OPF (MACOPF) formulation is utilized as the core algorithm to equip control and management functionalities for the operation of LV distribution networks. Efficient planning alternatives are proposed through co-optimization planning and operation stages for active network grids. An operational framework is also proposed to provide a DSO decision-making tool regarding the safe operation of LV distribution network.

Chapter 5 advanced the operational planning framework into a multi-objective one, while proper adaptations are proposed on the scheme to allow the incorporation of On-Load Tap Changer (OLTC) in the non-linear programming formulation. The construction of yearly synthetic profiles has been proposed to assess the evolution of DSO's operating costs in scenarios with increased DER integration in LV networks. The coordinated operation of a BESS (i.e. owned and operated by the DSO) investment has been compared with the option of retrofitting a typical transformer with OLTC hardware, both in active distribution networks.

6.2 Key findings and conclusions

The key findings and main conclusions of the thesis are segregated into two categories, the technical and the optimization – control based ones. The first category, refers to any proposed methodologies and techniques applied for optimization advancement and control contributions. Technical conclusions summarize the findings from case studies investigated regarding active network management and the subsequent coordinated controls among DER. Those may be summarized as follows:

Optimization and control based conclusions

- *The development of a tractable three-phase unbalanced multiperiod AC OPF scheme.* The computational techniques proposed based on the explicit calculation of the first and second order derivatives (i.e., Jacobian and Hessian of the Lagrangian and the objective function), in addition to pivotal adjustments in the Jacobian, ensured a tractable optimal control based on the exact AC power flows. The large scale formulation of the problem requires at least the explicit calculation of the first order derivative of the nonlinear equality constraints (J_E matrix) exploiting the sparse characteristics of these matrices; otherwise, memory leak can inevitably arise.
- *DER inter-temporal constraints lead to singular Jacobian matrix.* The interdependence of DER operating states (such as BESS or EV) create linear dependent rows on the gradients' matrix, which in turn cannot hold the linear dependency of constraint qualification. The resulting singularity of Jacobian matrix (i.e into the iterative process of primal-dual algorithm), can be addressed with pivotal elements once the problem arises, without any intervention on DERs' model. If the singularity is not treated, the optimizer will fail to converge, or converge to an erroneous point.
- *Sizing and placement of BESS based on synthetic profiles.* The co-optimization of planning and operation stages can take place using the proposed multiperiod AC OPF methodology.

The co-optimization of both stages can reduce the cost of BESS investment due to the consideration of DER operational flexibility. Nonetheless, the planning stage considering active network management may be a very demanding process.

- *The OLTC incorporation into nonlinear multiperiod programming framework*. The OLTC decision variables are typically introduced with the use of integer decision variables and solved with integer programming. The three-stage approach manages to incorporate of OLTC in the overall scheme, while it allows the introduction of technical and inter-temporal constraints for the equipment itself within the intermediate stage.

Technical conclusions and key findings

- The increasing integration of single phase DER in LV distribution may arise critical voltage unbalances, depending also on the loading conditions. Such voltage unbalances are quite underestimated in the literature due to the fact that most research works assume balanced conditions for the simplification of grid modeling. The PV incremental scenarios in Chapter 3, shown that MACOPF can assure up to 73% of PV integration avoiding any active power curtailment. Nonetheless, the subsequent Chapter shown that voltage unbalances and line congestion may be critical and further actions have to be taken. It is shown that proper coordination of DER themselves can alleviate unbalanced conditions. In particular, Chapter 4 examined scenarios with high integration of EVs that showed that coordinated charging could maintain voltage unbalances and other grid constraints including congestion management, admissible voltages. The investment on OLTC hardware or BESS cannot be the only effective measure due to the technical bottleneck of voltage unbalances. Hence, the coordinated smart charging mode of operation seems to be effective and necessary for such purposes. Concurrently, when single-phase PV installation provoke the issue of voltage unbalances, the management of smart inverters is vital.
- Following the previous finding, smart inverters should be available to contribute to the improvement of power quality conditions (i.e. admissible voltage magnitudes and acceptable voltage unbalances). Reactive power control is cheaper than curtailing active power –i.e. for the considered prices– from microgeneration to reduce overvoltages and tackle unbalances. The extensive usage of reactive power from smart inverters may lead to increase grid's power losses. Another issue that needs to be examined, particularly for reactive power support, is the fairness among the users' or an effective remuneration scheme. In any case future grid codes should consider the smart inverters' capability for support.
- The flexibility that can be provided by EVs was shown to be of significant importance in most of the examined cases. In the explored scenarios with increased EV integration, EV's spatial distribution in the grid along with their temporal availability, made them an adequate alternative to the mitigation of overvoltages –provoked by excessive active power injection from PVs–. In addition, the coordinated charging could guarantee that no congestions occured in distribution lines; yet, high EV availability to provide flexibility was deemed necessary. For instance, high EVs (65% and 85%) share a minimum 50% and 85% out

of total EVs, accordingly, need to follow the coordinated charging as per the case study in Chapter 4. For this particular case, the most binding constraint was the overloading of several distribution lines. Therefore, the coordination with BESS or OLTC is vital to ensure safe operation.

- Vehicle to Grid mode of operation appeared to be rather important in the explored scenarios. The equality constraint settled for all EVs to maintain their state of charge at the end of the determined horizon equal to the one at the beginning of simulation is restrictive for their operation. The V2G mode of operation takes place not only to reduce line currents, but also to create available charging slots to be used during sunny periods with expected overvoltage. Therefore, EVs that are parked at home all day present high availability, which is observed to be used in this way (i.e., charge during periods with high solar irradiance and discharge to avoid line congestions), providing benefits to the EV owners.
- OLTC appears to be the most efficient option to mitigate overvoltages when high PV integration is encountered, along with the accomplishment of loss minimization. Nonetheless, any phase unbalances could be treated by coordinating OLTC with other DER, or the installation of BESS. It was concluded that, for persistent phase imbalances, the OLTC can be also setup in offline mode to proper tap positions per winding—hence reducing the unbalances and the need of coordination with other assets or DER. Depending on the selected OLTC technology and whether the transformer can be retrofitted—as examined in this study—the OLTC is foreseen to be most efficient to address reversed power flows effects up to the secondary transformer level and the subsequent overvoltages.
- The investment in BESS solution is very dependent on the expected costs of their technological evolution and adoption from the market in the upcoming years. Considering a moderate BESS cost of 290€/kWh (i.e., regarding the expected adoption of BESS in the market) presents comparable results—or better results in some cases- with OLTC investment for the explored cases in Chapter 5. In mixed DER scenarios (i.e., PV and EV), BESS coordinated with DER outperforms the compared modes of operation, presenting the lowest DSO annual equivalent operational costs. Additionally, a BESS solution may provide lesser operating costs for the DSO, when installed in a distributed way; nevertheless, the coordination with DER appeared to be more preferable in the discussed scenarios, due to the increased spatio-temporal flexibility of EVs. It should be, also, stated as per Chapter 5 and the literature exploration, BESS costs may fall up to 200€/kWh in this decade if it is massively adopted by the market. If this assertion comes true, BESS investment cost will be reduced at about 30% from the considered one.
- The co-optimization of planning and operation stages considering the operational flexibility of DER can reduce significantly the size and number of BESS investments or distribution line reinforcement, or even act as investment deferral measure. In Chapter 5, up to 28% of reduction on the BESS capacity was derived, when 40% of EV share was used as an active measure. Any planning alternatives and decisions are dependent on the level of engagement of DER and the implied cost of the investment.

6.3 Outlook and suggestions for future work

This thesis explored several cases on unbalanced distribution grids operations; yet there are several suggestions and directions for future work to be examined. Some of them are outlined hereby as follows:

- In Chapter 3 the core algorithm based on MACOPF is solved as a nonlinear programming due to the exact consideration of AC power flow equations. The computational effort would be interesting to be compared with other approximative approaches either iterative linearized or convex ones.
- The centralized scheme formulated by MACOPF considers several information about availability or constraints related to end-users's –and their DER– privacy. Towards the deployment of Local Energy Communities the end-users' privacy is a great concern. Hence, possible decomposition of the proposed methodology into a distributed version, would be very crucial for investigation.
- In the thesis there is an assertion made regarding ideal Information and Communication (ICT) infrastructure for the substation operational centered schemes. All the simulations performed considered perfect (i.e. synchronized and accurate) dispatch of information between the sensory devices and the DTC. This assumption may be quite concrete since the scheduling period for the subsequent hours regarded 30 minutes time interval using in most cases averaged measurements. Despite the fact that in Chapter 4 there were suggestions made regarding the local management and processing of measurements at the DTC level, there weren't any implications and thorough analysis for cases with latency in communication or distorted signals as a matter packet losses. Therefore, this area of imperfect ICT could be explored to identify the necessary infrastructure requirements for such operational schemes, examining the behavior of them in real field setups where other sources of uncertainties do arise as well.
- Following the previous point, the substation centered optimization framework relies on the extensive knowledge of the grid topology and electrical characteristics. Hence, further analysis is required to ensure that its performance can take place in concordance and coordination with State Estimation engine, possibly accommodated in DTC as discussed in Chapter 4. It would be interesting to investigate the error between state estimation based methodologies and the exact resolution as the one presented in the thesis.
- The consideration of dynamic tariffs for the implementation of more advanced demand response schemes would possibly result to different management of DER flexibility. The end-users' engagement in the active network management may attract more flexibility capacities led by the pricing scheme adopted each time. In the proposed methodology inter-temporal costs were introduced in the mathematical formulation, but not explored in the simulations' phase.
- As discussed in Chapter 4, the communication of end-users' availability may take place via assigned contracts with Aggregators. This part of interaction could be analytically explored,

by investigating particularly the optimized portfolio by the aggregator with scheduling of operation arose by optimization-based DSO tools such as the MACOPF.

- More analytical modeling of BESS would be also an interesting extension. For instance, a cost function could be included on the objective function to reflect the degradation and life-cycle.
- The co-optimization of planning and operation stages was explored in Chapter 4 as mathematical advancement of the MACOPF. The exploitation of yearly synthetic profiles provided insight for a techno-economic assessment of the investment on OLTC hardware or a BESS solution in Chapter 5. There could be more sophisticated mathematical advancements to be applied for the creation of synthetic profiles to capture not only load growth, but also DER integration, which can be used thereafter for the optimization of planning stage. Alternatively, for planning purposes up to 5–10 years approximative methods for power flow equation ought to be used.
- The interior point algorithm for the resolution of MACOPF is commonly sensitive to the initial point selected. This essentially means that in some particular cases the optimizer may get trapped very fast into local minima, which in turn may not comprise an efficient operating point for the DSO. In this work a local database was proposed to provide initial inputs from previous occurrences of the tool with similar characteristics (i.e. based on the length and the structure of decision variables). It would be rather interesting to investigate the creation of initial points given by the convex approach of the problem to verify possible improvement either on time of convergence or the quality of solution obtained.

Appendix A

Appendix

A.1 Complementary data for benchmark LV distribution network and the connected DER

The network selected as a case study to perform the validation of the proposed scheme belongs to the IEEE benchmarked LV European network (Espinosa, 2015). The network corresponds to a real British low voltage feeder connected to the MV grid through a transformer of nominal power 800 kVA (Figure A.1). The transformer is modified and considered to be 20 kV to 400 V with nominal power of 150 kVA, since only one feeder is considered in the benchmark as well. The service cables to the 55 end-consumers are also included in the grid representation.

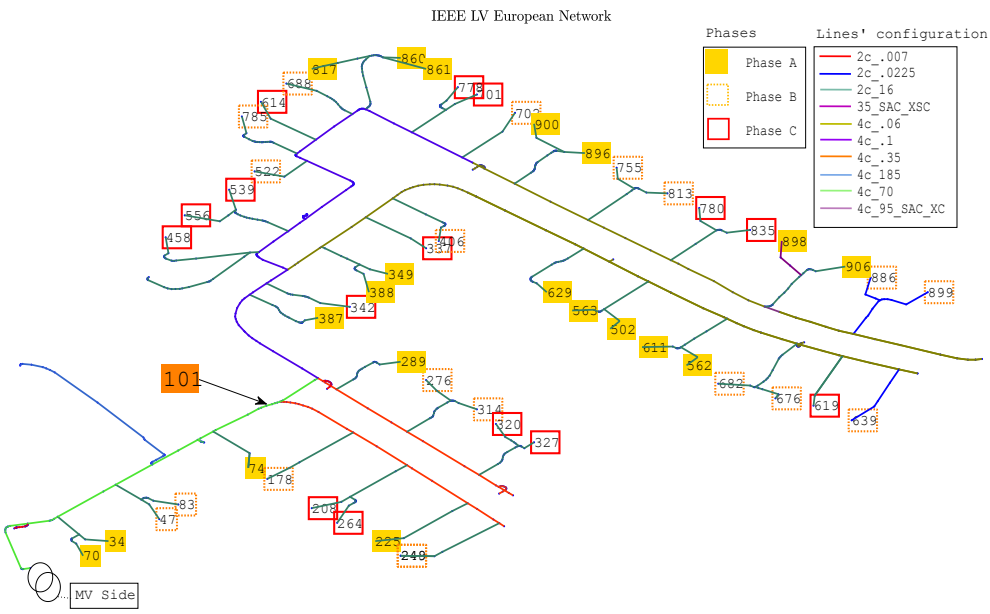

Figure A.1: The IEEE European LV benchmark network. Fifty-five consumers are connected to this case network.

The load and the microgeneration profiles used correspond to daily data for a summer period, which are extrapolated from a realistic data pool provided for the benchmarked grid, which can

be found in (Espinosa, 2015). All the consumers are single-phase and their phase connection is depicted in Figure A.1. All the microgeneration units are considered as single-phase PV rooftop installations that are connected to the same phase as the respective residential user. Note that $x.1, x.2, x.3$ implies connection at node x on phase a, b, c, accordingly.

Table A.1: Points of PV connections for the presented scenarios.

<table>
<tr><td rowspan="2">Points of PV connections</td><td>522.2/388.1/178.2/676.2/639.2/337.3/701.3/614.3/562.1/682.2/70.1/556.3/629.1/47.2/349.1/563.1/264.3/458.3/249.2/289.1</td><td>611.1/74.1/320.3/73.1/276.2/225.1/327.3/387.1/619.3/702.2</td><td>702.2/502.1/342.3/208.3/539.3/688.2/406.2</td><td>248.2/83.2/314.2/896.1/785.2/900.1/899.2/755.2/780.3/898.1/813.2</td></tr>
<tr><td colspan="4"></td></tr>
<tr><td rowspan="4">Scenarios [% of PV]</td><td>30%</td><td></td><td></td><td></td></tr>
<tr><td colspan="2">55%</td><td></td><td></td></tr>
<tr><td colspan="3">65%</td><td></td></tr>
<tr><td colspan="4">85%</td></tr>
</table>

Table A.2: Points of EV connections for the presented scenarios.

<table>
<tr><td rowspan="2">Points of EV connections</td><td>327.3/835.3/785.2/563.1/755.2/249.2/225.1/47.2/886.2/898.1/314.2/208.3/906.1/861.1/320.3/682.2/780.3/406.2/817.1/248.2</td><td>619.3/860.1/702.2/458.3/899.2/264.3/178.2/83.2/337.3/556.3</td><td>73.1/349.1/701.3/522.2/342.3/289.1</td></tr>
<tr><td colspan="3"></td></tr>
<tr><td rowspan="3">Scenarios [% of EV]</td><td>30%</td><td></td><td></td></tr>
<tr><td colspan="2">55%</td><td></td></tr>
<tr><td colspan="3">65%</td></tr>
</table>

A.2 Calculations of power flow and nonlinear derivatives

A.2.1 Branch current non-linear inequalities: Polar coordinates

As this constraint presents a nonlinear one, the analytical first and second derivative will be given to the optimizer for its acceleration. The formulation of complex current balance equation can provide an expressions with the state vectors as follows:

$$G(X) = I_{\text{nodal}} + I_{\text{inj}} \tag{A.1}$$

where $I_{\text{nodal}}, I_{\text{inj}}$ correspond to the complex nodal current injections and the injections from loads and generators accordingly. Expanding A.1 using the same notation as in (5.14) for a particular time step τ_k:

$$\begin{aligned} G(X) &= I_{\text{nodal}} + I_{\text{load}} - I_{\text{DER}} \\ &= Y_{\text{bus}} V_{\tau_k} + [S_{\text{load}}(x_{\tau_k}) - C_p \cdot S_{\text{DER}}(x_{\tau_k})]^* W^* \end{aligned} \tag{A.2}$$

where $W = [V_{\tau_k}]$.

For the first order derivative of complex current injections, the derivation with regard to the vector X is given in (A.3) and the subsequent derivative for a particular set of state and decision variable of time-step x_{τ_k} is given in (A.4). For the currents calculations, it is evident that there are two components for the assessment of the derivative i.e. $I_{\text{nodal}}, I_{\text{inj}}$. More analytically, it is:

$$\frac{\partial I_{\text{nodal},\tau_k}}{\partial X} = \left[\frac{\partial I_{\text{nodal}}}{\partial x_1} \quad \cdots \quad \boxed{\frac{\partial I_{\text{nodal}}}{\partial x_{\tau_k}}} \quad \cdots \quad \frac{\partial I_{\text{nodal}}}{\partial x_{H_t}} \quad \frac{\partial I_{\text{nodal}}}{\partial x_{H_t}} \quad \frac{\partial I_{\text{nodal}}}{\partial y_1} \quad \cdots \quad \frac{\partial I_{\text{nodal}}}{\partial y_{H_t}} \right]_{\tau_k} \tag{A.3}$$

Obviously, the partial derivatives of branch currents for period τ_k ($I_{b\tau_k}$) with regard to P_{g,τ_k} and Q_{g,τ_k} are zero entries to the Jacobian matrix, together with all the rest of the derivations that correspond to decision and control variables from other time-steps (e.g., $\partial I_{b\tau_k}/\partial x_1 = 0$).

$$\frac{\partial I_{\text{nodal},\tau_k}}{\partial x_\tau} = \left[\frac{\partial I_{\text{nodal}}}{\partial \Theta_\tau} \quad \frac{\partial I_{\text{nodal}}}{\partial \mathscr{V}_\tau} \quad \frac{\partial I_{\text{nodal}}}{\partial Pg_{\tau_k}} \quad \frac{\partial I_{\text{nodal}}}{\partial Qg_{\tau_k}} \right]_{\tau_k} = \left[\frac{\partial I_{\text{nodal}}}{\partial \Theta_{\tau_k}} \quad \frac{\partial I_{\text{nodal}}}{\partial \mathscr{V}_{\tau_k}} \quad \mathbf{0} \quad \mathbf{0} \right]_{\tau,k} \tag{A.4}$$

$$\frac{\partial I_{\text{nodal}}}{\partial \Theta_{\tau_k}} = Y_{\text{bus}} \cdot \frac{\partial V_{\tau_k}}{\partial \Theta_{\tau_k}} = jY_{\text{bus}} \cdot [V_{\tau_k}] \tag{A.5}$$

$$\frac{\partial I_{\text{nodal}}}{\partial V_{\tau_k}} = Y_{\text{bus}} \cdot \frac{\partial V_{\tau_k}}{\partial \mathscr{V}_{\tau_k}} = Y_{\text{bus}} \cdot [V_{\tau_k}][\mathscr{V}_{\tau_k}]^{-1} \tag{A.6}$$

$$\frac{\partial I_{\text{inj},\tau_k}}{\partial x_{\tau_k}} = \left[\frac{\partial I_{\text{inj}}}{\partial \Theta_{\tau_k}} \quad \frac{\partial I_{\text{inj}}}{\partial \mathscr{V}_{\tau_k}} \quad \frac{\partial I_{\text{inj}}}{\partial Pg_{\tau_k}} \quad \frac{\partial I_{\text{inj}}}{\partial Qg_{\tau_k}} \right]_{\tau_k} \tag{A.7}$$

$$\frac{\partial I_{\text{inj}}}{\partial \Theta_{\tau_k}} = j[S_{\text{load}} - C_g S_{\text{DER}}]^*[W^*] \tag{A.8}$$

$$\frac{\partial I_{\text{inj}}}{\partial \mathscr{V}_{\tau_k}} = -[S_{\text{load}} - C_g S_{\text{DER}}]^*[\mathscr{V}_{\tau_k}]^{-1}[W^*] \tag{A.9}$$

$$\frac{\partial I_{\text{inj}}}{\partial Pg_{\tau_k}} = -[W^*]C_p \tag{A.10}$$

$$\frac{\partial I_{\text{inj}}}{\partial Qg_{\tau_k}} = j[W^*]C_p \tag{A.11}$$

Therefore, compiling the above equations we obtain the full first-order derivative of the complex current balance equation:

$$G_{\Theta_{\tau_k}} = \frac{\partial G}{\partial \Theta_{\tau_k}} = \frac{\partial I_{\text{nodal}}}{\partial \Theta_{\tau_k}} + \frac{\partial I_{\text{inj}}}{\partial \Theta_{\tau_k}} = j(Y_{\text{bus}} \cdot [V_{\tau_k}] + [S_{\text{load}} - C_g S_{\text{DER}}]^*[W^*]) \tag{A.12}$$

$$G_{\mathscr{V}_{\tau_k}} = \frac{\partial G}{\partial \mathscr{V}_{\tau_k}} = \frac{\partial I_{\text{nodal}}}{\partial \mathscr{V}_{\tau_k}} + \frac{\partial I_{\text{inj}}}{\partial \mathscr{V}_{\tau_k}} = Y_{\text{bus}} \cdot [V_{\tau_k}][\mathscr{V}_{\tau_k}]^{-1} - [S_{\text{load}} - C_g S_{\text{DER}}]^*[\mathscr{V}_{\tau_k}]^{-1}[W^*] \tag{A.13}$$

$$G_{Pg_{\tau_k}} = \frac{\partial G}{\partial Pg_{\tau_k}} = \frac{\partial I_{\text{nodal}}}{\partial Pg_{\tau_k}} + \frac{\partial I_{\text{inj}}}{\partial Pg_{\tau_k}} = -[W^*]C_p \tag{A.14}$$

$$G_{Qg_{\tau_k}} = \frac{\partial G}{\partial Qg_{\tau_k}} = \frac{\partial I_{\text{nodal}}}{Qg_{\tau_k}} + \frac{\partial I_{\text{inj}}}{\partial Qg_{\tau_k}} = j[W^*]C_p \tag{A.15}$$

Accordingly, the second-order derivatives for the vector that correspond to the branch currents for time-step τ_k will be structured in proportion to the Lagrangian multiplier for inequality constraints, by the following matrix (A.16):

$$\begin{aligned}
\boldsymbol{\sigma}\frac{\partial^2 I_{\text{nodal},\tau_k}}{\partial x_{\tau_k}^2} &= \boldsymbol{\sigma}\frac{\partial}{\partial x_{\tau_k}}\left(\frac{I_{\text{nodal},\tau_k}}{\partial x_{\tau_k}}\right)^T \\
&= \begin{bmatrix} I_{\text{nodal},\Theta\Theta_{\tau_k}} & I_{\text{nodal}\Theta\mathscr{V}_{\tau_k}} & 0 & 0 \\ I_{\text{nodal}\mathscr{V}\Theta_{\tau_k}} & I_{\text{nodal}\mathscr{V}\mathscr{V}_{\tau_k}} & 0 & 0 \\ 0 & 0 & 0 & 0 \\ 0 & 0 & 0 & 0 \end{bmatrix} \\
&= \begin{bmatrix} \mathsf{A} & \mathsf{B} & 0 & 0 \\ \mathsf{B} & \mathsf{C} & 0 & 0 \\ 0 & 0 & 0 & 0 \\ 0 & 0 & 0 & 0 \end{bmatrix}
\end{aligned} \tag{A.16}$$

where

$$\begin{aligned}
I_{\text{nodal}\Theta\Theta_{\tau_k}}(\boldsymbol{\sigma}) &= \frac{\partial}{\partial\Theta_{\tau_k}}\left(j[V_{\tau_k}]Y_{\text{bus}}^T\right)\boldsymbol{\sigma} \\
&= -[Y_{\text{bus}}^T\boldsymbol{\sigma}][V_{\tau_k}] \\
&= \mathsf{A}
\end{aligned} \tag{A.17}$$

$$\begin{aligned}
I_{\text{nodal}\mathscr{V}\Theta_{\tau_k}}(\boldsymbol{\sigma}) &= \frac{\partial}{\partial\Theta_{\tau_k}}\left([V_{\tau_k}][\mathscr{V}_{\tau_k}]^{-1}Y_{\text{bus}}^T\right)\boldsymbol{\sigma}[V] \\
&= j[Y_{\text{bus}}^T\boldsymbol{\sigma}][V_{\tau_k}][\mathscr{V}_{\tau_k}]^{-1} \\
&= -jI_{\text{nodal}\Theta\Theta_{\tau_k}}\boldsymbol{\sigma}[\mathscr{V}_{\tau_k}]^{-1} \\
&= \mathsf{B}
\end{aligned} \tag{A.18}$$

$$\begin{aligned}
I_{\text{nodal}\Theta\mathscr{V}_{\tau_k}}(\boldsymbol{\sigma}) &= \frac{\partial}{\partial\mathscr{V}_{\tau_k}}\left(\left(\frac{\partial I_{\text{nodal}\tau_k}}{\partial V_{\tau_k}}\right)^T\boldsymbol{\sigma}\right) \\
&= j[Y_{\text{bus}}^T\boldsymbol{\sigma}][V_{\tau_k}][\mathscr{V}_{\tau_k}]^{-1} \\
&= I_{\text{nodal}\mathscr{V}\Theta_{\tau_k}}(\boldsymbol{\sigma})
\end{aligned} \tag{A.19}$$

$$\begin{aligned}
I_{\text{nodal}\mathscr{V}\mathscr{V}_{\tau_k}}(\boldsymbol{\sigma}) &= \frac{\partial}{\partial\mathscr{V}_{\tau_k}}\left(\left(\frac{\partial I_{\text{nodal}\tau_k}}{\partial V_{\tau_k}}\right)^T\boldsymbol{\sigma}\right) \\
&= \frac{\partial}{\partial\mathscr{V}_{\tau_k}}\left(j[Y_{bus}^T\boldsymbol{\sigma}][V_{\tau_k}][\mathscr{V}_{\tau_k}]^{-1}\right) \\
&= \mathbf{0} \\
&= \mathsf{C}
\end{aligned} \tag{A.20}$$

Now the assessment of the second-order derive of the other current component (I_{inj}) has to be discussed.

$$
\begin{aligned}
\boldsymbol{\sigma}\frac{\partial^2 I_{\text{inj},\tau_k}}{\partial x_{\tau_k}^2} &= \boldsymbol{\sigma}\frac{\partial}{\partial x_{\tau_k}}\left(\frac{I_{\text{inj},\tau_k}}{\partial x_{\tau_k}}\right)^T \\
&= \boldsymbol{\sigma}\begin{bmatrix} I_{\text{inj},\Theta\Theta_{\tau_k}} & I_{\text{inj}\Theta\mathscr{V}_{\tau_k}} & I_{\text{inj}\Theta P_{g\tau_k}} & I_{\text{inj}\Theta Q_{g\tau_k}} \\ I_{\text{inj}\mathscr{V}\Theta_{\tau_k}} & I_{\text{inj}\mathscr{V}\mathscr{V}_{\tau_k}} & I_{\text{inj}\mathscr{V}P_{g\tau_k}} & I_{\text{inj}\mathscr{V}Q_{g\tau_k}} \\ I_{\text{inj}P_g\Theta_{\tau_k}} & I_{\text{inj}P_g\mathscr{V}_{\tau_k}} & 0 & 0 \\ I_{\text{inj}Q_g\Theta_{\tau_k}} & I_{\text{inj}Q_g\mathscr{V}_{\tau_k}} & 0 & 0 \end{bmatrix} \\
&= \begin{bmatrix} \mathsf{G} & \mathsf{H} & \mathsf{K} & \mathsf{L} \\ \mathsf{M} & \mathsf{N} & \mathsf{T} & \mathsf{Y} \\ \mathsf{F} & \mathsf{P} & 0 & 0 \\ \mathsf{Q} & \mathsf{Z} & 0 & 0 \end{bmatrix}
\end{aligned} \tag{A.21}
$$

where

$$
\begin{aligned}
I_{\text{inj}\Theta\Theta_{\tau_k}}(\boldsymbol{\sigma}) &= \frac{partial}{\Theta_{\tau_k}}\left(I^T_{\text{inj}\Theta_{\tau_k}}\boldsymbol{\sigma}\right) \\
&= \frac{\partial}{\partial\Theta_{\tau_k}}\left(j[S_{\text{load}} - C_g S_{\text{DER}}]^*[W^*]\right)\boldsymbol{\sigma} \\
&= -[S_{\text{load}} - C_g S_{\text{DER}}]^*[\boldsymbol{\sigma}][W^*] \\
&= \mathsf{G}
\end{aligned} \tag{A.22}
$$

$$
\begin{aligned}
I_{\text{inj}\mathscr{V}\Theta_{\tau_k}}(\boldsymbol{\sigma}) &= \frac{\partial}{\Theta_{\tau_k}}\left(I^T_{\text{inj}\mathscr{V}_{\tau_k}}\boldsymbol{\sigma}\right) \\
&= \frac{\partial}{\partial\Theta_{\tau_k}}\left(-[S_{\text{load}} - C_g S_{\text{DER}}]^*[\mathscr{V}_{\tau_k}]^{-1}[W^*]\right)\boldsymbol{\sigma}[V] \\
&= -[S_{\text{load}} - C_g S_{\text{DER}}]^*\boldsymbol{\sigma}[\mathscr{V}_{\tau_k}]^{-1}[W^*] \\
&= \mathsf{M}
\end{aligned} \tag{A.23}
$$

$$
\begin{aligned}
I_{\text{inj}\Theta\mathscr{V}_{\tau_k}}(\boldsymbol{\sigma}) &= \frac{\partial}{\partial\mathscr{V}_{\tau_k}}\left(\left(\frac{\partial I_{\text{inj}\tau_k}}{\partial V_{\tau_k}}\right)^T\boldsymbol{\sigma}\right) \\
&= \frac{\partial}{\partial\mathscr{V}_{\tau_k}}\left(j(Y_{\text{bus}}\cdot[V_{\tau_k}] + [S_{\text{load}} - C_g S_{\text{DER}}]^*[W^*])\right) \\
&= -j(\boldsymbol{\sigma}) \\
&= \mathsf{H}
\end{aligned} \tag{A.24}
$$

$$
\begin{aligned}
I_{\text{inj}\mathscr{V}\mathscr{V}_{\tau_k}}(\boldsymbol{\sigma}) &= \frac{\partial}{\partial\mathscr{V}_{\tau_k}}\left(\left(\frac{\partial I_{\text{inj}\tau_k}}{\partial V_{\tau_k}}\right)^T\boldsymbol{\sigma}\right) \\
&= \frac{\partial}{\partial\mathscr{V}_{\tau_k}}\left(j[Y^T_{bus}\boldsymbol{\sigma}][V_{\tau_k}][\mathscr{V}_{\tau_k}]^{-1}\right) \\
&= \mathbf{0} \\
&= \mathsf{N}
\end{aligned} \tag{A.25}
$$

$$
\begin{aligned}
I_{\text{inj}\Theta Pg_{\tau_k}}(\boldsymbol{\sigma}) &= \frac{\partial}{\partial Pg_{\tau_k}}\left(\left(\frac{\partial I_{\text{inj}\tau_k}}{\partial\Theta_{\tau_k}}\right)^T\boldsymbol{\sigma}\right) \\
&= \frac{\partial}{\partial Pg_{\tau_k}}\left(j[S_{\text{load}} - C_g S_{\text{DER}}]^*[W^*]\right) \\
&= -j[\boldsymbol{\sigma}][W^*]C_p \\
&= j\mathsf{Q}^T \\
&= \mathsf{K}
\end{aligned} \tag{A.26}
$$

$$
\begin{aligned}
I_{\mathrm{inj}\Theta Qg_{\tau_k}}(\boldsymbol{\sigma}) &= \frac{\partial}{\partial Qg_{\tau_k}}\left(\left(\frac{\partial I_{\mathrm{inj}\tau_k}}{\partial \Theta_{\tau_k}}\right)^T \boldsymbol{\sigma}\right) \\
&= \frac{\partial}{\partial Qg_{\tau_k}}\left(\frac{\partial}{\partial Qp_{\tau_k}} j[S_{\mathrm{load}} - C_g S_{\mathrm{DER}}]^*[W^*]\right) \\
&= [\boldsymbol{\sigma}][W^*]C_p \\
&= -\mathsf{Q}^T \\
&= \mathsf{L}
\end{aligned}
\tag{A.27}
$$

$$
\begin{aligned}
I_{\mathrm{inj}\mathscr{V}Pg_{\tau_k}}(\boldsymbol{\sigma}) &= \frac{\partial}{\partial Pg_{\tau_k}}\left(\left(\frac{\partial I_{\mathrm{inj}\tau_k}}{\partial V_{\tau_k}}\right)^T \boldsymbol{\sigma}\right) \\
&= \frac{\partial}{\partial \mathscr{V}_{\tau_k}}\left(-[S_{\mathrm{load}} - C_g S_{\mathrm{DER}}]^*[\mathscr{V}_{\tau_k}]^{-1}[W^*]\right) \\
&= \mathsf{P}^T \\
&= \mathsf{T}
\end{aligned}
\tag{A.28}
$$

$$
\begin{aligned}
I_{\mathrm{inj}\mathscr{V}Qg_{\tau_k}}(\boldsymbol{\sigma}) &= \frac{\partial}{\partial Qg_{\tau_k}}\left(\left(\frac{\partial I_{\mathrm{inj}\tau_k}}{\partial V_{\tau_k}}\right)^T \boldsymbol{\sigma}\right) \\
&= \frac{\partial}{\partial \mathscr{V}_{\tau_k}}\left(-[S_{\mathrm{load}} - C_g S_{\mathrm{DER}}]^*[\mathscr{V}_{\tau_k}]^{-1}[W^*]\right) \\
&= -j\mathsf{P}^T \\
&= \mathsf{Y}
\end{aligned}
\tag{A.29}
$$

$$
\begin{aligned}
I_{\mathrm{inj}Pg\Theta_{\tau_k}}(\boldsymbol{\sigma}) &= \frac{\partial}{\partial \Theta_{\tau_k}}\left(\left(\frac{\partial I_{\mathrm{inj}\tau_k}}{\partial Pg_{\tau_k}}\right)^T \boldsymbol{\sigma}\right) \\
&= \frac{\partial}{\partial \Theta_{\tau_k}}\left(-jC_p^T[\boldsymbol{\sigma}][W^*]\right) \\
&= C_p^T[\boldsymbol{\sigma}][W^*] \\
&= -j\mathsf{Q} \\
&= \mathsf{F}
\end{aligned}
\tag{A.30}
$$

$$
\begin{aligned}
I_{\mathrm{inj}Pg\mathscr{V}_{\tau_k}}(\boldsymbol{\sigma}) &= \frac{\partial}{\partial \mathscr{V}_{\tau_k}}\left(\left(\frac{\partial I_{\mathrm{inj}\tau_k}}{\partial Pg_{\tau_k}}\right)^T \boldsymbol{\sigma}\right) \\
&= C_g^T[\boldsymbol{\sigma}][\mathscr{V}_{\tau_k}] \\
&= \mathsf{P}
\end{aligned}
\tag{A.31}
$$

$$
\begin{aligned}
I_{\mathrm{inj}Qg\Theta_{\tau_k}}(\boldsymbol{\sigma}) &= \frac{\partial}{\partial \Theta_{\tau_k}}\left(\left(\frac{\partial I_{\mathrm{inj}\tau_k}}{\partial Qg_{\tau_k}}\right)^T \boldsymbol{\sigma}\right) \\
&= \frac{\partial}{\partial \Theta_{\tau_k}}\left(-C_p^T[\boldsymbol{\sigma}][W^*]\right) \\
&= C_p^T[\boldsymbol{\sigma}][W^*] \\
&= \mathsf{Q}
\end{aligned}
\tag{A.32}
$$

$$
\begin{aligned}
I_{\text{inj}Qg\mathscr{V}_{\tau_k}}(\boldsymbol{\sigma}) &= \frac{\partial}{\partial \mathscr{V}_{\tau_k}}\left(\left(\frac{\partial I_{\text{inj}\tau_k}}{\partial Qg_{\tau_k}}\right)^T \boldsymbol{\sigma}\right) \\
&= \frac{\partial}{\partial \mathscr{V}_{\tau_k}}\left(jC_p^T[\boldsymbol{\sigma}][W^*]\right) \\
&= jC_p^T[\boldsymbol{\sigma}][\mathscr{V}_{\tau_k}]^{-1}[W^*] \\
&= -j\mathsf{P} \\
&= \mathsf{Z}
\end{aligned}
\tag{A.33}
$$

Assembling the overall expression of the second order derivative nodal current balance equations, it will be the summation of matrices (A.16) and (A.21). Therefore it is

$$
\begin{aligned}
G_{XX}(\boldsymbol{\sigma}) &= \boldsymbol{\sigma}\frac{\partial^2 I_{\text{nodal},\tau_k}}{\partial x_{\tau_k}^2} + \boldsymbol{\sigma}\frac{\partial^2 I_{\text{inj},\tau_k}}{\partial x_{\tau_k}^2} \\
&= \begin{bmatrix} \mathsf{A} & \mathsf{B} & 0 & 0 \\ \mathsf{B} & \mathsf{C} & 0 & 0 \\ 0 & 0 & 0 & 0 \\ 0 & 0 & 0 & 0 \end{bmatrix} + \begin{bmatrix} \mathsf{G} & \mathsf{H} & \mathsf{K} & \mathsf{L} \\ \mathsf{M} & \mathsf{N} & \mathsf{T} & \mathsf{Y} \\ \mathsf{F} & \mathsf{P} & 0 & 0 \\ \mathsf{Q} & \mathsf{Z} & 0 & 0 \end{bmatrix}.
\end{aligned}
\tag{A.34}
$$

Note that within the assessment of derivative several mathematical components are being stored and utilized in the iterative callback of the optimizer to take advantage of computation savings.

A.2.2 Power flow equality constraints: Cartesian coordinates

Hereby we simply provide the definition of the state variables, to provide the intuition why the Cartesian coordinates can simplify the assessment of the derivatives. Let the same notation as defined in previous sections. The vector for bus j $\upsilon_j = u_j + jw_j$. If U, W are the vectors representing the real and imaginary parts of the bus voltages accordingly, consider as D the inverse bus voltages $\frac{1}{\upsilon_j}$. Therefore, it is:

$$D = V^{-1} = [\mathscr{V}]^{-2}V^* \tag{A.35}$$

$$\Theta = \tan^{-1}([U]^{-1}W) \tag{A.36}$$

$$\mathscr{V} = (U^2 + W^2)^{\frac{1}{2}} \tag{A.37}$$

Assessing the fist-order derivatives it is:

$$\frac{\partial V}{\partial U} = [I]_{N_b} \tag{A.38}$$

$$\frac{\partial V}{\partial W} = j[I]_{N_b} \tag{A.39}$$

$$\frac{\partial D}{\partial U} = -[D]^2 \tag{A.40}$$

$$\frac{\partial D}{\partial W} = -j[D]^2 \tag{A.41}$$

$$\frac{\partial \Theta}{\partial U} = -[\mathscr{V}]^{-2}[W] \tag{A.42}$$

$$\frac{\partial \Theta}{\partial W} = [\mathscr{V}]^{-2}[U] \tag{A.43}$$

$$\frac{\partial \mathscr{V}}{\partial U} = [\mathscr{V}]^{-1}[U] \tag{A.44}$$

$$\frac{\partial \mathscr{V}}{\partial W} = [\mathscr{V}]^{-1}[W] \tag{A.45}$$

The above statement for variables can be used to reformulate the proposed MACOPF framework and explore the computational improvement.

References

Morad Mohamed Abdelmageed Abdelaziz, Hany E Farag, Ehab F El-Saadany, and Yasser Abdel-Rady I Mohamed. A novel and generalized three-phase power flow algorithm for islanded microgrids using a newton trust region method. *IEEE Transactions on Power Systems*, 28(1): 190–201, 2012. ISSN 0885-8950.

Hamdi Abdi, Soheil Derafshi Beigvand, and Massimo La Scala. A review of optimal power flow studies applied to smart grids and microgrids. *Renewable and Sustainable Energy Reviews*, 71:742–766, 2017. ISSN 1364-0321. doi: https://doi.org/10.1016/j.rser.2016.12.102. URL http://www.sciencedirect.com/science/article/pii/S1364032116311583.

Ajith Abraham and Swagatam Das. *Computational intelligence in power engineering*, volume 302. Springer, 2010. ISBN 3642140130.

S. Acha, T. C. Green, and N. Shah. Effects of optimised plug-in hybrid vehicle charging strategies on electric distribution network losses. In *IEEE PES T&D 2010*, pages 1–6. ISBN 2160-8555. doi: 10.1109/TDC.2010.5484397.

Jamshid Aghaei, Seyed Aboozar Bozorgavari, Sasan Pirouzi, Hossein Farahmand, and Magnus Korpås. Flexibility planning of distributed battery energy storage systems in smart distribution networks. *Iranian Journal of Science and Technology, Transactions of Electrical Engineering*, 2019. ISSN 2364-1827. doi: 10.1007/s40998-019-00261-z. URL https://doi.org/10.1007/s40998-019-00261-z.

Arturo Alarcon-Rodriguez, Edwin Haesen, Graham Ault, Johan Driesen, and Ronnie Belmans. Multi-objective planning framework for stochastic and controllable distributed energy resources. *IET Renewable Power Generation*, 3(2):227–238, 2009.

Bart Meersman Andreas Tuerk, Claudia Fruhmann. Synthesis document: Increasing the penetration of renewable energy sources in the distribution grid by developing control strategies and using ancillary services. Report, 2017.

Elpiniki Apostolaki-Iosifidou, Willett Kempton, and Paul Codani. Reply to shirazi and sachs comments on "measurement of power loss during electric vehicle charging and discharging". *Energy*, 142:1142 – 1143, 2018. ISSN 0360-5442. doi: https://doi.org/10.1016/j.energy.2017.10.080. URL http://www.sciencedirect.com/science/article/pii/S0360544217317851.

Xiaomin Bai. *Role of Demand Response*. John Wiley & Sons, Ltd, 2016. ISBN 9781118755471. doi: 10.1002/9781118755471.sgd008. URL http://dx.doi.org/10.1002/9781118755471.sgd008.

K. Baker, G. Hug, and Li Xin. Inclusion of inter-temporal constraints into a distributed newton-raphson method. In *2012 North American Power Symposium (NAPS)*, pages 1–6, a. doi: 10.1109/NAPS.2012.6336344.

K. Baker, D. Zhu, G. Hug, and X. Li. Jacobian singularities in optimal power flow problems caused by intertemporal constraints. In *2013 North American Power Symposium (NAPS)*, pages 1–6, b. doi: 10.1109/NAPS.2013.6666876.

P. Balram, Tuan Le Anh, and O. Carlson. Predictive voltage control of batteries and tap changers in distribution system with photovoltaics. In *2016 Power Systems Computation Conference (PSCC)*, pages 1–7. doi: 10.1109/PSCC.2016.7540847.

M. Bazrafshan and N. Gatsis. Comprehensive modeling of three-phase distribution systems via the bus admittance matrix. *IEEE Transactions on Power Systems*, 33(2):2015–2029, 2018a. ISSN 0885-8950. doi: 10.1109/TPWRS.2017.2728618.

M. Bazrafshan and N. Gatsis. Comprehensive modeling of three-phase distribution systems via the bus admittance matrix. *IEEE Transactions on Power Systems*, 33(2):2015–2029, 2018b. ISSN 0885-8950. doi: 10.1109/TPWRS.2017.2728618.

Regine Belhomme, Ramon Cerero, Giovanni Valtorta, and Philippe Eyrolles. The address project: Developing active demand in smart power systems integrating renewables. In *Power and Energy Society General Meeting, 2011 IEEE*, pages 1–8. IEEE. ISBN 1457710021.

A Bertani, Alberto Borghetti, Claudio Bossi, O Lamquet, S Masucco, A Morini, C Nucci, M Paolone, E Quaia, and E Silvestro. Management of low voltage grids with high penetration of distributed generation: concepts, implementations and experiments. In *CIGRE*. FR.

Ricardo J. Bessa, Jethro Dowell, and Pierre Pinson. *Renewable Energy Forecasting*. John Wiley & Sons, Ltd, 2016. ISBN 9781118755471. doi: 10.1002/9781118755471.sgd050. URL http://dx.doi.org/10.1002/9781118755471.sgd050.

H. Soleimani Bidgoli and T. H. Van Cutsem. Combined local and centralized voltage control in active distribution networks. *IEEE Transactions on Power Systems*, PP(99):1–1, 2017. ISSN 0885-8950. doi: 10.1109/TPWRS.2017.2716407.

Lorenz T Biegler and Victor M Zavala. Large-scale nonlinear programming using ipopt: An integrating framework for enterprise-wide dynamic optimization. *Computers & Chemical Engineering*, 33(3):575–582, 2009. ISSN 0098-1354.

Abdullah Bokhari, Ali Alkan, Rasim Dogan, Marc Diaz-Aguiló, Francisco De Leon, Dariusz Czarkowski, Zivan Zabar, Leo Birenbaum, Anthony Noel, and Resk Ebrahem Uosef. Experimental determination of the zip coefficients for modern residential, commercial, and industrial loads. *IEEE Transactions on Power Delivery*, 29(3):1372–1381, 2013.

A. Borghetti, M. Bosetti, S. Grillo, S. Massucco, C. A. Nucci, M. Paolone, and F. Silvestro. Short-term scheduling and control of active distribution systems with high penetration of renewable resources. *IEEE Systems Journal*, 4(3):313–322, 2010. ISSN 1932-8184. doi: 10.1109/JSYST.2010.2059171.

B. O. Brewin, S. C. E. Jupe, M. G. Bartlett, K. T. Jackson, and C. Hanmer. New technologies for low voltage distribution networks. In *2011 2nd IEEE PES International Conference and Exhibition on Innovative Smart Grid Technologies*, pages 1–8. ISBN 2165-4816. doi: 10.1109/ISGTEurope.2011.6162811.

Sergio Bruno and Massimo La Scala. Unbalanced three-phase optimal power flow for the optimization of mv and lv distribution grids. *From Smart Grids to Smart Cities: New Challenges in Optimizing Energy Grids*, pages 1–42, 2017. ISSN 1119116082.

Sergio Bruno, Silvia Lamonaca, Giuseppe Rotondo, Ugo Stecchi, and Massimo La Scala. Unbalanced three-phase optimal power flow for smart grids. *IEEE Transactions on Industrial Electronics*, 58(10):4504–4513, 2011. ISSN 0278-0046.

Samuel Burer and Adam N Letchford. Non-convex mixed-integer nonlinear programming: A survey. *Surveys in Operations Research and Management Science*, 17(2):97–106, 2012. ISSN 1876-7354.

Alessia Cagnano, Enrico De Tuglie, Marco Liserre, and Rosa A Mastromauro. Online optimal reactive power control strategy of pv inverters. *IEEE Transactions on Industrial Electronics*, 58 (10):4549–4558, 2011. ISSN 0278-0046.

F. Campos, L. Marques, and K. Kotsalos. Electric vehicle cpms and secondary substation management. In *8th Solar & 17th Wind Integration Workshop*.

Filipe Campos, Luís Marques, Nuno Silva, Francisco Melo, Luís Seca, Clara Gouveia, André Madureira, and Jorge Pereira. Adms4lv–advanced distribution management system for active management of lv grids. *CIRED-Open Access Proceedings Journal*, 2017(1):920–923, 2017. ISSN 2515-0855.

Florin Capitanescu. Critical review of recent advances and further developments needed in ac optimal power flow. *Electric Power Systems Research*, 136:57–68, 2016. ISSN 0378-7796.

Florin Capitanescu and Louis Wehenkel. Experiments with the interior-point method for solving large scale optimal power flow problems. *Electric Power Systems Research*, 95:276–283, 2013. ISSN 0378-7796.

Florin Capitanescu, Mevludin Glavic, Damien Ernst, and Louis Wehenkel. Interior-point based algorithms for the solution of optimal power flow problems. *Electric Power Systems Research*, 77(5):508–517, 2007. ISSN 0378-7796. doi: https://doi.org/10.1016/j.epsr.2006.05.003. URL http://www.sciencedirect.com/science/article/pii/S0378779606001209.

Florin Capitanescu, JL Martinez Ramos, Patrick Panciatici, Daniel Kirschen, A Marano Marcolini, Ludovic Platbrood, and Louis Wehenkel. State-of-the-art, challenges, and future trends in security constrained optimal power flow. *Electric Power Systems Research*, 81(8):1731–1741, 2011. ISSN 0378-7796.

Anya Castillo and Richard P O'Neill. Survey of approaches to solving the acopf (opf paper 4). *US Federal Energy Regulatory Commission, Tech. Rep*, 2013.

Anya Castillo, Paula Lipka, Jean-Paul Watson, Shmuel S Oren, and Richard P O'Neill. A successive linear programming approach to solving the iv-acopf. *IEEE Transactions on Power Systems*, 31(4):2752–2763, 2015. ISSN 0885-8950.

Smart Grid Coordination CEN-CENELEC-ETSI. Group: Smart grid reference architecture (november 2012). *URI: https://ec. europa. eu/energy/sites/ener/files/documents/xpert_group1_reference_architecture. pdf*, 2015.

A. Chaouachi, R. M. Kamel, R. Andoulsi, and K. Nagasaka. Multiobjective intelligent energy management for a microgrid. *IEEE Transactions on Industrial Electronics*, 60(4):1688–1699, 2013. ISSN 0278-0046. doi: 10.1109/TIE.2012.2188873.

T-H Chen and J-D Chang. Open wye-open delta and open delta-open delta transformer models for rigorous distribution system analysis. In *IEE Proceedings C (Generation, Transmission and Distribution)*, volume 139, pages 227–234. IET. ISBN 2053-7921.

Carol S Cheng and Dariush Shirmohammadi. A three-phase power flow method for real-time distribution system analysis. *IEEE Transactions on Power Systems*, 10(2):671–679, 1995. ISSN 0885-8950.

Konstantina Christakou, Dan-Cristian Tomozei, Jean-Yves Le Boudec, and Mario Paolone. Ac opf in radial distribution networks–part i: On the limits of the branch flow convexification and the alternating direction method of multipliers. *Electric Power Systems Research*, 143:438–450, 2017. ISSN 0378-7796.

R. M. Ciric, A. P. Feltrin, and L. F. Ochoa. Power flow in four-wire distribution networks-general approach. *IEEE Transactions on Power Systems*, 18(4):1283–1290, 2003. ISSN 0885-8950. doi: 10.1109/tpwrs.2003.818597.

Smart Energy Demand Coalition. Mapping demand response in europe today. *Tracking Compliance with Article*, 15, 2014.

Smart Energy Demand Coalition. Explicit demand response in europe. *Mapping the Markets*, 2017.

Thomas Coleman, Mary Ann Branch, and Andrew Grace. Optimization toolbox. *For Use with MATLAB. User's Guide for MATLAB 5, Version 2, Relaese II*, 1999.

A. O' Connell, D. Flynn, and A. Keane. Rolling multi-period optimization to control electric vehicle charging in distribution networks. *IEEE Transactions on Power Systems*, 29(1):340–348, 2014. ISSN 0885-8950. doi: 10.1109/TPWRS.2013.2279276.

H. Costa, M. Miranda, J. Ramos, L. Seca, A. Madureira, D. Lemos, R. Santana, M. Louro, P. G. Matos, L. Rosa, and N. Silva. Voltage control demonstration for lv networks with controllable der; the sustainable project approach. In *CIRED Workshop 2016*, pages 1–5, a. doi: 10.1049/cp.2016.0640.

H. M. Costa, J. Sumaili, A. G. Madureira, and C. Gouveia. A multi-temporal optimal power flow for managing storage and demand flexibility in lv networks. In *2017 IEEE Manchester PowerTech*, pages 1–6, b. doi: 10.1109/PTC.2017.7981166.

Levy Ferreira Costa, Giovanni De Carne, Giampaolo Buticchi, and Marco Liserre. The smart transformer: A solid-state transformer tailored to provide ancillary services to the distribution grid. *IEEE Power Electronics Magazine*, 4(2):56–67, 2017. ISSN 2329-9207.

Vander Menengoy da Costa, Nelson Martins, and Jose Luiz R Pereira. Developments in the newton raphson power flow formulation based on current injections. *IEEE Transactions on power systems*, 14(4):1320–1326, 1999. ISSN 0885-8950.

L. Degroote, B. Renders, B. Meersman, and L. Vandevelde. Neutral-point shifting and voltage unbalance due to single-phase dg units in low voltage distribution networks. In *2009 IEEE Bucharest PowerTech*, pages 1–8. doi: 10.1109/PTC.2009.5281998.

E. Demirok, P. C. González, K. H. B. Frederiksen, D. Sera, P. Rodriguez, and R. Teodorescu. Local reactive power control methods for overvoltage prevention of distributed solar inverters in low-voltage grids. *IEEE Journal of Photovoltaics*, 1(2):174–182, 2011. ISSN 2156-3381. doi: 10.1109/JPHOTOV.2011.2174821.

A. L. Dimeas and N. D. Hatziargyriou. Operation of a multiagent system for microgrid control. *IEEE Transactions on Power Systems*, 20(3):1447–1455, 2005. ISSN 0885-8950. doi: 10.1109/TPWRS.2005.852060.

Predrag Djapic, Charlotte Ramsay, Danny Pudjianto, Goran Strbac, Joseph Mutale, Nick Jenkins, and Ron Allan. Taking an active approach. *IEEE Power and Energy Magazine*, 5(4):68–77, 2007. ISSN 1540-7977.

ERSE-Entidade Reguladora dos Serviços Energéticos. Parâmetros de regulação para o período 2015-2017. *Lisboa: Entidade Reguladora dos Serviços Energéticos*, 2014.

Anamika Dubey, Anjan Bose, Michael Liu, and Luis Nando Ochoa. Paving the way for advanced distribution management systems applications: Making the most of models and data. *IEEE Power and Energy Magazine*, 18(1):63–75, 2020. ISSN 1540-7977.

Roger C. Dugan. Reference guide: The open distribution system simulator (opendss). 2016.

Efacec. Ev homecharger. 2018. URL http://electricmobility.efacec.com/wp-content/uploads/2016/10/CS195I1404C1_HC.pdf.

N. Efkarpidis, T. De Rybel, and J. Driesen. Optimization control scheme utilizing small-scale distributed generators and oltc distribution transformers. *Sustainable Energy, Grids and Networks*, 8:74–84, 2016a. ISSN 23524677. doi: 10.1016/j.segan.2016.09.002.

N. Efkarpidis, T. De Rybel, and J. Driesen. Technical assessment of centralized and localized voltage control strategies in low voltage networks. *Sustainable Energy, Grids and Networks*, 8:85–97, 2016b. ISSN 23524677. doi: 10.1016/j.segan.2016.09.003.

Nikolaos Efkarpidis, Tom De Rybel, and Johan Driesen. Optimal placement and sizing of active in-line voltage regulators in flemish lv distribution grids. *IEEE Transactions on Industry Applications*, 52(6):4577–4584, 2016c. ISSN 0093-9994.

Cherrelle Eid, Paul Codani, Yannick Perez, Javier Reneses, and Rudi Hakvoort. Managing electric flexibility from distributed energy resources: A review of incentives for market design. *Renewable and Sustainable Energy Reviews*, 64:237–247, 2016. ISSN 1364-0321. doi: https://doi.org/10.1016/j.rser.2016.06.008. URL http://www.sciencedirect.com/science/article/pii/S1364032116302222.

G Erbach. Promotion of renewable energy sources in the eu. *Depth Analysis, European Parliamentary Research Service, PE*, 583:1–20, 2016.

Alejandro Navarro Espinosa. Dissemination document "low voltage networks models and low carbon technology profiles". 2015.

M. Et-Taoussi, H. Ouadi, and H. E. Chakir. Hybrid optimal management of active and reactive power flow in a smart microgrid with photovoltaic generation. *Microsystem Technologies*, 2019. ISSN 1432-1858. doi: 10.1007/s00542-019-04354-x. URL https://doi.org/10.1007/s00542-019-04354-x.

Vasileios A. Evangelopoulos, Pavlos S. Georgilakis, and Nikos D. Hatziargyriou. Optimal operation of smart distribution networks: A review of models, methods and future research. *Electric Power Systems Research*, 140:95–106, 2016. ISSN 03787796. doi: 10.1016/j.epsr.2016.06.035.

Pedro Faria, João Spínola, and Zita Vale. Distributed energy resources scheduling and aggregation in the context of demand response programs. *Energies*, 11(8):1987, 2018. ISSN 1996-1073. URL http://www.mdpi.com/1996-1073/11/8/1987.

P. Fortenbacher, M. Zellner, and G. Andersson. Optimal sizing and placement of distributed storage in low voltage networks. In *2016 Power Systems Computation Conference (PSCC)*, pages 1–7. doi: 10.1109/PSCC.2016.7540850.

Stephen Frank and Steffen Rebennack. An introduction to optimal power flow: Theory, formulation, and examples. *IIE Transactions*, 48(12):1172–1197, 2016. ISSN 0740-817X. doi: 10.1080/0740817X.2016.1189626. URL https://doi.org/10.1080/0740817X.2016.1189626.

Stephen Frank, Ingrida Steponavice, and Steffen Rebennack. Optimal power flow: a bibliographic survey i. *Energy Systems*, 3(3):221–258, 2012. ISSN 1868-3967.

J. García-Villalobos, I. Zamora, K. Knezović, and M. Marinelli. Multi-objective optimization control of plug-in electric vehicles in low voltage distribution networks. *Applied Energy*, 180: 155–168, 2016. ISSN 0306-2619. doi: http://dx.doi.org/10.1016/j.apenergy.2016.07.110. URL http://www.sciencedirect.com/science/article/pii/S0306261916310406.

Jean Charles Gilbert and Cédric Josz. *Plea for a semidefinite optimization solver in complex numbers*. Thesis, 2017.

MJ Gorman and JJ Grainger. Transformer modelling for distribution system studies. ii. addition of models to y/sub bus/and z/sub bus. *IEEE transactions on power delivery*, 7(2):575–580, 1992. ISSN 0885-8977.

Marion Gottschalk, Mathias Uslar, and Christina Delfs. *The smart grid architecture model–SGAM*, pages 41–61. Springer, 2017.

C Gouveia, D Rua, CL Moreira, and JA Peças Lopes. *Coordinating distributed energy resources during microgrid emergency operation*, pages 259–303. Springer, 2014.

John J Grainger and William D Stevenson. *Power system analysis*, volume 621. McGraw-Hill New York, 1994.

Etta Grover-Silva, Robin Girard, and George Kariniotakis. Optimal sizing and placement of distribution grid connected battery systems through an socp optimal power flow algorithm. *Applied Energy*, 219:385–393, 2018. ISSN 0306-2619. doi: https://doi.org/10.1016/j.apenergy.2017.09.008. URL http://www.sciencedirect.com/science/article/pii/S0306261917312813.

Dian M Grueneich. The next level of energy efficiency: The five challenges ahead. *The Electricity Journal*, 28(7):44–56, 2015. ISSN 1040-6190.

vS. Harbo and B. Biegel. Contracting flexibility services. In *IEEE PES ISGT Europe 2013*, pages 1–5. ISBN 2165-4816. doi: 10.1109/ISGTEurope.2013.6695262.

N Hatziargyriou, O Vlachokyriakou, T Van Cutsem, J Milanovic, P Pourbeik, C Vournas, M Hong, R Ramos, J Boemer, and P Aristidou. Task force on contribution to bulk system control and stability by distributed energy resources connected at distribution network. *IEEE PES, Piscataway, NJ, USA, Rep. PES-TR22*, 2017.

Nikos Hatziargyriou. *Microgrids: architectures and control*. Wiley Online Library, 2014. ISBN 1118720644.

Adrian Hauswirth, Saverio Bolognani, Gabriela Hug, and Florian Dörfler. Generic existence of unique lagrange multipliers in ac optimal power flow. *arXiv preprint arXiv:1806.06615*, 2018.

M. Heleno, D. Rua, C. Gouveia, A. Madureira, M. A. Matos, J. P. Lopes, N. Silva, and S. Salustio. Optimizing pv self-consumption through electric water heater modeling and scheduling. In *2015 IEEE Eindhoven PowerTech*, pages 1–6. doi: 10.1109/PTC.2015.7232636.

Miguel Heleno, Manuel A. Matos, and J. A. Peças Lopes. A bottom-up approach to leverage the participation of residential aggregators in reserve services markets. *Electric Power Systems Research*, 136:425–433, 2016. ISSN 03787796. doi: 10.1016/j.epsr.2016.03.025.

Miguel Luis Delgado Heleno. Provision of advanced ancillary services through demand side integration. 2016.

Joern Hoppmann, Jonas Volland, Tobias S Schmidt, and Volker H Hoffmann. The economic viability of battery storage for residential solar photovoltaic systems–a review and a simulation model. *Renewable and Sustainable Energy Reviews*, 39:1101–1118, 2014. ISSN 1364-0321.

IEA. Web data-base. *http://www.iea.org/*, 2020.

J. P. Iria, F. J. Soares, A. G. Madureira, and M. Heleno. Availability of household loads to participate in demand response. In *2014 IEEE 8th International Power Engineering and Optimization Conference (PEOCO2014)*, pages 252–257. doi: 10.1109/PEOCO.2014.6814435.

R. A. Jabr. Optimal power flow using an extended conic quadratic formulation. *IEEE Transactions on Power Systems*, 23(3):1000–1008, 2008. doi: 10.1109/TPWRS.2008.926439.

Robert Wilson James Northcote-Green. *Control and Automation of Electrical Power Distribution Systems*. Taylor & Francis, 2013.

Teng Jen-Hao. A direct approach for distribution system load flow solutions. *IEEE Transactions on Power Delivery*, 18(3):882–887, 2003. ISSN 0885-8977. doi: 10.1109/TPWRD.2003.813818.

J. Jiricka, M. Kaspirek, L. Kolar, and M. Zahradka. Smart substation mv/lv. *CIRED - Open Access Proceedings Journal*, 2017(1):1482–1486, 2017. ISSN 2515-0855. doi: 10.1049/oap-cired.2017.0143.

R. Kamphuis, J. P. Wijbenga, J. S. van der Veen, P. Macdougall, and M. Faeth. Dream: An ict architecture framework for heterarchical coordination in power systems. In *2015 IEEE Eindhoven PowerTech*, pages 1–4. doi: 10.1109/PTC.2015.7232832.

S Karagiannopoulos, P Aristidou, and G Hug. Co-optimisation of planning and operation foractive distribution grids. In *2017 IEEE Manchester PowerTech*. IEEE, a.

S. Karagiannopoulos, P. Aristidou, and G. Hug. Data-driven local control design for active distribution grids using off-line optimal power flow and machine learning techniques. *IEEE Transactions on Smart Grid*, pages 1–1, 2019. ISSN 1949-3053. doi: 10.1109/TSG.2019.2905348.

Stavros Karagiannopoulos, Petros Aristidou, and Gabriela Hug. A centralised control method for tackling unbalances in active distribution grids. In *2018 Power Systems Computation Conference (PSCC)*. IEEE, b.

Stavros Karagiannopoulos, Line Roald, Petros Aristidou, and Gabriela Hug. Operational planning of active distribution grids under uncertainty. In *To be confirmed*. Leeds, c.

Stavros Karagiannopoulos, Petros Aristidou, and Gabriela Hug. Hybrid approach for planning and operating active distribution grids. *IET Generation, Transmission & Distribution*, 11(3): 685–695, 2017. ISSN 1751-8695.

S. Karambelkar, L. Mackay, S. Chakraborty, L. Ramirez-Elizondo, and P. Bauer. Distributed optimal power flow for dc distribution grids. In *2018 IEEE Power & Energy Society General Meeting (PESGM)*, pages 1–5. ISBN 1944-9925. doi: 10.1109/PESGM.2018.8586629.

E. L. Karfopoulos, K. A. Panourgias, and N. D. Hatziargyriou. Distributed coordination of electric vehicles providing v2g regulation services. *IEEE Transactions on Power Systems*, 31(4):2834–2846, 2016. ISSN 1558-0679. doi: 10.1109/TPWRS.2015.2472957.

K. Kotsalos, L. Marques, G. Sampaio, J. Pereira, C. Gouveia, H. Teixeira, R. Fernandes, and F. Campos. On the development of a framework for the advanced monitoring of lv grids. In *2019 International Conference on Smart Energy Systems and Technologies (SEST)*, pages 1–6, a. ISBN null. doi: 10.1109/SEST.2019.8848989.

Konstantinos Kotsalos, Nuno Silva, Ismael Miranda, and Helder Leite. Scheduling of operation in low voltage distribution networks with multiple distributed energy resources. In *Proceedings of the CIRED Workshop 2017 , Ljubljana, Slovenia*, b.

Konstantinos Kotsalos, Ismael Miranda, Nuno Silva, and Helder Leite. A horizon optimization control framework for the coordinated operation of multiple distributed energy resources in low voltage distribution networks. *Energies*, 12(6):1182, 2019a. ISSN 1996-1073. URL http://www.mdpi.com/1996-1073/12/6/1182.

Konstantinos Kotsalos, André Simões, Luis Marques, Filipe Campos, Clara Gouveia, Henrique Teixeira, Gil Sampaio, and Jorge Pereira. (adms4lv)–improved observability of lv grids based on advanced analytics. 2019b. ISSN 2960241509.

P. Kotsampopoulos, N. Hatziargyriou, B. Bletterie, and G. Lauss. Review, analysis and recommendations on recent guidelines for the provision of ancillary services by distributed generation. In *2013 IEEE International Workshop on Inteligent Energy Systems (IWIES)*, pages 185–190. doi: 10.1109/IWIES.2013.6698583.

D. Kourounis, A. Fuchs, and O. Schenk. Towards the next generation of multiperiod optimal power flow solvers. *IEEE Transactions on Power Systems*, PP(99):1–1, 2018. ISSN 0885-8950. doi: 10.1109/TPWRS.2017.2789187.

A. Kulmala, S. Repo, and P. Järventausta. Coordinated voltage control in distribution networks including several distributed energy resources. *IEEE Transactions on Smart Grid*, 5(4):2010–2020, 2014. ISSN 1949-3053. doi: 10.1109/TSG.2014.2297971.

Prabha Kundur, Neal J Balu, and Mark G Lauby. *Power system stability and control*. McGraw-hill New York, 1994.

Christian Körner, Matthias Hennig, Ronald Schmid, and K Handt. Gaining experience with a regulated distribution transformer in a smart grid environment. 2012.

Sébastien Le Digabel. Algorithm 909: Nomad: Nonlinear optimization with the mads algorithm. *ACM Transactions on Mathematical Software (TOMS)*, 37(4):44, 2011. ISSN 0098-3500.

Q. Li and V. Vittal. The convex hull of the ac power flow equations in rectangular coordinates. In *2016 IEEE Power and Energy Society General Meeting (PESGM)*, pages 1–5. ISBN 1944-9933. doi: 10.1109/PESGM.2016.7741777.

S. Lilla, C. Orozco, A. Borghetti, F. Napolitano, and F. Tossani. Day-ahead scheduling of a local energy community: an alternating direction method of multipliers approach. *IEEE Transactions on Power Systems*, pages 1–1, 2019. ISSN 1558-0679. doi: 10.1109/TPWRS.2019.2944541.

Kerstin Lindén and Inger Segerqvist. Modelling of load devices and studying load/system characteristics. *Licentiate thesis*, 1992.

Marco Liserre, Giampaolo Buticchi, Markus Andresen, Giovanni De Carne, Levy Ferreira Costa, and Zhi-Xiang Zou. The smart transformer: Impact on the electric grid and technology challenges. *IEEE Industrial Electronics Magazine*, 10(2):46–58, 2016. ISSN 1932-4529.

Xiaohu Liu, Andreas Aichhorn, Liming Liu, and Hui Li. Coordinated control of distributed energy storage system with tap changer transformers for voltage rise mitigation under high photovoltaic penetration. *IEEE Transactions on Smart Grid*, 3(2):897–906, 2012. ISSN 1949-3053 1949-3061. doi: 10.1109/tsg.2011.2177501.

J. A. P. Lopes, F. J. Soares, and P. M. R. Almeida. Integration of electric vehicles in the electric power system. *Proceedings of the IEEE*, 99(1):168–183, 2011. ISSN 0018-9219. doi: 10.1109/JPROC.2010.2066250.

J. A. Peças Lopes, N. Hatziargyriou, J. Mutale, P. Djapic, and N. Jenkins. Integrating distributed generation into electric power systems: A review of drivers, challenges and opportunities. *Electric Power Systems Research*, 77(9):1189–1203, 2007. ISSN 03787796. doi: 10.1016/j.epsr.2006.08.016.

João A Peças Lopes, Filipe Joel Soares, and Pedro M Rocha Almeida. Integration of electric vehicles in the electric power system. *Proceedings of the IEEE*, 99(1):168–183, 2010. ISSN 0018-9219.

M. Lotfi, C. Monteiro, M. Shafie-khah, and J. P. S. Catalão. Evolution of demand response: A historical analysis of legislation and research trends. In *2018 Twentieth International Middle East Power Systems Conference (MEPCON)*, pages 968–973. doi: 10.1109/MEPCON.2018.8635264.

Steven H Low. Convex relaxation of optimal power flow—part i: Formulations and equivalence. *IEEE Transactions on Control of Network Systems*, 1(1):15–27, 2014. ISSN 2325-5870.

Atte Mikael Löf. Testing of low voltage network automation. 2013.

A. Madureira, C. Gouveia, C. Moreira, L. Seca, and J. P. Lopes. Coordinated management of distributed energy resources in electrical distribution systems. In *2013 IEEE PES Conference on Innovative Smart Grid Technologies (ISGT Latin America)*, pages 1–8, a. doi: 10.1109/ISGT-LA.2013.6554446.

A. Madureira, J. P. Lopes, A. Carrapatoso, and N. Silva. The new role of substations in distribution network management. pages 863–863, 2009. doi: 10.1049/cp.2009.1034.

A. G. Madureira, J. C. Pereira, N. J. Gil, J. A. Peças Lopes, G. N. Korres, and N. D. Hatziargyriou. Advanced control and management functionalities for multi-microgrids. *European Transactions on Electrical Power*, 21(2):1159–1177, 2011. ISSN 1430144X. doi: 10.1002/etep.407.

André Madureira, Ricardo Bessa, Luis Seca, Jorge Pereira, António A Messias, Diogo A Lopes, and Pedro G Matos. Advanced system architecture and algorithms for smart distribution grids: the sustainable approach. In *CIRED2015-23rd International Conference on Electricity Distribution*, b.

S. Maharjan, Q. Zhu, Y. Zhang, S. Gjessing, and T. Basar. Dependable demand response management in the smart grid: A stackelberg game approach. *IEEE Transactions on Smart Grid*, 4(1): 120–132, 2013. ISSN 1949-3053. doi: 10.1109/TSG.2012.2223766.

Marios Maniatopoulos, Dimitris Lagos, Panos Kotsampopoulos, and Nikos Hatziargyriou. Combined control and power hardware in-the-loop simulation for testing smart grid control algorithms. *IET Generation, Transmission & Distribution*, 11(12):3009–3018, 2017. ISSN 1751-8695.

Carlo Masetti. Revision of european standard en 50160 on power quality: Reasons and solutions. In *Harmonics and Quality of Power (ICHQP), 2010 14th International Conference on*, pages 1–7. IEEE. ISBN 1424472466.

Manuel A. Matos, Luís Seca, André G. Madureira, Filipe J. Soares, Ricardo J. Bessa, Jorge Pereira, and João Peças Lopes. *Control and Management Architectures*. John Wiley & Sons, Ltd, 2016. ISBN 9781118755471. doi: 10.1002/9781118755471.sgd058. URL http://dx.doi.org/10.1002/9781118755471.sgd058.

P. Godinho Matos, P.R. Daniel, A.M. Veiga, A. Aires Messias, M. São Miguel Oliveira, and P. Líbano Monteiro. Inovgrid, a smart vision for a next generation distribution system. *IET Conference Proceedings*, pages 0536–0536. URL http://digital-library.theiet.org/content/conferences/10.1049/cp.2013.0787.

Ann McCabe. *A Regulatory Perspective on Transforming the Power Sector*, pages 97–115. Springer, 2019.

Ismael Miranda, Nuno Silva, and Helder Leite. Technical and economic assessment for optimal sizing of distributed storage. In *Innovative Smart Grid Technologies (ISGT Europe), 2012 3rd IEEE PES International Conference and Exhibition on*, pages 1–6. IEEE. ISBN 146732597X.

Ismael Miranda, Helder Leite, and Nuno Silva. Coordination of multifunctional distributed energy storage systems in distribution networks. *IET Generation, Transmission & Distribution*, 10(3):726–735, 2016. ISSN 1751-8687. doi: 10.1049/iet-gtd.2015.0398. URL http://digital-library.theiet.org/content/journals/10.1049/iet-gtd.2015.0398.

Daniel K Molzahn and Ian A Hiskens. Moment-based relaxation of the optimal power flow problem. In *Power Systems Computation Conference (PSCC), 2014*, pages 1–7. IEEE. ISBN 8393580137.

James A Momoh, Rambabu Adapa, and ME El-Hawary. A review of selected optimal power flow literature to 1993. i. nonlinear and quadratic programming approaches. *IEEE transactions on power systems*, 14(1):96–104, 1999. ISSN 0885-8950.

A. Navarro, L. F. Ochoa, and D. Randles. Monte carlo-based assessment of pv impacts on real uk low voltage networks. In *2013 IEEE Power & Energy Society General Meeting*, pages 1–5, a. ISBN 1932-5517. doi: 10.1109/PESMG.2013.6672620.

Alejandro Navarro, Luis F Ochoa, and Dan Randles. Monte carlo-based assessment of pv impacts on real uk low voltage networks. In *Power and Energy Society General Meeting (PES), 2013 IEEE*, pages 1–5. IEEE, b. ISBN 1479913030.

Jorge Nocedal. *Knitro: An integrated package for nonlinear optimization*, pages 35–60. Springer, 2006.

Jorge Nocedal and Stephen J Wright. Numerical optimization, second edition. *Numerical optimization*, pages 497–528, 2006.

Luis F Ochoa and Pierluigi Mancarella. Low-carbon lv networks: Challenges for planning and operation. In *Power and Energy Society General Meeting, 2012 IEEE*, pages 1–2. IEEE. ISBN 1467327298.

Alison O'Connell, Damian Flynn, and Andrew Keane. Rolling multi-period optimization to control electric vehicle charging in distribution networks. *IEEE Transactions on Power Systems*, 29 (1):340–348, 2014. ISSN 0885-8950.

P. C. Olival, A. G. Madureira, and M. Matos. Advanced voltage control for smart microgrids using distributed energy resources. *Electric Power Systems Research*, 146:132–140, 2017. ISSN 03787796. doi: 10.1016/j.epsr.2017.01.027.

F. Olivier, P. Aristidou, D. Ernst, and T. Van Cutsem. Active management of low-voltage networks for mitigating overvoltages due to photovoltaic units. *IEEE Transactions on Smart Grid*, 7(2): 926–936, 2016a. ISSN 1949-3053. doi: 10.1109/TSG.2015.2410171.

Frederic Olivier, Petros Aristidou, Damien Ernst, and Thierry Van Cutsem. Active management of low-voltage networks for mitigating overvoltages due to photovoltaic units. *IEEE Transactions on Smart Grid*, 7(2):926–936, 2016b. ISSN 1949-3053 1949-3061. doi: 10.1109/tsg.2015.2410171.

Frédéric Olivier, Daniele Marulli, Damien Ernst, and Raphaël Fonteneau. Foreseeing new control challenges in electricity prosumer communities. In *Proc. of the 10th Bulk Power Systems Dynamics and Control Symposium–IREP'2017*, a.

Frédéric Olivier, Antonio Sutera, Pierre Geurts, Raphaël Fonteneau, and Damien Ernst. Phase identification of smart meters by clustering voltage measurements. In *2018 Power Systems Computation Conference (PSCC)*, pages 1–8. IEEE, b. ISBN 1910963100.

Gerardo Osório, Miadreza Shafie-khah, Pedro Coimbra, Mohamed Lotfi, and João Catalão. Distribution system operation with electric vehicle charging schedules and renewable energy resources. *Energies*, 11(11):3117, 2018.

Omid Palizban and Kimmo Kauhaniemi. Energy storage systems in modern grids—matrix of technologies and applications. *Journal of Energy Storage*, 6:248–259, 2016. ISSN 2352-152X.

doi: https://doi.org/10.1016/j.est.2016.02.001. URL http://www.sciencedirect.com/science/article/pii/S2352152X1630010X.

Rasmus Pedersen. *Power Management and Voltage Control using Distributed Resources*. Thesis. URL 10.5278/vbn.phd.engsci.00154.

Rasmus Pedersen, Christoffer Sloth, Gorm Bruun Andresen, and Rafael Wisniewski. Disc: A simulation framework for distribution system voltage control. In *Control Conference (ECC), 2015 European*, pages 1056–1063. IEEE. ISBN 3952426938.

Eefje Peeters, Régine Belhomme, Carlos Batlle, François Bouffard, Seppo Karkkainen, Daan Six, and Maarten Hommelberg. Address: Scenarios and architecture for active demand development in the smart grids of the future. In *Electricity Distribution-Part 1, 2009. CIRED 2009. 20th International Conference and Exhibition on*, pages 1–4. IET. ISBN 1849191263.

Kyriacos Petrou, Andreas Procopiou, Luis F Ochoa, Tom Langstaff, and John Theunissen. Residential battery controller for solar pv impact mitigation: A practical and customer-friendly approach. 2019. ISSN 2960241509.

F Pilo, S Jupe, F Silvestro, C Abbey, A Baitch, B Bak-Jensen, C Carter-Brown, G Celli, K El Bakari, and M Fan. Working group c6. 19: Planning and optimization methods for active distribution systems. *Cigre C6*, 8, 2014.

Rui Pinto, Ricardo Bessa, and Manuel Matos. Surrogate model of multi-period flexibility from a home energy management system. *arXiv preprint arXiv:1703.08825*, 2017a.

Rui Pinto, Ricardo J. Bessa, and Manuel A. Matos. Multi-period flexibility forecast for low voltage prosumers. *Energy*, 141:2251–2263, 2017b. ISSN 0360-5442. doi: https://doi.org/10.1016/j.energy.2017.11.142. URL http://www.sciencedirect.com/science/article/pii/S0360544217320005.

Rui Pinto, Ricardo J. Bessa, Jean Sumaili, and Manuel A. Matos. Distributed multi-period three-phase optimal power flow using temporal neighbors. *Electric Power Systems Research*, 182: 106228, 2020. ISSN 0378-7796. doi: https://doi.org/10.1016/j.epsr.2020.106228. URL http://www.sciencedirect.com/science/article/pii/S0378779620300353.

SuSTAINABLE project. Definition of overall system architecture (d2.3). Report, 2012.

Jairo Quirós-Tortós, Luis F Ochoa, Alejandro Navarro-Espinosa, Mary Gillie, and Richard Hartshorn. Probabilistic impact assessment of electric vehicle charging on residential uk lv networks. In *CIRED*, pages 1–5.

Seyed-Ehsan Razavi, Ehsan Rahimi, Mohammad Sadegh Javadi, Ali Esmaeel Nezhad, Mohamed Lotfi, Miadreza Shafie-khah, and João P. S. Catalão. Impact of distributed generation on protection and voltage regulation of distribution systems: A review. *Renewable and Sustainable Energy Reviews*, 105:157–167, 2019. ISSN 1364-0321. doi: https://doi.org/10.1016/j.rser.2019.01.050. URL http://www.sciencedirect.com/science/article/pii/S1364032119300668.

Hannu Reponen, Anna Kulmala, Ville Tuominen, and Sami Repo. Rtds simulations of coordinated voltage control in low voltage distribution network. In *PES Innovative Smart Grid Technologies Conference Europe (ISGT-Europe), 2016 IEEE*, pages 1–6. IEEE. ISBN 1509033580.

P. Richardson, D. Flynn, and A. Keane. Optimal charging of electric vehicles in low-voltage distribution systems. *IEEE Transactions on Power Systems*, 27(1):268–279, 2012. ISSN 0885-8950. doi: 10.1109/TPWRS.2011.2158247.

P. Richardson, Michael Moran, J. Taylor, A. Maitra, and Andrew Keane. *Impact of electric vehicle charging on residential distribution networks: An Irish demonstration initiative*, volume 2013. 2013. doi: 10.1049/cp.2013.0873.

Justino Rodrigues, Carlos Moreira, and Joao Abel Lopes. Smart transformers as active interfaces enabling the provision of power-frequency regulation services from distributed resources in hybrid ac/dc grids. *Applied Sciences*, 10:1434, 2020. doi: 10.3390/app10041434.

Afshin Samadi, Ebrahim Shayesteh, Robert Eriksson, Barry Rawn, and Lennart Söder. Multi-objective coordinated droop-based voltage regulation in distribution grids with pv systems. *Renewable Energy*, 71:315–323, 2014. ISSN 0960-1481. doi: https://doi.org/10.1016/j.renene.2014.05.046. URL http://www.sciencedirect.com/science/article/pii/S0960148114003073.

K. Samarakoon, J. Ekanayake, and N. Jenkins. Investigation of domestic load control to provide primary frequency response using smart meters. *IEEE Transactions on Smart Grid*, 3(1):282–292, 2012. ISSN 1949-3053. doi: 10.1109/TSG.2011.2173219.

Enrique Santacana, Gary Rackliffe, Le Tang, and Xiaoming Feng. Getting smart. *IEEE Power and Energy Magazine*, 8(2):41–48, 2010. ISSN 1540-7977.

Baljinnyam Sereeter, Kees Vuik, and Cees Witteveen. Newton power flow methods for unbalanced three-phase distribution networks. *Energies*, 10(10):1658, 2017.

M Shahidehpour and M Fotuhi-Friuzabad. Grid modernization for enhancing the resilience, reliability, economics, sustainability, and security of electricity grid in an uncertain environment. *Scientia Iranica*, 23(6):2862–2873, 2016. ISSN 1026-3098.

Farhad Shahnia, Ritwik Majumder, Arindam Ghosh, Gerard Ledwich, and Firuz Zare. Voltage imbalance analysis in residential low voltage distribution networks with rooftop pvs. *Electric Power Systems Research*, 81(9):1805–1814, 2011. ISSN 0378-7796. doi: https://doi.org/10.1016/j.epsr.2011.05.001. URL http://www.sciencedirect.com/science/article/pii/S0378779611001040.

I. Sharma, C. Cañizares, and K. Bhattacharya. Smart charging of pevs penetrating into residential distribution systems. *IEEE Transactions on Smart Grid*, 5(3):1196–1209, 2014. ISSN 1949-3053. doi: 10.1109/TSG.2014.2303173.

E. Shayesteh, M. Parsa Moghaddam, S. Taherynejhad, and M. K. Sheikh-EL-Eslami. Congestion management using demand response programs in power market. In *2008 IEEE Power and Energy Society General Meeting - Conversion and Delivery of Electrical Energy in the 21st Century*, pages 1–8. ISBN 1932-5517. doi: 10.1109/PES.2008.4596877.

D. Shirmohammadi, H. W. Hong, A. Semlyen, and G. X. Luo. A compensation-based power flow method for weakly meshed distribution and transmission networks. *IEEE Transactions on Power Systems*, 3(2):753–762, 1988. ISSN 0885-8950. doi: 10.1109/59.192932.

N Silva. Smart grid solutions and current projects deployment: Inovgrid project. 2010.

Nuno Silva, Pedro Manuel Silva, Luis Seca, André Madureira, Jorge Pereira, and Francisco Melo. Lv scada-how to effectively manage lv networks with limited topology and electrical characteristics data. In *23rd CIRED 2015*.

M. W. Siti, D. V. Nicolae, A. A. Jimoh, and A. Ukil. Reconfiguration and load balancing in the lv and mv distribution networks for optimal performance. *IEEE Transactions on Power Delivery*, 22(4):2534–2540, 2007. ISSN 1937-4208. doi: 10.1109/TPWRD.2007.905581.

Tiago Soares, Marco Silva, Tiago Sousa, Hugo Morais, and Zita Vale. Energy and reserve under distributed energy resources management—day-ahead, hour-ahead and real-time. *Energies*, 10 (11):1778, 2017. ISSN 1996-1073. URL http://www.mdpi.com/1996-1073/10/11/1778.

Iver Bakken Sperstad and Håkon Marthinsen. Optimal power flow methods and their application to distribution systems with energy storage: a survey of available tools and methods. *SINTEF Energi. Rapport*, 2016. ISSN 8259436779.

Thomas Stetz, Frank Marten, and Martin Braun. Improved low voltage grid-integration of photovoltaic systems in germany. *IEEE Transactions on sustainable energy*, 4(2):534–542, 2012. ISSN 1949-3029.

Brian Stott and Ongun Alsac. Fast decoupled load flow. *IEEE transactions on power apparatus and systems*, (3):859–869, 1974. ISSN 0018-9510.

Brian Stott and Ongun Alsaç. Optimal power flow: Basic requirements for real-life problems and their solutions. In *SEPOPE XII Symposium, Rio de Janeiro, Brazil*.

X. Su, M. A. S. Masoum, and P. J. Wolfs. Multi-objective hierarchical control of unbalanced distribution networks to accommodate more renewable connections in the smart grid era. *IEEE Transactions on Power Systems*, 31(5):3924–3936, 2016. ISSN 0885-8950. doi: 10.1109/TPWRS.2015.2501845.

Xiangjing Su, Mohammad A. S. Masoum, and Peter J. Wolfs. Optimal pv inverter reactive power control and real power curtailment to improve performance of unbalanced four-wire lv distribution networks. *IEEE Transactions on Sustainable Energy*, 5(3):967–977, 2014. ISSN 1949-3029 1949-3037. doi: 10.1109/tste.2014.2313862.

Hongbo Sun, Daniel Nikovski, Tetsufumi Ohno, Tomihiro Takano, and Yasuhiro Kojima. A fast and robust load flow method for distribution systems with distributed generations. *Energy Procedia*, 12:236–244, 2011. ISSN 1876-6102.

O. Sundstrom and C. Binding. Flexible charging optimization for electric vehicles considering distribution grid constraints. *IEEE Transactions on Smart Grid*, 3(1):26–37, 2012. ISSN 1949-3053. doi: 10.1109/TSG.2011.2168431.

National Travel Survey. National travel survey: England 2016. Report.

B. D. Tavares, J. Sumaili, F. J. Soares, A. G. Madureira, and R. Ferreira. Assessing the impact of demand flexibility on distribution network operation. In *2017 IEEE Manchester PowerTech*, pages 1–6. doi: 10.1109/PTC.2017.7981196.

Adrian Timbus, Mats Larsson, and Cherry Yuen. Active management of distributed energy resources using standardized communications and modern information technologies. *IEEE Transactions on Industrial Electronics*, 56(10):4029–4037, 2009. ISSN 0278-0046.

William F Tinney and Clifford E Hart. Power flow solution by newton's method. *IEEE Transactions on Power Apparatus and systems*, (11):1449–1460, 1967. ISSN 0018-9510.

R. Tonkoski, L. A. C. Lopes, and T. H. M. El-Fouly. Coordinated active power curtailment of grid connected pv inverters for overvoltage prevention. *IEEE Transactions on Sustainable Energy*, 2(2):139–147, 2011. ISSN 1949-3029. doi: 10.1109/TSTE.2010.2098483.

G. L. Torres and V. H. Quintana. An interior-point method for nonlinear optimal power flow using voltage rectangular coordinates. *IEEE Transactions on Power Systems*, 13(4):1211–1218, 1998. ISSN 0885-8950. doi: 10.1109/59.736231.

P. Trichakis, P. F. Lyons, R. Hair, and P. C. Taylor. Predicting the technical impacts of high levels of small-scale embedded generators on low-voltage networks. *IET Renewable Power Generation*, 2(4):249–262, 2008. ISSN 1752-1416 1752-1424. doi: 10.1049/iet-rpg:20080012.

I Tsiropoulos, D Tarvydas, and N Lebedeva. Li-ion batteries for mobility and stationary storage applications scenarios for costs and market growth. *Publications Office of the European Union: Luxembourg*, 2018.

E Union. Directive 2009/72/ec of the european parliament and of the council of 13 july 2009 concerning common rules for the internal market in electricity and repealing directive 2003/54/ec. *Off. J. Eur. Union L*, 211:55–93, 2009.

Daniel Filipe Bonito Vieira. *O papel dos Sistemas de Informação Geográfica no planeamento, projecto e manutenção da Rede de Distribuição de Energia Eléctrica*. Thesis, 2015.

José Carlos M Vieira, Walmir Freitas, and Andre Morelato. Phase-decoupled method for three-phase power-flow analysis of unbalanced distribution systems. *IEE Proceedings-Generation, Transmission and Distribution*, 151(5):568–574, 2004. ISSN 1359-7051.

Andreas Wachter. *An interior point algorithm for large-scale nonlinear optimization with applications in process engineering*. Thesis, 2003.

Yaw-Juen Wang. Analysis of effects of three-phase voltage unbalance on induction motors with emphasis on the angle of the complex voltage unbalance factor. *IEEE Transactions on energy conversion*, 16(3):270–275, 2001. ISSN 0885-8969.

S. Weckx and J. Driesen. Load balancing with ev chargers and pv inverters in unbalanced distribution grids. *IEEE Transactions on Sustainable Energy*, 6(2):635–643, 2015a. doi: 10.1109/TSTE.2015.2402834.

S. Weckx, C. Gonzalez, and J. Driesen. Combined central and local active and reactive power control of pv inverters. *IEEE Transactions on Sustainable Energy*, 5(3):776–784, 2014. ISSN 1949-3029. doi: 10.1109/TSTE.2014.2300934.

Sam Weckx and Johan Driesen. Load balancing with ev chargers and pv inverters in unbalanced distribution grids. *IEEE Transactions on Sustainable Energy*, 6(2):635–643, 2015b. ISSN 1949-3029.

Joakim Widén, Ewa Wäckelgård, Jukka Paatero, and Peter Lund. Impacts of distributed photovoltaics on network voltages: Stochastic simulations of three swedish low-voltage distribution grids. *Electric power systems research*, 80(12):1562–1571, 2010. ISSN 0378-7796.

Allen J. Wood, Bruce F. Wollenberg, and Gerald B. Sheblé. *Power Generation, Operation, and Control (3rd Edition)*, book section 8. John Wiley & Sons. ISBN 978-0-471-79055-6. URL https://www.wiley.com/en-us/Power+Generation%2C+Operation%2C+and+Control%2C+3rd+Edition-p-9780471790556.

Andreas Wächter and Lorenz T. Biegler. On the implementation of an interior-point filter line-search algorithm for large-scale nonlinear programming. *Mathematical Programming*, 106(1): 25–57, 2006. ISSN 1436-4646. doi: 10.1007/s10107-004-0559-y. URL https://doi.org/10.1007/s10107-004-0559-y.

L. W. Yao and J. A. Aziz. Modeling of lithium ion battery with nonlinear transfer resistance. In *2011 IEEE Applied Power Electronics Colloquium (IAPEC)*, pages 104–109. doi: 10.1109/IAPEC.2011.5779865.

Alireza Zakariazadeh, Shahram Jadid, and Pierluigi Siano. Smart microgrid energy and reserve scheduling with demand response using stochastic optimization. *International Journal of Electrical Power & Energy Systems*, 63:523–533, 2014. ISSN 01420615. doi: 10.1016/j.ijepes.2014.06.037.

Maximilian J Zangs, Peter BE Adams, Timur Yunusov, William Holderbaum, and Ben A Potter. Distributed energy storage control for dynamic load impact mitigation. *Energies*, 9(8):647, 2016.

Fan Zhang and Carol S Cheng. A modified newton method for radial distribution system power flow analysis. *IEEE Transactions on Power Systems*, 12(1):389–397, 1997. ISSN 0885-8950.

Jizhong Zhu. *Optimal Power Flow*, pages 297–364. John Wiley & Sons, Inc, 2015a. ISBN 9781118887004. doi: 10.1002/9781118887004.ch8. URL http://dx.doi.org/10.1002/9781118887004.ch8.

Jizhong Zhu. *Optimization of Power System Operation*. John Wiley & Sons, Inc, 2015b. ISBN 9781118887004. doi: 10.1002/9781118887004.ch1. URL http://dx.doi.org/10.1002/9781118887004.ch1.

R. D. Zimmerman. Ac power flows, generalized opf costs and their derivatives using complex matrix notation. Report, 2010.

Ray D Zimmerman and Carlos E Murillo-Sánchez. Matpower 6.0 user's manual. *Power Systems Engineering Research Center*, 9, 2016.

Ray D Zimmerman and Hongye Wang. Matpower interior point solver mips 1.3 user's manual. 2016.